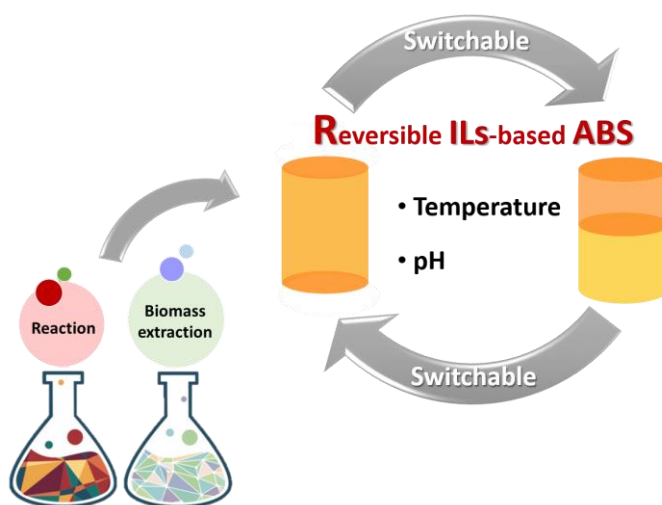




Ana Maria da
Conceição Ferreira

Soluções aquosas de líquidos iónicos como
solventes sustentáveis em processos de separação

Ionic liquids aqueous solutions as sustainable
solvents in separation processes





Ana Maria da
Conceição Ferreira

**Soluções aquosas de líquidos iónicos como
solventes sustentáveis em processos de separação**

**Ionic liquids aqueous solutions as sustainable
solvents in separation processes**

Tese apresentada à Universidade de Aveiro para cumprimento dos requisitos necessários à obtenção do grau de Doutor em Engenharia Química, realizada sob a orientação científica do Doutora Mara Guadalupe Freire Martins, Investigadora Coordenadora do Departamento de Química, CICECO, da Universidade de Aveiro, e coorientação do Professor Doutor João Manuel da Costa e Araújo Pereira Coutinho, Professor Catedrático do Departamento de Química, CICECO, da Universidade de Aveiro.

Apoio financeiro do POCTI no âmbito do III Quadro Comunitário de Apoio.

O doutoramento agradece o apoio financeiro da FCT e do FSE no âmbito do III Quadro Comunitário de Apoio (SFRH/BD/92200/2013).

Parte da investigação que conduziu aos resultados aqui apresentados foi financiada pelo Conselho Europeu de Investigação ao abrigo do Sétimo ProgramaQuadro da União Europeia (FP7/2007-2013)/ERC no. 337753



“Stories help make us who we are”

o júri

President

Prof. Dr. António José Arsénia Nogueira
Professor Catedrático do Departamento de Biologia da Universidade de Aveiro

Prof. Dr. José António Couto Teixeira
Professor Catedrático do Departamento de Engenharia Biológica da Universidade do Minho

Prof.^a Dr.^a Isabel Maria Delgado Jana Marrucho Ferreira
Professora com Agregação do Instituto Superior Técnico da Universidade de Lisboa

Prof. Dr. Armando Jorge Domingues Silvestre
Professor Associado com Agregação do Departamento de Química da Universidade de Aveiro

Prof. Dr. Álvaro Silva Lima
Professor Titular do Programa de Pós-Graduação em Engenharia de Processos da Universidade Tiradentes, Aracaju-SE, Brasil

Dr.^a Mara Guadalupe Freire Martins
Investigadora Coordenadora do Departamento de Química, CICECO – Instituto de Materiais de Aveiro, da Universidade de Aveiro

Agradecimentos

Obrigada à mãe, ao pai e às vaquinhas. Obrigada por me apoiarem, apesar de não entender muito bem esta vida de estudante, e por estarem sempre dispostos a ajudar.

Obrigada aos amores da minha vida (3 Mosqueteiros, Os BrOs, 5 princesas, Brigada Smile, 9.º I, Helena, sexy man, sister-prima) que me aturam a mim e aos meus desvaneios. Obrigada por estarem presentes na minha vida, pelas conversas filosóficas, pelas jantaradas. Obrigada por me fazerem acreditar que sou capaz; com vocês a caminhada tornou-se mais fácil. Já disse hoje que vos adoro?!

Um grande obrigado a todos os membros do Path e do Mini-Path, pelo apoio e por me terem acolhido tão bem, durante esta labuta. Obrigada ao meu grupo de dança Path favorito, vocês proporcionaram-me um final de tese muito mais descontraído e divertido ;).

Por último, mas não menos importante, aos meus orientadores, à Dr.^a Mara Freire e ao Prof. João Coutinho, obrigada pelo acompanhamento feito durante estes 4 anos, ou melhor dizendo 8 anos, mas, principalmente, por todas as oportunidades dadas, pela paciência e confiança depositadas em mim.

palavras-chave

Líquido iônico, zwitterião, água, solvente, extração, sistema aquoso bifásico, sistema reversível, separação, processo integrado.

Resumo

Este trabalho compreende o desenvolvimento de solventes e processos de separação sustentáveis, eficientes e rentáveis, através da aplicação de soluções aquosas de líquidos iônicos (LIs). Em particular mostra-se o potencial de soluções aquosas de LIs como solventes alternativos para a extração de compostos de valor acrescentado a partir de biomassa, evitando portanto a utilização de solventes orgânicos voláteis, assim como a sua utilização na formação de sistemas aquosos bifásicos (SAB) como processos de separação. No primeiro conjunto de resultados demonstra-se que soluções aquosas de LIs apresentam uma elevada capacidade para extrair cafeína e hidroximatairesinol (HMR) de borras de café e de nós de abeto da Noruega, respetivamente. O primeiro trabalho nesta vertente mostra a importância do conceito de hidrotropia, atuando como o principal fator responsável pelo elevado desempenho das soluções aquosas de LIs na extração de compostos de valor acrescentado a partir de biomassa, enquanto que o segundo trabalho demonstra a utilização de LIs biocompatíveis, permitindo a utilização direta dos extratos de biomassa em aplicações nutracêuticas e de cosmética. As soluções aquosas de LIs também foram estudadas na criação de SAB reversíveis, como plataformas de separação alternativas, assim como no desenvolvimento de sistemas integrados de reação-separação. As respetivas transições de fase ocorrem por aplicação de estímulos externos, tais como pH e temperatura, e a sua aplicação foi demonstrada na separação de misturas de aminoácidos, e ácidos nucleicos e proteínas. Por fim, demonstra-se a utilização de SAB reversíveis como processos integrados de produção e separação. Os SAB reversíveis obtidos por alterações de pH foram aplicados na produção de hidroximetilfurfural (HMF) a partir de frutose em meio ácido, seguido da sua separação em condições alcalinas (induzindo a formação de duas fases). Por outro lado, e tirando partido da natureza biocompatível dos constituintes dos SAB, estudaram-se SAB reversíveis através da alteração da temperatura em processos biocatalíticos. A reação ocorre em meio homogéneo, catalisada pela lacase, onde pequenas alterações de temperatura induzem a formação de duas fases e a completa separação da enzima do respetivo produto. Estes sistemas permitem também a recuperação e reutilização das fases/constituintes dos SAB, contribuindo para o desenvolvimento de processos sustentáveis. Embora seja ainda necessária investigação adicional sobre a viabilidade destes solventes e sistemas para aplicação em larga escala, os resultados aqui apresentados mostram a relevância de soluções aquosas de LIs como solventes alternativos e no desenvolvimento de processos de separação.

Keywords

Ionic liquid, zwitterion, water, solvent, extraction, aqueous biphasic system, switchable/reversible system, separation, integrated process.

Abstract

This work is focused on the development of sustainable and cost-effective solvents and separation processes, particularly by applying aqueous solutions of ionic liquids (ILs). It is shown the potential of ILs aqueous solutions as alternative solvents to extract value-added compounds from biomass, avoiding the use of the commonly applied volatile organic solvents, and their use as phase-forming components of aqueous biphasic systems (ABS) to develop reversible and/or integrated separation platforms.

In the first set of results, it is demonstrated the high performance of ILs aqueous solutions to extract caffeine and hydroxymatairesinol (HMR) from spent coffee grounds (SCG) and Norway spruce knots, respectively. In the first work it is shown the relevance of the hydrotropy concept as the major factor behind the improved extraction performance of ILs aqueous solutions, whereas in the second work biocompatible ILs were applied and proposed to be used directly with the biomass extracts in nutraceutical and cosmetic applications. Still focused on the use of ILs aqueous solutions, these were then explored in the creation of reversible aqueous biphasic systems (ABS) as alternative separation platforms, followed by the development of integrated production-separation strategies. Transitions from monophasic to biphasic regimes were shown to occur by changes in pH and temperature (applied as external stimulus). Examples on their use in the separation of mixtures of amino acids and of nucleic acids from proteins are given. Finally, it is shown the applicability of reversible ABS as integrated production-separation processes. pH-driven ABS were applied in the production of hydroxymethylfurfural (HMF) from fructose at acidic media, followed by their separation at alkaline conditions (inducing the two phases separation). On the other hand, and taking advantage of the biocompatible nature of the ABS phase-forming components, thermoreversible ABS were used in biocatalytic processes. A reaction catalysed by laccase occurs in the homogenous solution, after which small temperature changes induce the two-phase formation and the complete separation of the enzyme from the respective product. These systems also allow the recovery and reuse of the ABS phases, contributing towards the development of sustainable production and separation processes. Although additional research on these solvents and systems scale-up feasibility is still required, the results here presented unveil the relevance of IL aqueous solutions as alternative solvents and on the development of efficient separation processes.

Contents

1. Introduction	1
1.1. Scopes and Objectives.....	3
1.2. Bioactive compounds, solvents and separation processes.....	6
1.3. Ionic liquids (ILs).....	8
1.3.1. ILs as alternative solvents for the extraction of value-added compounds from biomass.....	10
1.3.2. ILs as phase-forming components of aqueous biphasic systems (ABS) to be used in separation processes.....	17
1.3.3. Reversible systems composed of ILs	26
1.4. Additional remarks.....	29
1.5. References.....	31
2. Materials and experimental procedure.....	35
2.1. Extraction of value-added compounds from biomass using ILs aqueous solutions.....	37
2.1.1. Extraction of caffeine from spent coffee grounds using aqueous solutions of ionic liquids and salts	37
2.1.2. Extraction of 7-hydroxymatairesinol from Norway Spruce knots using aqueous solutions of ionic liquids.....	38
2.2. Reversible IL-based ABS.....	43
2.2.1. pH-responsive aqueous biphasic systems formed by ionic liquids and polymers.....	43
2.2.2. Temperature-responsive aqueous biphasic systems composed of ammonium-based zwitterions and salts	46
2.3. Integrated IL-based processes.....	48
2.3.1. Integrated production-separation platforms applying reversible pH-driven aqueous biphasic systems	48
2.3.2. Integrated production-separation platforms applying thermoreversible aqueous biphasic systems.....	50

2.4. References.....	52
3. Extraction of value-added compounds from biomass using ILs aqueous solutions	53
3.1. Extraction of caffeine from spent coffee grounds using aqueous solutions of ionic liquids and salts	55
Abstract	55
Introduction.....	56
Results and discussion.....	57
Conclusions.....	61
References.....	62
3.2. Extraction of 7-hydroxymatairesinol from Norway Spruce knots using aqueous solutions of ionic liquids	63
Abstract	63
Introduction.....	64
Results and discussion.....	66
Conclusions.....	73
References.....	74
4. Reversible IL-based ABS.....	77
4.1. pH-responsive aqueous biphasic systems formed by ionic liquids and polymers	79
Abstract	79
Introduction.....	80
Results and discussion.....	81
Conclusions.....	88
References.....	88
4.2. Temperature-responsive aqueous biphasic systems composed of ammonium-based zwitterions and salts.....	91
Abstract	91
Introduction.....	92

Results and discussion.....	93
Conclusions.....	98
References.....	98
5. Integrated IL-based processes.....	101
5.1. Integrated production-separation platforms applying reversible pH-driven aqueous biphasic systems.....	103
Abstract	103
Introduction.....	104
Results and discussion.....	105
Conclusions.....	111
References.....	112
5.2. Integrated production-separation platforms applying thermoreversible aqueous biphasic systems.....	115
Abstract	115
Introduction.....	116
Results and discussion.....	117
Conclusions.....	123
References.....	123
6. Conclusions & Future work.....	125
List of Publications	131
Appendix A	135
Appendix B	147
Appendix C	173

List of figures

Figure 1.1. Layout of the current thesis.	4
Figure 1.2. (A) Chemical structures of some IL cations and anions usually employed in the extraction and separation of value-added compounds. (B) Allusive scheme to the ILs “designer solvents” characteristic. (C) Chemical structures of tetraalkylammonium-based ZIs.	9
Figure 1.3. Scheme of SLE applied to solid biomass samples.....	11
Figure 1.4. Chemical structures of some compounds extracted from biomass using IL aqueous solutions.	14
Figure 1.5. (A) Scheme of phase diagrams determination. (B) Schematic representation of an ABS phase diagram in an orthogonal representation. TCB - Binodal curve, C - Critical point, TB - Tie-line, T - composition of the top phase, B - composition of the bottom phase, and X, Y and Z – initial mixture compositions of biphasic mixtures.	18
Figure 1.6. Chemical structures of some compounds that may be extracted from vegetable sources used in IL-based ABS.	20
Figure 1.7. Chemical structure of some amino acids usually investigated with IL-based ABS.....	23
Figure 1.8. Illustration of reversible IL-based liquid-liquid systems.....	27
Figure 1.9. (A) Schematic illustration of typical phase diagrams with LCST- and UCST-type phase behaviour. (B) Schematic representation of phase transition with the addition of acidic or alkaline species in aqueous media. (C) Schematic representation of phase transition with the addition of CO ₂ /N ₂	28
Figure 3.1.1. Chemical structures of the ILs and salts investigated, and of caffeine.	58
Figure 3.1.2. Influence of the hydrotropes (ILs, salts and the mixture ILs + salts) concentration in the solubility of caffeine in aqueous solutions at 25 °C (-*-) NaCl, (-◆-) Na[Tos], (-●-) [C ₄ C ₁ im]Cl, (—) [C ₄ C ₁ im][Tos], (-■-) NaCl + [C ₄ C ₁ im][Tos] (1:1 in a mole basis) and (-X-) Na[Tos] + [C ₄ C ₁ im]Cl (1:1 in a mole basis). (—) The black line corresponds to the solubility of caffeine in water under the same conditions.	59
Figure 3.1.3. Extraction yields of caffeine from SCG using aqueous solutions of ILs, salts, and their mixtures at T = 25 °C, t = 30 min, and solid-liquid ratio = 1:10. IL/salt. Concentration of the ILs, salts, or mixtures: (purple bars) 0.25 M, (green bars) 0.50 M, (blue bars) 0.75 M and (orange bars) 1.00 M. (—) The black line corresponds to the caffeine extraction using water at the same conditions.	60
Figure 3.2.1. (A) Chemical structures of HMR, (B) betaine and (C) betaine analogues.	64
Figure 3.2.2. Chemical structures of the ionic liquids used in the extraction of HMR from Norway spruce knots.....	66

Figure 3.2.3. Yield of HMR extracted from Norway Spruce knots with different aqueous solutions of ILs (at 0.5 M), acetone and water (T = 25 °C, t = 180 min) for a S/L ratio= 0.10 (blue bars) and for a S/L ratio = 0.02 (orange bars). Ratio of HMR2/ HMR1 for a S/L ratio= 0.10 (●) and for a S/L ratio= 0.02 (●).	67
Figure 3.2.4. Response surface (top) and contour plots (bottom) on the yield of total HMR extracted using aqueous solutions of [(C ₂) ₃ NC ₂]Br at 25 °C with the combined effects of: (A) extraction time (t (min)) and IL concentration (C (M)); (B) solid-liquid ratio (S/L ratio) and concentration (C (M)); and (C) solid-liquid ratio (S/L ratio) and extraction time (t (min))......	69
Figure 3.2.5. IC ₅₀ values (mg·mL ⁻¹) after 0.5 (green bars), 1.5 (blue bars) and 2h (yellow bars) of exposure to DPPH.	71
Figure 3.2.6. (A) Cell viability when exposed to increasing concentrations of pure IL (▲), HMR in the IL-water solution (■) and precipitated HMR-rich extract (●). (B) Cell viability when exposed to increasing concentrations of the IL (▲) used for the extractions of HMR.	72
Figure 3.2.7. (A) Macrophage cellular oxidative stress in the presence of the different samples of HMR and pure IL. Scale bar: 20 μm. (B) Cellular oxidative stress in LPS-stimulated macrophages treated with precipitated HMR, HMR in IL solution and pure IL. Scale bar: 20μm.	73
Figure 3.2.8. Schematic overview of the proposed process for the extraction of HMR from Norway Spruce knots using aqueous solutions of AGB-based ILs.	73
Figure 4.1.1. Phase diagrams of ABS composed of PPG 400 + water + [Ch][C ₁ CO ₂] at pH ≈ 9 (●), pH ≈ 8 (●), pH ≈ 7 (●), pH ≈ 6 (●) and pH ≈ 5 (●).	82
Figure 4.1.2. Illustration of the pH-driven behaviour of [Ch][C ₁ CO ₂]-based ABS; two dyes were added to better illustrate the phase separation.....	84
Figure 4.1.3. (A) Scheme of the separation of the DNA from HSA. (B) DNA extraction efficiency to the IL-rich phase (EE%, bars) and HSA yield (Y%, symbols) in ABS formed by: (orange bars) [Ch][C ₁ CO ₂], (green bars) [Ch][C ₂ CO ₂], (blue bars) [Ch][Gly] and (yellow bars) [Ch]Cl.....	85
Figure 4.1.4. (A) A ₂₆₀ to A ₂₈₀ ratio for DNA samples after recovery from the IL-rich phase. (B) Circular dichroism (CD) spectra of samples of DNA:HSA at different weight ratio after recovery from the IL-rich phase at pH 5. (C) CD spectra of the DNA:HSA sample at a 1:1 weight ratio after recovery from the IL-rich phase at different pH values.	87
Figure 4.2.1. Chemical structures and acronyms of the ZIs used.....	93
Figure 4.2.2. (A) Salt anion effect in the phase diagrams of ternary systems composed of water, N ₅₅₅ C3S and potassium-based salts at 25 °C: K ₃ PO ₄ (□), K ₃ C ₆ H ₅ O ₇ (◆), K ₂ CO ₃ (○), K ₂ HPO ₄ (+) and KH ₂ PO ₄ (△). (B) ZIs alkyl chains length effect in the phase diagrams of ternary systems composed of water, K ₃ PO ₄ and ZIs at 25 °C: N ₅₅₅ C3S (□), N ₃₃₃ C3S (+), N ₂₂₂ C3S (▲), N ₁₁₁ C4S (○) and N ₁₁₁ C3S (◆).	94

Figure 4.2.3. Temperature (T) effect in the phase diagrams of ternary systems composed of ZI + K_3PO_4 + water at 25 °C (▲), 35 °C (◆), and 45 °C (○): (A) $N_{555}C3S$, (B) $N_{333}C3S$, and (C) $N_{111}C3S$	96
Figure 4.2.4. Illustration of the thermoreversible behaviour of ZI-based ABS.....	97
Figure 4.2.5. Partition of L-tryptophan (Try) and glycine (Gly) in $N_{111}C3S$ - and $N_{555}C3S$ -based ABS formed at 25 °C and 45 °C, respectively: $EE_{Try}\%$ (green bars), $EE_{Gly}\%$ (blue bars).	97
Figure 5.1.1. Chemical structures of the ILS investigated.	106
Figure 5.1.2. Ternary phase diagrams of an IL-based ABS at 25 °C, at pH ≈ 9 (▲) and pH ≈ 5 (◆). In all the investigated ABS, the top phase corresponds to the IL-rich phase while the bottom phase is mainly composed of salt and water.	106
Figure 5.1.3. Phase diagrams of ABS composed of $[P_{4444}]Cl$ + water + $K_3C_6H_5O_7/C_6H_8O_7$ at pH ≈ 9 (▲), pH ≈ 8 (○), pH ≈ 7 (◆), pH ≈ 6 (□) and pH ≈ 5 (—).	107
Figure 5.1.4. Production of HMF through fructose dehydration in presence (or not) of citric acid and ILS, at 80 °C for 80 min.....	110
Figure 5.1.5. Selective separation of HMF (red bars) from fructose (yellow bars) that did not react through the addition of KOH and formation of ABS.	111
Figure 5.2.1. (A) Chemical structures and acronyms of the ZIs used. (B) Chemical structure of PEG with the molecular formula $H-(O-CH_2-CH_2)_n-OH$	118
Figure 5.2.2. Temperature effect in the phase diagrams of ternary systems composed of ZI + PEG 6000 + H_2O at 25 °C (▲), 35 °C (●) and 45 °C (■). (A) $N_{111}C3S$ - and (B) $N_{555}C3S$ -based ABS. There is no formation of ABS comprising PEG 6000 and $N_{555}C3S$ at 45°C.....	119
Figure 5.2.3. (A) Oxidation of ABTS using laccase and their selective separation from the reaction product by changes in temperature. (B) Extraction efficiencies of laccase ($EE\%$, yellow bars) and extraction efficiencies of the green-coloured $ABTS^+$ radical ($EE\%$, green bars) in ABS formed by PEG 6000 and $N_{555}C3S$ or $N_{111}C3S$	121
Figure 5.2.4. (A) Flowchart of the integrated reaction-separation process developed, including the enzyme and ZI-rich phase recyclability. (B) Relative laccase activity in the ZI-rich phase in 5 cycles of oxidative reaction, comprising both the recovery and reuse of the enzyme and ZI-rich phase.....	122

List of symbols

$[i]$	Concentration of component i	R^2	Correlation coefficient
€_{biom}	Cost associated to the biomass	$r_{\text{IL lost}}$	Ratio of IL lost during the recycling approach
€_{IL}	Price <i>per</i> kg of IL	S	Selectivity
€_{prod}	Price <i>per</i> kg of compound extracted from the biomass	S/L ratio	Solid-liquid ratio
A_i	Absorbance of component i	T	Temperature
α	Axial point	t	Time
β_i	Adjusted coefficients for the independent variable i or non-proportional costs of the process	V_{IL}	Volume of the IL needed to treat one kg of biomass
C_{prod}	Extracted concentration of the target compound in the biomass	wt%	Weight fraction percentage
$EE_i\%$	Extraction efficiency percentage of component i	X_i	Independent variable i
δ	Proportional costs of the process	$Y_i\%$	Recovery yield of component i
K_i	Partition coefficient of component i	σ	Standard deviation
K_{ow}	Octanol-water partition coefficient	R^2	Correlation coefficient
$\text{p}K_a$	Acidic dissociation constant	$r_{\text{IL lost}}$	Ratio of IL lost during the recycling approach

List of acronyms

Ionic liquid cations

$[(C_2)_3NC_2]^+$	Triethyl[2-ethoxy-2-oxoethyl]ammonium	$[C_4C_{1im}]^+$	1-Butyl-3-methylimidazolium
$[(C_3)_3NC_2]^+$	Tri(n-propyl)[2-ethoxy-2-oxoethyl]ammonium	$[C_4C_{1pip}]^+$	1-Butyl-1-methylpiperidinium
$[(C_4)_3NC_2]^+$	Tri(n-butyl)[2-ethoxy-2-oxoethyl]ammonium	$[C_4C_{1py}]^+$	1-Butyl-3-methylpyridinium
$[(HSO_3)C_4C_{1im}]^+$	1-(4-Sulfonylbutyl)-3-methylimidazolium	$[Ch]^+$	Cholinium
$[aC_{1im}]^+$	1-Allyl-3-methylimidazolium	$[C_nC_{1im}]^+$	1-Alkyl-3-methylimidazolium
$[C_{12}C_{1im}]^+$	1-Dodecyl-3-methylimidazolium	$[N_{0002}]^+$	Ethylammonium
$[C_{14}C_{1im}]^+$	1-Tetradecyl-3-methylimidazolium	$[N_{110(2OH)}]^+$	<i>N,N</i> -Dimethylethanolammonium
$[C_1PyrNC_2]^+$	<i>N</i> -(1-methylpyrrolidyl-2-ethoxy-2-oxoethyl)ammonium	$[N_{1100}]^+$	<i>N,N</i> -Dimethylammonium
$[C_2C_{1im}]^+$	1-Ethyl-3-methylimidazolium	$[N_{111(C_{2O}(O)_{12})}]^+$	2-(Dodeoxy)- <i>N,N,N</i> -trimethyl-2-oxoethanaminium
$[C_4C_1C_{1im}]^+$	1-Butyl-2,3-dimethylimidazolium	$[P_{4444}]^+$	Tetrabutylphosphonium

Ionic liquid anions

$[BF_4]^-$	Tetrafluoroborate	$[Lac]^-$	Lactate
$[C_1CO_2]^-$	Acetate	$[N(C_1)_2CO_2]^-$	Dimethylcarbamate
$[C_1SO_3]^-$	Methylsulfonate	$[N(CN)_2]^-$	Dicyanamide
$[C_1SO_4]^-$	Methylsulphate	$[NO_3]^-$	Nitrate
$[C_2CO_2]^-$	Propanoate	$[NTf_2]^-$	Bis(trifluoromethylsulfonyl)imide
$[C_7CO_2]^-$	Octanoate	$[Tos]^-$	Tosylate
$[CF_3SO_3]^-$	Trifluoromethanesulfonate	Br^-	Bromide
$[Gly]^-$	Glycolate	Cl^-	Chloride
$[HSO_4]^-$	Hydrogenosulphate	OH^-	Hydroxide

Zwitterions

N ₁₁₁ C3S	<i>N,N,N</i> -Trimethyl-3-sulfonyl-1-propaneammonium
N ₁₁₁ C4S	<i>N,N,N</i> -Trimethyl-4-sulfonyl-1-butaneammonium
N ₂₂₂ C3S	<i>N,N,N</i> -Triethyl-3-sulfonyl-1-propaneammonium
N ₃₃₃ C3S	<i>N,N,N</i> -Tripropyl-3-sulfonyl-1-propaneammonium
N ₅₅₅ C3S	<i>N,N,N</i> -Tripentyl-3-sulfonyl-1-propaneammonium

Common salts

		MgCl ₂	Magnesium chloride
CaCl ₂	Calcium chloride	Na[Tos]	Sodium tosylate
K ₂ CO ₃	Potassium carbonate	Na ₂ CO ₃	Sodium carbonate
K ₂ HPO ₄	Potassium hydrogen phosphate	Na ₂ HPO ₄	Sodium hydrogen phosphate
K ₃ C ₆ H ₅ O ₇	Potassium citrate	Na ₂ SO ₄	Sodium sulfate
K ₃ PO ₄	Potassium phosphate	Na ₃ C ₆ H ₅ O ₇	Sodium citrate
KCH ₃ CO ₂	Potassium acetate	NaCl	Sodium chloride
KCl	Potassium chloride	NaH ₂ PO ₄	Sodium dihydrogen phosphate
KH ₂ PO ₄	Potassium dihydrogen phosphate	NaHCO ₃	Sodium hydrogen carbonate
KOH	Potassium hydroxide		

List of abbreviations

AA	Amino acid	IL	Ionic liquid
ABS	Aqueous biphasic systems	LCC-ILs	Long-chain alkyl carboxylates ILs
ABTS	2,2'-azino-bis(3-ethylbenzothiazoline-6-sulfonic acid)	LCST	Lower critical solution temperature
AGB	Analogues of glycine-betaine	LLE	Liquid-liquid extraction
AGB-ILs	Analogues of glycine-betaine ionic liquids	LPS	Lipopolysaccharide
AK	Adenylate kinase	MAE	Microwave-assisted extraction
BSA	Bovine serum albumin	MIBK	Methyl-iso-butylketone
CD	Circular Dichroism	N ₂	Nitrogen
DAD	Detector Diode Array	NaPA	Sodium polyacrylate
DCFH-DA	2',7'-dichlorodihydrofluorescein diacetate	NMR	Nuclear magnetic resonance
DMEM	Dulbecco's Modified Eagle's Medium	PBS	Phosphate buffered saline
DMSO	Dimethyl sulfoxide	PEG	Poly(ethylene)glycol
DNA	Deoxyribonucleic acid	PPG	Polypropylene glycol
DPPH	2,2-Diphenyl-2-picrylhydrazyl	RID	Refractive Index Detector
DSC	Differential scanning calorimetry	ROS	Reactive oxygen species
FBS	Fetal bovine serum	RSM	Response surface methodology
FDA	Food and drug administration	SCG	Spent coffee grounds
FTIR	Fourier transform infrared spectroscopy	SEM	Scanning electron microscope
Gly	Glycine	SLE	Solid-liquid extraction
GRAS	Generally recognized as safe	TGA	Thermogravimetric analyses
HBSS	Hanks' balanced salt solution	TL	Tie-line
HMF	5-hydroxymethylfurfural	TLL	Tie-line length
HMR	Hydroxymatairesinol	Try	L-tryptophan
HMR1	(7 <i>R</i> ,8 <i>R</i> ,8' <i>R</i>)-(-)- <i>allo</i> -hydroxymatairesinol	UAE	Ultrasound assisted extraction
HMR2	(7 <i>S</i> ,8 <i>R</i> ,8' <i>R</i>)-(-)-7-hydroxymatairesinol	UCST	Upper critical solution temperature
HPLC	High performance liquid chromatography	UV-Vis	Ultraviolet- Visible
HSA	Human serum albumin	ZI	Zwitterion

1. INTRODUCTION

1.1. Scopes and Objectives

The current work is based on the use of aqueous solutions of ionic liquids (ILs) as alternative solvents for the extraction, separation and/or purification of value-added (bio)compounds, and on the design of cost-effective, sustainable and integrated extraction/recovery or production/recovery strategies. ILs have been chosen as alternative solvents due to their unique properties, namely a negligible vapour pressure under atmospheric conditions, low flammability and high thermal and chemical stabilities.¹ ILs are also recurrently recognized by their high solvation aptitude for organic and inorganic compounds, and as enhanced stabilizing media for proteins, nucleic acids, among others.¹ Mainly due to their designer ability, ILs have been largely investigated in the past decades in a wide plethora of applications.

In this work, tailored and better processes using ILs have been developed for the extraction or production and separation of value-added biocompounds. In particular, three types of processes have been developed: (i) extraction/recovery of biocompounds from solid biomass samples; (ii) separation/recovery of biocompounds from aqueous samples; and (iii) integrated production/separation processes involving value-added compounds. In the extraction of target compounds from solid biomass matrices, two examples are presented, namely the extraction of caffeine from spent coffee grounds (SCG), and hydroxymatairesinol (HMR) from the knots of *Norway Spruce*. In the second type of process, new reversible IL-based aqueous biphasic systems (ABS) are described in the separation of deoxyribonucleic acid (DNA) from human serum albumin (HSA), and aromatic from aliphatic amino acids. In the last approach, two integrated processes based on ABS are presented, namely by the production and purification of 5-hydroxymethylfurfural (HMF), and by performing integrated catalytic reactions and separations steps using laccase. For a better understanding of the current thesis organization, a schematic representation is given in **Figure 1.1**.

An increased demand in the consumption of natural compounds, majorly extracted from biomass, has been observed in the past years.² Biomass contains various types of bioactive compounds which can be used in nutraceutical, cosmetic, and pharmaceutical products, particularly due to their beneficial biological activities, such as anticancer, antimicrobial, antioxidant, and analgesic effects.² However, conventional extraction processes for value-added natural compounds may display several disadvantages, such as low efficiency and non-selectivity, time-consuming, high energetic input, and degradation of the targeted compounds.² Furthermore, traditional methods generally involve the use of large quantities of toxic and volatile organic solvents leading to additional concerns on environmental and human health

issues.² Aiming at finding more effective and biocompatible and environmentally-friendly solvents and processes, aqueous solutions of ILs were investigated as alternative solvents for the extraction of value-added compounds from biomass.

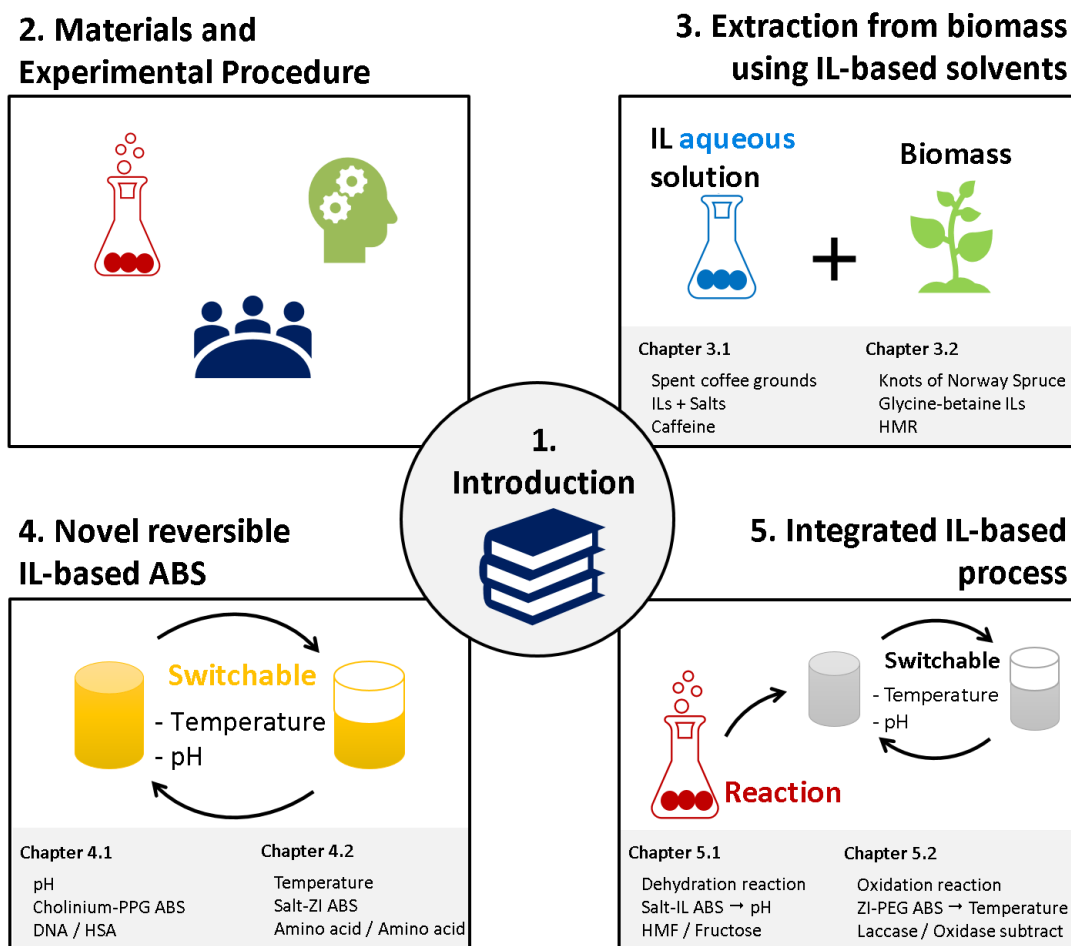


Figure 1.1. Layout of the current thesis.

In this line, **Chapter 3** describes two examples of the application of ILs aqueous solutions on the extraction of caffeine and HMR from biomass. Usually, IL-based solid-liquid extractions lead to promising results since ILs can act as powerful hydrotropes³ or may be designed to present surface-active properties,^{4, 5} allowing an increase in the solubility of several biomolecules in aqueous solutions of ILs, and therefore leading to higher extraction yields. In **Chapter 3.1** it is investigated the potential of aqueous solutions composed of ILs and conventional salts, as well as mixtures of both compounds, to dissolve and extract caffeine from SCG, aiming at better understanding the hydrotropy-based mechanism ruling the high-performance of ILs aqueous solutions to extract value-added compounds from biomass. Aqueous solutions of ILs and salts containing hydrotrope ions display a higher caffeine solubilisation and extraction capacity. The obtained results allowed to conclude that the IL/salt isolated ions and not the original ion-pair

play the primary role on the hydrotrophy-based extraction mechanism. Although high extraction efficiencies are usually obtained with aqueous solutions of ILs, one of the main problems associated to the extraction of biocompounds from biomass using aprotic ILs is connected to their recovery from the IL-rich solution, since these cannot be recovered by evaporation.² There have been some proposals in this direction, either by applying back-extraction using organic solvents or by inducing precipitation with anti-solvents.² In a subsequent research work, described in **Chapter 3.2**, aqueous solutions of biocompatible ILs, namely analogues of glycine-betaine (AGB), were used for the extraction of HMR from knots of *Norway Spruce*, in which it is avoided the requirement of removing the IL or an additional recovery step. The extraction yields obtained showed to be better than those obtained with traditional volatile organic solvents. Furthermore, studies on the cytotoxicity of the ILs aqueous solutions supported their biocompatible nature and high antioxidant activity of the HMR-rich extracts. It was shown that aqueous solutions of ILs containing HMR have the potential to be used directly in cosmetic, nutraceutical and pharmaceutical applications without requiring an additional step for the HMR recovery and IL recycling.

In the past few years, IL-based ABS have been largely explored for the separation and purification of a broad range of compounds, mainly due to their superior performance as alternative extraction and purification platforms.^{4, 6, 7} In addition, in liquid-liquid systems, research on dynamic and reversible biphasic systems has also been conducted. These phase-transitions are achieved by changes in pH⁸ or temperature,⁹ as well as by the addition of CO₂/N₂.¹⁰ **Chapter 4** comprises several examples on the development of new reversible IL-based ABS and on their application for the separation of DNA from HSA, and of aromatic from aliphatic amino acids. These systems, as those studied in **Chapter 5**, have potential to be remarkable separation processes by taking advantage of their switchable behaviour. **Chapter 4.1** addresses the development of pH-triggered IL-based ABS, in which cholinium-based ILs and polypropylene glycol (PPG) were used as phase-forming components. The phase transitions were achieved by playing with the speciation of the IL anion according to the medium pH. Changes between homogeneous and biphasic regimes occur in a wide range of pH values and compositions, which can be tailored to a target separation process. Due to their biocompatible nature, these systems were used in the selective separation of DNA from HSA (the major protein present in human serum samples). In the following work, novel reversible IL-based ABS without changes on the phases' compositions were designed, *i.e.* thermoreversible systems. **Chapter 4.2** addresses the ability of water-soluble ammonium-based zwitterions (ZIs) – in which both the cation and anion are covalently tethered to each other - to form ABS with salts, followed by the study on their temperature-induced switchable behaviour. These thermoreversible systems were applied in

the separation of a wide range of compounds, such as in the separation of aromatic (L-tryptophan) and aliphatic (glycine) amino acids.

In the two previously described chapters, switchable systems were proposed. According to the new gathered insights, integrated production-separation IL-based ABS processes were then developed - **Chapter 5. Chapter 5.1** comprises the study of pH-driven reversible IL-based ABS, formed by imidazolium- and phosphonium-based ILs, and salts. In this work it is shown that reversible IL-based ABS can be prepared by playing with the speciation behaviour of the organic salt (potassium citrate) used in the ABS formulation. These systems were studied as integrated production-purification platforms, in which HMF was produced from fructose at acidic pH, and then separated from the unreacted precursor by an increase in the pH and consequent formation of two-phase systems. **Chapter 5.2** is focused on the use of ZIs to form ABS aiming at finding more biocompatible thermoreversible ABS that can be used to extract and purify biocompounds. The temperature-dependency of the solubility curves of ABS composed of poly(ethylene)glycol (PEG) of different molecular weights and various ZIs were evaluated. The investigated systems display a thermoreversible behaviour and were investigated as integrated reaction/separation processes. An enzymatic reaction involving laccase was carried out at the monophasic region, after which small changes in temperature induces the formation of two phases and the complete separation of the enzyme from the products in a single-step.

1.2. Bioactive compounds, solvents and separation processes

The use of bioactive compounds in different commercial sectors, such as in the pharmaceutical, nutraceutical and cosmetic industries, has faced a significant increase in the last years. In particular, the discrimination between natural and synthetic products has received enormous attention, and an increased demand on the consumption of natural compounds over their synthetic counterparts has been observed.¹¹ Natural bioactive compounds have several beneficial biological activities, such as anticancer, antimicrobial, antioxidant, antidiarrheal, and analgesic effects (among others).¹² Based on their beneficial biological activities and applications, the development of cost-effective and sustainable extraction processes of value-added compounds from natural sources has gained remarkable relevance in recent years.

Different extraction techniques have been used to extract bioactive compounds from biomass, such as soxhlet extraction, and high-pressure, mechanical-, ultrasound-, and microwave-assisted (among others).⁷ These extractions from solid biomass samples (solid-liquid extractions, SLE) consists in the extraction and dissolution of a given compound from a solid matrix in a given solvent. Unless completely selective solvents are identified, extractions from

biomass usually result in a complex extract. Therefore, after the extraction step, induced precipitation, distillation and chromatography, among others, are used as separation/purification techniques. Most of these techniques generally involve the use of volatile and often toxic organic solvents, additionally leading to environmental and human concerns.¹³ Furthermore, the costs associated to the final product are strongly dependent on the downstream processing, namely the type of techniques used and number of steps required.¹³ Thus, it is of crucial relevance to explore alternative solvents with more environmentally-friendly characteristics than those currently used, and to develop cost-effective and sustainable extraction and purification techniques, which could be ideally incorporated in a integrated process.

Novel approaches have been proposed, seeking both sustainable extraction and purification techniques and safer/"greener" solvents (*e.g.* solvents produced from renewable resources, water, supercritical fluids, deep eutectic solvents and ILs).¹⁴ Among these, ILs are one of the most studied alternative solvents for extraction and separation purposes.^{2, 15, 16} For instance, ILs or their mixtures with water/organic solvents have been applied directly in the SLE of value-added compounds from biomass, such as alkaloids, terpenoids, phenolic compounds, among others, and in liquid-liquid extractions (LLE) aiming the separation of target products. In these studies, aqueous solutions of ILs are the preferred choice, although the use of pure ILs or ILs with organic solvents mixtures were also addressed. ILs aqueous solutions have been described as more efficient and selective solvents. The high extraction efficiency afforded by ILs aqueous solutions has been described as a result of the ability of some ILs for disrupting the biomass organized structure.⁷ However, it has been also shown that ILs aqueous solutions may act as enhanced solvents due to hydrotrope-⁷ or micelle-mediated phenomena,⁷ thus increasing the solubility of target products and extraction yield. In general, aqueous solutions of ILs display a higher solubilisation and extraction performance when compared to the respective pure solvents,² as well as decreased viscosity.

LLE is usually performed using organic solvents immiscible with water.¹⁷ Compared to chromatography, liquid-liquid systems offer technological simplicity and low cost, as well as the capability to provide high yields, improved purification factors, enhanced selectivity and the possibility of combining the recovery and purification steps. Aiming at avoiding the use of organic solvents in LLE, in 1958, Albertson introduced the ABS concept for the separation of (bio)molecules by their partitioning between two liquid aqueous phases.¹⁸ Both phases are mainly composed of water, thus affording an amenable media for (bio)molecules.⁴ In addition to these largely studied polymer-polymer and polymer-salt ABS, in recent years, Gutowski *et al.*¹⁹ demonstrated that ABS can also be formed by the addition of inorganic salts to aqueous

solutions of hydrophilic ILs. IL-based ABS have shown remarkable advantages when compared to more traditional polymer-based ones, namely by providing low viscous solvent media and by allowing the tailoring of extraction efficiencies and selectivity.⁴

1.3. Ionic liquids (ILs)

ILs are ionic compounds that belong to the molten salts group, and generally defined as presenting a melting temperature below 100 °C; often, they are denominated by room temperature ILs when they are liquid at temperatures close to room temperature.²⁰ They are typically composed of a large and unsymmetrical cation and an organic or inorganic anion.²⁰ The low melting temperatures of ILs are a result of the weak intermolecular interactions derived from the large size ions and their charge distribution, and lack of an ordered crystalline structure.²⁰

The ionic nature of ILs is responsible for some of their unique properties, such as their negligible vapour pressure under atmospheric conditions, low flammability, high thermal and chemical stabilities, large liquid temperature range, high ionic conductivity and excellent microwave-absorbing ability.^{21, 22} ILs are also recurrently recognized by their high solvating aptitude for organic and inorganic compounds, from synthetically produced to natural extracted ones, and as good stabilizing media for proteins, nucleic acids, among others.^{2, 4} Amongst the large range of ILs that can be synthesized, the most commonly studied are nitrogen-based, with some examples of their cation chemical structures given in **Figure 1.2A**. The cation can be of a different nature, and additionally designed by changing the size of the alkyl side chains and addition of functional groups.²² Furthermore, the anion can be of a very different chemical nature, such as halogens, sulphates, cyano-based, fluorinated, etc. (**Figure 1.2A**). Based on the vast number of cation/anion combinations it is possible to tune their physicochemical properties aiming at designing a specific IL for a target application, and so, ILs are commonly described as “designer solvents” (**Figure 1.2B**).²³⁻²⁵ This feature overcomes the limited selectivity of common volatile organic solvents, allowing the design of more effective solvents for extraction purposes and more efficient separation platforms.

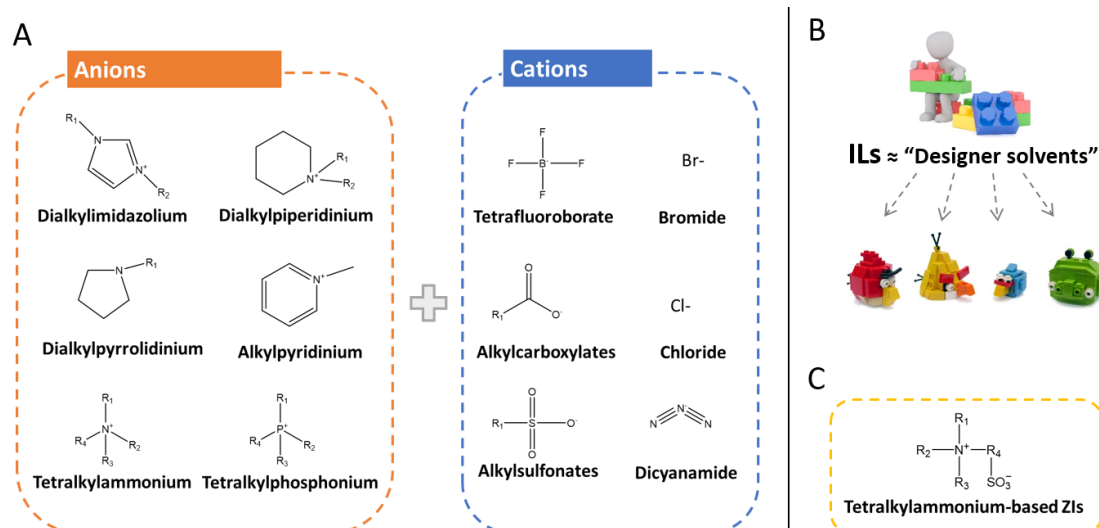


Figure 1.2. (A) Chemical structures of some IL cations and anions usually employed in the extraction and separation of value-added compounds. (B) Allusive scheme to the ILs "designer solvents" characteristic. (C) Chemical structures of tetraalkylammonium-based ZIs.

In addition to the existence of over six hundred of common solvents used by industry, most aprotic ILs are an ambient-friendly alternative due to their combination of non-volatility and non-flammability,^{21, 23} eliminating solvent losses to the atmosphere, and consequently decreasing both the environmental footprint and the cost of the process.⁷ This is the main reason behind the categorization of ILs as "green solvents". However, the fact of displaying a negligible vapour pressure is not enough to assure that these compounds are in fact "green", although losses to atmosphere are completely avoided when compared to traditional volatile organic solvents. Properties such as toxicity and biodegradability must be also accessed. For instance, even the most hydrophobic ILs have a non-negligible miscibility with water, which can result in the contamination of aqueous streams.^{26, 27} In recent years, several studies were conducted to evaluate the toxicity and biodegradability of ILs,^{26, 28} either by the combination of different anions and cations or by changing the alkyl side chain length and number of alkyl groups at the cation ring. These studies showed that the ILs toxicity is primordially determined by the cation nature and increases with the increase of the length of the alkyl side chain (increase in hydrophobicity).²⁷ Commonly, the anion has a smaller influence on toxicity than the cation, and generally, short cation alkyl chains or more hydrophilic ILs display lower toxicity.²⁸ The solubility of ILs in water decreases with their hydrophobicity, *i.e.*, the most toxic ILs are those that usually exhibit lower mutual solubilities with water, and hence, their environmental impact in aquatic streams can be "minimized".²⁶

Although aprotic ILs cannot enter into the environment by evaporation, they can enter into the biosphere by water streams. Therefore, the synthesis of "greener" ILs and studies on their

applications are nowadays one of the major topics of research within the ILs community. Starting materials must be non-toxic and ideally should be renewable. Low cost synthetic routes and easy preparation should also be filled. In this direction, some novel ILs have been reported, such as those composed of cholinium-²⁹ and glycine-betaine-based cations, combined with anions derived from amino acids,³⁰ carboxylic acids,³¹ etc.

Recently, a new class of zwitterionic-type molten salts (ZIs) was described, displaying similar chemical structures to ILs, but in which the cation and anion are covalently tethered to each other (**Figure 1.2C**).³² Since the ion pairs remain covalently linked it is avoided the formation of ion pairs or ion-exchange mechanism, particularly relevant when dealing with separation processes. With the proposal of ZIs, new avenues were opened in electrochemistry,³³ as suitable additives for systematically controlling the water content of hydrophobic ILs, and in separation processes.³²

1.3.1. ILs as alternative solvents for the extraction of value-added compounds from biomass

Biomass, is a unique, ubiquitous, and sustainable renewable resource for the production of biomaterials and biochemicals with wide commercial application. In SLE approaches, the biomass is placed in direct contact with the IL-based solvent, and operational conditions such as temperature, extraction time, and solid-liquid ratio are optimized (**Figure 1.3**). The two phases are then separated by filtration, decantation or centrifugation. The appropriate solvent is chosen based on a set of characteristics, such as polarity, selectivity, density, surface tension, viscosity, chemical and thermal stability, corrosion behaviour, cost, toxicity, and required operating temperature. After the SLE step, a new step is required to purify and/or recover the target compound, which may be attained by distillation, a new LLE step, by chromatographic approaches, among others.

SLE techniques using ILs as solvents have also been applied with microwave-assisted extraction (MAE),^{34, 35} ultrasound assisted extraction (UAE)^{36, 37} and enzyme-assisted^{38, 39} processes to enhance the extraction efficiency, while attempting to decrease the extraction time and amount of solvent used. More specially, UAE increases the mass transfer, being the best option when dealing with thermally sensitive value-added compounds, while MAE allows a fast heat transfer into the solvent solution, being the best option when considerable viscous solutions are used (*e.g.* pure or highly concentrated ILs solutions).

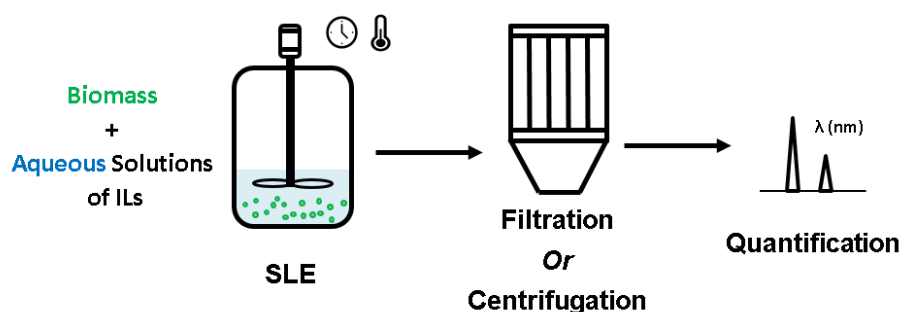


Figure 1.3. Scheme of SLE applied to solid biomass samples.

Various works have been published addressing the use of ILs, mixture of ILs and mixtures of ILs with organic solvents for the extraction of essential oils, such as limonene from orange peels⁴⁰ and coumarin from *Cinnamomum cassia bark*,⁴¹ extraction of shikimic acid from *Illicium verum*⁴² and *Ginkgo biloba* leaves,⁴³ extraction of lipids from *Chlorella microalgae*,^{44, 45} extraction of polysaccharides and lipids from brown algae⁴⁶, among others.^{2, 7} Although there is a large number of possible cation-anion combinations in ILs, most studies published up to date are still focused on imidazolium-based ILs. The pioneering work applying ILs to extract valued-added compounds from biomass was demonstrated in 2006, by Bioniqs Ltd.⁴⁷ The authors demonstrated the successful application of protic and distillable ILs to extract artemisinin, a sesquiterpene lactone, from *Artemisia annua*. A protic and biodegradable IL, $[\text{N}_{110(2\text{OH})}][\text{C}_7\text{CO}_2]$ (definition of the ILs is provided in the **List of acronyms**), was found to be the best IL investigated and, under the optimum conditions, high extraction yields were obtained when compared to those obtained by hexane at high temperatures.⁴⁷ After this proof of principle, the number of investigations regarding the use of ILs for the extraction of value-added compounds materials from biomass significantly increased. Regarding the use of IL-based solvents, four types have been reported: (i) pure ILs, (ii) ILs mixture, (iii) ILs/organic solvents mixtures and (iv) aqueous solutions of ILs.

After the pioneering work shown by Bioniqs Ltd,⁴⁷ Chowdhury *et al.*⁴⁸ suggested the application of SLE for the extraction of ellagic and gallic acids, pyrocatechol and (+)-catechin from *Acacia catechu* (catechu) and *Terminalia chebula* (myrobolan), also using a protic and distillable IL ($[\text{N}_{1100}][\text{N}(\text{C}_1)_2\text{CO}_2]$), at room temperature. High extraction efficiencies for both catechu (85%) and myrobolan (75%) biomass were obtained, while with water as the main solvent the extraction efficiencies are 64 and 52%, respectively.⁴⁸ In 2011, Bica *et al.*⁴⁰ showed that pure ILs ($[\text{C}_4\text{C}_1\text{im}]\text{Cl}$, $[\text{aC}_1\text{im}]\text{Cl}$ and $[\text{C}_2\text{C}_1\text{im}][\text{C}_1\text{CO}_2]$) can dissolve orange peels and extract limonene, commonly used in cosmetics, as a flavouring chemical, and as a biodegradable insecticide. The complete dissolution of orange peels was observed after 3 h with $[\text{C}_2\text{C}_1\text{im}][\text{C}_1\text{CO}_2]$, with a yield of the isolated orange oil of 4.9%.⁴⁰ The liquid solutions were then

subjected to vacuum distillation at 60–65 °C and a distilled fraction composed of two layers, limonene and water, was finally obtained allowing the isolation of limonene.⁴⁰ Recently, Mehta *et al.*⁴¹ also developed an efficient processing scheme for the extraction of essential oil, *i.e.*, coumarin from *Cinnamomum cassia bark* but in these case using a protic IL - [N₀₀₀₂][NO₃] combined with aprotic [C₄C₁im]-based ILs for biomass dissolution, and further creation of a biphasic system with diethyl ether. With the mixture of [N₀₀₀₂][NO₃] and [C₄C₁im][C₁CO₂], an yield of 4.7% of essential oil was obtained, although some degradation of the IL was observed.⁴¹ With the mixture of [C₄C₁im]Cl and [N₀₀₀₂][NO₃] a similar yield (4.6%) was obtained, but without any degradation observed.⁴¹ The authors demonstrated that the addition of these ILs allow to tailor the viscosity, solvation ability, and extraction efficiency of ILs, described as a synergic effect of IL ions (protic + aprotic).⁴¹ After the extraction of the essential oil, the cellulosic material and free lignin were regenerated from the biomass-IL solution through the addition of a mixture of acetone and water.⁴¹ In general, all of these results clearly support the high ability of pure ILs to enhance the target products extraction yields, either by destroying the biomass lignocellulosic part and/or by improving the solvent solvation capacity.

Ressmann *et al.*⁴² explored an alternative and effective method for the extraction of shikimic acid via dissolution of *Illicium verum* in presence of Brønsted acidic IL solutions. The authors investigated the conversion of shikimic acid into ethyl ester in ethanol solutions of [(HSO₃)C₄C₁im][HSO₄], [(HSO₃)C₄C₁im][NTf₂], [(HSO₃)C₄C₁im]Br and [(HSO₃)C₄C₁im]Cl.⁴² The authors obtained high conversions into ethyl ester (81 to 99%), although the complete conversion was only attained with [(HSO₃)C₄C₁im][NTf₂].⁴² The sulfonic acid side chain was demonstrated to be the main factor behind the efficient catalytic activity.⁴² The reactive dissolution of star anise seeds was then studied in [(HSO₃)C₄C₁im][HSO₄]-ethanol solutions, where the increase of the IL concentration leads to an increase in the extraction yield. Moreover, the application of microwave irradiation drastically reduced the reaction time (from 24 h to 30 min).⁴² Based on these results, Ressmann *et al.*⁴² developed an in situ process for the conversion of shikimic acid that uses a mixture of ethanol with 3-pentanone catalysed by [(HSO₃)C₄C₁im][HSO₄] or [(HSO₃)C₄C₁im][NTf₂].⁴² ILs act both as solvents and as catalysts toward the in situ synthesis of shikimic acid ethyl ester and its ketal ester.⁴² Although the process reported does not allow the recovery of the IL, it eliminates the use of the toxic and corrosive thionyl chloride commonly employed, while reducing the number of operational steps with improved yield. In the same context, Usuki *et al.*⁴³ suggested the extraction and isolation of the same biomolecule from *Ginkgo biloba* leaves using pure [C₄C₁im]Cl. At optimum conditions, the extraction yield of shikimic acid was 2.5 times higher than that obtained with methanol at 80 °C,

and 2 times higher than with dimethylformamide at 150 °C. However, no attempts at shikimic acid conversion were carried out by the authors.⁴³

Young *et al.*⁴⁴ reported an enhanced performance of [C₂C₁im][C₁SO₄]-methanol solutions for the dissolution of biomass and extraction of lipids from *Chlorella microalgae*. Later, Kim *et al.*⁴⁵ investigated in more detail the IL cation and anion effects on the lipids extraction efficiency. It was possible to conclude that the lipids extraction is mainly driven by the IL anion nature and that hydrophilic ILs are the most favourable. [C₄C₁im][CF₃SO₃], [C₄C₁im][C₁SO₄] and [C₂C₁im][C₁SO₄] lead to the best extraction results (125, 118 and 119 mg g⁻¹ of dried weight, respectively) compared with the commonly applied method of Bligh and Dyer (106 mg g⁻¹ of dried weight).⁴⁵ On the other hand, Malihan *et al.*⁴⁶ placed emphasis on sugars extraction, such as the polysaccharide laminara, although they also reported the extraction of lipids from brown algae. In this work, several mineral acids were tested together with [C₄C₁im]Cl, and where the combination [C₄C₁im]Cl/HCl dictates the higher extraction performance observed for carbohydrates.⁴⁶ More recently, Ma *et al.*⁴⁹ optimized the extraction of bioactive compounds (rutin, quercetin, and scoparone) from *Herba artemisiae scopariae*, also using IL-methanol solutions. The [C₄C₁im]Br-methanol solutions, at a reflux temperature of 60 °C during 60 min, allowed to extracted a similar yield to that afforded by pure methanol.⁴⁹ It was demonstrated that the use of [C₄C₁im]Br at low concentrations in methanol was enough to tuning the polarity of the extraction solvent while keeping a low viscosity.

Although pure ILs, mixture of ILs or solutions of ILs and organic solvents appear as good alternatives to conventional volatile organic solvents, from a greener and low-cost perspective, aqueous solutions of ILs appear as a more promising option. With this perspective in mind, various works have been published addressing the use of ILs aqueous solutions for the SLE of value-added compounds from biomass. Most of these works report on the extraction of alkaloids, *e.g.* glaucine from *Glaucium flavum Cr.* (Papaveraceae),^{50, 51} caffeine from *Paullinia cupana* (guarana seeds, Sapindaceae),⁵² galantamine, narwedine, and unguiminorine from the aerial parts of *Leucojum aestivum L.* (Amaryllidaceae),⁵³ and piperine from *Piper nigrum* (Black Pepper).⁵⁴ Others works include the extraction of more hydrophobic bioactive compounds (tocopherol, perillyl alcohol, rutin, and ginkgolides) from soybean;⁵⁵ phycobiliproteins, chlorophylls and carotenoids from the red macroalgae *Gracilaria sp.*,⁵⁶ cynaropicrin from *C. cardunculus L.* leaves,⁵⁷ triterpenic acids (ursolic, oleanolic, betulinic acids) from apple peels,⁵⁸ saponins from leaves and aerial parts of *Ilex paraguariensis* (mate) and *Camellia sinensis* (tea),⁵⁹ and polyphenols and saponins from *Ziziphus joazeiro* and *Agave sisalana*.⁶⁰ The chemical structures of some of these compounds are depicted in **Figure 1.4**.

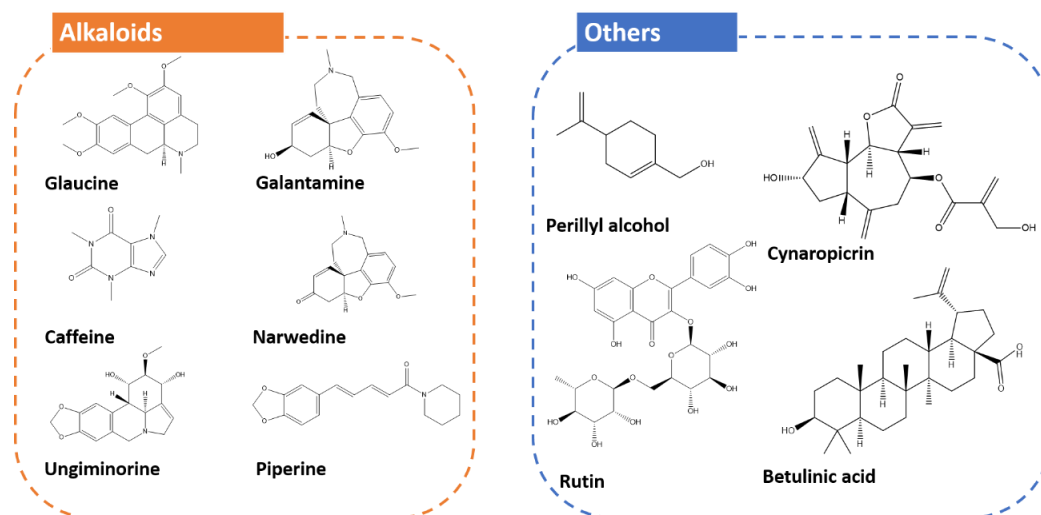


Figure 1.4. Chemical structures of some compounds extracted from biomass using IL aqueous solutions.

Bogdanov *et al.*⁵⁰ reported the successful substitution of methanol by a $[C_4C_1im][C_1CO_2]$ aqueous solution for the extraction of glaucine from *Glaucium flavum*. In fact, aqueous solutions of IL show the best results, namely 85% of extraction yield of glaucine, overcoming the yield obtained with methanol (< 60%) under similar conditions (80 °C, 1 h).⁵⁰ Overall, the authors demonstrated the role played by the organic imidazolium cation on the extraction process. Moreover, it was observed a significant reduction in the extraction time (from 12 h to 1 h) with the increase of extraction temperature (from 25 °C to 80 °C).⁵⁰ This trend is related with the increase of the diffusion coefficient and decrease of the IL solution viscosity at higher temperatures. Later, Bogdanov *et al.*⁵¹ reported a more detailed work on the kinetics, modelling and mechanism of glaucine extraction from *Glaucium flavum*. The authors performed consecutive extractions of biomass fresh samples using the same solvent up to saturation, avoiding the need of the IL recycling, while also contributing to a reduction of the process cost.⁵¹ Finally, the authors showed the recovery of glaucine from the IL by a back-extraction step with chloroform, that unfortunately decreases the “green” character of the proposed process.⁵¹ Cláudio *et al.*⁵² and Svinyarov and co-workers⁵³ investigated the extraction of caffeine from guarana seeds and the extraction of galantamine, narwedine, and ungimnorine from the aerial parts of *L. aestivum*, using aqueous solutions of a series of imidazolium-, pyrrolidinium-, and ammonium-based ILs. At the optimal conditions, aqueous solutions of $[C_4C_1im]Cl$ were found to be the best solvent in both studies. Cláudio *et al.*⁵² obtained outstanding extraction yields of caffeine, up to 9 wt%, in comparison to the traditional method employing hazardous organic solvents where the maximum yield of caffeine achieved was of 4.30 wt% (by soxhlet extraction using methylene chloride).⁵² Finally, the authors studied the recuperation of caffeine from the IL medium by a back-extraction step, where butanol was identified as the best solvent.

Bica and co-workers⁵⁴ reported the extraction of piperine from black pepper by SLE using aqueous solutions of surface-active ILs ($[C_nC_{1m}]^+$, with $n = 10, 12,$ and 14 , combined with different anions, as well as with a long chain biodegradable and betain-derived IL, $[N_{111}(C_{20}(O)_{12})]Cl$. Only for IL concentrations above the critical micellar concentration (CMC), the authors were able to obtain high extraction yields of piperine (4.0 wt%).⁵⁴ In this work, the ability of the IL to self-aggregate in aqueous media seems to be the main favourable factor for the enhanced extraction yields observed.⁵⁴ Although piperine is an alkaloid and an aromatic compound, it is of a hydrophobic nature, as shown by its higher octanol–water partition coefficient [$\log(K_{ow})$ of piperine = 2.30 vs $\log(K_{ow})$ of caffeine = -0.13], thus requiring the creation of hydrophobic cores produced by surface-active ILs to increase its dispersion/solubility in aqueous media.⁵⁴ The biodegradable IL revealed a high-performance on the extraction of piperine and can be used as a prospective alternative to volatile solvents commonly used (chloroform, toluene and methanol). Jin *et al.*⁵⁵ proposed a family of new water/IL mixtures, using amphiphilic anionic functional long-chain carboxylate ILs (LCC-ILs), for the simultaneous dissolution of biomass (soybean) and extraction of hydrophobic bioactive compounds (tocopherol, perillyl alcohol, rutin, and ginkgolides). The water/LCC-IL mixtures investigated allow extraction yields 2 to 12 times higher than that achieved with common organic solvents.⁵⁵ The authors also demonstrated the formation of nanomicelles when tocopherol is dissolved in water/LCC-IL mixtures,⁵⁵ meaning that the formation of IL aggregates achieved by the use of surface-active ILs allows the incorporation of hydrophobic bioactive compounds into the micelle core, thereby enhancing the extraction yield, a similar result to that found by Bica and co-workers.⁵⁴ In the same line, Ventura and co-workers⁵⁶ carried out the extraction of phycobiliproteins, chlorophylls and carotenoids from the red macroalgae *Gracilaria sp.* The results obtained demonstrate that hydrophilic ILs better extract phycobiliproteins, while those of lower hydrophilicity are better extraction solvents for chlorophylls and carotenoids.⁵⁶ Faria *et al.*⁵⁷ also showed that aqueous solutions of surface-active ILs are more efficient to the cynaropicrin extraction from *C. cardunculus L.* leaves, as well as for the extraction of triterpenic acids from apple peels,⁵⁸ a residue of food industries. The authors combined solubility and extraction studies to better understand the molecular-level mechanisms and ILs chemical structures which improve the extraction efficiency. At the best conditions, using an extraction time of 60 min and a concentration of $[C_{14}C_{1m}]Cl$ at 0.50 M, extraction yields of 3.73 wt% of cynaropicrin⁵⁷ and 2.62 wt% of triterpenic acids⁵⁸ were attained from *C. cardunculus L.* leaves and apple peels, respectively. The authors obtained significantly higher values compared to the values obtained with volatile organic solvents, such as chloroform or acetone in similar conditions.⁵⁷ Furthermore, these works also studied the recovery of the target compound from

the IL aqueous solution by the addition of water as an anti-solvent.^{57,58} In summary, all of these results support the idea that more hydrophilic bioactive compounds are better extracted with aqueous solutions of hydrophilic ILs, particularly displaying a hydrotropic character, while more hydrophobic compounds are better extracted by aqueous solutions of ILs with surface-active properties.

In general, imidazolium-based ILs, combined with chloride, bromide, acetate, dicyanamide, and tetrafluoroborate anions, have been the preferential choice to be used in aqueous solutions for extraction purposes from biomass. Thus, there is still a need on identifying more benign and sustainable ILs for such strategies. In this line, Ribeiro *et al.*⁵⁹ applied aqueous solutions of cholinium-based ILs as potential alternatives to imidazolium counterparts for the SLE of polyphenols and saponins from the leaves and aerial parts of *Ilex paraguariensis* (mate) and *Camellia sinensis* (tea). The authors concluded that [Ch]Cl was the best solvent option for the extraction of saponins (70%) and phenolic compounds, either from mate or tea.⁵⁹ In a following work, the same group of authors⁶⁰ studied thirteen ILs and nine deep eutectic solvents to extract saponins from two plant sources. Depending on the matrix type, distinct results of extraction and selectivity (over polyphenolics) were obtained.⁶⁰ From the results obtained, two deep eutectic solvents, [Ch]Cl:[Ch][C₁CO₂] and [Ch]Cl:[Ch][C₂CO₂] in water/ethanol mixtures were selected as the optimal solvents for the extraction of saponins from *Ziziphus joazeiro* and *Agave sisalana*, respectively.⁶⁰

In summary, ILs and their mixtures with alcohols or water are remarkable extraction solvents for value-added compounds from biomass. Neat ILs may act as solvents and as pre-treatment strategies of biomass, which usually presents a compact ordered and rigid structure, inducing pronounced changes in the morphological structure of biomass (usually visualized by scanning electron microscope, SEM) and a better access of the solvent to the target compounds. Yet, the use of aqueous solutions presents several advantages, such as the increase in the solubility of the target compounds by a hydrotropic or micelle-mediated solubilization phenomena, leading thus to remarkable extraction yields. Moreover, aqueous solutions allow the decrease of the high viscosity of most ILs, enhancing mass transfer and reducing energetic inputs. In these mixtures, the greenest and low cost solvent (water) is used, which in addition to sustainable features, also contributes to increase the solvent selectivity for target chemicals.

In all of these works, and unless a completely selective solvent is identified, the biomass extracts obtained are a combination of several bioactive compounds. However, only few works carried out the separation, purification and/or recovery of the extracted value-added compounds. In fact, in most of the published works, no information on the purity degree of the target compounds is usually given.² The other lacuna identified in such type of published works

comprises the lack of attempts for the IL recovery for further use (solvent recycling). Although scarce, some approaches, such as back-extraction using organic solvents,⁵² distillation of the volatile compounds (*e.g.* essential oils),⁶¹ induced precipitation with anti-solvents,⁶² and adsorption on macroporous materials⁶³ or anion-exchange resins,⁶⁴ have been described, also showing that it is possible to recover and reuse the IL-based solvents without losses on their extraction efficiency.² Since almost all ILs used in solid-liquid extractions from biomass are completely miscible with water, they can be also used to form ABS, as already demonstrated in some works.^{59, 65-68}

1.3.2. ILs as phase-forming components of aqueous biphasic systems (ABS) to be used in separation processes

After the extraction step mainly carried out by SLE techniques described before, after any reaction involving the production of bio-based products, or when dealing with complex natural matrices, separation techniques need to be employed aiming at recovering the target compounds, and for which IL-based LLE approaches have been studied. In addition to liquid-liquid systems formed by non-miscible ILs with the second liquid phase, a large interest has been given to IL-based ABS. These systems were proposed as potential alternatives to polymer-rich ones, with a set of important advantages: low viscosity, quick phase separation, and high and tailored extraction efficiency.⁴ In fact, a high extractive performance may be achieved by the manipulation of the IL chemical structure and mixture composition, by increasing the affinity of the specific compound to a given phase. IL-based ABS were originally proposed to be formed by ILs and inorganic salts in aqueous media.¹⁹ After this pioneering work, it was shown that these systems can be formed with a wide plethora of salts, and that the influence of the salt ions in the liquid-liquid demixing is well described by the Hofmeister series (ions classification based on their salting-out/-in ability).⁶⁹ Generally, it is accepted that the inorganic/organic salts of high charge density lead to the salting-out of the IL, creating a second aqueous phase.⁶⁹ In addition, it was demonstrated that IL-based ABS can be formed by combining ILs with carbohydrates, polymers or amino acids in aqueous media.⁴

For the design of effective ABS as separation and purification processes, their phase diagrams and respective tie-lines are required. This information is crucial to define mixture compositions able to form two-phase systems and know the coexisting phase's compositions. All ABS have a unique phase diagram under a set of conditions, such as temperature, pressure and pH. Usually, the ABS phase diagrams are determined through the cloud point titration method (**Figure 1.5A**).⁴ **Figure 1.5B** depicts an example of a phase diagram of an ABS composed of a IL, a salt and water, and the respective binodal curve.⁴ This phase diagram is shown in an orthogonal representation,

in which the amount of water is omitted, corresponding to the amount required to reach 100 wt% for a given mixture composition. The binodal curve, TCB, represents the separation between the miscible and immiscible regions, *i.e.*, above the binodal curve it is located the biphasic region, while below it is the monophasic region. The larger the biphasic region, the higher the ability of the phase-forming components to form liquid-liquid systems. Three mixture compositions at the biphasic region are also identified as X, Y and Z in **Figure 1.5B**. These mixtures are along the same tie-line (TL), meaning that all these mixtures present the same top (T_{IL} , T_{Salt}) and bottom phase compositions (B_{IL} , B_{Salt}).⁴ What changes in these mixtures is the phases' volume or weight. The tie-line length (TLL) is a numerical indicator of the composition difference between the two phases and is often used to correlate with the trends observed in solutes partitioning between the phases.⁴ The critical point of the ternary system is Point C, where the two binodal nodes meet, *i.e.*, the compositions of the two coexisting phases become equal, and the biphasic system ceases to exist.⁴

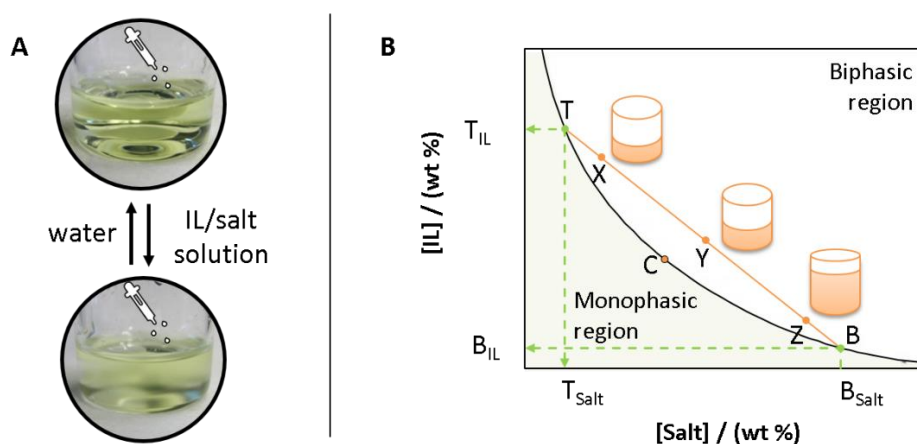


Figure 1.5. (A) Scheme of phase diagrams determination. (B) Schematic representation of an ABS phase diagram in an orthogonal representation. TCB - Binodal curve, C - Critical point, TB - Tie-line, T - composition of the top phase, B - composition of the bottom phase, and X, Y and Z – initial mixture compositions of biphasic mixtures.

IL-based ABS have been largely investigated for the separation of the most distinct added-value compounds and/or biomolecules.⁴ IL-based ABS usually lead to a high extraction performance when compared to the traditional polymer-salt and salt-salt systems, which display a restricted polarity difference between the coexisting phases. It should be however noted that there are several approaches to manipulate the partitioning of a specific solute between the coexisting phases: (i) use of different phase-forming components; (ii) change of the ternary mixture composition, temperature or pH; and (iii) addition of co-solvents, anti-solvents or amphiphilic compounds.⁴ In a large part of the studies comprising ABS with ILs, it has been

demonstrated that a proper choice of the IL and salting-out agent could lead to the complete extraction of the target solute, high selectivity and concentration factors up to 1000 times.⁷⁰ Although IL-based ABS were mostly studied at a laboratory scale, the scale-up of traditional ABS formed by polymers has already been demonstrated and is currently used in the purification of proteins at industrial level.⁷¹ In this sub-chapter some relevant studies concerning the application of IL-based ABS for the separation and fractionation of value-added compounds are reviewed and discussed. These value-added compounds comprise alkaloids, phenolic acids, terpenoids, amino acids, proteins and enzymes.

In recent years, there has been a great interest in the investigation of IL-based ABS as separation platforms of products extracted from vegetable sources.¹⁶ It should be however remarked that most of these studies only evaluated the extraction performance of IL-based ABS for target compounds, using pure and commercial compounds instead of natural extracts and/or more complex matrices. These compounds include alkaloids (codeine, papaverine, caffeine, nicotine, xanthine, theophylline and theobromine), phenolic compounds (vanillin and phenolic acids, such as gallic, vanillic, syringic and caffeic acid, eugenol, propyl gallate and syringaldehyde), terpenoids (β -carotene), among others, with relevant antifungal, anti-inflammatory, and antioxidant properties. The chemical structures of some of these compounds are depicted in **Figure 1.6**.

The capacity of ABS composed of ILs and inorganic salts,⁷² carbohydrates⁷³ or amino acids⁷⁴ has been extensively studied for the extraction of caffeine. The highest extraction efficiencies are obtained with ABS formed by ILs and salts, given the salting-out effect exerted by the salt that promotes the migration of the alkaloid to the opposite phase (IL-rich phase).⁷² Passos *et al.*⁷⁵ studied the effect of the cation alkyl chain length on the extraction of a large number of alkaloids (nicotine, caffeine, theophylline and theobromine). The authors⁷⁵ studied ABS constituted by $[C_nC_{1m}]Cl$, with $n = 4-10$, with potassium citrate (at controlled pH), and observed a maximum in the partition as a function of the alkyl side chain size. The authors⁷⁵ also concluded that the pH of the medium, and hence the alkaloid speciation, does not change the results observed. This maximum was justified by the self-aggregation of ILs of larger alkyl chains, an inherent characteristic of these ILs and that was shown to occur in ABS, being confirmed by transmission electron microscopy. In addition to ABS composed of ILs and salts, Pereira *et al.*⁷⁶ studied IL-polymer-based ABS for the extraction of 3 alkaloids. In almost all ABS, a preferential migration of caffeine to the polymer-rich phase was observed, while nicotine and xanthine partitioned to the IL-rich phase (opposite).⁷⁶ Based on these results, these ABS appear as promising alternatives to fractionate complex mixtures enriched in alkaloids. Li *et al.*⁷⁷ used IL-based ABS as an extraction strategy for the analysis of opium alkaloids (codeine and papaverine)

in complex matrixes, *i.e.*, human fluids. After optimization of the operating conditions, the researchers obtained extraction efficiencies of 93% for papaverine and 65% for codeine using ABS constituted by $[C_4C_{1im}]Cl$ and K_2HPO_4 (definition of the salts is provided in the **List of acronyms**).

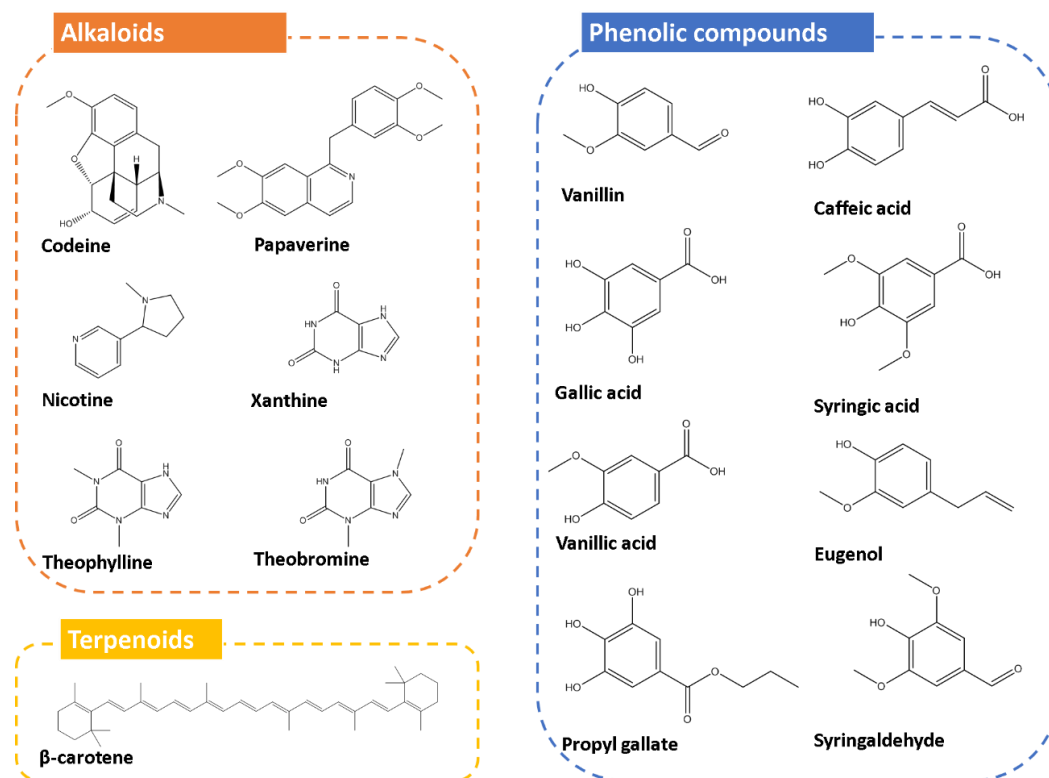


Figure 1.6. Chemical structures of some compounds that may be extracted from vegetable sources used in IL-based ABS.

ABS have also been studied in the separation of a wide range of phenolic compounds with antioxidant and anti-inflammatory activities, which have an important role in the prevention of cancer, hypertension and neurodegenerative and cardiovascular diseases. Aiming their purification from real matrixes, several works were reported regarding the application of IL-based ABS for the separation of vanillin,^{78, 79} phenolic acids, such as gallic,⁷⁹⁻⁸² vanillic,^{79, 81, 82} syringic,^{81, 82} eugenol,⁸³ propyl gallate,⁸³ caffeic acid⁷⁹ and syringaldehyde.⁷⁹

To avoid the use of organic solvents in the purification of extracts containing antioxidants, namely vanillin, Cláudio *et al.*⁷⁸ studied the application of ABS constituted by ILs and an inorganic salt (K_3PO_4). The authors evaluated the effect of the IL chemical structure, the equilibrium temperature and the initial concentration of vanillin in the partitioning of this antioxidant between the two phases. In all situations, vanillin migrates preferentially to the IL-rich phase. The partition coefficients of vanillin at 25 °C ranged from 2.7 to 49.6. A maximum was observed in the ABS composed of the $[C_nC_{1im}]Cl$ series of ILs, being these results in agreement with the

findings of Passos *et al.*⁷⁵ in the extraction of alkaloids. The authors finally evaluated the viscosity and density of the coexisting phases to appraise the process scale-up viability, verifying that the viscosity of these systems is substantially lower than that observed in ABS constituted by polymers.⁷⁸ In a latter work, Cláudio *et al.*⁸⁰ focused their studies in the potential of ABS formed by a wide variety of ILs and three salts (Na_2SO_4 , K_3PO_4 and $\text{K}_2\text{HPO}_4/\text{KH}_2\text{PO}_4$) for the extraction of gallic acid. In general, the extraction of gallic acid into the IL-rich phase decreases in the following order: Na_2SO_4 (pH 3-8) \gg $\text{K}_2\text{HPO}_4/\text{KH}_2\text{PO}_4$ (pH 7) $>$ K_3PO_4 (pH 13). Although K_3PO_4 is the strongest salting-out species, the authors have demonstrated that the pH of the aqueous medium plays a major role in the partitioning of antioxidants.⁸⁰ For pH values below the acidic dissociation constant (pK_a) of gallic acid ($\text{pK}_a=4.4$), the uncharged molecule preferentially partitions to the IL-rich phase, while its conjugate base partitions preferentially to the salt-rich phase. These results led the authors to propose a subsequent work on the back-extraction of antioxidants present in biomass, as well as on the recovery and reuse of the IL-rich phases without loss of extraction efficiency.⁸² Two types of IL-based ABS were studied for the extraction of phenolic acids (gallic, syringic and vanillic acids), namely IL + Na_2CO_3 and IL + Na_2SO_4 , in order to tailor the pH values of the coexisting phases. From the several $[\text{C}_4\text{C}_1\text{im}]$ -based ILs investigated, the most promising were $[\text{C}_4\text{C}_1\text{im}][\text{CF}_3\text{SO}_3]$ and $[\text{C}_4\text{C}_1\text{im}][\text{N}(\text{CN})_2]$, that were used in sequential two-step cycles (comprising both the product and IL recoveries).⁸² In four sequential partitioning experiments involving phenolic acids, extraction efficiencies ranging between 73 and 99% were attained, while allowing the regeneration of the IL.⁸²

More recently, Almeida *et al.*⁸¹ propose the use of ILs as additives (at 5 or 10 wt%) in ABS formed by PEG and salts in order to reduce the costs of the overall extraction/purification, foreseeing the extraction of gallic, vanillic and syringic acids. The results obtained show that all antioxidants preferentially migrate to the polymer-rich phase, which corresponds to the phase where ILs are enriched.⁸¹ The authors have demonstrated that the addition of small amounts of IL leads to an increase in extraction efficiencies of all phenolic acids, ranging from 80 to 99%, thus validating the ILs ability to adjust the polarity/affinity of the phases.⁸¹ In the same line of investigation, Santos *et al.*⁸³ studied the possibility of optimizing the extraction efficiency of other antioxidants, namely eugenol and propyl gallate, using ILs as additives, and results of complete extraction were achieved in a single-step. In general, higher extraction efficiencies were attained using the IL + salt ABS (from 75.9 to 100%) than with PEG + salt + IL ABS (between 47.1 to 100%).⁸³ The poorer efficiency of polymer-based ABS was suggested to be a result of less tuned and non-specific interactions, contrarily to what is observed in systems where the ILs are present. π - π stacking interactions (between ILs aromatic cations and antioxidants aromatic rings) and other antioxidant-IL interactions may be decisive for the success of the separation

process.⁸³ These results were further interpreted in more detail by Sousa *et al.*⁸⁴, who studied a larger range of ABS, ILs and natural compounds. In general, the addition of ILs as adjuvants to polymer-based ABS changes the coexisting phases' characteristics, and thereby modifies the partition of biomolecules. An increase in the extraction of more hydrophobic biomolecules is observed when using ILs as adjuvants in PEG-salt systems, whereas IL + salt ABS perform better in the extraction of more hydrophilic biomolecules.⁸⁴ In summary, the favourable partition of more hydrophilic biomolecules in IL + salt ABS seems to be ruled by specific solute-IL interactions, while the favourable partition of more hydrophobic biomolecules in PEG + salt and PEG + salt + IL seems to be governed by the phases hydrophobicity/polarity. Recently, Passos *et al.*⁸⁵ demonstrated the existence of specific IL-solute interactions in some IL-based ABS, which in part explain the large extraction efficiencies usually obtained with these systems involving ILs.

In a recent work, Santos *et al.*⁷⁹ proposed an ABS approach to fractionate five phenolic compounds resulting from lignin depolymerisation, namely caffeic acid, vanillic acid, gallic acid, vanillin and syringaldehyde. ABS formed by sodium polyacrylate 8000 (NaPA 8000) and PEG 8000 were used, in which cationic and anionic commercial surfactants and ionic liquids with surface-active nature ($[C_{12}C_{1im}]Cl$ and $[C_{14}C_{1im}]Cl$) were used as electrolytes at concentrations below 1 wt%.⁷⁹ The recovery, partition coefficients and selectivity of each system were evaluated, and recoveries ranging between 40.73% for syringaldehyde to 82.52% for caffeic acid were reported.⁷⁹ The investigated systems were finally used in the design of an integrated process comprising the fractionation of phenolic compounds, their isolation and recycling of the phase-forming components.⁷⁹

Terpenoids can be extracted from plants, algae and fungi.⁸⁶ Their interest is due to the fact that they present biological activities against cancer and processes of inflammation and malaria, justifying a great interest in their extraction from biomass and purification.⁸⁶ Despite their high potential, only two works evaluated the ability of ABS constituted by ILs in the extraction of β -carotene.^{72, 73} Louros *et al.*⁷² studied ABS constituted by ILs with a strong hydrophobic nature (phosphonium-based ILs) and showed a high ability for extracting hydrophobic solutes, namely β -carotene, with partition coefficients in the order of 61. Freire *et al.*⁷³ also achieved good partition coefficients, ranging between 5.5 and 24.0, using a more benign approach - ABS formed by ILs and carbohydrates. It was demonstrated that the main driving force for the partitioning of β -carotene is related with the inherent ability of carbohydrates to be hydrated (or not) and their consequent salting-out ability.⁷³ In summary, all the described works support the high extraction performance of IL-based ABS and that a large range of partition coefficients may be obtained for natural compounds extracted from vegetable sources by changing the IL chemical structure, the second phase-forming component nature, and mixture composition.

In addition to the value-added compounds described before, IL-based ABS have also been studied in the separation of amino acids and proteins. Amino acids are important compounds in several biotechnological processes, and the development of methods for their separation and purification is still the subject of intense investigation.⁸⁷ Some amino acids, such as L-tryptophan, L-phenylalanine and L-tyrosine, can be produced by bacterial fermentation. In this context, the application of IL-based ABS can be a promising alternative for integrated amino acid extraction within continuous fermentation processes.⁸⁸ L-tryptophan,^{73, 87, 89-95} L-tyrosine^{93, 95} and L-phenylalanine^{94, 95} and L-Lysine⁹⁵, whose chemical structures are described in **Figure 1.7**, are the most studied amino acids with IL-based ABS.

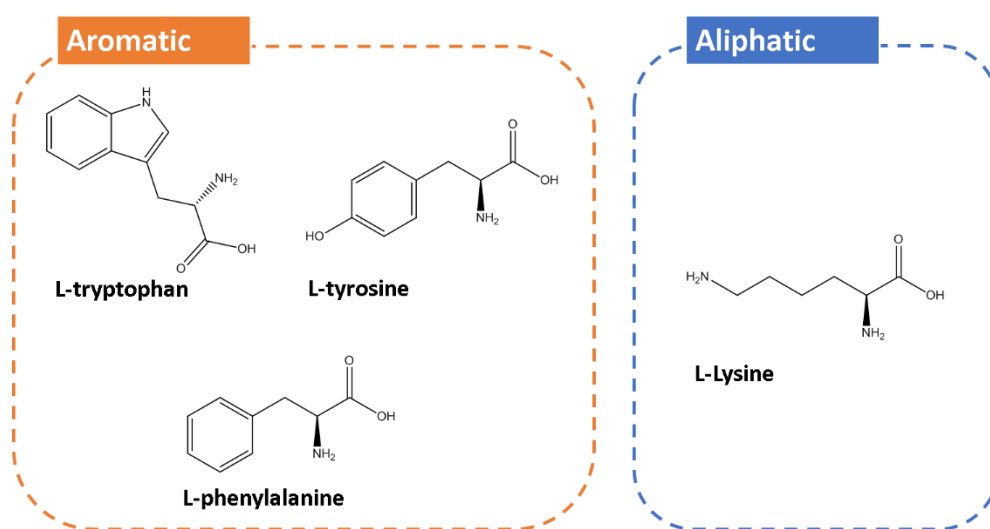


Figure 1.7. Chemical structure of some amino acids usually investigated with IL-based ABS.

Neves *et al.*⁸⁷ and Ventura *et al.*⁸⁹ studied the ability of ABS formed by a large number of ILs and K_3PO_4 to extract L-tryptophan. The authors have shown that depending on the nature of the IL, partition coefficients ranging from 10 to 120 to the IL-rich phase can be obtained,^{87, 89} and that these values are significantly higher than those obtained with conventional ABS formed by polymers (in the order of 0.1-3),⁹⁶ as well as with liquid-liquid systems formed by hydrophobic ILs and water (in the order of 1-7).⁹⁷ Moreover, it was demonstrated that the influence of the IL cation seems to be more important than the influence of the IL anion in terms of extraction performance for amino acids.⁸⁷ Pereira *et al.*⁹⁰ studied ILs as adjuvants in traditional aqueous systems formed by polymer-salt combinations for the extraction of L-tryptophan. The results obtained indicate that the addition of small quantities of IL to traditional systems regulates the partition coefficient and allows to control the extraction efficiency of the various systems by a suitable selection of the IL chemical structure. These systems⁹⁰ have been proposed as alternatives to the usual approach of polymers functionalization,⁹⁸ which is much more

expensive and time-consuming. Hamzehzadeh *et al.*⁹¹ carried out a study in the same line of research, with results in agreement with those obtained by Pereira *et al.*⁹⁰

Although ABS composed of inorganic salts and ILs have been intensively explored for liquid-liquid extraction purposes of a wide variety of biomolecules, more recently, the application of biodegradable and less toxic salts has been also studied to extract amino acids. ABS composed of ILs and potassium citrate, as an organic and biodegradable salt, were studied.^{92, 93} In all systems, amino acids preferentially partition to the IL-rich phase, with extraction efficiencies ranging between 72 and 99%, obtained in a single-step.^{92, 93} In the same line and with the intention of replacing the inorganic salts in the formation of ABS, Freire *et al.*⁷³ studied the ability of ABS consisting of ILs and carbohydrates to extract amino acids. The systems studied allow an extraction efficiency of *ca.* 50% of amino acids to the IL-rich phase in a single-step. A new class of ABS combining ILs with organic buffers for the extraction of amino acids (L-phenylalanine and L-tryptophan)⁹⁴ was recently proposed. Unlike ABS consisting of ILs and salts, in these systems, amino acids may migrate preferentially to the IL- or to the GB-rich phase, with extraction efficiencies ranging between 22.4 and 100.0% in a single-step.⁹⁴ Based on the results obtained, the authors proposed the use of these systems for the fractionation of complex mixtures of amino acids by optimizing the composition of the mixture and pH of the coexisting phases.⁹⁴ Recently, Capela *et al.*⁹⁵, based on the particular ability of aliphatic amino acids to form ABS with ILs, showed these systems can be used to selectively separate mixtures of aliphatic and aromatic amino acids usually present in protein hydrolysates or in fermentation broths. With the exception of the L-Proline + [P₄₄₄₄]Br ABS, the remaining studied phosphonium-based ABS showed the preferential migration of aromatic amino acids to the IL-rich phase while aliphatic amino acids are enriched in the opposite layer, allowing their effective separation.⁹⁵ Extraction efficiencies of the IL-rich phase for aromatic amino acids (L-phenylalanine, L-tryptophan and L-tyrosine) ranging between 40 and 85%, and extraction efficiencies of the opposite phase for aliphatic amino acid (L-lysine) ranging between 91% and 98%, were obtained in a single-step.⁹⁵ Phosphonium-based ABS were also demonstrated to act as remarkable separation techniques when compared with ABS formed by imidazolium-based ILs. The selectivity values for phosphonium-based ILs range between 1.5 and 121, corresponding to significantly higher values than those found with imidazolium-based systems (from 0.01 to 0.07).⁹⁵ Finally, the authors evaluated the possibility of recovering the aromatic amino acids from the IL-rich phase, reaching recovery values of 93% while removing 79% of the IL present.⁹⁵ As highlighted before, the range of extraction efficiency values obtained in the discussed works indicate that the manipulation of the amino acids partitioning between the coexisting phases is easily achieved by properly selecting the IL chemical structure.

IL-based ABS have been also investigated for the extraction of proteins, a field in which ABS play a significant role due to their water-rich media and the labile nature of proteins.^{73, 87, 89-95} The proteins and enzymes most studied with IL-based ABS are albumin, cytochrome c, lysozyme, myoglobin, trypsin, and lipases. Given that proteins are produced or are present in complex matrices, traditional methods for proteins and enzymes purification require several steps, such as salt precipitation, dialysis, ionic and affinity chromatography, or electrophoresis, being highly complex, time-consuming and expensive. Therefore, there is a strong interest in the exploration of IL-based ABS as alternative separation strategies.

Ruiz-Angel *et al.*⁹⁹ evaluated the efficiency of extraction of ABS constituted by ILs and polymers to 4 proteins (cytochrome c, myoglobin, ovalbumin, haemoglobin). The authors⁹⁹ concluded that the partition coefficients using IL-based systems are generally 2 to 3 orders of magnitude higher than those obtained with ABS of the polymer-polymer or polymer-salt type. Complete extractions of bovine serum albumin (BSA) have been obtained in a single-step using ABS composed of ILs and salts^{100, 101} or ILs and polymers,^{102, 103} by an adequate manipulation of the IL chemical structure and composition of the system. In most of these works a salt with buffer capacity was used. To avoid this requirement, self-buffering ILs have been proposed for the formation of ABS and extraction of proteins.^{100, 102} The stability of the proteins after the extraction process was evaluated by Fourier transform infrared spectroscopy and circular dichroism, where it was proved that proteins maintain their secondary structure in the IL-rich phase after the extraction step.^{100, 101}

IL-based ABS are also a good option for the extraction of enzymes, as well as a medium for biocatalysis itself. ABS with ILs have already been studied in the extraction of other proteins and enzymes from real matrices, like extracellular media, *e.g.* in the purification of lipase produced by *Bacillus* sp. ITP-001.¹⁰⁴ The authors achieved lipase purification factors ranging between 26 and 51, and recovery factors ranging between 91 and 96%,¹⁰⁴ which correspond to higher values than those achieved with polymer-based ABS.¹⁰⁵ Later, the same group of authors demonstrated that ABS containing ILs as adjuvants lead to higher purification factors as result of a preferential partition of the contaminating proteins to the upper phase (polymer-rich), while the target enzyme preferentially migrates to the lower phase (salt-rich).¹⁰⁶ After optimization of the extraction conditions, the authors proposed the purification of lipase by two pathways: (i) with a pre-purification step; and (ii) without any pre-purification step.¹⁰⁶ The highest obtained purification factors correspond to 103.5 and 245.0 for steps (ii) and (i), respectively.¹⁰⁶ Although it has been observed a decrease in the lipase purification in step (ii), this one does not require a pre-purification step.¹⁰⁶ This approach allows thus to significantly reduce the costs of the purification process, while satisfying the purification factors required by the industrial sectors.

With the same purpose, Dreyer and Kragl¹⁰⁷ demonstrated the application of ABS constituted by ammonium-based ILs for the purification of two dehydrogenases from cellular extracts of *Escherichia coli*, *Lactobacillus brevis* and *Thermophilic bacterium* (partition coefficients *ca.* 3). In addition to the separation step, the authors demonstrated an increase in the enzymes activity of up to 400% in the presence of IL.¹⁰⁷ All of the described works support the high potential of IL-based ABS in the purification of proteins and enzymes from real matrices, and on keeping their stability and/or increasing activity.

Passos *et al.*¹⁰⁸ developed a new and efficient approach for extraction of proteins applying thermoreversible IL-based ABS. Contrarily to most IL-based ABS constituted by aprotic ILs, which display a weak dependence on temperature, it was found that ABS formed by protic ILs and polymers are highly temperature dependent, allowing therefore to trigger reversible phase separations by small changes in temperature. With the investigated systems, extraction efficiencies higher than 95% were obtained for cytochrome c and azocasein. The reversible behavior of these systems was demonstrated for three times, with no losses on the proteins extraction performance. This work was one of the pioneering works showing the reversible nature of IL-based ABS, highlighting the possibility of using these systems as separation strategies.¹⁰⁸

1.3.3. Reversible systems composed of ILs

The ability to induce reversible phase transitions between homogeneous solutions and biphasic liquid-liquid systems, at pre-defined and suitable operating conditions, can be used in the design of integrated production-separation processes.¹⁰⁹ Given the advantages of ILs as solvents or as phase-forming components of liquid-liquid systems discussed in the previous sub-chapters, dynamic and reversible biphasic systems constituted by ILs have aroused great interest in the scientific community. It was already demonstrated that mixtures involving ILs and other solvents can be adjusted between the homogeneous regime and a two-phase system by changes in temperature^{110, 111} or pH,^{10, 110} also achieved by the addition of CO₂/N₂.¹⁰ This type of switchable systems thus allow to carry out reactions or extractions in the monophasic region, which after the application of an external stimulus may result in the creation of two-phase liquid-liquid systems feasible for separation and/or purification steps (**Figure 1.8**). This approach also contributes to a more feasible recovery of the target products and phase-forming components (**Figure 1.8**), allowing their recyclability.

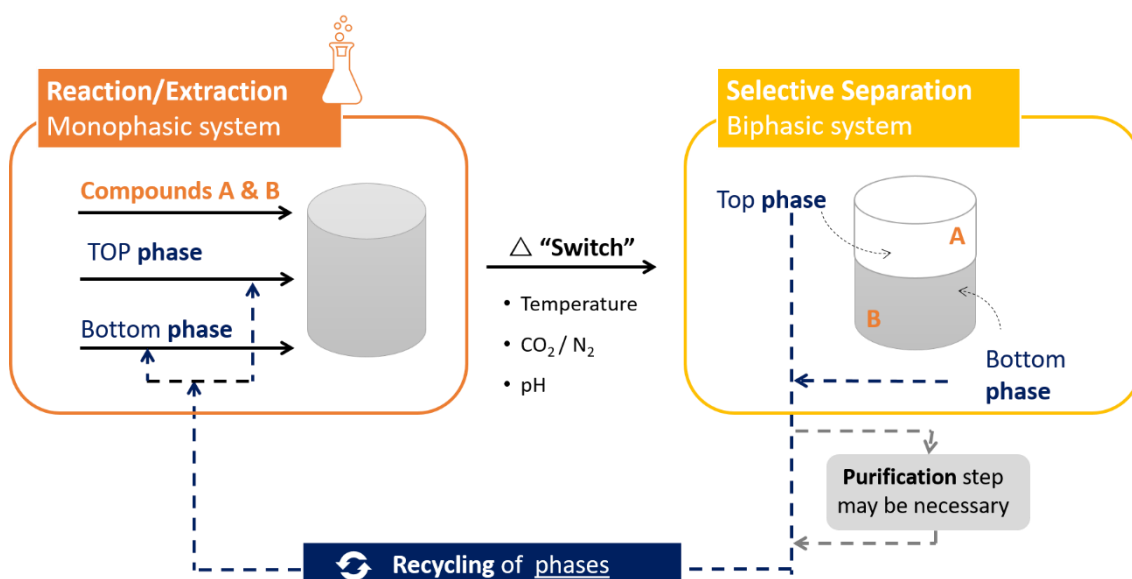


Figure 1.8. Illustration of reversible IL-based liquid-liquid systems.

Regarding the formation of liquid-liquid systems by changes in temperature, these may display an upper critical solution temperature (UCST, where the biphasic region decreases with an increase in temperature)^{110, 112-116} or a lower critical solution temperature (LCST, where the biphasic region increases with an increase in temperature)¹¹⁷⁻¹¹⁹ - **Figure 1.9A**. These systems with temperature-dependent phase transitions have been used in the separation of proteins,¹¹⁹ metals^{114, 116} and catalysts,¹¹³ although no complex mixtures or attempts on purification have been addressed. Furthermore, most UCST and LCST of systems comprising ILs often occur at temperatures far from room temperature, and when considering binary mixtures composed of water and hydrophobic ILs these are confined to mixture compositions imposed by the critical point of each phase diagram.^{110, 114-116} Therefore, the design of novel IL-based systems with an UCST or LCST close to room temperature has been object of a great deal of work; yet, only a restricted number of systems has been identified.^{118, 119} In addition to ILs, thermoreversible systems formed by hydrophobic ZIs and water have also been reported,¹²⁰⁻¹²² although no examples on their advantages as separation processes have been given.

Reversible liquid-liquid systems composed of hydrophobic ILs and water have been achieved through changes in pH.¹¹⁰ More specifically, the alkalinisation of the biphasic mixture moves the system to the monophasic regime because the IL respective alkali-salt becomes water soluble. The subsequent acidification of the solution leads to the regeneration of the hydrophobic IL and to phase separation¹¹⁰ (**Figure 1.9B**). Instead of adding acid or alkali salt aqueous solutions, some authors proposed CO₂ and N₂ flushing (**Figure 1.9C**). For example, Xiong *et al.*¹²³ showed that the addition of CO₂ to liquid-liquid systems formed by hydrophobic ILs and water leads to the creation of monophasic solutions, *i.e.* by turning the IL hydrophilic and consequently completely

miscible with water. Ohno and co-workers¹²⁴ also have proposed IL-based liquid-liquid systems, yet achieved in the opposite way. By adding CO₂ to a water-miscible IL there is the protonation of the IL carboxylate group resulting in two-phase separation, which is a reversible phenomenon by bubbling with N₂.¹²⁴ Jessop *et al.*¹²⁵ showed that IL-based liquid-liquid systems could be formed in the presence of an organic solvent (decane). The flushing of an alcohol and an amine base with CO₂ results in the formation of an IL immiscible with the non-polar solvent. The process can be reverted by exposing the system to N₂. These systems have been used for the separation of metals,¹¹⁰ and for the synthesis/separation of gold (Au) porous films¹²³ and polystyrene.¹²⁵ In general, most of the research in dynamic/reversible liquid-liquid extractions using ILs has been focused in the direct use of hydrophobic ILs^{110, 114-116, 118, 119, 123, 124} and non-miscible aqueous or organic solvents.^{112, 113, 117, 125 115}

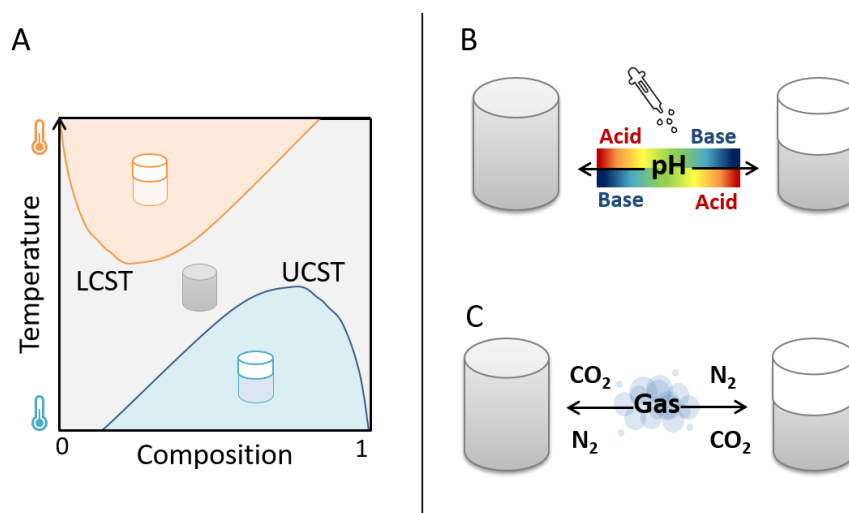


Figure 1.9. (A) Schematic illustration of typical phase diagrams with LCST- and UCST-type phase behaviour. (B) Schematic representation of phase transition with the addition of acidic or alkaline species in aqueous media. (C) Schematic representation of phase transition with the addition of CO₂/N₂.

Besides all the advantages mentioned in the previous sub-chapter regarding the high performance of IL-based ABS, their reversible behaviour to develop integrated processes has not been explored. Most works published up to date only reported phase diagrams at several temperatures and pH values. For instance, it was demonstrated that the phase diagrams of ABS composed of ILs and salts, amino acids or carbohydrates display an UCST behaviour, *i.e.* the phase separation ability decreases with an increase in the temperature. At higher temperatures, the interactions between the IL and water are more favourable, enhancing thus their mutual solubilities and reducing their ability to form ABS.¹²⁶ On the other hand, it was demonstrated that ABS formed by ILs and polymers follow the opposite trend, where an increase in the temperature results in an increase of the immiscibility domain.¹²⁶⁻¹²⁸ This behaviour was

explained based on the disruption of the hydrogen-bonding interactions between the polymer and water at higher temperatures.¹²⁶ Song *et al.*¹²⁸ and Li *et al.*¹²⁷ further demonstrated that it is possible to obtain a second ABS from the polymer-rich phase by an increase in the temperature, offering the possibility of the polymer recovery and further refinement in proteins partitioning. As previously mentioned, Passos *et al.*¹⁰⁸ demonstrated that ABS formed by protic ILs and polymers are thermoreversible since there is a more strong dependence of the phase diagrams with temperature. These systems were evaluated in terms of their reversibility behaviour and ability to separate two model/pure proteins. The pH effect in IL-based ABS has also been demonstrated, with alkaline salt solutions being more able to induce liquid-liquid demixing (**Figure 1.9B**).⁸ In general, at acidic pH values the ability of conventional salts to induce the phases separation is lower, since salts will be more protonated and will display a lower salting-out ability.⁸ However, Kurnia *et al.*¹²⁹ showed that the mechanisms associated to the pH dependency of ABS formation can be more complex. The authors reported that the IL-based ABS formation is dominated by the ability of the higher valency and completely dissociated salting-out ions to interact with water, and to form hydration complexes.¹²⁹ This ability is connected to the salts speciation in aqueous solution according to the medium pH. This work allowed to better understand why some salt ions work better at alkaline pH values, while others display a better performance at acidic conditions.¹²⁹ Switchable pH-driven ABS, in particular by the addition of CO₂/N₂, were already demonstrated in the literature, with applications in the separation of aliphatic and aromatic amines.^{130, 131}

Although some works exist in the literature demonstrating the switchable behaviour of IL-based ABS, their investigation as tailored, effective, and integrated processes was lagged behind. The pH and temperature dependency of IL-based ABS could be used to switch between monophasic and biphasic regions and to create reversible phase transitions, which are particularly relevant in the design of integrated processes.

1.4. Additional remarks

ILs have a high potential as alternatives solvents for the extraction and purification of value-added compounds from the most diverse sources. The most relevant property contributing to these outputs is their “designer” ability, which allows the tailoring of the extraction and purification performance. In this chapter, it was shown and described the current thesis layout, and overviewed the potential and suitability of IL-based solvents for solid-liquid extractions from biomass, followed by IL-based separation processes by the application of ABS. Despite the efforts made by different authors to screen different ILs and to evaluate various process

conditions, most studies are based on ILs comprising imidazolium cations and fluorinated anions, which are not only more expensive, but also moderately toxic and of low biodegradability.²⁶⁻²⁸ More recent works are moving into a different direction, *i.e.* by applying more sustainable ILs solvents and separation systems. ILs based on quaternary ammoniums, such as cholinium-based, have been largely investigated in the last decade.⁷ Still, there is still a long path to explore all the potential of more biocompatible ILs, both as extraction solvents and in separation processes. In this thesis, and although some works comprise the use imidazolium-based ILs, special emphasis has been placed in the use of more benign IL alternatives, such as cholinium- and glycine-betaine-based.

The use of aqueous solutions of ILs for the extraction of value-added compounds from biomass is a particularly good strategy since aqueous solutions of ILs allow to decrease the high viscosity associated to most neat ILs, while contributing to an increase of the biocompatible nature of the solvent and to a decrease of the overall solvent cost. Furthermore, ILs have shown to be successful in the extraction of small extractable compounds by favouring their solubility in aqueous solutions, either by a hydrotropic⁷ or micelle-mediated effect.⁷ In spite of the high efficiency of ILs aqueous solutions for the extraction of bioactive compounds, the non-volatile nature of aprotic ILs represents a major drawback when envisaging the target product recovery since a simple evaporation step cannot be applied.² Although some attempts exist in this direction, some of these techniques are laborious and expensive, and additionally require the use of volatile organic solvents that the ILs aim to replace. Aiming at overcoming this major drawback in the ILs recovery, one possibility can be the no need of ILs recovering. If ILs are carefully and properly selected they can be used together with the extracted targeted compounds, thus avoiding one additional recovery step in the process. To this end, ILs which may enhance the extracts biological properties, while not displaying cytotoxic features, appear as a promising option.

Although not directly shown in this thesis, the solid-liquid and liquid-liquid strategies discussed in this chapter can be combined towards the development of integrated processes, *e.g.* by extracting value-added compounds from biomass using IL aqueous solutions followed by the addition of a second phase-forming component to create an ABS for separation purposes. Some examples on this direction can be found in the literature.^{59, 65, 66} Taking advantage of the characteristics of the switchable IL-based ABS developed, a different type of an integrated process (production-separation) was however developed. In fact, in recent years, the development of switchable systems has attracted a large attention.⁸⁻¹⁰ However, the research in dynamic liquid-liquid extractions using ILs has been focused in the direct use of hydrophobic ILs and non-miscible aqueous or organic solvents. Taking in account all the advantages previously

mentioned regarding the high performance of IL-based ABS and their water-rich media, their reversible behaviour was here studied, combined with examples on their use to develop integrated processes. More specifically, temperature- and pH-driven reversible phase transitions were accomplished with IL-based ABS.

From the works overviewed in this chapter, it is clear that the use of appropriate ILs leads to high extraction yields, recovery yields and purification factors. Still, there is a quite number of requirements to address aiming at fully developing cost-effective and sustainable extraction and separation processes involving ILs, namely to: (i) identify efficient, low-cost and biocompatible ILs able to compete with the commonly used solvents; (ii) develop integrated processes, particularly focused on decreasing the number of steps involved and process cost; (iii) develop efficient strategies for the value-added compounds recovery and IL recycling; (iv) perform scale-up studies of the optimized processes; and (v) carry out economic and life cycle analysis of the developed processes. Although there is still a long way to follow, IL-based solvent and separation processes display relevant advantages and hopefully may become an industrial reality in the following decades.

1.5. References

1. A. Jordan and N. Gathergood, *Chem. Soc. Rev.*, 2015, **44**, 8200-8237.
2. H. Passos, M. G. Freire and J. A. P. Coutinho, *Green Chem.*, 2014, **16**, 4786-4815.
3. A. F. M. Cláudio, M. C. Neves, K. Shimizu, J. N. Canongia Lopes, M. G. Freire and J. A. P. Coutinho, *Green Chem.*, 2015, **17**, 3948-3963.
4. M. G. Freire, A. F. Cláudio, J. M. Araújo, J. A. P. Coutinho, I. M. Marrucho, J. N. Canongia Lopes and L. P. Rebelo, *Chem. Soc. Rev.*, 2012, **41**, 4966-4995.
5. K. S. M. S. Raghavarao, T. V. Ranganathan, N. D. Srinivas and R. S. Barhate, *Clean Technol. Envir.*, 2003, **5**, 136-141.
6. Q. Ren, H. Xing, Z. Bao, B. Su, Q. Yang, Y. Yang and Z. Zhang, *Chinese J. Anal. Chem.*, 2013, **21**, 937-952.
7. S. P. M. Ventura, F. A. e Silva, M. V. Quental, D. Mondal, M. G. Freire and J. A. P. Coutinho, *Chem. Rev.*, 2017, **117**, 6984-7052.
8. M. T. Zafarani-Moattar and S. Hamzehzadeh, *Fluid Phase Equilib.*, 2011, **304**, 110-120.
9. Y. Qiao, W. Ma, N. Theyssen, C. Chen and Z. Hou, *Chem. Rev.*, 2017, **117**, 6881-6928.
10. P. G. Jessop, S. M. Mercer and D. J. Heldebrant, *Energy Environ. Sci.*, 2012, **5**, 7240-7253.
11. J. Pokorný, *Eur. J. Lipid Sci. Technol.*, 2007, **109**, 883-883.
12. S. Sasidharan, Y. Chen, D. Saravanan, K. M. Sundram and L. Yoga Latha, *Afr. J. Tradit. Complement Altern. Med.*, 2011, **8**, 1-10.
13. H. Walter, D. E. Brooks and D. Fisher, *Partitioning in Aqueous Two-Phase Systems: Theory, Methods, Uses, and Applications to Biotechnology.*, London Academic Press., 2nd ed. edn., 1985.
14. C. Capello, U. Fischer and K. Hungerbühler, *Green Chem.*, 2007, **9**, 927-934.
15. B. Tang, W. Bi, M. Tian and K. H. Row, *J. Chromatogr. B*, 2012, **904**, 1-21.
16. M. M. Pereira, J. A. P. Coutinho and M. G. Freire, *Ionic Liquids in the Biorefinery Concept: Challenges and Perspectives*, The Royal Society of Chemistry, 2016, DOI: 10.1039/9781782622598-00227, 227-257.
17. M. Martínez-Aragón, S. Burghoff, E. L. V. Goetheer and A. B. de Haan, *Sep. Purif. Technol.*, 2009, **65**, 65-72.
18. P. E. R. Å. Albertsson, *Nature*, 1958, **182**, 709-711.
19. K. E. Gutowski, G. A. Broker, H. D. Willauer, J. G. Huddleston, R. P. Swatloski, J. D. Holbrey and R. D. Rogers, *J. Am. Chem. Soc.*, 2003, **125**, 6632-6633.
20. K. N. Marsh, J. A. Boxall and R. Lichtenthaler, *Fluid Phase Equilib.*, 2004, **219**, 93-98.

21. M. J. Earle, J. M. S. S. Esperança, M. A. Gilea, J. N. Canongia Lopes, L. P. N. Rebelo, J. W. Magee, K. R. Seddon and J. A. Widegren, *Nature*, 2006, **439**, 831-834.
22. R. D. Rogers and K. R. Seddon, *Science*, 2003, **302**, 792-793.
23. T. Welton, *Chem. Rev.*, 1999, **99**, 2071-2084.
24. P. Wasserscheid and T. Welton, *Front Matter*, Wiley-VCH Verlag GmbH & Co. KGaA, 2008.
25. J. Ranke, S. Stolte, R. Störmann, J. Arning and B. Jastorff, *Chem. Rev.*, 2007, **107**, 2183-2206.
26. M. G. Freire, P. J. Carvalho, R. L. Gardas, I. M. Marrucho, L. M. N. B. F. Santos and J. A. P. Coutinho, *J. Phys. Chem. B*, 2008, **112**, 1604-1610.
27. M. G. Freire, P. J. Carvalho, A. M. S. Silva, L. M. N. B. F. Santos, L. P. N. Rebelo, I. M. Marrucho and J. A. P. Coutinho, *J. Phys. Chem. B*, 2009, **113**, 202-211.
28. K. M. Docherty and J. C. F. Kulpa, *Green Chem.*, 2005, **7**, 185-189.
29. Q.-P. Liu, X.-D. Hou, N. Li and M.-H. Zong, *Green Chem.*, 2012, **14**, 304-307.
30. K. Fukumoto, M. Yoshizawa and H. Ohno, *J. Am. Chem. Soc.*, 2005, **127**, 2398-2399.
31. S. T. Handy, M. Okello and G. Dickenson, *Org. Lett.*, 2003, **5**, 2513-2515.
32. Y. Mieno, Y. Kohno, S. Saita and H. Ohno, *Chem. Eur. J.*, 2016, **22**, 12262-12265.
33. M. Yoshizawa, M. Hirao, K. Ito-Akita and H. Ohno, *J. Mater. Chem.*, 2001, **11**, 1057-1062.
34. S.-y. Wang, L. Yang, Y.-g. Zu, C.-j. Zhao, X.-w. Sun, L. Zhang and Z.-h. Zhang, *Ind. Eng. Chem. Res.*, 2011, **50**, 13620-13627.
35. L. Yang, X. Sun, F. Yang, C. Zhao, L. Zhang and Y. Zu, *Int. J. Mol. Sci.*, 2012, **13**, 5163-5178.
36. C.-h. Ma, S.-y. Wang, L. Yang, Y.-g. Zu, F.-j. Yang, C.-j. Zhao, L. Zhang and Z.-h. Zhang, *Chem. Eng. Process.*, 2012, **57-58**, 59-64.
37. W. Wang, Q. Li, Y. Liu and B. Chen, *Ultrason. Sonochem.*, 2015, **24**, 13-18.
38. Y. Sun, S. Ding, H. Huang and Y. Hu, *Bioresour. Bioprocess.*, 2017, **4**, 1-8.
39. T. Liu, X. Sui, L. Li, J. Zhang, X. Liang, W. Li, H. Zhang and S. Fu, *Analytica chimica acta*, 2016, **903**, 91-99.
40. K. Bica, P. Gaertner and R. D. Rogers, *Green Chem.*, 2011, **13**, 1997-1999.
41. M. J. Mehta and A. Kumar, *Chem. Asian J.*, 2017, **12**, 3150-3155.
42. A. K. Ressmann, P. Gaertner and K. Bica, *Green Chem.*, 2011, **13**, 1442-1447.
43. T. Usuki, N. Yasuda, M. Yoshizawa-Fujita and M. Rikukawa, *Chem. Commun.*, 2011, **47**, 10560-10562.
44. G. Young, F. Nippgen, S. Titterbrandt and M. J. Cooney, *Sep. Purif. Technol.*, 2010, **72**, 118-121.
45. Y.-H. Kim, Y.-K. Choi, J. Park, S. Lee, Y.-H. Yang, H. J. Kim, T.-J. Park, Y. Hwan Kim and S. H. Lee, *Bioresour. Technol.*, 2012, **109**, 312-315.
46. L. B. Malihan, G. M. Nisola and W.-J. Chung, *Bioresour. Technol.*, 2012, **118**, 545-552.
47. B. Ltd, *Extraction of Artemisinin using Ionic Liquids*; , Project Report 003- 001/1; , York, U.K, 2016.
48. S. A. Chowdhury, R. Vijayaraghavan and D. R. MacFarlane, *Green Chem.*, 2010, **12**, 1023-1028.
49. W. Ma and K. H. Row, *J. Liq. Chromatogr. Relat. Technol.*, 2017, **40**, 459-466.
50. M. G. Bogdanov, I. Svinyarov, R. Keremedchieva and A. Sidjimov, *Sep. Purif. Technol.*, 2012, **97**, 221-227.
51. M. G. Bogdanov and I. Svinyarov, *Sep. Purif. Technol.*, 2013, **103**, 279-288.
52. A. F. M. Cláudio, A. M. Ferreira, M. G. Freire and J. A. P. Coutinho, *Green Chem.*, 2013, **15**, 2002-2010.
53. M. G. Bogdanov, R. Keremedchieva and I. Svinyarov, *Sep. Purif. Technol.*, 2015, **155**, 13-19.
54. K. Ressmann Anna, R. Zirbs, M. Pressler, P. Gaertner and K. Bica, *Z. Naturforsch. B*, 2013, **68**, 1129-1137.
55. W. Jin, Q. Yang, B. Huang, Z. Bao, B. Su, Q. Ren, Y. Yang and H. Xing, *Green Chem.*, 2016, **18**, 3549-3557.
56. M. Martins, F. A. Vieira, I. Correia, R. A. S. Ferreira, H. Abreu, J. A. P. Coutinho and S. P. M. Ventura, *Green Chem.*, 2016, **18**, 4287-4296.
57. E. L. P. de Faria, M. V. Gomes, A. F. M. Cláudio, C. S. R. Freire, A. J. D. Silvestre and M. G. Freire, *Biophys. Rev.*, 2018, **0**, 1-11.
58. E. L. P. de Faria, S. V. Shabudin, A. F. M. Cláudio, M. Válega, F. M. J. Domingues, C. S. R. Freire, A. J. D. Silvestre and M. G. Freire, *ACS Sustain. Chem. Eng.*, 2017, **5**, 7344-7351.
59. B. D. Ribeiro, M. A. Z. Coelho, L. P. N. Rebelo and I. M. Marrucho, *Ind. Eng. Chem. Res.*, 2013, **52**, 12146-12153.
60. B. D. Ribeiro, M. A. Z. Coelho and I. M. Marrucho, *Eur. Food Res. Technol.*, 2013, **237**, 965-975.
61. J. Jiao, Q.-Y. Gai, Y.-J. Fu, Y.-G. Zu, M. Luo, W. Wang and C.-J. Zhao, *J. Food Eng.*, 2013, **117**, 477-485.
62. A. K. Ressmann, K. Strassl, P. Gaertner, B. Zhao, L. Greiner and K. Bica, *Green Chem.*, 2012, **14**, 940-944.
63. C. Lu, X. Luo, L. Lu, H. Li, X. Chen and Y. Ji, *J. Sep. Sci.*, 2013, **36**, 959-964.
64. R. Zirbs, K. Strassl, P. Gaertner, C. Schroder and K. Bica, *RSC Adv.*, 2013, **3**, 26010-26016.
65. P. L. Santos, L. N. S. Santos, S. P. M. Ventura, R. L. de Souza, J. A. P. Coutinho, C. M. F. Soares and Á. S. Lima, *Chem. Eng. Res. Des.*, 2016, **112**, 103-112.
66. Z. Tan, F. Li and X. Xu, *Sep. Purif. Technol.*, 2012, **98**, 150-157.

67. Á. S. Lima, C. M. F. Soares, R. Paltram, H. Halbwirth and K. Bica, *Fluid Phase Equilib.*, 2017, **451**, 68-78.
68. Z. J. Tan, C. Y. Wang, Z. Z. Yang, Y. J. Yi, H. Y. Wang, W. L. Zhou and F. F. Li, *Molecules (Basel, Switzerland)*, 2015, **20**, 17929-17943.
69. S. Shahriari, C. M. S. S. Neves, M. G. Freire and J. A. P. Coutinho, *J. Phys. Chem. B*, 2012, **116**, 7252-7258.
70. H. F. D. Almeida, M. G. Freire and I. M. Marrucho, *Green Chem.*, 2017, **19**, 4651-4659.
71. R. Hatti-Kaul, *Aqueous Two-Phase Systems: Methods and Protocols*, 2000.
72. C. L. S. Louros, A. F. M. Cláudio, C. M. S. S. Neves, M. G. Freire, I. M. Marrucho, J. Pauly and J. A. P. Coutinho, *Int. J. Mol. Sci.*, 2010, **11**, 1777-1791.
73. M. G. Freire, C. L. S. Louros, L. P. N. Rebelo and J. A. P. Coutinho, *Green Chem.*, 2011, **13**, 1536-1545.
74. M. Domínguez-Pérez, L. I. N. Tomé, M. G. Freire, I. M. Marrucho, O. Cabeza and J. A. P. Coutinho, *Sep. Purif. Technol.*, 2010, **72**, 85-91.
75. H. Passos, M. P. Trindade, T. S. M. Vaz, L. P. da Costa, M. G. Freire and J. A. P. Coutinho, *Sep. Purif. Technol.*, 2013, **108**, 174-180.
76. J. F. B. Pereira, S. P. M. Ventura, F. A. e Silva, S. Shahriari, M. G. Freire and J. A. P. Coutinho, *Sep. Purif. Technol.*, 2013, **113**, 83-89.
77. Y. Yan-Ying, Z. Wei and C. Shu-Wen, *Chinese J. Anal. Chem.*, 2007, **35**, 1726-1730.
78. A. F. M. Cláudio, M. G. Freire, C. S. R. Freire, A. J. D. Silvestre and J. A. P. Coutinho, *Sep. Purif. Technol.*, 2010, **75**, 39-47.
79. J. H. P. M. Santos, M. Martins, A. J. D. Silvestre, J. A. P. Coutinho and S. P. M. Ventura, *Green Chem.*, 2016, **18**, 5569-5579.
80. A. F. M. Cláudio, A. M. Ferreira, C. S. R. Freire, A. J. D. Silvestre, M. G. Freire and J. A. P. Coutinho, *Sep. Purif. Technol.*, 2012, **97**, 142-149.
81. M. R. Almeida, H. Passos, M. M. Pereira, Á. S. Lima, J. A. P. Coutinho and M. G. Freire, *Sep. Purif. Technol.*, 2014, **128**, 1-10.
82. A. F. M. Cláudio, C. F. C. Marques, I. Boal-Palheiros, M. G. Freire and J. A. P. Coutinho, *Green Chem.*, 2014, **16**, 259-268.
83. J. H. Santos, F. A. e Silva, S. P. M. Ventura, J. A. P. Coutinho, R. L. de Souza, C. M. F. Soares and Á. S. Lima, *Biotechnol. Prog.*, 2015, **31**, 70-77.
84. R. d. C. S. Sousa, M. M. Pereira, M. G. Freire and J. A. P. Coutinho, *Sep. Purif. Technol.*, 2018, **196**, 244-253.
85. H. Passos, T. B. V. Dinis, E. V. Capela, M. V. Quental, J. Gomes, J. Resende, P. P. Madeira, M. G. Freire and J. A. P. Coutinho, *Phys. Chem. Chem. Phys.*, 2018, **20**, 8411-8422.
86. P. K. Ajikumar, K. Tyo, S. Carlsen, O. Mucha, T. H. Phon and G. Stephanopoulos, *Mol. Pharm.*, 2008, **5**, 167-190.
87. C. M. S. S. Neves, S. P. M. Ventura, M. G. Freire, I. M. Marrucho and J. A. P. Coutinho, *J. Phys. Chem. B*, 2009, **113**, 5194-5199.
88. M. Ikeda, *Appl. Microbiol. Biotechnol.*, 2006, **69**, 615-626.
89. S. P. M. Ventura, C. M. S. S. Neves, M. G. Freire, I. M. Marrucho, J. Oliveira and J. A. P. Coutinho, *J. Phys. Chem. B*, 2009, **113**, 9304-9310.
90. J. F. B. Pereira, A. S. Lima, M. G. Freire and J. A. P. Coutinho, *Green Chem.*, 2010, **12**, 1661-1669.
91. S. Hamzehzadeh and M. Vasireh, *Fluid Phase Equilib.*, 2014, **382**, 80-88.
92. H. Passos, A. R. Ferreira, A. F. M. Cláudio, J. A. P. Coutinho and M. G. Freire, *Biochem. Eng. J.*, 2012, **67**, 68-76.
93. M. T. Zafarani-Moattar, S. Hamzehzadeh and S. Nasiri, *Biotechnol. Prog.*, 2012, **28**, 146-156.
94. A. Luis, T. B. Dinis, H. Passos, M. Taha and M. G. Freire, *Biochem. Eng. J.*, 2015, **101**, 142-149.
95. E. V. Capela, M. V. Quental, P. Domingues, J. A. P. Coutinho and M. G. Freire, *Green Chem.*, 2017, **19**, 1850-1854.
96. M. Lu and F. Tjerneld, *Journal of chromatography. A*, 1997, **766**, 99-108.
97. L. I. N. Tomé, V. R. Catambas, A. R. Teles, M. G. Freire, I. M. Marrucho and J. A. P. Coutinho, *Sep. Purif. Technol.*, 2010, **72**, 167-173.
98. J. Li and W. J. Kao, *Biomacromolecules*, 2003, **4**, 1055-1067.
99. M. J. Ruiz-Angel, V. Pino, S. Carda-Broch and A. Berthod, *J. chromatogr. A*, 2007, **1151**, 65-73.
100. M. Taha, F. A. e Silva, M. V. Quental, S. P. M. Ventura, M. G. Freire and J. A. P. Coutinho, *Green Chem.*, 2014, **16**, 3149-3159.
101. M. M. Pereira, S. N. Pedro, M. V. Quental, A. S. Lima, J. A. P. Coutinho and M. G. Freire, *J. Biotechnol.*, 2015, **206**, 17-25.
102. M. Taha, M. V. Quental, I. Correia, M. G. Freire and J. A. P. Coutinho, *Process Biochem.*, 2015, **50**, 1158-1166.
103. M. V. Quental, M. Caban, M. M. Pereira, P. Stepnowski, J. A. P. Coutinho and M. G. Freire, *Biotechnol. J.*, 2015, **10**, 1457-1466.

104. S. P. M. Ventura, R. L. F. de Barros, J. M. de Pinho Barbosa, C. M. F. Soares, A. S. Lima and J. A. P. Coutinho, *Green Chem.*, 2012, **14**, 734-740.
105. J. M. P. Barbosa, R. L. Souza, A. T. Fricks, G. M. Zanin, C. M. F. Soares and Á. S. Lima, *J. Chromatogr. B*, 2011, **879**, 3853-3858.
106. R. L. Souza, R. A. Lima, J. A. P. Coutinho, C. M. F. Soares and Á. S. Lima, *Sep. Purif. Technol.*, 2015, **155**, 118-126.
107. S. Dreyer and U. Kragl, *Biotechnol. Bioeng.*, 2008, **99**, 1416-1424.
108. H. Passos, A. Luís, J. A. P. Coutinho and M. G. Freire, *Sci. Rep.*, 2016, **6**, 1-7.
109. J. Luo, T. Xin and Y. Wang, *New J. Chem.*, 2013, **37**, 269-273.
110. P. Nockemann, B. Thijs, S. Pittois, J. Thoen, C. Glorieux, K. Van Hecke, L. Van Meervelt, B. Kirchner and K. Binnemans, *J. Phys. Chem. B*, 2006, **110**, 20978-20992.
111. Y. Kohno and H. Ohno, *Chem. Commun.*, 2012, **48**, 7119-7130.
112. C. T. Wu, K. N. Marsh, A. V. Deev and J. A. Boxall, *J. Chem. Eng. Data*, 2003, **48**, 486-491.
113. D. E. Bergbreiter, P. L. Osburn, A. Wilson and E. M. Sink, *J. Am. Chem. Soc.*, 2000, **122**, 9058-9064.
114. T. V. Hoogerstraete, B. Onghena and K. Binnemans, *Int. J. Mol. Sci.*, 2013, **14**, 21353-21377.
115. A. J. L. Costa, M. R. C. Soromenho, K. Shimizu, I. M. Marrucho, J. M. S. S. Esperança, J. N. C. Lopes and L. P. N. Rebelo, *J. Phys. Chem. B*, 2012, **116**, 9186-9195.
116. B. Onghena, J. Jacobs, L. Van Meervelt and K. Binnemans, *Dalton Trans.*, 2014, **43**, 11566-11578.
117. J. M. Crosthwaite, S. N. V. K. Aki, E. J. Maginn and J. F. Brennecke, *J. Phys. Chem. B*, 2004, **108**, 5113-5119.
118. K. Fukumoto and H. Ohno, *Angew. Chem. Int. Ed.*, 2007, **119**, 1884-1887.
119. Y. Kohno, S. Saita, K. Murata, N. Nakamura and H. Ohno, *Polym. Chem.*, 2011, **2**, 862-867.
120. S. Saita, Y. Mieno, Y. Kohno and H. Ohno, *Chem. Commun.*, 2014, **50**, 15450-15452.
121. Y. Fukaya and H. Ohno, *Phys. Chem. Chem. Phys.*, 2013, **15**, 14941-14944.
122. Y. Mieno, Y. Kohno, S. Saita and H. Ohno, *Chem. Eur. J.*, 2016, **22**, 12262-12265.
123. D. Xiong, G. Cui, J. Wang, H. Wang, Z. Li, K. Yao and S. Zhang, *Angew. Chem. Int. Ed.*, 2015, **54**, 7265-7269.
124. Y. Kohno, H. Arai and H. Ohno, *Chem. Commun.*, 2011, **47**, 4772-4774.
125. L. Phan, D. Chiu, D. J. Heldebrant, H. Huttenhower, E. John, X. Li, P. Pollet, R. Wang, C. A. Eckert, C. L. Liotta and P. G. Jessop, *Ind. Eng. Chem. Res.*, 2008, **47**, 539-545.
126. F. A. e Silva, J. F. B. Pereira, K. A. Kurnia, S. P. M. Ventura, A. M. S. Silva, R. D. Rogers, J. A. P. Coutinho and M. G. Freire, *Chem. Commun.*, 2017, **53**, 7298-7301.
127. Z. Li, X. Liu, Y. Pei, J. Wang and M. He, *Green Chem.*, 2012, **14**, 2941-2950.
128. C. P. Song, R. N. Ramanan, R. Vijayaraghavan, D. R. MacFarlane, E.-S. Chan, J. A. P. Coutinho, L. Fernandez and C.-W. Ooi, *J. Chem. Thermodyn.*, 2017, **115**, 191-201.
129. K. A. Kurnia, M. G. Freire and J. A. P. Coutinho, *J. Phys. Chem. B*, 2014, **118**, 297-308.
130. D. Xiong, Z. Li, H. Wang and J. Wang, *Green Chem.*, 2013, **15**, 1941-1948.
131. D. Xiong, H. Wang, Z. Li and J. Wang, *ChemSusChem*, 2012, **5**, 2255-2261.

2. MATERIALS AND EXPERIMENTAL PROCEDURE

2.1. Extraction of value-added compounds from biomass using ILs aqueous solutions

2.1.1. Extraction of caffeine from spent coffee grounds using aqueous solutions of ionic liquids and salts

Materials

Spent coffee grounds (SPG) were supplied by the *Cafeteria* of the Chemistry Department of University of Aveiro, Aveiro, Portugal. Samples were dried until constant weight (≈ 6 days at $60\text{ }^{\circ}\text{C}$). Their initial humidity content was $(59.5 \pm 2.5)\%$. Pure caffeine (purity $\geq 98.5\%$) was acquired from Marsing & Co. Ltd.

Several aqueous solutions of salts, ILs, and their mixtures were investigated. Sodium tosylate ($\text{Na}[\text{Tos}]$, purity $> 90\%$) was supplied from Alfa Aesar, and sodium chloride (NaCl , purity $\approx 99.0\%$) was acquired from Chem Lab. The ILs studied were $[\text{C}_4\text{C}_1\text{im}][\text{Tos}]$ (purity $\approx 98.0\%$) and $[\text{C}_4\text{C}_1\text{im}]\text{Cl}$ (purity $\approx 99.0\%$), both purchased at Iolitec. All IL samples were dried, for at least 24 h under vacuum, before use. Their purities (purity $> 98\%$) were further confirmed by ^1H and ^{13}C nuclear magnetic resonance (NMR). The definition of the ILs used is provided in the **List of acronyms**.

The mobile phase used in the high performance liquid chromatography (HPLC) analysis was composed of methanol (purity $\geq 99.99\%$) from Fisher Chemical, and ultra-pure water (purity $\geq 99.99\%$) from Merck, both HPLC grade. Syringe filters ($0.45\text{ }\mu\text{m}$) acquired at GE healthcare, Whatman, were used.

Experimental procedure

Caffeine solubility

Pure caffeine (solid solute) was added in excess amounts to each aqueous solution and the mixture equilibrated in an air oven ($25 \pm 0.5\text{ }^{\circ}\text{C}$), under constant agitation (750 rpm), using an Eppendorf Thermomixer Comfort equipment. Equilibration time was established as 72 h after carrying out related kinetic studies. After saturation, all samples were centrifuged at the same temperature of equilibration in a Hettich Mikro 120 centrifuge, during 20 min at 4500 rpm, to separate the macroscopic solid and liquid phases. Then, samples of the liquid phase were carefully collected and diluted in ultra-pure water, and the amount of caffeine was quantified through HPLC-DAD (detector diode array) at 274 nm. In all experiments, control samples at the same compositions, but without solute, were studied. At least three individual samples were used for the quantification of caffeine at each aqueous solution.

Caffeine extraction

All aqueous solutions (containing salts, ILs or their mixtures) were gravimetrically prepared within 10^{-4} g (using an analytical balance Mettler Toledo Excellence - XS205 Dual Range). Mixtures of SCG and aqueous solutions were also prepared by weight, in sealed glass vials. The extractions were carried out in commercial Carousel Radleys Tech equipment able to both stirring and maintain the temperature within ± 0.5 °C. In all experiments the stirring was kept constant at 300 rpm, as well as, the temperature at 25 °C and the solid-liquid ratio of 1:10. After extraction, the overall solution was filtered under vacuum using a 0.45 μm cellulose membrane, and the caffeine extracted and present in the liquid solutions was quantified through HPLC-DAD at 274 nm.

Quantification of caffeine

The quantification of caffeine in each solution was carried out by HPLC-DAD (Shimadzu, model PROMINENCE). HPLC analyses were performed with an analytical C18 reversed-phase column (250 \times 4.60 mm), kinetex 5 μm C18 100 A, from Phenomenex. The mobile phase consisted of 25% of methanol and 75% of ultra-pure water. The separation was conducted in isocratic mode, at a flow rate of 1.0 mL \cdot min $^{-1}$ and using an injection volume of 10 μL . DAD was set at 274 nm. Each sample was analysed at least in duplicate. The column oven and the autosampler were operated at a controlled temperature of 25 °C. At these conditions, caffeine display a retention time of 6.6 min. Calibration curves were prepared using pure (commercial) caffeine. The amount of caffeine present in the SCG was calculated according to the weight of pure caffeine present in the extract divided by the total weight of dried biomass.

2.1.2. Extraction of 7-hydroxymatairesinol from Norway Spruce knots using aqueous solutions of ionic liquids**Materials**

Norway spruce knots (90%–95% actual knot material) were separated from over-thick industrial wood chips by sedimentation in water, after drying and grinding.¹ Before extraction, knots were immersed in liquid nitrogen and milled to pass through a 40–60 mesh sieve. A reference sample of 7-hydroxymatairesinol (HMR, HMR1/HMR2, > 96% purity) was prepared by precipitation with potassium acetate (KCH₃CO₂) and flash silica chromatography of a spruce knot extract, according to the literature.²

The solvents used for the extraction included distilled water, acetone (purity ≥ 99.99 %) from VWR chemicals, and aqueous solutions of ILs. The ILs [C₄C₁im]Cl (purity $\approx 99.0\%$), [C₄C₁im][Tos]

(purity \approx 98.0%), $[\text{C}_4\text{C}_1\text{im}][\text{C}_1\text{CO}_2]$ (purity \approx 98.0%) and $[\text{C}_4\text{C}_1\text{im}]\text{Br}$ (purity \approx 99.0%) were purchased from Iolitec. The ILs $[\text{C}_1\text{PyrNC}_2]\text{Br}$, $[(\text{C}_2)_3\text{NC}_2]\text{Br}$, $[(\text{C}_3)_3\text{NC}_2]\text{Br}$ and $[(\text{C}_4)_3\text{NC}_2]\text{Br}$ have been synthesized and characterized by us according to the literature.³ All IL samples were dried, for at least 24 h, under vacuum and at a moderate temperature (\approx 50 °C) before use. Their purities were further confirmed by ^1H and ^{13}C NMR spectra and showed to be \geq 98-99%. The water content of all ILs, after the drying procedure, was $<$ 1000 ppm as determined by Karl-Fischer titration. The definition of the ILs used is provided in the **List of acronyms**.

The mobile phase used in the HPLC analysis was composed of methanol (purity \geq 99.99%) from Fisher Chemical, and ultra-pure water (purity \geq 99.99%) from Merck, both HPLC grade. Syringe filters (0.45 μm) acquired at GE healthcare, Whatman, were used.

2,2-Diphenyl-2-picrylhydrazyl hydrate (DPPH) was acquired from Sigma-Aldrich. LPS from *Escherichia coli* (serotype O26:B6), penicillin and streptomycin were obtained from Sigma Chemical Co. (St. Louis, MO, USA). Dulbecco's Modified Eagle's Medium (DMEM), fetal bovine serum (FBS), 2',7'-dichlorodihydrofluorescein diacetate (DCFH-DA) and Hoechst 33342 were purchased at Fisher Scientific (Leicestershire, UK).

The potassium acetate (purity $>$ 99%) used for the precipitation of HMR and the ascorbic acid (purity $>$ 99.7%) used in the antioxidant activity assays were acquired from Sigma-Aldrich.

Experimental procedure

Solubility of HMR

HMR was added in excess amount to IL aqueous solutions, and was then equilibrated in an air oven (at 25 ± 0.5 °C) under constant agitation using an Eppendorf Thermomixer Comfort equipment. Previously optimized equilibration conditions were established: a stirring velocity of 750 rpm and an equilibration time of at least 72 h. After the saturation was reached, samples were centrifuged at the same temperature of equilibration in a Hettich Mikro 120 centrifuge, during 20 min at 4500 rpm to separate the macroscopic solid and liquid phases. After centrifugation, samples were put in an air bath equipped with a Pt 100 probe and a PID controller at the temperature used in equilibrium assays during 2 h. Then, the samples of the liquid phase were carefully collected and diluted in ultra-pure water, and the amount of HMR was quantified by HPLC-DAD. At least three individual samples were used in the quantification of HMR.

HMR extraction

Solid-liquid extractions of HMR from Norway Spruce knots were carried out using a commercial Carousel from Radleys Tech able to both stir and maintain the temperature within ± 0.5 °C, and protected from light. In all experiments the stirring was kept constant

at 1000 rpm. All aqueous solutions containing known amounts of ILs and biomass were prepared gravimetrically within $\pm 10^{-4}$ g. Several concentrations of IL, and different solid-liquid ratios, and times of extraction were ascertained. The temperature was set at 25 °C. For comparison purposes water and acetone were also used in the extractions. After the extraction step, water, acetone or ILs aqueous solutions were separated from biomass by centrifugation (at 4000 rpm for 30 min, using a centrifuge 5804, Eppendorf).

Quantification of HMR

The quantification of HMR in each solution was carried out by HPLC-DAD (Shimadzu, model PROMINENCE). HPLC analyses were performed with an analytical C18 reversed-phase column (250 × 4.60 mm), kinetex 5 μ m C18 100 A, from Phenomenex. The mobile phase consisted of 40% of methanol and 60% of ultra-pure water. The separation was conducted in isocratic mode, at a flow rate of 0.8 mL·min⁻¹ and using an injection volume of 10 μ L. DAD was set at 280 nm. Each sample was analysed at least in duplicate. The column oven and the autosampler were operated at a controlled temperature of 30 °C. Calibration curves were prepared using the pure HMR sample dissolved in methanol. HMR1 and HMR2 display a retention time of 8.4 and 7.8 min, respectively, and the sum of their areas was used for calibration purposes. The HMR1/2 ratio was calculated from the relative proportion of the two chromatographic peaks.

Response Surface methodology (RSM)

A RSM was applied to simultaneously analyse various factors (operational conditions) and to identify the most significant parameters which enhance the HMR extraction yield. In a 2^k surface response methodology there are *k* factors that contribute to a different response, and the data are treated according to a second order polynomial equation:

$$y = \beta_0 + \sum \beta_i X_i + \sum \beta_{ii} X_i^2 + \sum_{i < j} \beta_{ij} X_i X_j \quad (\text{Eq. 2.1.1})$$

where *y* is the response variable and β_0 , β_i , β_{ii} and β_{ij} are the adjusted coefficients for the intercept, linear, quadratic and interaction terms, respectively, and X_i and X_j are independent variables. This model allows the drawing of surface response curves and through their analysis the optimal conditions can be determined.⁴ [(C₂)₃NC₂]Br was selected to perform a 2³ factorial planning with the aim of optimizing the extraction yield of HMR. The 2³ factorial planning has been defined by the central point (zero level), the factorial points (1 and -1, level one) and the axial points (level α) – **Appendix A.2, Table A.2.1**. The independent variables coded levels used in the factorial planning are presented in **Appendix A.2, Table A.2.2**. The axial points are encoded at a distance α from the central point:

$$\alpha = (2^k)^{1/4} \quad (\text{Eq. 2.1.2})$$

The obtained results were statistically analysed with a confidence level of 95%. Student's t-test was used to check the statistical significance of the adjusted data. The adequacy of the model was determined by evaluating the lack of fit, the regression coefficient (and the F-value obtained from the analysis of variance (ANOVA) that was generated. The Statsoft Statistica 10.0© software was used for all statistical analyses, and Matlab 2015b, The MathWorks, for representing the response surfaces and contour plots.

Reuse of Biomass

The reuse of the biomass was investigated at 25 °C, using aqueous solutions of $[(C_2)_3NC_2]Br$ at 1.5 M, in 4 successive extractions at the optimized operational conditions (solid-liquid ratio of 0.1 or 0.01 during 280 min, and at 25 °C). After each extraction the solid-liquid mixture was filtered and a new IL aqueous solution was added to the same biomass sample.

Precipitation of HMR

The IL solution of $[(C_2)_3NC_2]Br$ was saturated by using it in 5 consecutive extraction cycles. The extract containing HMR in the ILs aqueous solutions was heated up to 60°C, and potassium acetate was added until saturation, aiming at recovering HMR by induced precipitation. This salt was chosen based on literature data.² Taking advantage of the solubility dependence on temperature, the initial mixture was also placed at 6°C in order to induce the precipitation of HMR. HMR was identified as the major compound present in the precipitate (55.28% of the total weight analysed, as addressed by HPLC-DAD).

Antioxidant activity assays

The antioxidant activity of the HMR-rich extracts was determined using the DPPH scavenging assay. The principle of this assay is based on the colour change of the DPPH[•] solution from purple to yellow, as the radical is quenched by the antioxidant.⁵ This change in colour was monitored by visible spectroscopy at 517 nm, using a BioTeck Synergy HT microplate reader. The antioxidant activity is expressed in IC₅₀ values, defined as the inhibitory concentration of the extract necessary to decrease the initial DPPH radical concentration by 50%, as well as in g of ascorbic acid equivalents *per kg* of dry weight ($\mu\text{g AAE mg}^{-1}$ of extract).⁶ Taking into account the IC₅₀ definition, a lower IC₅₀ value reflects a better DPPH radical scavenging activity.

Briefly, 3.34 mL of a DPPH solution (1 mM) in methanol was mixed with different volumes of the different HMR extracts in the several aqueous solutions. Then, 1:1 (v:v) methanol:water was added until the volume of 4 mL was reached. Samples were kept in the dark for 0.5, 1 h, and 2 h, at room temperature, and the decrease in the absorbance at 517 nm determined.⁶ A blank

control was used, with 250 μL of DPPH solution in methanol, in which methanol was added until a volume of 4 mL was reached. Ascorbic acid was used as a positive control. The DPPH radical scavenging activity, AA (%), is determined according to the following equation:

$$AA (\%) = \frac{(A_0 - A_1)}{A_0} \times 100 \quad (\text{Eq. 2.1.3})$$

where A_0 is the absorbance of the control and A_1 is the absorbance of the sample at 517 nm.

Cell culture

Raw 264.7, a mouse leukaemic monocyte macrophage cell line from American Type Culture Collection (ATCC number: TIB-71), was cultured in DMEM supplemented with 10% non-inactivated FBS, 100 $\text{U}\cdot\text{mL}^{-1}$ penicillin, and 100 $\mu\text{g}\cdot\text{mL}^{-1}$ streptomycin at 37°C in a humidified atmosphere of 95% air and 5% CO_2 . Cells were routinely inspected for morphological changes by microscope observation and subcultured every two days until passage 25.

Cell viability assays

In order to investigate the biocompatibility of the HMR extracts, their effect on the macrophage viability/metabolic activity by a resazurin assay was assessed.⁷ Briefly, 0.05×10^6 cells/well in a 96 well plate were exposed to known concentrations of the various HMR extracts during 24h. Two hours before the end of exposure, resazurin solution was added to each well to a final concentration of 50 μM . Absorbance was then read at 570 and 600 nm in a BioTeck Synergy HT microplate reader.

In-vitro cell viability and antioxidant activity assays

The potential antioxidant activity of $[(\text{C}_2)_3\text{NC}_2]\text{Br}$ -HMR-rich extracts was addressed by their capacity to prevent lipopolysaccharide (LPS)-induced oxidative stress in macrophages. Raw cells were plated at 0.05×10^6 per well of a μ -Chamber slide (IBIDI GmbH, Germany), allowed to stabilize overnight and then stimulated with 1 $\mu\text{g}\cdot\text{mL}^{-1}$ LPS during 16h. Compounds to be tested were added 1h prior to LPS stimulation. At the end of incubation, period cells were washed three times with Hanks' balanced salt solution (HBSS, in mM: 1.3 CaCl_2 , 0.5 MgCl_2 , 5.3 KCl , 138 NaCl , 0.44 KH_2PO_4 , 4.2 NaHCO_3 , and 0.34 Na_2HPO_4 (pH 7.4) and then loaded with 5 μM DCFH-DA and 0.5 $\mu\text{g}\cdot\text{mL}^{-1}$ Hoechst in HBSS, for 30 min at 37 °C in the dark. Cells were washed three times with HBSS, and analysed with an Axio Observer Z1 fluorescent microscope (Zeiss Group, Oberkochen, Germany) at 63X magnification.

2.2. Reversible IL-based ABS

2.2.1. pH-responsive aqueous biphasic systems formed by ionic liquids and polymers

Materials

Cholinium-based salts studied in this work were [Ch]Cl (purity \approx 99%) and [Ch]OH (*ca.* 46 wt% in water), both acquired from Sigma-Aldrich, [Ch][C₁CO₂] (purity \approx 98%) purchased from Iolitec and [Ch][C₂CO₂], [Ch][Gly] and [Ch][Lac] synthesized by us according to standard protocols⁸. It should be remarked that [Ch]Cl does not fall within the IL category due to its higher melting point. However, it is described as part of the cholinium-based ILs group for comparison purposes. Before use, all ILs were purified and dried for a minimum of 24 h at constant agitation, at moderate temperature (\approx 80 °C) and under vacuum (to reduce their volatile impurities to negligible values). After this step, the purity of each IL was confirmed by ¹H and ¹³C NMR spectra and found to be > 98%. The definition of the ILs used is provided in the **List of acronyms**.

The polymer polypropylene glycol (PPG) of average molecular weight 400 g·mol⁻¹, PPG 400, was used, supplied by Sigma-Aldrich and used as received.

The aqueous biphasic systems (ABS) studied at different pH values were established using hydrochloric acid (37% in aqueous solution) and glycolic acid (purity \approx 99%), both purchased from Sigma-Aldrich, acetic acid (purity \geq 99.5%), purchased from José Manuel Gomes dos Santos, propanoic acid (purity \approx 99%), acquired from Merck, and butanoic acid (purity \geq 99%) and lactic acid (purity 88%-92%), both acquired from Riedel-de-Haën.

For the demonstration of the ABS pH-triggered reversibility sudan III from Merck, and pigment blue 27 from Daicolor, were used as standard dyes.

For the extraction assays, deoxyribonucleic acid (DNA) from Salmon supplied by Sigma-Aldrich, and human serum albumin (HSA, 96%) acquired from Alfa Aesar, were used.

Experimental procedure

Determination of the ABS phase Diagrams and Tie-lines (TLs)

The ternary phase diagrams (PPG 400 + IL + water) were determined at several pH values with the following ILs: [Ch]Cl (from pH 5 to 1), [Ch][C₁CO₂] (from pH 9 to 5), [Ch][C₂CO₂] (from pH 8 to 5), [Ch][Gly] (from pH 7 to 4) and [Ch][Lac] (from pH 7 to 4). Each pH values was reached by adding the acid which corresponds to the precursor of the IL anion studied. The ternary phase diagrams were determined through the cloud point titration method⁹ at (25 \pm 1) °C and atmospheric pressure. Aqueous solutions of PPG 400 at \approx 65 wt% and aqueous solutions of the different hydrophilic ILs/acid mixtures at variable concentrations (from 60 to 80 wt%) were prepared gravimetrically and used for the determination of the binodal curves. Drop-wise

addition of each aqueous IL solution to a PPG 400 aqueous solution was carried out until the detection of a cloudy solution (biphasic region), followed by the drop-wise addition of ultra-pure water until the detection of a clear and limpid solution (monophasic region). Whenever necessary, the addition of the PPG solution to the IL was also carried out to complete the phase diagrams. The ternary system compositions were determined by weight quantification within $\pm 10^{-4}$ g.

The determination of the TLs was carried out by a gravimetric approach initially proposed by Merchuk *et al.*¹⁰. Ternary mixtures composed of IL/Acid + PPG + water at the biphasic region were gravimetrically prepared within $\pm 10^{-4}$ g, vigorously agitated, and left under equilibrium for 12 h at (25 ± 1) °C. Both phases were then separated and individually weighted. Each TL was determined through the relationship between the top phase composition, the overall system composition, and weight of the two phases.³

The pH of each aqueous phase was determined at (25 ± 1) °C using an HI 9321 Microprocessor pH meter (HANNA instruments).

pH-triggered reversibility

Aiming at studying the possibility of moving from monophasic to biphasic regimes in IL-based ABS by a proper tailoring of the pH, an initial ternary mixture was chosen based on the determined phase diagrams: PPG 400 (34 wt %) + IL (13 wt %) + water (53 wt %). The pH of this system is *ca.* 9. In order to reach the monophasic regime, an aqueous solution of each acid at 50 wt%, corresponding to the IL anion precursor, was drop wise added under constant agitation until the mixture became homogeneous (monophasic). Then, an aqueous solution of cholinium hydroxide, at 46 wt %, was added under agitation to reach the pH value of 9. It should be remarked that the pH of the aqueous solutions was experimentally determined in all addition steps. To better illustrate the phase separation phenomenon and these systems reversibility, two dyes, namely Sudam III and pigment blue 27 (≈ 0.30 mg of each), were added to the overall ABS.

Extraction of HSA and DNA

In the studied ABS, the top phase corresponds to the PPG-rich aqueous phase while the bottom phase is mainly composed of IL and water. The ternary mixtures compositions used in the partitioning experiments were chosen based on the phase diagrams determined for each ABS. In particular, a common mixture composition was prepared for all systems investigated: 30 wt% of PPG 400, 20 wt% of IL/Acid and 50 wt% of water. Only for three systems composed of [Ch][C₁CO₂] at pH 5 and [Ch][Pro] at pH 5 (50 wt% of PPG, 20 wt% of IL and 30 wt% of water at pH 5), and [Ch][Gly] at pH 4 (50 wt% of PPG, 20 wt% of IL and 30 wt% of water at pH 4), were

used due to the smaller biphasic region obtained with these ILs at lower pH values. DNA and HSA were introduced at the concentrations of $0.5 \text{ g}\cdot\text{L}^{-1}$ and $1.0 \text{ g}\cdot\text{L}^{-1}$, respectively, as part of the water added to each ABS.

The selective partition of DNA and HSA in each ABS was first addressed by carrying out experiments with each individual biomolecule. Each ABS mixture was stirred, centrifuged for 30 min at 3500 rpm, and left to equilibrate for at least 10 min at $(25 \pm 1) \text{ }^\circ\text{C}$ to achieve the complete of partitioning of each biomolecule between the two phases. After equilibrium, both phases were carefully separated, and the HSA and DNA in each phase quantified by UV-spectroscopy, using a BioTeck Synergy HT microplate reader, at a wavelength of 280 and 260 nm, respectively. Previously established calibration curves were used. At least three individual experiments were performed, allowing to determine the average in the extraction efficiency, as well as the respective standard deviations. The interference of the PPG and ILs with the quantification method was also taken into account and blank control samples were always employed.

Purification of DNA using the [Ch][Gly]-based ABS

Standard aqueous mixtures of DNA and HSA in different weight fraction ratios (1:1 to 1:5) were prepared in 1 mL milli-Q water, and vortex for 30 min for complete solubilization. The studied weight ratio of DNA to HSA correspond to concentrations of $0.5 \text{ g}\cdot\text{L}^{-1}$ and $1.0 \text{ g}\cdot\text{L}^{-1}$ of HSA and DNA, respectively, in the water added to create each ABS. After mixing, each system was left at $(25 \pm 1) \text{ }^\circ\text{C}$ for 24 h, allowing the precipitation of HSA and thus the purification of DNA. After the protein precipitation, all ABS were centrifuged at 1000 rpm for 2 min, and left at $(25 \pm 1) \text{ }^\circ\text{C}$ for 2 h. After equilibrium and precipitation of the protein, the phases were carefully separated and quantified in terms of DNA and HSA content by UV-Vis spectroscopy (Shimadzu UV-1800 UV-Vis spectrometer, USA), allowing to determine the extraction efficiencies and yields. The purification level of DNA was confirmed by the UV-Vis absorbance ratio of the IL-rich phase at 260 nm and 280 nm (A_{260}/A_{280} ratio).

After the purification step, the stability of DNA in each ABS at different pH values was confirmed by UV-Vis (Shimadzu UV-1800 UV-Vis spectrometer, USA) and circular dichroism (CD, Jasco J-1500 CD spectrometer, Japan) spectroscopies. To appraise the long-term stability of DNA in the IL-rich phase, samples were kept $(25 \pm 1) \text{ }^\circ\text{C}$ for several months, in which UV-Vis and CD spectra were acquired periodically.

2.2.2. Temperature-responsive aqueous biphasic systems composed of ammonium-based zwitterions and salts

Materials

The reagents used in the ZIs synthesis were 1,3-propanesultone (purity $\geq 99\%$), triamylamine (purity $\geq 98\%$), tripropylamine (purity $\geq 98\%$) and trimethylamine (*ca.* 13% v/v in acetonitrile) from Tokyo Chemical Industry Co. The following organic solvents, purchased from Kanto Chemical Co., Inc, were also used: acetonitrile (purity $\geq 99.5\%$), diethyl ether (purity $\geq 99\%$), ethyl acetate (purity $\geq 99.5\%$), hexane (purity $\geq 96\%$) and methanol (purity $\geq 99.8\%$). Deuterium oxide, D₂O (99.8 atom% D) from ACROS Organics was used in nuclear magnetic resonance (NMR) experiments.

To prepare ABS, the following salts were used: dipotassium hydrogenphosphate (K₂HPO₄, purity $\geq 9\%$), tripotassium citrate monohydrate (K₃C₆H₅O₇·H₂O, purity $\geq 99\%$), tripotassium phosphate (K₃PO₄, purity $\geq 95\%$), potassium carbonate, (K₂CO₃, purity $\geq 99.5\%$), potassium dihydrogenphosphate (KH₂PO₄, purity $\geq 99\%$), and trisodium citrate (Na₃C₆H₅O₇, purity $\geq 99\%$), all from Wako Pure Chemical Industries, Ltd, and sodium dihydrogenphosphate dihydrate (NaH₂PO₄·2H₂O, purity $\geq 99\%$) from Kanto Chemical Co., Inc.

L-Tryptophan (purity 99%) and glycine (purity > 99%) were acquired from Acros Organics. The quantification of aliphatic amino acids was carried out using the ninhydrin reagent (2% solution) from Sigma.

Experimental procedure

Synthesis of zwitterions

Five ZIs were prepared. For the synthesis of N₅₅₅C3S and N₃₃₃C3S, trialkylamine and 1,3-propanesultone were dissolved in acetonitrile, and the resulting solution was mixed under dry nitrogen gas atmosphere. The obtained solution was stirred for two days at 80 °C. After the removal of acetonitrile by evaporation, the residual liquid was repeatedly washed with excess amounts of anhydrous diethyl ether. The resultant solid was purified by recrystallization with ethyl acetate/methanol, and the obtained white powder was dried in vacuum at 60 °C for 24 h. For the synthesis of N₂₂₂C3S, trialkylamine and 1,3-propanesultone were dissolved in acetonitrile, and the resulting solution was mixed under a dry nitrogen gas atmosphere. The obtained solution was stirred for 5h at 80 °C. The white powder obtained was repeatedly washed with excess amounts of anhydrous diethyl ether, and then dried in vacuum at 60 °C for 24 h, without the need of a recrystallization step. The same procedure was used in the synthesis of N₁₁₁C3S and N₁₁₁C4S. However, the reaction temperature was of 0 °C to avoid the evaporation

of trimethylamine. The chemical structure and purity of the synthesized ZIs were confirmed by ^1H NMR spectroscopy and elemental analysis. The definition of the ZIs used is provided in the **List of acronyms**.

Differential scanning calorimetry

Differential scanning calorimetry (DSC) was performed with a Hitachi DSC7000X at a heating rate of 2 °C/min.

Thermogravimetric analysis

Thermogravimetric analyses (TGA) were performed with an EXSTAR TG/DTA 7200 system (Seiko Instruments, Inc.) at a heating rate of 10 °C/min under nitrogen atmosphere.

Determination of the ABS phase diagrams

The binodal curves of each ABS were determined through the cloud point titration method, at 25, 35, and 45 °C (± 1 °C) and atmospheric pressure. Aqueous solutions of salt at 20-50 wt% and aqueous solutions of each ZI with concentrations ranging from 50 to 70 wt% were prepared and used. Repetitive drop wise addition of the aqueous salt solution to the aqueous solution of each ZI was carried out under constant stirring until the detection of a cloudy (biphasic) solution, followed by the drop wise addition of ultrapure water until the finding of a monophasic region (clear and limpid solution). Whenever necessary, and to better characterize the solubility curves, the addition of the ZI aqueous solution to the salt aqueous solution was carried out. The ternary system compositions were determined by weight quantification within $\pm 10^{-3}$ g.

Partition of amino acids

Aqueous solutions of amino acids were prepared at 1 g·dm⁻³ (4.9×10^{-3} mol·L⁻¹) for L-tryptophan and at 0.75 g·L⁻¹ (1.0×10^{-2} mol·L⁻¹) for glycine. The following mixtures compositions were used to carry out the separation of amino acids: 30 wt% of N₅₅₅C3S + 4 wt% of K₃PO₄ and 19.5 wt% of N₁₁₁C3S + 19.5 wt% of K₃PO₄. The extractions were carried out at 45 °C and 25 °C in N₅₅₅C3S- and N₁₁₁C3S-based ABS, respectively. Each mixture was vigorously stirred and left to equilibrate for at least 12 h, a time established in previous optimizing experiments, to achieve the complete partitioning of each amino acid between the coexisting phases. After a careful separation of both phases, the quantification of L-tryptophan was carried by UV-spectroscopy, using a BioTeck Synergy HT microplate reader, at a wavelength of 279 nm. To quantify the glycine present in each phase, 75 μL of ninhydrin reagent was added to 100 μL of an adequately diluted sample of each ABS phase. After incubation at 80 °C during 30 min, ethanol at 50% (v/v) was added to stop the reaction. Then glycine was quantified by UV-spectroscopy at a wavelength of 570 nm.^{11, 12} At least three individual systems were prepared in order to determine the average in the amino acids partition coefficients and extraction efficiencies, as well as the

respective standard deviations. Possible interferences of the ZI and K_3PO_4 with the analytical method were taken into account, and control samples were always prepared at the same weight fraction composition, using pure water instead of the amino acid aqueous solution. The partition coefficients of L-tryptophan (K_{TrY}) and glycine (K_{Gly}) are defined as the ratio of the concentration of each amino acid in the ZI-rich phase to that in the salt-rich phase. The selectivity is defined as the ratio between the partition coefficient of L-tryptophan and the partition coefficient of glycine. The percentage extraction efficiency of L-tryptophan ($EE_{TrY}\%$) and glycine ($EE_{Gly}\%$) are defined as the percentage ratio between the amount of each amino acid in the ZI-rich aqueous phase or salt-rich phase and that in the total mixture.

2.3. Integrated IL-based processes

2.3.1. Integrated production-separation platforms applying reversible pH-driven aqueous biphasic systems

Materials

The salts $K_3C_6H_5O_7 \cdot H_2O$, purity $\geq 99\%$, from Sigma–Aldrich, and potassium hydroxide (KOH, pure) from Pronalab, were used. Citric acid monohydrate ($C_6H_8O_7 \cdot H_2O$, purity $\geq 99\%$) from Fisher Scientific was used.

The ILs used were $[C_4C_1im]Cl$ (purity $\approx 99\%$), $[C_4C_1py]Cl$ (purity $> 98\%$), $[C_4C_1pip]Cl$ (purity $\approx 99\%$), $[P_{4444}]Cl$ (purity $\approx 98\%$), $[C_4C_1im]Br$ (purity $\approx 99\%$) and $[C_4C_1C_1im]Cl$ (purity $\approx 98\%$). All imidazolium-, pyridinium-, and pyrrolidinium-based ILs were purchased from Iolitec. The $[P_{4444}]Cl$ was kindly supplied by Cytec Industries Inc. Before use, each IL was dried for a minimum of 24h, at moderate temperature (60 °C), under constant agitation and vacuum. The definition of the ILs used is provided in the **List of acronyms**.

For the production of 5-hydroxymetilfurfural (HMF) it was used D-(-)-fructose (purity $\geq 98\%$) from Panreac. Pure HMF (purity $\geq 99\%$) from Sigma-Aldrich was used as a standard and to establish the calibration curve required for HMF quantification by HPLC-DAD. The following solvents were additionally used for HPLC-DAD analysis: methanol (purity $\geq 99.99\%$) from Fisher Chemical, and ultra-pure water (purity $\geq 99.99\%$) from Merck. Syringe filters (0.45 μm) acquired at GE healthcare Whatman were used.

Experimental procedure

Determination of the ABS phase diagrams and tie-lines (TLs)

The binodal curves were determined through the cloud point titration method at (25 ± 1) °C and atmospheric pressure, using aqueous solutions of salt at around 50 wt% and aqueous solutions of the different hydrophilic ILs with concentrations ranging from 60 to 90 wt%. It was carried out the addition of the salt aqueous solution to the IL aqueous solution, and *vice-versa*, to determine the phase diagrams. All the additions were carried out under constant stirring. The ternary system compositions were determined by weight quantification within $\pm 10^{-4}$ g.

The determination of the TLs was carried out by a gravimetric approach initially proposed by Merchuk *et al.*¹⁰. Ternary mixtures composed of IL + $K_3C_6H_5O_7/C_6H_8O_7$ + water at the biphasic region were gravimetrically prepared within $\pm 10^{-4}$ g, vigorously agitated, and left under equilibrium for 12 h at (25 ± 1) °C. Both phases were then separated and individually weighted. Each TL was determined through the relationship between the top phase composition, the overall system composition, and weight of the two phases.⁹

The pH of each aqueous phase was determined at (25 ± 1) °C using an HI 9321 Microprocessor pH meter (HANNA instruments).

Production and separation of HMF

Fructose (0.30 g), an aqueous solution of citric acid at 50 wt% (0.75 g, pH \approx 1.5) and IL (1 g) were added to a glass reaction vial, and left for reaction under a constant temperature of 80 °C, during 80 min. The reaction system was cooled down to room temperature, and potassium hydroxide was added up to pH \approx 7 (with the simultaneous formation of two phases, IL-based ABS). The amounts of HMF and fructose in the two phases were analysed by HPLC-DAD and HPLC-RID (refractive index detector), respectively. This procedure for each system has been repeated at least for three times.

Quantification of HMF and fructose by HPLC

The quantification of HMF and fructose in the ABS coexisting phases was carried out by HPLC-DAD (DIONEX ultimate 3000 DAD). HPLC analyses were performed with an analytical C18 reversed-phase column (250×4.60 mm 10 μ), SPHERISORB S10 ODS 2. The mobile phase consisted of a mixture of methanol and water (1:4, v:v). The separation was conducted in isocratic mode, at a flow rate of 0.6 mL·min⁻¹ and using an injection volume of 20 μ L. DAD was set at 284 nm. Each sample was analysed at least in duplicate. The column oven was operated at a controlled temperature of 35 °C. Calibration curves were previously prepared using the pure/standard HMF dissolved in ultra-pure water. At the described conditions, HMF displays a

retention time of 6.9 min. Blank control samples were used to evaluate the possible interferences of the salt and ILs in the quantification.

The quantification of fructose in each phase was carried out by HPLC-RID (Gilson Model 131). HPLC analyses were performed with a sugar-alcohol column (250 × 4.60 mm 8 μ), REZEX RCU-USP, from Phenomenex. The mobile phase consisted of 100% of ultra-pure water. The separation was conducted in isocratic mode, at a flow rate of 0.1 mL·min⁻¹ and using an injection volume of 20 μL. Each sample was analysed at least in duplicate. The column oven was operated at a controlled temperature of 60 °C. Calibration curves were prepared using the pure/standard fructose sample dissolved in ultra-pure water. At the described conditions, fructose displays a retention time of 17.7 min. Blank control samples were used to evaluate the possible interferences of the salt and ILs in the quantification.

2.3.2. Integrated production-separation platforms applying thermoreversible aqueous biphasic systems

Materials

The reagents used in the ZIs synthesis were 1,3-propanesultone (purity ≥ 99%), triamylamine (purity ≥ 98%), tripropylamine (purity ≥ 98%) and trimethylamine (*ca.* 13% v/v in acetonitrile) from Tokyo Chemical Industry Co. The following organic solvents, purchased from Kanto Chemical Co., Inc, were also used: acetonitrile (purity ≥ 99.5%), diethyl ether (purity ≥ 99%), ethyl acetate (purity ≥ 99.5%), hexane (purity ≥ 96%) and methanol (purity ≥ 99.8%). Deuterium oxide, D₂O (99.8 atom% D) from ACROS Organics was used in nuclear magnetic resonance (NMR) experiments.

To prepare ABS, different polyethylene glycol (PEG) of different molecular weights, namely 1540, 2000, 4000 and 6000 g·mol⁻¹ (abbreviated as PEG 1540, PEG 2000, PEG 4000 and PEG 6000, respectively) were used. They were obtained from Wako Pure Chemical Industries, Ltd, with the exception of PEG 2000 that was obtained from Kanto Chemical Co., Inc.

Commercial laccase from *Trametes versicolor*, kindly supplied by Sigma, and 2,2'-azino-bis(3-ethylbenzothiazoline-6-sulfonic acid (ABTS), acquired from Sigma, were used. The salts and compounds used to prepared the citrate/phosphate buffer were citric acid monohydrate (C₆H₈O₇·H₂O, purity > 99%) from Fisher Scientific, and sodium phosphate dibasic (Na₂HPO₄, purity >99%) from Merck.

Experimental procedure

Determination of the ABS phase diagrams and tie-lines (TLs)

The ABS binodal curves were determined through the cloud point titration method, at 25, 35, and 45 °C (± 1 °C) and atmospheric pressure. Aqueous solutions of polymer at 50-70 wt% and aqueous solutions of each ZI with concentrations ranging from 50 to 70 wt% were prepared and used. Repetitive drop wise addition of the aqueous polymer solution to the aqueous solution of ZI was carried out under constant stirring until the detection of a cloudy solution, followed by the drop wise addition of ultrapure water until the finding of a clear and limpid solution. Whenever necessary, and to better characterize the solubility curves, the addition of the ZI aqueous solution to the polymer aqueous solution also was carried out. The ternary system compositions were determined by weight quantification within $\pm 10^{-3}$ g.

TLs were determined by a gravimetric method originally described by Merchuk *et al.*¹⁰.

Oxidation reaction and separation of laccase

The following mixtures compositions were used to carry out the enzymatic catalysis: 39 wt% of N₅₅₅C3S + 13 wt% of PEG 6000 and 20 wt% of N₁₁₁C3S + 20 wt% of PEG 6000. The oxidation reaction in aqueous PEG/ZI monophasic systems was investigated using laccase solutions prepared with a concentration circa 50 g·L⁻¹ dissolved in PBS (phosphate buffered saline at 0.01M and pH \approx 7.4 at 25 °C), as well as aqueous solutions of ABTS with a concentration of 0.8 g·L⁻¹ dissolved in PBS. In each system, a small amount of the solution containing laccase (\approx 250 μ L) and a small amount of the solution containing ABTS (\approx 50 μ L) were added to the phase-forming components to reach a total weight of 1 g. The oxidative reactions were carried out at 45 °C and 25 °C in N₅₅₅C3S- and N₁₁₁C3S-based ABS, respectively. Each mixture was carefully mixed during 1 min. Then, the reaction systems were cooled down to 25 °C or heated up to 45 °C in N₅₅₅C3S- and N₁₁₁C3S-based ABS, respectively. A careful separation of both phases was then performed. The quantification of oxidized ABTS in each phase was carried by UV-Vis spectrophotometer (Shimadzu UV-1800 UV-Vis spectrometer, USA), at a wavelength of 420 nm. Laccase was quantified by its activity, for which 10 μ L of each phase was mixed with 50 μ L of ABTS, and 700 μ L of citrate/phosphate buffer (0.1M) at pH 4.5. The increase in absorbance/min was recorded in a UV-Vis spectrophotometer (Shimadzu UV-1800 UV-Vis spectrometer, USA) at 420 nm. Each procedure has been repeated at least three times to determine the average in the compounds extraction efficiencies, as well as the respective standard deviations. Possible interferences of the ZI and polymer with the analytical method were taken into account, and control samples were always prepared using PBS solutions instead of laccase and ABTS aqueous solutions. The percentage extraction efficiency of oxidase ABTS ($EE_{ABTS}\%$) and laccase ($EE_{laccase}\%$) are defined as

the percentage ratio between the amount of oxidase ABTS/active laccase in the ZI-rich aqueous phase or PEG-rich phase and that in the total mixture. The ZI interference or the bottom-phase interference in the laccase activity was also evaluated by preparing 5 mixtures, all of them with 50 μL of a laccase solution, and 37 μL of PBS, ZI or bottom-rich phase.

Recovery and stability of laccase

To investigate the recovery and stability of laccase, five consecutive cycles of oxidative reaction of ABTS were performed. Each cycle (reaction + separation) was carried out in a maximum of 1 h. The laccase activity was assayed as previously described. After reaction, the formation of ABS was induced by changes in temperature. The upper phase was removed (substrate-rich phase), a fresh substrate solution was added (same volume of solution removed with a composition determined by the TL - **Appendix C.2, Table C.2.9**), and a new cycle was initiated. The 5 cycles were carried out in a maximum of 5 h. The operational stability along the cycles was evaluated by the relative enzyme activity. The relative laccase activity (%) is defined as the ratio of the enzyme activity at the end of each cycle in respect to the enzyme activity in the first cycle.

An ultrafiltration step was finally applied to the PEG-rich phase using amicons with a cut-off of 3 kDa. 2 cycles at 10000 rpm, 20 min each, were applied. The phases obtained were analysed by Fourier-transform infrared spectroscopy (FTIR) and UV-Vis spectroscopies to address the presence of polymer, ZI and ABTS.

2.4. References

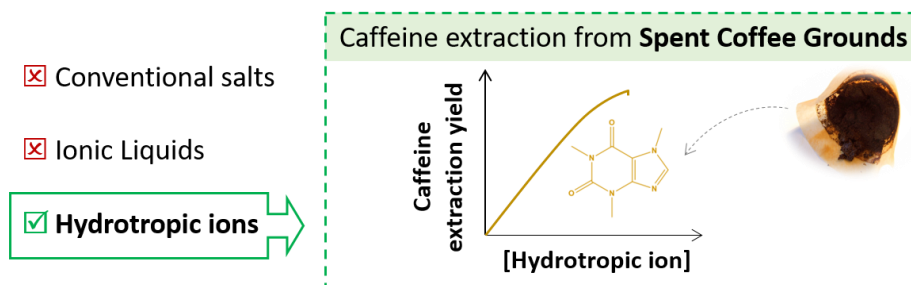
1. B. Holmbom, S. Willfoer, J. Hemming, S. Pietarinen, L. Nisula, P. Eklund and R. Sjoeholm, *Materials, Chemicals, and Energy from Forest Biomass*, American Chemical Society, 2007, **954**, 350-362.
2. S. M. Willför, A. I. Smeds and B. R. Holmbom, *J. Chromatogr. A*, 2006, **1112**, 64-77.
3. A. Messadi, A. Mohamadou, S. Boudesocque, L. Dupont, P. Fricoteaux, A. Nguyen-Van-Nhien and M. Courty, *J. Mol. Liq.*, 2013, **184**, 68-72.
4. M. I. I. Rodrigues and A. Francisco, *Planejamento de Experimentos e Optimização de Processos*, Campinas, Brazil, 2005.
5. M. N. Alam, N. J. Bristi and M. Rafiquzzaman, *Saudi Pharm. J.*, 2013, **21**, 143-152.
6. D. Huang, B. Ou and R. L. Prior, *J. Agric. Food Chem.*, 2005, **53**, 1841-1856.
7. J. O'Brien, I. Wilson, T. Orton and F. Pognan, *Eur. J. Biochem.*, 2000, **267**, 5421-5426
8. N. Muhammad, M. I. Hossain, Z. Man, M. El-Harbawi, M. A. Bustam, Y. A. Noaman, N. B. Mohamed Alitheen, M. K. Ng, G. Hefter and C.-Y. Yin, *J. Chem. Eng. Data*, 2012, **57**, 2191-2196.
9. M. G. Freire, A. F. M. Claudio, J. M. M. Araujo, J. A. P. Coutinho, I. M. Marrucho, J. N. C. Lopes and L. P. N. Rebelo, *Chem. Soc. Rev.*, 2012, **41**, 4966-4995.
10. J. C. Merchuk, B. A. Andrews and J. A. Asenjo, *J. Chromatogr. B Biomed. Sci. Appl.*, 1998, **711**, 285-293.
11. S. Moore and W. H. Stein, *J. Biol. Chem.*, 1954, **211**, 907-913.
12. D. L. Jones, A. G. Owen and J. F. Farrar, *Soil Biol. Biochem.*, 2002, **34**, 1893-1902.

3. EXTRACTION OF VALUE- ADDED COMPOUNDS FROM BIOMASS USING ILS AQUEOUS SOLUTIONS

3.1. Extraction of caffeine from spent coffee grounds using aqueous solutions of ionic liquids and salts

Chapter based on a manuscript under preparation:¹

A. M. Ferreira, H. M. D. Gomes, J. A. P. Coutinho and M. G. Freire



Instead of the IL/salt cation-anion pair, isolated ions in aqueous media are the key factors contributing to the enhanced solubility and extraction yield of value-added compounds from biomass achieved by a hydrotropic effect.

Abstract

Caffeine is a well-known alkaloid with antibacterial and antifungal properties, which can be used as a natural pesticide. The extraction of caffeine for this purpose is particularly relevant if carried out from biomass wastes. Some methods to extract caffeine from biomass are of low efficiency and require a large consumption of hazardous organic solvents and/or energy requests. Therefore, the extraction of caffeine from biomass or related wastes using more benign and cost-effective solvents and processes is of great interest. Spent coffee is a major residue from the preparation of drinkable coffee, with no significant commercial value, and usually discarded as a solid waste. In this context, in this work, we investigated the potential of aqueous solutions of ILs, salts, and their mixtures as alternative solvents to dissolve and extract caffeine from spent coffee grounds. ILs and salts were chosen aiming at better understanding the hydrotrope-mediated phenomenon. It is shown that salts or ILs containing anions that may act as hydrotropes, such as sodium tosylate (Na[Tos]) and [C₄C₁im][Tos], are the best solvents to improve the solubility of caffeine and its extraction from biomass. Studies with mixtures of ILs and salts allowed to conclude that this effect is derived from the ions present in aqueous

¹**Contributions:** M.G.F. and J.A.P.C. conceived and directed this work. A.M.F. and H.M.D.G. acquired the experimental data. A.M.F., M.G.F. and J.A.P.C. interpreted the experimental data. The manuscript was mainly written by A.M.F., M.G.F. and J.A.P.C.

solution and not from the initial IL/salt cation-anion pair. The trend obtained in the extraction yields of caffeine from biomass follows the ILs/salts tendency on improving the caffeine solubility, supporting that hydrotropy plays a major role when applying aqueous solutions of ILs or salts to extract value-added compounds from biomass. All the caffeine content in the SCG samples was extracted with aqueous solutions of adequate ILs or salts at 0.75 M, at a solid-liquid ratio of 1:10, at 25 °C, avoiding therefore the use of volatile organic solvents and energy-intensive conditions.

Introduction

Spent coffee grounds (SCG) are the most abundant coffee by-product (45%), being generated in coffee beverage preparation and instant coffee manufacturing, with productions of 6 million tons of this residue *per* year.¹ SCG are not adequately valorized; when used, these residues are typically burned for energy production or as fertilizers.² However, this inexpensive and abundant resource is rich in valuable compounds, such as essential oils, tannins and polyphenols,³ as well as in caffeine (5-10 mg·g⁻¹, depending on the coffee source).⁴ These compounds have relevant antioxidant, anti-inflammatory, radical scavenger, and antimicrobial properties^{5,6} and could be used in food, dietary, pharmaceutical and agrochemical industries.⁷ Recent studies showed also the importance of SCG as a source of an antioxidant dietary fiber.⁸ Moreover, caffeine-containing drinks are very popular around the world; the Food and Drug Administration (FDA) regulated that any added caffeine must be labelled on human consumption products owing to possible adulteration and health concerns.⁹ Another worthy example is the current controversy on the consumption/use of natural *versus* synthetic value-added-enriched products.¹⁰ Human consumers usually prefer natural value-added compounds,¹⁰ and thus their extraction from natural sources has gained a tremendous importance in the past years.¹¹

Conventional extraction processes of value-added compounds from biomass or wastes may present several drawbacks, such as low efficiency and non-selectivity, time-consuming, requirement of a high energetic input, and/or possible degradation of the targeted compounds. Traditional methods generally involve the use of large amounts of volatile organic solvents, leading to some safety and environmental concerns. Moreover, the use of hazardous solvents in the extraction step may prevent the targeted high-value chemicals to be used for human consumption. The extraction of caffeine from biomass is typically carried out with supercritical CO₂, that although selective and efficient requires a high initial investment on equipment, or by applying volatile organic solvents, such as chloroform, methylene chloride, dichloromethane, ethanol, *n*-hexane and others.^{12, 13} Caffeine is usually extracted with non-polar solvents or supercritical solvents due to its moderate hydrophobic character and low solubility in water

($16 \text{ g}\cdot\text{L}^{-1}$ at room temperature,¹⁴ $\log(K_{ow}) = -0.13$,³⁷ where K_{ow} is defined as the octanol-water partition coefficient).¹⁵

In recent years, aqueous solutions of ionic liquids (ILs) have been reported as efficient alternative solvents for the extraction of value-added compounds from biomass.¹¹ Some authors claimed that the high extraction efficiency achieved using ILs aqueous solutions is related with the ability of ILs to disrupt the biomass structure, allowing an easier access to the target compounds.^{11, 16, 17} Nevertheless, given that aqueous solutions are used, the disruption of the lignocellulosic matrix is highly improbable. On the other hand, Cláudio *et al.*¹⁸ suggested that the ILs aqueous solutions enhanced performance as extraction solvents results from their ability to enhance the solubility of target compounds. In this previously published work,¹⁸ ILs were identified as a novel class of hydrotropes, thus able to increase the solubility of hydrophobic solutes in aqueous solutions by the creation of IL-solute aggregates. Although pure ILs have been described as potential solvents for the extraction of value-added compounds from biomass, aqueous solutions of ILs also display a high potential and additional advantages due to the use of lower amounts of IL.¹¹ Aqueous solutions of ILs have thus benefits in terms of solvent toxicity and cost, and leads to a reduction of the overall viscosity of the extraction media, thus enhancing the mass transfer phenomena and reducing energy consumption.

Independently of the major factor ruling the enhanced capacity of aqueous solutions, they have shown to act as remarkable solvents for the extraction of a wide variety of bioactive components from vegetable sources,¹¹ such as in the extraction of several alkaloids, namely caffeine from *Paullinia cupana* (guarana seeds, Sapindaceae),¹⁹ glaucine from *Glaucium flavum* Cr. (Papaveraceae),²⁰ galantamine, narwedine, N-desmethygalantamine, and unguiminorine from the aerial parts of *Leucojum aestivum* L. (Amaryllidaceae)²¹, and piperine from *Piper nigrum* (Black Pepper).²² In all these works, IL aqueous solutions have been described as more efficient and selective solvents than volatile organic solvents typically used.

In order to better understand the phenomenon behind the improved performance of ILs aqueous solutions, in this work we investigated the solubility of caffeine in aqueous solutions of common (salt) hydrotropes, ILs, and their mixtures, followed by investigations on their use to extract caffeine from SCG.

Results and discussion

Caffeine (**Figure 3.1.1**) is a moderate hydrophobic ($\log(K_{ow}) = -0.13$)¹⁵ with a water solubility of $16 \text{ g}\cdot\text{L}^{-1}$ at room temperature.¹⁴ Therefore, caffeine extraction from biomass is usually carried out with volatile organic solvents. Aiming at identifying alternative solvents able to improve its extraction from biomass, we first investigated the potential of IL aqueous solutions to solubilize

caffeine. The solubility of caffeine was determined in several aqueous solutions of ILs at different concentrations, in aqueous solutions of conventional salts (some well-known hydrotropes) and in IL-salt mixtures aqueous solutions at 25 °C. More specifically, we appraised the potential of IL and salt ions to act as hydrotropes. Aqueous solutions containing the ILs [C₄C₁im][Tos] and [C₄C₁im]Cl, the salts sodium tosylate (Na[Tos]) and sodium chloride (NaCl), and mixtures of Na[Tos] and [C₄C₁im]Cl (1:1 in a mole basis), and mixtures of [C₄C₁im][Tos] and NaCl (1:1 in a mole basis), were investigated. The chemical structures of the ILs and salts investigated are given in **Figure 3.1.1**, and ILs definition is provided in the **List of acronyms**.

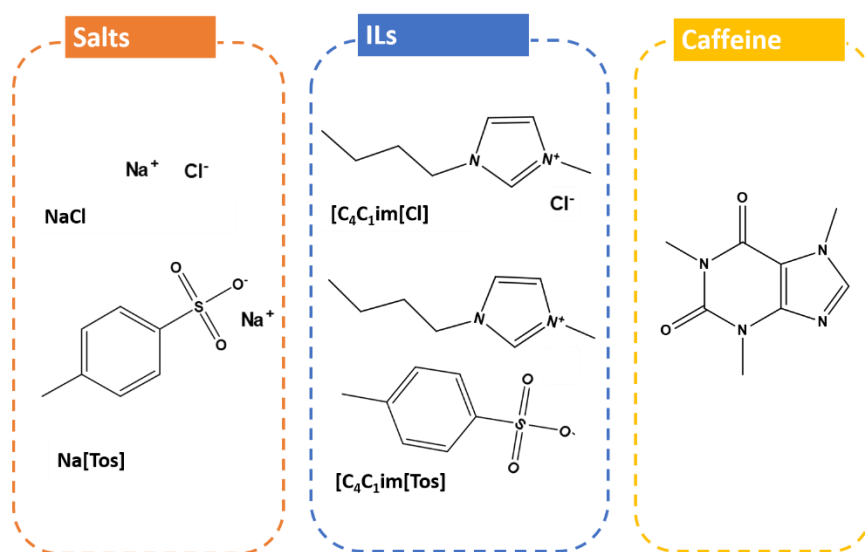


Figure 3.1.1. Chemical structures of the ILs and salts investigated, and of caffeine.

Figure 3.1.2 depicts the solubility of caffeine at 25 °C in the studied aqueous solutions (*cf.* the **Materials and experimental procedure** Chapter, **section 2.2.1**, for further details). Detailed experimental solubility data are reported in **Appendix A.1 (Table A.1.1)**. The solubility of caffeine in water at 25 °C is $22.8 \pm 0.2 \text{ g}\cdot\text{L}^{-1}$, being in agreement with literature data^{23, 24} ($22.6 \pm 0.3 \text{ g}\cdot\text{L}^{-1}$).²³ From the studied salts and ILs, Na[Tos], [C₄C₁im][Tos], mixtures of [C₄C₁im]Cl and Na[Tos] (1:1 in a mole basis), and mixtures of [C₄C₁im][Tos] and NaCl (1:1 in a mole basis), lead to an increase in the solubility of caffeine, whereas NaCl acts as a salting-out species, leading to a decrease in the caffeine solubility when compared with pure water. An improvement in the solubility of caffeine up to 2.5-fold ($\approx 58.5 \text{ g}\cdot\text{L}^{-1}$) has been observed using 1 M of [C₄C₁im][Tos] or Na[Tos].

The hydrotropic capacity of the various ILs and salts investigated on the caffeine solubility improvement follows the order: [C₄C₁im][Tos] \approx Na[Tos] > [C₄C₁im]Cl + Na[Tos] (1:1 in a mole basis) \approx [C₄C₁im][Tos] + NaCl (1:1 in a mole basis) > [C₄C₁im]Cl > NaCl. Hydrotropes form three-dimensional aggregates with localized hydrophobic regions which are responsible for the

increased aqueous solubility of hydrophobic compounds.²⁵ In general, ILs or salts with the [Tos]⁻ anion, a well-known hydrotrope, are the most proficient to improve the alkaloid solubilization. Although in a smaller extent, the IL [C₄C₁im]Cl also enhances the caffeine solubility, meaning that [C₄C₁im]⁺ also acts as a hydrotrope. On the other hand, NaCl has a salting-out effect on the caffeine solubility, being in agreement with the literature.²⁴ Furthermore, mixtures of NaCl with [C₄C₁im][Tos] and Na[Tos] with [C₄C₁im]Cl (**Figure 3.1.2**) show the same ability to solubilize caffeine. From a chemical point of view they present the same ions in aqueous media, at the same concentrations. Therefore, the enhancement or decrease in the caffeine solubility is a result of the ions ability to act as hydrotropes and not of the original ion pair itself. The hydrotropic ability of all species investigated depends on their concentration, although more evident up to 0.25 M, after which a less pronounced increase in the caffeine solubility is observed. In summary, chloride and sodium ions do not present a hydrotropic behavior, *i.e.* do not contribute to enhance the solubility of caffeine, while the tosylate and imidazolium ions show a hydrotropic capacity.

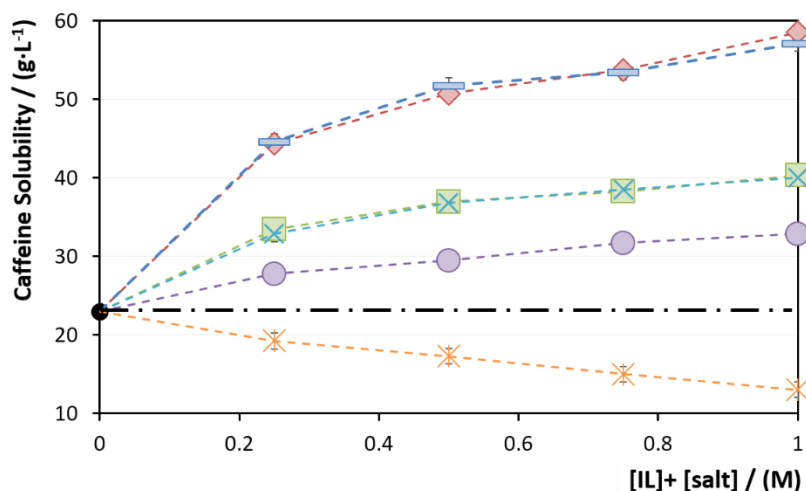


Figure 3.1.2. Influence of the hydrotropes (ILs, salts and the mixture ILs + salts) concentration in the solubility of caffeine in aqueous solutions at 25 °C (-*-*) NaCl, (-♦-) Na[Tos], (-●-) [C₄C₁im]Cl, (-■-) [C₄C₁im][Tos], (-■-) NaCl + [C₄C₁im][Tos] (1:1 in a mole basis) and (-×-) Na[Tos] + [C₄C₁im]Cl (1:1 in a mole basis). (—) The black line corresponds to the solubility of caffeine in water under the same conditions.

The relevance of the results obtained was then evaluated in terms of these solvents applicability in extraction processes, namely in the extraction of caffeine from biomass wastes. Different aqueous solutions of ILs, salts and ILs + salts at various concentrations were investigated as alternative extraction solvents of caffeine from SCG. The extraction of caffeine

from SCG was carried out at a biomass-solvent ratio of 1:10, at 25 °C, during 30 min. Caffeine was quantified by HPLC-DAD, with the respective extraction yields (weight of extracted caffeine in respect to the dried weight of SCF) shown in **Figure 3.1.3** (detailed results are given in **Appendix A.1, Table A.1.2**). Further details on the experimental procedure and materials are provided in the **Materials and experimental procedure** Chapter, **section 2.1.1**.

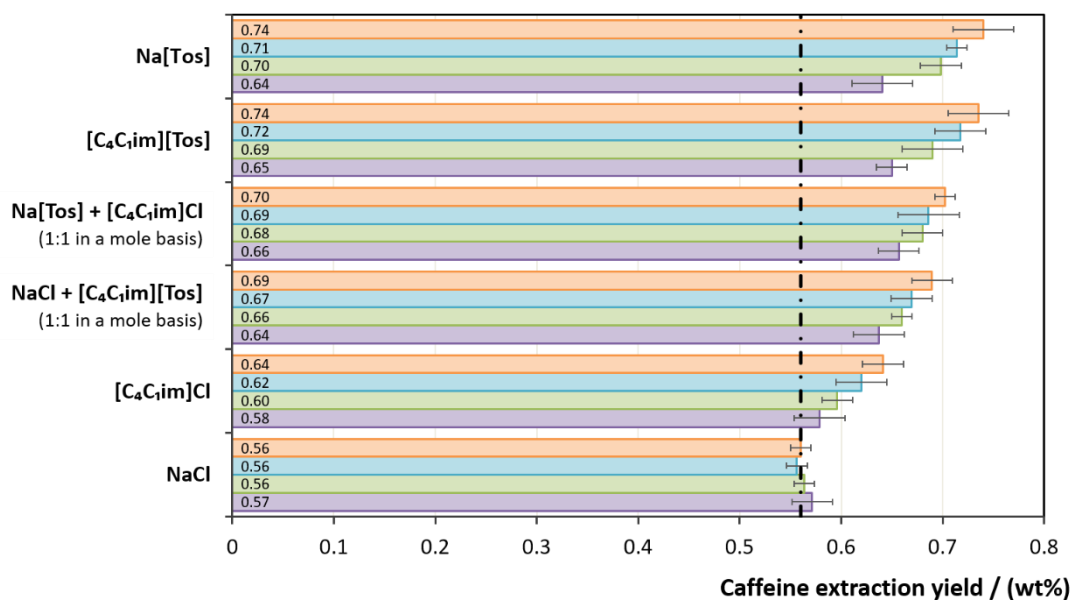


Figure 3.1.3. Extraction yields of caffeine from SCG using aqueous solutions of ILs, salts, and their mixtures at $T = 25\text{ °C}$, $t = 30\text{ min}$, and solid-liquid ratio = 1:10. IL/salt. Concentration of the ILs, salts, or mixtures: (purple bars) 0.25 M, (green bars) 0.50 M, (blue bars) 0.75 M and (orange bars) 1.00 M. (—)) The black line corresponds to the caffeine extraction using water at the same conditions.

The maximum content of caffeine in SCG is $0.72 \pm 0.20\text{ wt\%}$, as determined by us by soxhlet extraction with pure ethanol, whereas the extraction yield of caffeine at 25 °C using pure water as solvent is $0.56 \pm 0.02\text{ wt\%}$. In general, the trend on the caffeine extraction yield is in agreement with the tendency obtained with the caffeine solubility using the different ILs/salts aqueous solutions. An improved caffeine extraction is observed with aqueous solutions containing the tosylate anion, namely with Na[Tos] and [C₄C₁im][Tos]. In fact, these solutions allow to extract all caffeine present in the SCG samples. Mixtures of ILs and salts incorporating [Tos]⁻ also perform better than [C₄C₁im]Cl, thus confirming that the tosylate anion is a stronger hydrotrope than the imidazolium-based cation. The mixtures of NaCl with [C₄C₁im][Tos], and of Na[Tos] with [C₄C₁im]Cl, have a similar ability to extract caffeine, as observed with the solubility studies, thus confirming that the solubilization and extraction of caffeine depends on the ions hydrotropic character and not on the initial ion pair. In general, all these aqueous solutions lead

to higher extraction yields than that observed with pure water. On the other hand, aqueous solutions of NaCl display a negligible effect on the caffeine extraction, leading to extraction yields similar to that obtained with pure water. In summary, the commonly reported high efficiencies of ILs aqueous solutions to extract value-added compounds from biomass is, in fact, an effect derived from the ions themselves, independently of being an IL or a conventional salt. Although the biomass disruption may occur in some extent, the gathered results confirm that it is the hydrotrophy phenomenon that plays a major role towards the observed enhanced solubility of target compounds. It should be however remarked that this effect is depend on the solute nature. For instance, for more hydrophobic solutes, such as triterpenic acids²⁶ and cynaropicrin,²⁷ it was demonstrated that aqueous solutions of surface-active ILs perform better than aqueous solutions containing hydrotrope-based ILs.

The interest in caffeine as a natural pesticide has increased over the past few years, as well as the number of published works on extraction studies of caffeine from a broad range of biomass sources (coffee, tea, guarana, and mate), applying several extraction methods (microwave-assisted, ultrasound-assisted, etc.) and different solvents (n-hexane, ethanol, among others).^{4, 11, 13, 28, 29} In this work, high extraction yields of caffeine have been obtained using aqueous solutions of ILs, salts or their mixtures, thus not requiring the use of volatile organic solvents, at moderate temperatures and without using energy-intensive methods. Aqueous solutions of ILs or salts containing hydrotropes ions are therefore improved extraction solvents of moderately hydrophobic value-added compounds from biomass.

Conclusions

In this work, aqueous solutions of ILs, salts, and their mixtures were investigated as alternative solvents to improve the solubility and extraction of caffeine from biomass wastes, namely SCG. It was shown that aqueous solutions of ILs or salts containing the tosylate anion, a well-known hydrotrope, act as the best solvents. Studies with mixtures of ILs and salts demonstrated that the ions in solution, and not the initial ion pair, are the key factor for improving solubility and extraction yields. The extraction yields obtained as a function of the different ILs/salts investigated follow the trend obtained in the caffeine solubility, meaning that hydrotrophy plays a major role towards the typically observed improved extractions from biomass when using ILs aqueous solutions. The total caffeine content in the original matrix can be extracted with aqueous solutions of adequate ILs or salts at 0.75 M, at a solvent-liquid ratio of 1:10, and at 25 °C, avoiding thus the need of using volatile organic solvents and more sophisticated equipment and high energetic inputs.

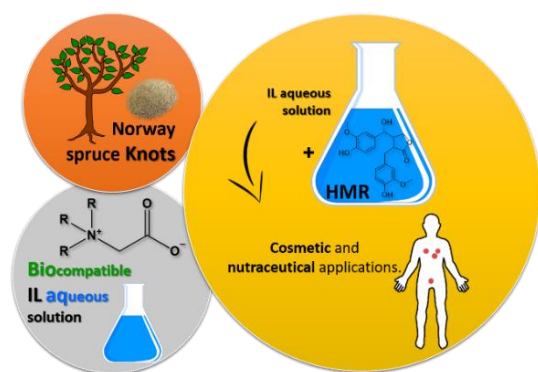
References

1. Y. I. K. T. V. Makarova, *J. Phys. Chem.*, 1974, **48**, 385-387.
2. F. Leifa, A. Pandey and C. R. Soccol, *J. Basic Microbiol.*, 2000, **40**, 187-197.
3. P. Esquivel and V. M. Jiménez, *Food Res. Int.*, 2012, **46**, 488-495.
4. R. Cruz, M. M. Cardoso, L. Fernandes, M. Oliveira, E. Mendes, P. Baptista, S. Morais and S. Casal, *J. Agric. Food Chem.*, 2012, **60**, 7777-7784.
5. W.-J. Yen, B.-S. Wang, L.-W. Chang and P.-D. Duh, *J. Agric. Food Chem.*, 2005, **53**, 2658-2663.
6. A. Panusa, A. Zuurro, R. Lavecchia, G. Marrosu and R. Petrucci, *J. Agric. Food Chem.*, 2013, **61**, 4162-4168.
7. K. Stanton, C. Tibazarwa, H. Certa, W. Greggs, D. Hillebold, L. Jovanovich, D. Woltering and R. Sedlak, *Integr. Environ. Assess. Manag.*, 2010, **6**, 155-163.
8. N. Martinez-Saez, A. T. Garcia, I. D. Perez, M. Rebollo-Hernanz, M. Mesias, F. J. Morales, M. A. Martin-Cabrejas and M. D. Del Castillo, *Food Chem.*, 2017, **216**, 114-122.
9. L. Zhang, D. M. Kujawinski, E. Federherr, T. C. Schmidt and M. A. Jochmann, *Anal. Chem.*, 2012, **84**, 2805-2810.
10. J. Pokorný, *Eur. J. Lipid Sci. Technol.*, 2007, **109**, 629-642.
11. H. Passos, M. G. Freire and J. A. P. Coutinho, *Green Chem.*, 2014, **16**, 4786-4815.
12. K. Ramalakshmi and B. Raghavan, *Crit. Rev. Food Sci. Nutr.*, 1999, **39**, 441-456.
13. R. J. Clarke and R. Macrae, *Coffee: Technology*, Springer Netherlands, Dordrecht, 1987, **2**, 59-71.
14. V. Zeindlhofer, D. Khlan, K. Bica and C. Schröder, *Rsc Adv.*, 2017, **7**, 3495-3504.
15. Chemspider, The free chemical database, <http://www.chemspider.com>, (accessed April 2017).
16. S. P. M. Ventura, F. A. e Silva, M. V. Quental, D. Mondal, M. G. Freire and J. A. P. Coutinho, *Chem. Rev.*, 2017, **117**, 6984-7052.
17. Q. Hou, M. Ju, W. Li, L. Liu, Y. Chen and Q. Yang, *Molecules*, 2017, **22**, 1-24.
18. A. F. M. Cláudio, M. C. Neves, K. Shimizu, J. N. Canongia Lopes, M. G. Freire and J. A. P. Coutinho, *Green chem.*, 2015, **17**, 3948-3963.
19. A. F. M. Cláudio, A. M. Ferreira, M. G. Freire and J. A. P. Coutinho, *Green Chem.*, 2013, **15**, 2002-2010.
20. M. G. Bogdanov, I. Svinjarov, R. Keremedchieva and A. Sidjimov, *Sep. Purif. Technol.*, 2012, **97**, 221-227.
21. I. Svinjarov, R. Keremedchieva and M. G. Bogdanov, *Sep. Sci. Technol.*, 2016, **51**, 2691-2699.
22. G. Raman and V. G. Gaikar, *Ind. Eng. Chem. Res.*, 2002, **41**, 2966-2976.
23. A. Shalmashi and F. Golmohammad, *Lat. Am. appl. res.*, 2010, **40**, 283-285.
24. A. Al-Maaieh and D. R. Flanagan, *J. Pharm. Sci.*, 2002, **91**, 1000-1008.
25. T. K. Hodgdon and E. W. Kaler, *Curr. Opin. Colloid Interface Sci.*, 2007, **12**, 121-128.
26. E. L. P. de Faria, S. V. Shabudin, A. F. M. Cláudio, M. Válega, F. M. J. Domingues, C. S. R. Freire, A. J. D. Silvestre and M. G. Freire, *ACS Sustain. Chem. Eng.*, 2017, **5**, 7344-7351.
27. E. L. P. de Faria, M. V. Gomes, A. F. M. Cláudio, C. S. R. Freire, A. J. D. Silvestre and M. G. Freire, *Biophys. Rev.*, 2018, **0**, 1-11.
28. A. Pietsch, *The Craft and Science of Coffee*, Academic Press, 2017, DOI: <https://doi.org/10.1016/B978-0-12-803520-7.00010-4>, 225-243.
29. R. J. Clarke, in *Encyclopedia of Food Sciences and Nutrition (Second Edition)*, Academic Press, Oxford, 2003, DOI: <https://doi.org/10.1016/B0-12-227055-X/00272-8>, pp. 1506-1511.

3.2. Extraction of 7-hydroxymatairesinol from Norway Spruce knots using aqueous solutions of ionic liquids

Chapter based on the published manuscript:²

A. M. Ferreira, E. S. Morais, A. C. Leite, A. Mohamadou, B. Holmbom, T. Holmbom, B. M. Neves, J. A. P. Coutinho, M. G. Freire and A. J. D. Silvestre, "Enhanced Extraction and Biological Activity of 7-hydroxymatairesinol obtained from Norway Spruce knots using Aqueous Solutions of Ionic Liquids", *Green Chem.*, 2017, **19**, 2626-2635



Biocompatible aqueous solutions of ILs rich in 7-hydroxymatairesinol (HMR) can be safely used in cosmetic and nutraceutical applications.

Abstract

In the past few years, an increasing demand for therapeutic drugs obtained from natural products has been faced. 7-Hydroxymatairesinol (HMR) has been commercialized as a nutritional supplement due to its anticarcinogenic and antioxidant properties. Aqueous solutions of analogues of glycine-betaine ionic liquids (AGB-ILs) were here studied as alternative solvents for the extraction of HMR from knots of Norway Spruce trees, in which extraction yields up to 9.46 wt% were obtained at a room temperature and in a short-time. Furthermore, it was found that the antioxidant potential of IL aqueous solutions enriched in HMR are more promising than the recovered HMR-rich solid extracts, and that these solutions can be safely used in nutraceutical and cosmetic applications. These results bring new perspectives into the design of new integrated approaches for the extraction and direct application of natural-derived high-value compounds using adequate ILs, without requiring an additional step involving the target product recovery and solvent recycling.

²Contributions: M.G.F., J.A.P.C. and A.J.S.D. conceived and directed this work. A.M. synthesized the ILs. A.M.F., E.S.M., A.C.L. and B.M.N. acquired the experimental data. In particular, A.M.F. determined all experimental data regarding the extraction of HMR and respective optimization. A.M.F., B.M.N., B.H., T.H., M.G.F., J.A.P.C. and A.J.S.D interpreted the experimental data. The manuscript was mainly written by A.M.F., M.G.F. and A.J.S.D with contributions from the remaining authors.

Introduction

Lignans are a specific family of phenolic compounds (comprising a 2,3-dibenzylbutane skeleton) that possess a large number of relevant biological properties, and thus have been used in nutraceutical and pharmacological applications.^{1, 2} Norway Spruce (*Picea abies*) knots, *i.e.* the part of branches embedded in the stem, are an exceptional source of lignans (5–15 wt%), such as hydroxymatairesinol (HMR), matairesinol, α -conidendrin, conidendrinic acid, isolariciresinol, secoisolariciresinol, liovile, picearesinol, lariciresinol, and pinoresinol.^{1, 3} HMR represents 65–80% of the total lignans content,⁴ and although it is found in several biomass sources, Norway Spruce knots are one of the most attractive sources. HMR (**Figure 3.2.1A**) occurs naturally in Spruce knots as a mixture of two stereoisomers differing in the stereochemistry of C-7, namely (*7R,8R,8'R*)-(-)-*allo*-hydroxymatairesinol (HMR1) and (*7S,8R,8'R*)-(-)-7-hydroxymatairesinol (HMR2). The most abundant isomer is HMR2, usually present in a 3:1 HMR2:HMR1 ratio.⁵ HMR has attracted a large attention since it is a direct metabolic precursor of the mammalian lignan enterolactone (ENL), presenting therefore promising biological properties.⁴ In fact, the daily intake of HMR increases the blood levels of ENL with proved benefits in the prevention of breast and prostate cancers, in menopause, and in heart diseases; additionally, HMR displays a strong antioxidant activity.⁴ Due to its valuable properties, HMR is commercialized as a nutritional supplement since 2006.⁶

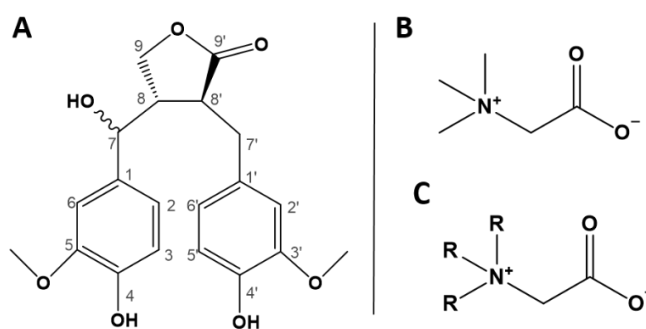


Figure 3.2.1. (A) Chemical structures of HMR, (B) betaine and (C) betaine analogues.

Currently, HMR is extracted from knots using volatile organic solvents, such as acetone, and mixtures of ethanol or acetone with water.¹ Others methods/solvents for the extraction of lignans have been reported, including supercritical fluid extraction, pressurized liquid extraction, microwave-assisted extraction, and ultrasonic-based extraction.¹ However, these methods require the use of sophisticated equipment and are energy-consuming.⁷ To overcome some of the concerns associated to the use of volatile organic compounds, either regarding their environmental footprint or when used for the extraction of target compounds envisioned for

human consumption, ionic liquids (ILs) and their aqueous solutions have emerged as promising solvents.⁸ Pure ILs have been proposed as alternative solvents for the extraction of natural compounds from biomass,⁸ but they usually display high viscosity and melting points above room temperature. Aqueous solutions of ILs were additionally proposed, while being able to overwhelm some of these drawbacks.⁸ In addition to the use of a greener and lower cost solvent, i.e. water, aqueous solutions of ILs display a lower viscosity, enhancing thus the mass transfer and reducing energy consumption.⁸ Furthermore, ILs aqueous solutions have been described as more efficient and selective solvents.⁹ The high efficiency achieved using ILs aqueous solutions has been related with the ability of ILs to disrupt the biomass structure;⁸ yet, a more sound explanation, and particularly when dealing with aqueous solutions, conveys on the enhanced solubility of biomolecules in aqueous solutions of ILs when compared with their solubility in the respective pure solvents. The solubility of biomolecules in aqueous solutions of ILs goes through a maximum along the IL concentration – a phenomenon that has been attributed to the ILs ability to act as hydrotropes by the formation of IL–biomolecule aggregates.¹⁰

Although ILs present favourable environmental characteristics compared to conventional organic solvents, their potential toxicity and low biodegradability should also be taken into consideration.¹¹⁻¹⁵ In fact, most studies reported in the literature regarding the use of ILs for the extraction of natural compounds are based on imidazolium ILs,⁸ which are not the best choice when considering their cost, toxicity and biodegradability. Aiming at moving towards more sustainable solvents, the synthesis of ILs from non-toxic starting materials and their applications are nowadays major topics of research.¹⁶ In addition to the well-studied cholinium-based ILs, those derived from glycine-betaine (GB-ILs) (**Figure 3.2.1B**) or its analogues (AGB-ILs)¹⁷ (**Figure 3.2.1C**), a naturally occurring and low cost amino acid, can be seen as promising alternatives as extraction solvents, yet still underexplored. Despite their advantages, there is only a single study reporting on the use of GB-ILs ($[N_{111}(C_{20}(O)_{12})]Cl$) in the extraction of value-added compounds from biomass.¹⁸ Glycine-betaine can be found in sugar beet molasses (up to 27 wt%), an underexplored by-product of the sugar industry.¹⁷ Moreover, GB and its derivatives are usually used as food supplements,¹⁹ and in cosmetic lotions and formulations.²⁰

Given the valuable properties of HMR and advantages of the AGB-ILs described before, we propose here the use of aqueous solutions of AGB-ILs as alternative solvents for the extraction of HMR from Norway Spruce knots by solid-liquid extractions at low temperatures (25 °C). Furthermore, the biological properties of the aqueous IL solutions containing HMR, such as their antioxidant activity and cytotoxicity, were assessed, showing that there is no need to recover the HMR from the extraction media and that these can be directly used in nutraceutical and cosmetic applications.

Results and discussion

Several aqueous solutions of ILs were investigated to infer their ability to extract HMR from Norway Spruce knots. The definition of the ILs used is provided in the **List of acronyms**, and their chemical structure is provided in the **Figure 3.2.2**. The experimental procedure and materials sources and purity are given in the **Materials and experimental procedure** Chapter (**section 2.1.2**). For an initial evaluation of the ILs aqueous solutions performance to extract HMR, aqueous solutions of imidazolium-based and AGB-based ILs at 0.5 M were used, as well as water and acetone. The results obtained are given in **Figure 3.2.3**, reporting HMR extraction yields for the different ILs at 0.5 M, where the extraction yield corresponds to the percentage ratio between the weight of extracted HMR (1 and 2) and the weight of dry biomass.

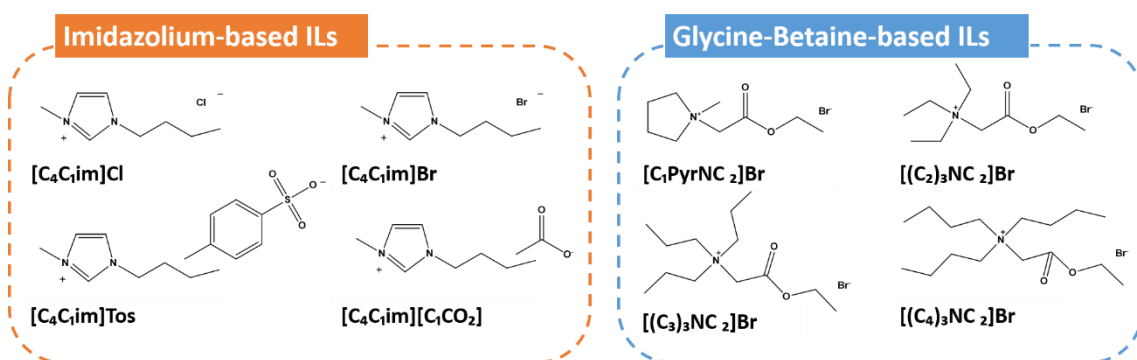


Figure 3.2.2. Chemical structures of the ionic liquids used in the extraction of HMR from Norway spruce knots.

The obtained extraction yields of HMR with ILs aqueous solutions range between 5.1 and 7.4 wt% (**Figure 3.2.3**, with detailed data provided in **Appendix A.2, Table A.2.3**), corresponding to higher yields than those achieved with water (4.4 wt%) or acetone (5.0 wt%). These results show the relevance of ILs in increasing the extraction yield of aqueous solutions for hydrophobic compounds, such as HMR (octanol-water partition coefficient (K_{ow}); $\log(K_{ow}) \approx 2.1$).²¹ The extraction yield of HMR also depends on the IL chemical structure, with the aqueous solutions of $[C_4C_1im][Br]$ and $[C_4C_1im][Tos]$ appearing as the best solvents, meaning that ILs composed of aromatic ions lead to higher extractions yields. Electron-rich aromatic π -systems can establish $\pi \cdots \pi$ and strong hydrogen-bonding interactions with target solutes such as HMR. These favourable interactions seem to be responsible for the slightly increased extraction performance of imidazolium-based ILs over AGB-ILs. It should be noted that the ratio of the two stereoisomers does not significantly change with the IL chemical structure. However, considering the ratio of HMR2:HMR1 of about 3:1, it seems that aqueous solutions of ILs are more effective for the extraction of HMR1 than of HMR2.

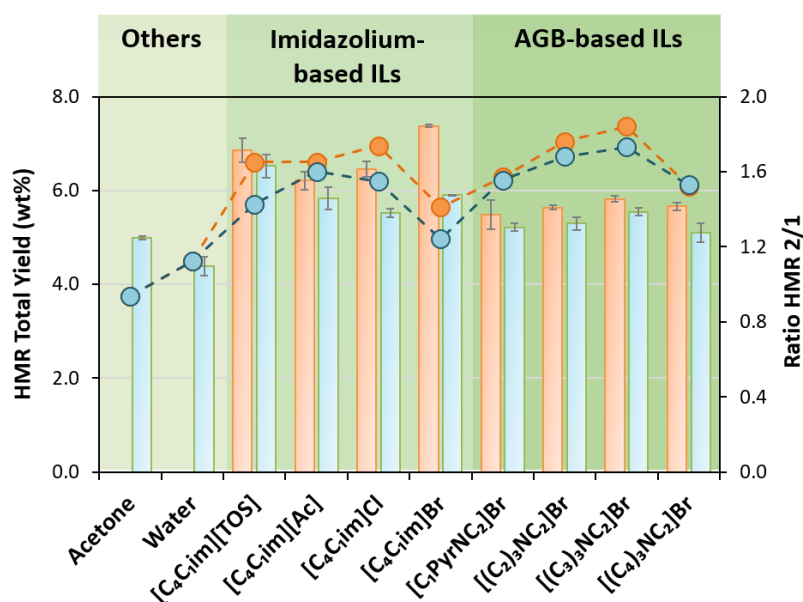


Figure 3.2.3. Yield of HMR extracted from Norway Spruce knots with different aqueous solutions of ILs (at 0.5 M), acetone and water ($T = 25\text{ }^{\circ}\text{C}$, $t = 180\text{ min}$) for a S/L ratio= 0.10 (blue bars) and for a S/L ratio = 0.02 (orange bars). Ratio of HMR2/ HMR1 for a S/L ratio= 0.10 (●) and for a S/L ratio= 0.02 (●).

Based on the results discussed above and considering on one hand that imidazolium-based IL only slightly increased the extraction yield, and, on the other hand, the lower cost and lower toxicity of $[(\text{C}_2)_3\text{NC}_2]\text{Br}$, this last IL was used to optimize the extraction operational conditions by a response surface methodology (RSM). The selection of short chain length IL derivatives is also valuable given that the toxicity of ILs increases with the increase of their alkyl side chains length.^{15, 22}

A RSM was used to optimize the operational conditions to improve the HMR extraction yield. This methodology allows to explore the relationship between the response (extraction yield of HMR) and the independent variables/conditions which influence the extraction yield.²³ To this end, a 2^3 (3 factors and 2 levels) factorial planning was executed. The parameters studied were the extraction time (t , min), solid-liquid ratio (S/L ratio, weight of dried biomass per weight of solvent) and IL concentration (C , M). The influence of the three variables on the extraction yields of HMR is illustrated in **Figure 3.2.4**. Variance analysis (ANOVA) was used to estimate the statistical significance of the variables and their interactions. The experimental points used in the factorial planning, the model equation, the extraction yield of HMR obtained experimentally and the respective calculated values, and the correlation coefficients obtained, as well as all the statistical analyses, are shown in the **Appendix A.2 (Tables A.2.4 to A.2.6, Figures A.2.1 to A.2.3)**. The R^2 value obtained is 0.954 and the average relative deviation between the experimental and the predicted values is 0.33%. Thus, no significant differences were observed between the experimental and calculated responses, supporting the good description of the

experimental results by the statistical models developed. The statistical analysis shown in the **Appendix A.2** and the data depicted in **Figure 3.2.4** show that the IL concentration is the most significant parameter, with a region of maximum extraction yield at moderate IL concentrations (1.5 M). In fact, this result is in close agreement with the ILs ability to act as hydrotropes,¹⁰ where a maximum in the solubility of biomolecules with the IL concentration is observed. The extraction time also influences the HMR extraction yield. In general, the amount of extracted HMR increases with time, reaching a maximum at 280 min. The solid-liquid ratio is also relevant, although with a behaviour that depends on the other variables. Albeit all parameters have a significant effect on the extraction yields of HMR, as can be seen in the pareto chart shown in the **Appendix A.2 (Figure A.2.1)**, their significance decreases in the order: C (M) > t (min) > S/L ratio. The optimized conditions found for the extraction of HMR at 25 °C are an IL concentration of 1.5 M, an extraction time of 280 min, and a solid-liquid ratio of 0.01, giving an HMR yield of 9.46 wt%. Regarding the evaluation of higher extraction times, as can be seen in the **Appendix A.2 (Table A.2.7)**, at the other optimized conditions the change of the extraction time does not bring significant differences in the HMR extraction yield, falling within the associated uncertainties. These results highlight the potential of IL aqueous solutions to extract HMR from biomass at mild conditions. It should be also noticed that this value is higher and in the same range to that obtained by soxhlet extraction with acetone (8.42 wt%), using longer extraction times (at least 360 minutes) and higher temperatures (60-80 °C).¹

We further investigated the reuse of the biomass (detailed experimental procedure is described in the **Materials and experimental procedure** Chapter, **section 2.1.2**, and detailed results are given in the **Appendix A.2, Figure A.2.4** and **Table A.2.8**) to ascertain if all HMR present was extracted in a single extraction step. Although we could use a soxhlet extraction to infer the total amount of HMR present in the studied biomass, this approach is not feasible since we obtained higher HMR extraction yields using the optimized operational conditions with IL aqueous solutions. Therefore, the best way to address if the total amount of HMR present in the biomass was extracted is to use several “fresh” and consecutive aqueous solutions of ILs aiming at avoiding limitations in the extractions that could arise from the solvents saturation. This type of experiments allowed us to conclude that the studied biomass contains *ca.* 10.5 wt% of HMR, as discussed below. As expected, when a lower solid-liquid ratio is used, the complete extraction of HMR from knots is almost achieved. However, to maximise the cost-efficiency and sustainability character of the developed process, it would be valuable to saturate the IL solution on the target compound; however, this variable was not considered in the multifactorial optimization. Thus, from a critical perspective, the use of a higher solid-liquid ratio is a better approach since the IL aqueous solution saturation is faster achieved, although in this approach

a small amount of HMR (2-3 wt%) still remains in the biomass and is lost. Even so, a lower quantity of solvent is employed, resulting thus in a lower consumption of solvents and on more sustainable extraction technologies. Envisaging the industrial application of the process under study, that should be economic and fast, a solid-liquid ratio 0.10 is the most advisable and was chosen to carry out the following studies.

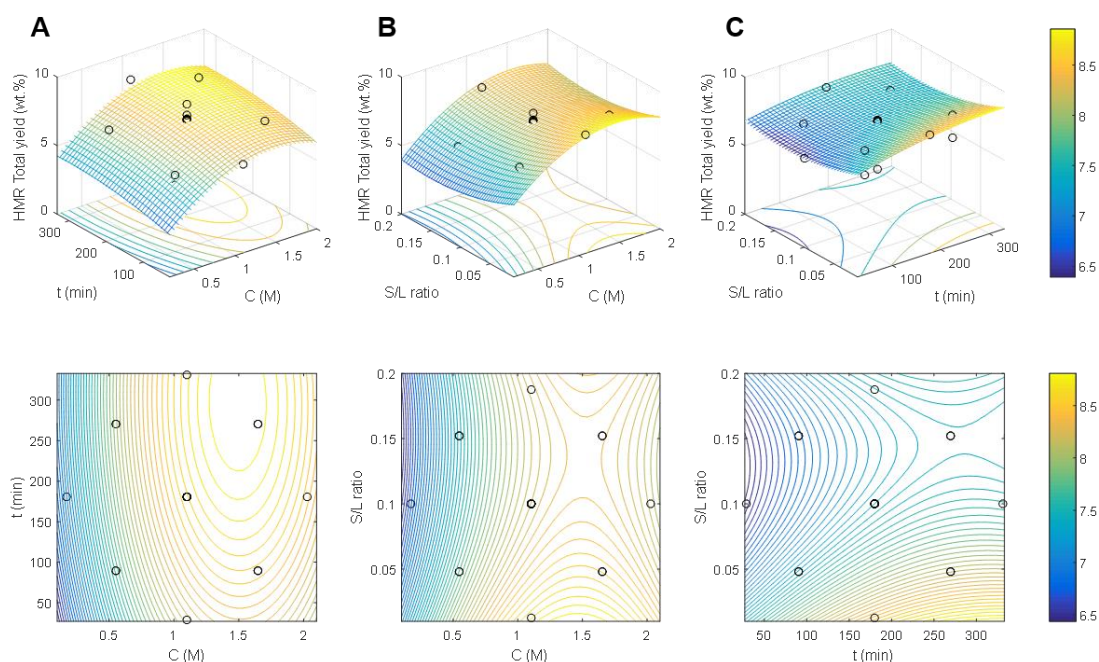


Figure 3.2.4. Response surface (top) and contour plots (bottom) on the yield of total HMR extracted using aqueous solutions of $[(C_2)_3NC_2]Br$ at 25 °C with the combined effects of: **(A)** extraction time (t (min)) and IL concentration (C (M)); **(B)** solid-liquid ratio (S/L ratio) and concentration (C (M)); and **(C)** solid-liquid ratio (S/L ratio) and extraction time (t (min)).

Aiming at developing a more cost-effective and environmentally-friendly extraction technique, the reusability of the extraction solvent without any pre-extraction step was investigated. The detailed experimental procedure is described in the **Materials and experimental procedure** Chapter, **section 2.1.2**, and detailed results are given in **the Appendix A.2 (Figure A.2.5)**. To this end, the 1.5 M $[(C_2)_3NC_2]Br$ aqueous solution was used in six successive extractions at the following operational conditions: solid-liquid ratio of 0.1 for 280 min at 25 °C. After each extraction, the solid-liquid mixture was filtered and the aqueous solution was reused with a new batch of Norway spruce knots. Remarkably, in the first five samples, *ca.* 7 wt% of HMR was extracted in each step, with the overall solution reaching a HMR total concentration around 5-times higher ($36.3 \text{ g}\cdot\text{L}^{-1}$). This means that the IL aqueous solution was far from saturation and can be reused for at least five times without any loss in extraction performance.

We also determined the HMR (standard) solubility at 25 °C in a solution of $[(C_2)_3NC_2]Br$ at 1.5 M, where a saturation value of $37.5 \text{ g}\cdot\text{L}^{-1}$ was found, supporting the experimentally demonstrated use of the IL aqueous solutions for five consecutive extraction steps.

In spite of the high efficiency of ILs aqueous solutions for the extraction of bioactive compounds, the non-volatile nature of aprotic ILs represents a major drawback when envisaging the target product recovery since a simple evaporation step cannot be applied.^{8, 24} There are some proposed alternatives for the recovery of the target products or IL removal, such as back-extraction using organic solvents,^{9, 25} distillation of the compounds,²⁶ induced precipitation with anti-solvents,^{27, 28} and adsorption on macroporous materials²⁹ or anion-exchange resins;³⁰ yet, some of these techniques are laborious and costly.⁸ Accordingly, we started by studying the possibility of precipitating HMR from the IL-aqueous solutions using potassium acetate (data shown in the **Appendix A.2, Figure A.2.6**), often used to form an adduct with HMR.^{31, 32} By applying this process we were able to recover 75% of the extracted HMR with a purity of 65%. However, considering that in this work we used biocompatible ILs derived from glycine-betaine, which are currently used as food supplements,¹⁹ and in cosmetic formulations,²⁰ and although a recovery step by the induced precipitation of HMR could be feasible as well as the IL recycling, we evaluated the possibility of using directly the aqueous IL-HMR-rich extracts without the need of an additional isolation/recovery step. To appraise this possibility, the biological properties (antioxidant activity and cytotoxicity) of the IL-HMR-extract aqueous solutions were assessed. The detailed experimental procedure is described in the **Materials and experimental procedure** Chapter, **section 2.1.2**.

The antioxidant activity of the aqueous solutions of ILs containing HMR, as well as of HMR extracts obtained from its recovery from the IL aqueous solutions or organic solvents, was determined using the 2,2-diphenyl-2-picrylhydrazyl hydrate (DPPH) radical scavenging assay, with ascorbic acid as the reference. The extracts obtained by acetone extraction and aqueous IL solutions show IC_{50} values on the same range, as show in **Figure 3.2.5** (details in **Appendix A.2, Table A.2.9**), and are not influenced by the presence of the IL (and as confirmed by null IC_{50} values of the aqueous solution of IL used as control). On the other hand, the precipitated extract from the IL aqueous solution presents the lowest antioxidant activity, further supporting the usefulness of directly using IL aqueous solutions containing HMR instead of recovering it, which also implies an additional step in the process. HMR is in indeed the major phenolic compound extracted from the selected biomass; yet, other phenolic compounds commonly found Norway spruce knots³³ can also be extracted while contributing to the higher antioxidant activity observed. Due to their lower amounts, they may not precipitate by the addition of potassium acetate. Moreover, according to Willför *et al.*³⁴ some synergistic effects may occur in less pure

extracts, thus leading to a higher antioxidant activity.³⁴ All HMR-rich extracts display a lower antioxidant capacity than ascorbic acid (**Figure 3.2.5**); however, when compared to other phenolic extracts, such as polyphenolic extracts obtained from *Terminalia chebula* (IC₅₀ of 14 µg·mL⁻¹),³⁵ *Cynara cardunculus* L. var. *altilis* (IC₅₀ of 34.3 ± 2.3 µg·mL⁻¹),³⁶ and *Malpighia emarginata* DC (405 to 1744 mg AAE 100 g⁻¹ of fruit),³⁷ we obtained a high antioxidant activity (21.8 ± 7.0 µg AAE mg⁻¹ of extract).^{1, 2, 6}

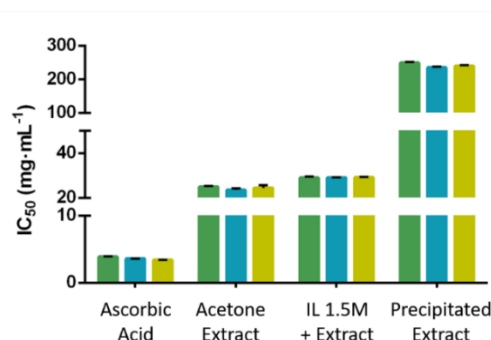


Figure 3.2.5. IC₅₀ values (mg·mL⁻¹) after 0.5 (green bars), 1.5 (blue bars) and 2h (yellow bars) of exposure to DPPH.

In order to address the potential applications of the IL aqueous solutions containing HMR, their cytotoxicity and cellular antioxidant/anti-inflammatory activity were determined. The detailed experimental procedure is described in the **Materials and experimental procedure** Chapter, **section 2.1.2**. A macrophage cell line was used since these cells are central players in inflammatory responses. When the cells are stimulated with a strong inflammation inducer, bacterial lipopolysaccharide (LPS), this leads to the production of reactive oxygen species (ROS) causing oxidative stress. This can be used as a tool to assess cellular antioxidant activity of the produced HMR-rich extracts. First, the cell viability was studied at different IL and extract concentrations (**Figure 3.2.6A**). For the HMR extract in aqueous IL solutions there is a decrease in the cell viability for concentrations above 100 µg·mL⁻¹ of HMR. This toxicity results from the presence of the IL since the precipitated HMR-rich extract does not affect the cells viability at higher concentrations. Cell viability assays were also carried out for aqueous solutions of [(C₂)₃NC₂]Br at different concentrations (**Figure 3.2.6B**), showing that concentrations of IL above 1.5 mM start to affect the cells. Nevertheless, and according to the US Food and Drug Administration (FDA), the HMR consumption by humans cannot exceed 500 µg·mL⁻¹, and at concentrations of 1000 µg·mL⁻¹, HMR causes an increase in adenylylase kinase (AK) activity which is responsible for the loss of cell membrane integrity.³⁸ Therefore, a daily maximum consumption of 1 mg *per* kg of body weight is recommended.³⁸ Then, it was studied the effect of the precipitated HMR-rich extract, [(C₂)₃NC₂]Br and HMR extract in aqueous [(C₂)₃NC₂]Br (all

at $100 \mu\text{g}\cdot\text{mL}^{-1}$) on the cellular oxidative stress, with the respective results provided in **Figure 3.2.7A**. In general, none of the samples shows oxidative damage in the cells at the tested concentrations, as shown by the lack of green colouration in the second and third lines of **Figure 3.2.7A**. Finally, we addressed the capacity of the precipitated HMR and HMR in IL aqueous solutions to reduce LPS-induced oxidative stress (**Figure 3.2.7B**). Overall, HMR has indeed considerable cellular antioxidant activity, reducing the LPS-induced production of ROS, as shown by the decrease of intensity in the cells' green colour, when compared with the cells stimulated only with LPS. The aqueous solution of $[(\text{C}_2)_3\text{NC}_2]\text{Br}$, on the other hand, does not display a significant antioxidant activity. These results are in agreement with the results obtained in the DPPH assays discussed above. Moreover, commercially available HMR has been tested in the ROS induced oxidative stress⁴ in THP-1 acute monocytic leukaemia cells, with similar results to ours, showing that with $100\text{--}300 \mu\text{M}$ ($0.37\text{--}1.12 \text{ mg}\cdot\text{mL}^{-1}$) of HMR there is a significant reduction of ROS levels. Thus, the HMR extracts in aqueous solutions of $[(\text{C}_2)_3\text{NC}_2]\text{Br}$ have a similar behaviour to a commercially available extract with a reported purity of 91%,⁴ confirming their potential for direct applications in nutraceutical formulations.

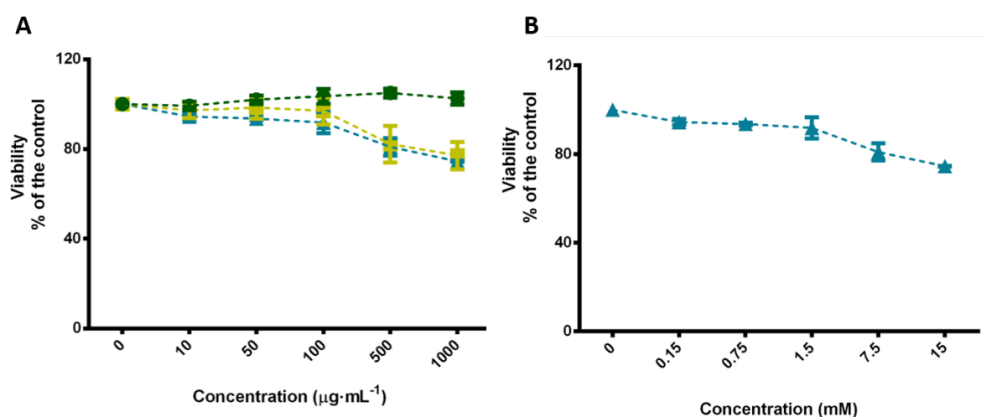


Figure 3.2.6. (A) Cell viability when exposed to increasing concentrations of pure IL (▲), HMR in the IL-water solution (■) and precipitated HMR-rich extract (●). (B) Cell viability when exposed to increasing concentrations of the IL (▲) used for the extractions of HMR.

Finally, the equation suggested by Passos *et al.*⁸ was used to evaluate the scale-up viability of the proposed extraction process. The proposed equation⁸ is a simplified model that relates the return associated to the extraction of a particular value-added compound when ILs are used as extraction solvents. In our case, the cost of the IL is the main factor behind the final product cost, mainly because we do not propose the recycling of the IL and instead it is in the final HMR-rich formulations. Therefore, for this process to be economically viable it is necessary to employ ILs with a cost lower than $11 \text{ €}\cdot\text{kg}^{-1}$, which is perfectly achievable if the process is scaled-up and

industrial reagents are acquired³⁹ (cf. the **Appendix A.2** with detailed information in the subsection “Analysis of the scale-up potential of the proposed process”).

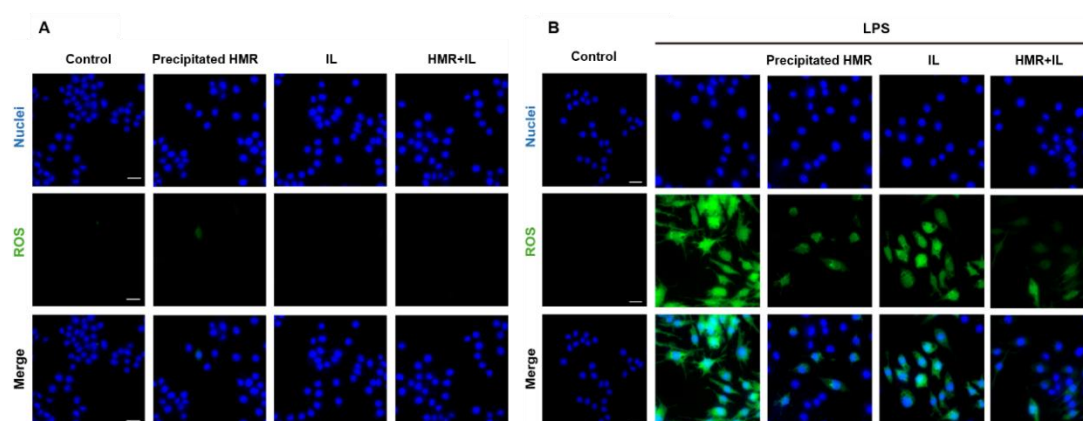


Figure 3.2.7. (A) Macrophage cellular oxidative stress in the presence of the different samples of HMR and pure IL. Scale bar: 20 μm . (B) Cellular oxidative stress in LPS-stimulated macrophages treated with precipitated HMR, HMR in IL solution and pure IL. Scale bar: 20 μm .

In summary, the cost-efficient extraction method presented here, summarized in **Figure 3.2.8**, using aqueous solutions of AGB-ILs instead of volatile organic solvents, opens new perspectives for the recovery of HMR from biomass sources, while envisaging their widespread use (at a lower cost) in cosmetic and nutraceutical applications. It should be however highlighted that after the extraction of the target HMR with IL aqueous solutions, the remaining biomass can further be used in other applications within an integrated biorefinery approach.

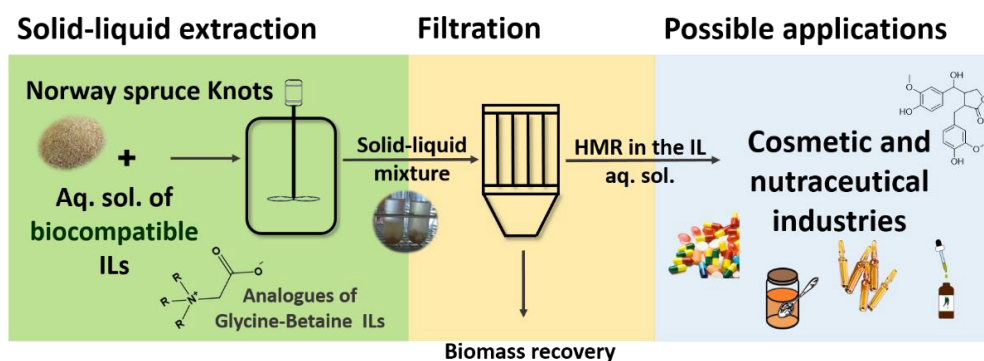


Figure 3.2.8. Schematic overview of the proposed process for the extraction of HMR from Norway Spruce knots using aqueous solutions of AGB-based ILs.

Conclusions

Aiming at developing a more sustainable approach for the HMR extraction from biomass, we here demonstrate the outstanding performance of ILs aqueous solutions as alternative solvents. A RSM was applied and the best results correspond to HMR extraction yields up to 9.45 wt%,

obtained at 25 °C using an aqueous solution of 1.5 M of $[(C_2)_3NC_2]Br$, a solid-liquid ratio of 0.01, and for 280 min. This yield is higher than that obtained with volatile organic solvents, using higher temperatures and with longer extraction times. Finally, the HMR extracts obtained, especially the HMR extract in $[(C_2)_3NC_2]Br$ aqueous solution, present a high antioxidant activity, and thus ROS damage inhibition in vitro, without being harmful to the cells, proving that aqueous solutions of ILs containing HMR have the potential to be safely used in cosmetic and nutraceutical applications. In summary, this study brings new perspectives on the use of aqueous solutions of appropriate ILs to replace the commonly used volatile organic solvents for the extraction of lignans and similar components from biomass, without requiring an additional step of the product recovery/isolation – a major drawback when dealing with non-volatile ILs.

References

1. S. M. Willför, A. I. Smeds and B. R. Holmbom, *J. Chromatogr. A*, 2006, **1112**, 64-77.
2. R. R. J. Arroo, A. W. Alfermann, M. Medarde, M. Petersen, N. Pras and J. G. Woolley, *Phytochem. Rev.*, 2002, **1**, 27-35.
3. S. Willför, L. Nisula, J. Hemming, M. Reunanen and B. Holmbom, *Journal*, 2004, **58**, 335.
4. M. Cosentino, F. Marino, R. C. Maio, M. Gioacchino Delle Canne, M. Luzzani, S. Paracchini and S. Lecchini, *Int. Immunopharmacol.*, 2010, **10**, 339-343.
5. E. Spilioti, B. Holmbom, A. G. Papavassiliou and P. Moutsatsou, *Mol Nutr Food Res*, 2014, **58**, 749-759.
6. B. Holmbom, S. Willfoer, J. Hemming, S. Pietarinen, L. Nisula, P. Eklund and R. Sjoeholm, *Materials, Chemicals, and Energy from Forest Biomass*, American Chemical Society, 2007, **954**, 350-362.
7. Y. Xiao and H. Zhang, *Anal. Chim. Acta.*, 2012, **712**, 78-84.
8. H. Passos, M. G. Freire and J. A. P. Coutinho, *Green Chem.*, 2014, **16**, 4786-4815.
9. A. F. M. Cláudio, A. M. Ferreira, M. G. Freire and J. A. P. Coutinho, *Green Chem.*, 2013, **15**, 2002-2010.
10. A. F. M. Cláudio, M. C. Neves, K. Shimizu, J. N. Canongia Lopes, M. G. Freire and J. A. P. Coutinho, *Green Chem.*, 2015, **17**, 3948-3963.
11. A. Romero, A. Santos, J. Tojo and A. Rodriguez, *J. Hazard. Mater.*, 2008, **151**, 268-273.
12. J. G. Huddleston, A. E. Visser, W. M. Reichert, H. D. Willauer, G. A. Broker and R. D. Rogers, *Green Chem.*, 2001, **3**, 156-164.
13. M. G. Freire, P. J. Carvalho, R. L. Gardas, I. M. Marrucho, L. M. N. B. F. Santos and J. A. P. Coutinho, *J. Phys. Chem. B*, 2008, **112**, 1604-1610.
14. D. Coleman and N. Gathergood, *Chem. Soc. Rev.*, 2010, **39**, 600-637.
15. P. G. Jessop, *Green Chem.*, 2011, **13**, 1391-1398.
16. A. Jordan and N. Gathergood, *Chem. Soc. Rev.*, 2015, **44**, 8200-8237.
17. Y. De Gaetano, A. Mohamadou, S. Boudesocque, J. Hubert, R. Plantier-Royon and L. Dupont, *J. Mol. Liq.*, 2015, **207**, 60-66.
18. K. Ressmann Anna, R. Zirbs, M. Pressler, P. Gaertner and K. Bica, *Z. Naturforsch. B*, 2013, **68**, 1129-1137.
19. J. R. Hoffman, N. A. Ratamess, J. Kang, S. L. Rashti and A. D. Faigenbaum, *J. Int. Soc. Sports Nutr.*, 2009, **6**, 7-7.
20. Z. F. Nsimba, M. Paquot, L. G. Mvumbi and M. Deleu, *Biotechnol. Agron. Soc. Environ.*, 2010, **14**, 737-748.
21. Chemspider, The free chemical database, <http://www.chemspider.com>, (accessed October 2016).
22. D. Coleman and N. Gathergood, *Chem. Soc. Rev.*, 2010, **39**, 600-637.
23. M. I. I. Rodrigues and A. Francisco, *Planejamento de Experimentos e Optimização de Processos*, Campinas, Brazil, 2005.
24. Q. Ren, H. Xing, Z. Bao, B. Su, Q. Yang, Y. Yang and Z. Zhang, *Chin. J. Chem. Eng.*, 2013, **21**, 937-952.
25. F. Postleb, D. Stefanik, H. Seifert and R. Giernoth, *Journal*, 2013, **68**, 1123.
26. J. Jiao, Q.-Y. Gai, Y.-J. Fu, Y.-G. Zu, M. Luo, W. Wang and C.-J. Zhao, *J. Food Eng.*, 2013, **117**, 477-485.
27. A. K. Ressmann, K. Strassl, P. Gaertner, B. Zhao, L. Greiner and K. Bica, *Green Chem.*, 2012, **14**, 940-944.

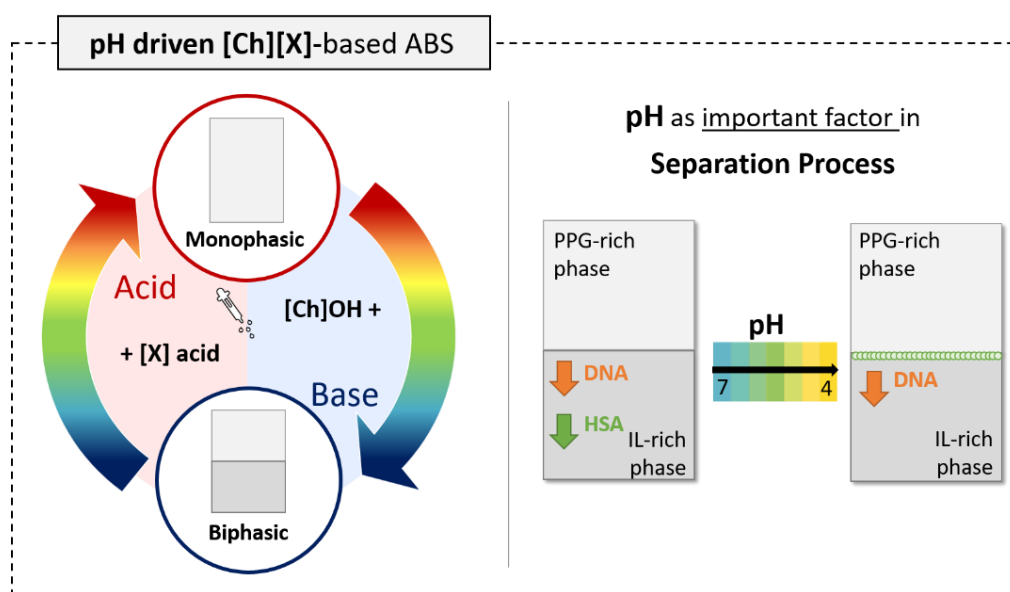
28. R. Ferreira, H. Garcia, A. F. Sousa, M. Petkovic, P. Lamosa, C. S. R. Freire, A. J. D. Silvestre, L. P. N. Rebelo and C. S. Pereira, *New J. Chem.*, 2012, **36**, 2014-2024.
29. C. Lu, X. Luo, L. Lu, H. Li, X. Chen and Y. Ji, *J. Sep. Sci.*, 2013, **36**, 959-964.
30. R. Zirbs, K. Strassl, P. Gaertner, C. Schroder and K. Bica, *RSC Adv.*, 2013, **3**, 26010-26016.
31. M. Cosentino, F. Marino, M. Ferrari, E. Rasini, R. Bombelli, A. Luini, M. Legnaro, M. G. D. Canne, M. Luzzani, F. Crema, S. Paracchini and S. Lecchini, *Pharmacol. Res.*, 2007, **56**, 140-147.
32. A. I. Smeds, I. Češková, P. C. Eklund and S. M. Willför, *Holzforschung*, 2012, **66**, 553-567.
33. S. Willför, J. Hemming, M. Reunanen, C. Eckerman and B. Holmbom, *Holzforschung*, 2003, **57**, 27-36.
34. S. M. Willfor, M. O. Ahotupa, J. E. Hemming, M. H. Reunanen, P. C. Eklund, R. E. Sjöholm, C. S. Eckerman, S. P. Pohjamo and B. R. Holmbom, *J. Agric. Food Chem.*, 2003, **51**, 7600-7606.
35. S. Saha and R. J. Verma, *J. Taibah Univ. Sci.*, 2016, **10**, 805-812.
36. P. A. B. Ramos, S. A. O. Santos, Â. R. Guerra, O. Guerreiro, C. S. R. Freire, S. M. Rocha, M. F. Duarte and A. J. D. Silvestre, *Ind. Crops and Prod.*, 2014, **61**, 460-471.
37. L. Delva and R. Goodrich-Schneider, *Int. J. Food Sci. Tech.*, 2013, **48**, 1048-1056.
38. H. M. C. Ltd, New Dietary Ingredient Notification for 7-Hydroxymatairesinol (HMR) Potassium Acetate Complex <http://www.fda.gov/ohrms/dockets/dockets/95s0316/95s-0316-rpt0235-05-Contents-vol167.pdf>, (accessed December 2016).
39. Alibaba, <https://www.alibaba.com>, (accessed March 2017).

4. REVERSIBLE IL-BASED ABS

4.1. pH-responsive aqueous biphasic systems formed by ionic liquids and polymers

Based on the manuscript under preparation:³

A. M. Ferreira, M. V. Quental, M. Sharma, D. Mondal, J. A. P. Coutinho and M. G. Freire.



Switchable pH-driven ionic-liquid-based aqueous biphasic systems and pH relevance on the design of effective separation platforms.

Abstract

Novel pH-triggered aqueous biphasic systems (ABS) composed of water, polypropylene glycol and cholinium-based ionic liquids (ILs) constituted by anions derived from carboxylic acids are here disclosed. Reversible phase transitions are achieved by the IL anion speciation at different pH values, promoted by the addition of the IL anion respective acid or cholinium hydroxide aiming at not changing the original species in aqueous media. Changes between homogeneous and biphasic regimes occur in a wide range of pH values and compositions, which can be tailored to a target separation process. Finally, it is shown the pH relevance in the design of these systems as effective separation platforms, in which the separation of deoxyribonucleic acid (DNA) from human serum albumin (HSA) may be achieved in a single-step.

³Contributions: M.G.F., J.A.P.C. and D.M. conceived and directed this work. A.M.F., M.V.Q. and M.S. acquired the experimental data. A.M.F., D.M., M.G.F. and J.A.P.C. interpreted the obtained experimental data. The manuscript was mainly written by A.M.F. and M.G.F. with contributions from the remaining authors.

Introduction

Large efforts have been carried out aiming at finding sustainable and efficient isolation/purification processes for biomolecules,¹ in which aqueous biphasic systems (ABS) can be considered. ABS are composed of two immiscible aqueous-rich phases, formed by polymer-polymer, polymer-salt or salt-salt mixtures in aqueous media.² ABS were first reported in the 50's as more benign liquid-liquid separation techniques for proteins, enzymes, viruses, cells, cell organelles, and other biological materials, mainly due to their water-rich environment.³ However, conventional ABS show a limited polarity range at the coexisting phases, hindering high extraction efficiencies to be attained in a single-step. This drawback may be overcome by employing ionic liquids (ILs) as phase-forming components of ABS⁴ since these can be tailored by taking advantage of the ILs designer solvents ability. IL-based ABS were first reported in 2003 by Rogers and co-workers.⁵ Compared to polymer-based ABS, IL-containing systems present additional advantages, such as low viscosity, rapid phase separation and high extraction efficiencies and selectivity.^{6,7} Although a large number of studies has been reported on IL-based ABS, most investigated systems are composed of imidazolium-based ILs and inorganic salts.⁷ Trying to overcome some of the toxicity and biodegradability concerns associated to these ILs and salts, more recently, novel ABS formed by more biocompatible species have been reported,⁸ e.g. formed by cholinium-based ILs and polymers. Cholinium-based ILs, designed from a water-soluble essential nutrient which supports several biological functions,⁹ may be tailored to be non-toxic and biodegradable. Polymers such as polyethylene glycol (PEG) or polypropylene glycol (PPG) are able to form ABS with ILs and display high biodegradability, low toxicity, low cost, relatively low melting temperatures, and low volatility.¹⁰⁻¹²

Although not explored up to date, cholinium-based ILs, if combined with anions that suffer speciation as a function of the pH, can be used to create reversible ABS. In fact, in the past few years, a large interest has been devoted to the investigation of reversible biphasic systems constituted by ILs, induced either by changes in pH, including the addition of CO₂/N₂, or temperature.¹³⁻¹⁹ Most of these works correspond however to binary systems formed by hydrophobic ILs and water^{14-16, 18, 19} or organic solvents.^{14, 17} Albeit additional advantages can be achieved with hydrophilic ILs and ternary systems such as ABS, namely a more effective tailoring of phase transitions by both applying external stimulus and playing with the ternary mixture compositions, the investigation of their reversible nature was lagged behind.¹³ Temperature-dependent reversible IL-based ABS have been reported, particularly formed by protic ILs and polymers.¹³ In addition to these, reversible IL-based ABS can be formed by employing phase-forming components susceptible to pH changes.

In this work we demonstrate the reversible nature of ABS formed by water, PPG 400 (polypropylene glycol with a molecular weight of $400 \text{ g}\cdot\text{mol}^{-1}$) and cholinium alcanoate ILs. All species were chosen so that the pH-driven phenomenon could be achieved by the IL anion speciation (by the addition of the respective acid or [Ch]OH to avoid changes in the species present in solution). Due to their biocompatible nature, the significant pH effect on these systems was further investigated to selectively separate deoxyribonucleic acid (DNA) from human serum albumin (HSA), relevant in the pre-treatment of human serum samples. Due to their relevance in molecular biology and gene therapy, in the last years, there has been an increased interest on the development of sustainable and cost-effective isolation methods for DNA.²⁰ Apart from being a biological information carrier, DNA has also been recognized as a key component in pharmaceutical applications and as a building block of functional materials.²¹⁻²³ Traditionally, the purification of nucleic acids requires the use of hazardous organic solvents, such as phenol, chloroform, formamide, dimethyl sulfoxide (DMSO), etc., which may additionally affect their structural integrity.²⁴ ILs have been already described as suitable solvents and storage media for DNA.²⁵⁻²⁸ Furthermore, Prasad and co-workers^{29, 30} demonstrated that cholinium-based ILs are able to preserve the structural integrity of DNA up to one year. These results suggest that cholinium-based ILs are appropriate solvents for DNA processing. However, no studies on the use of these ILs as phase-forming components of ABS to purify DNA have been found in the literature. There is however one report on the use of IL-based ABS to separate DNA,³¹ although the authors only carried out partition studies of pure DNA with these systems and used the water-unstable IL $[\text{C}_4\text{C}_1\text{im}][\text{BF}_4]$ ³² and the inorganic salt potassium dihydrogenphosphate (KH_2PO_4) as phase-forming components of ABS.

Results and discussion

Aiming at studying the possibility of moving from monophasic to biphasic regimes in IL-based ABS by a proper tailoring of the pH, the liquid-liquid phase diagrams of systems composed of water, PPG 400, and several hydrophilic ILs, namely $[\text{Ch}][\text{C}_1\text{CO}_2]$, $[\text{Ch}][\text{C}_2\text{CO}_2]$, $[\text{Ch}][\text{Lac}]$, and $[\text{Ch}][\text{Gly}]$ were determined at different pH values and at $25 \text{ }^\circ\text{C}$. $[\text{Ch}]\text{Cl}$ was also investigated as an ABS phase-forming component for comparison purposes. The definition of the ILs used is provided in the **List of acronyms**, and details about their synthesis procedure are given in the **Materials and experimental procedure** Chapter (**section 2.2.1**). Aiming at changing the pH, the IL anion corresponding acids were added as part of the aqueous solutions (*cf.* the **Materials and experimental procedure** Chapter, **section 2.2.1**). In summary, the reversible IL-based ABS here disclosed are reached by playing with the speciation of the IL anion. **Figure 4.1.1** shows the principle of the reversible process under investigation, where the transitions between the

monophasic and the biphasic regimes are attained by the alternate addition of an acidic (IL anion corresponding acid; in the example given it corresponds to acetic acid) or an alkaline ([Ch][OH]) species to the overall aqueous system. These compounds (IL anion corresponding acids and [Ch][OH]) were chosen to be able to change the pH of the aqueous medium while keeping the original species in the original systems.

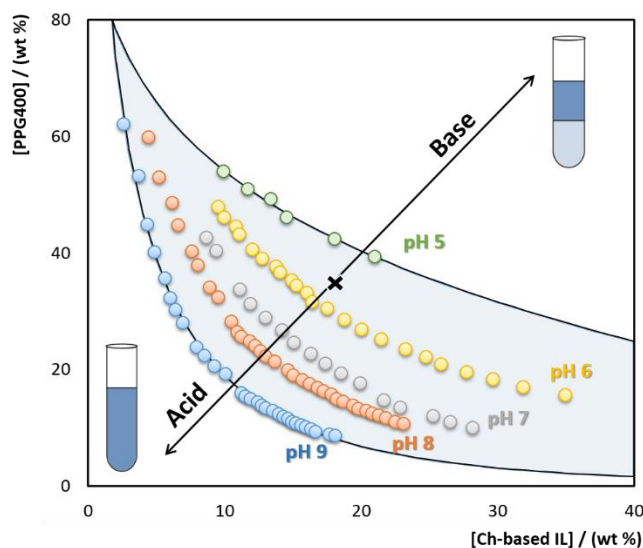


Figure 4.1.1. Phase diagrams of ABS composed of PPG 400 + water + [Ch][C₁CO₂] at pH ≈ 9 (●), pH ≈ 8 (●), pH ≈ 7 (●), pH ≈ 6 (●) and pH ≈ 5 (●).

The ternary phase diagrams at 25 °C for the ABS composed of [Ch][C₁CO₂] and PPG 400 at different pH values are illustrated in **Figure 4.1.1**. The detailed experimental procedure is given in the **Materials and experimental procedure** Chapter (**section 2.2.1**), and the remaining results, *i.e.*, the experimental weight fraction data, the representation of the phase diagrams for the remaining ILs, and a summary on the ability or non-ability of a given IL to form ABS at a specific pH value are given in the Appendix B.1 (**Tables B.1.1 to B.1.7**, and **Figure B.1.1**). For mixture compositions above each solubility curve there is the formation of a two-phase system, while mixture compositions below the same curve result in the formation of a homogeneous solution (no phase separation). In the studied ABS, the top phase corresponds to the PPG-rich aqueous phase while the bottom phase is mainly composed of IL and water.

From the overall results obtained it is clear that the pH decrease is not favourable for ABS formation. Higher pH values promote the two-phase formation since there is the IL anion deprotonation, resulting in stronger salting-out species according to the Hofmeister series,³³ and thus requiring lower amounts of IL or polymer to undergo liquid-liquid demixing. These findings are in agreement with previously published works on the evaluation of the pH effect in IL-based

ABS (although their switchable behaviour was not addressed).³⁴⁻³⁶ In general, and for all ILs, there is a decrease on the ability for ABS formation with the pH decrease (see **Appendix B.1, Figure B.1.1**). As expected, only the ABS composed of [Ch]Cl is weakly affected by a pH-driven phenomenon. The marginal decrease in the ability for ABS formation with [Ch]Cl as the pH moves towards the acidic region results from the HCl addition, which inherently means a less concentrated [Ch]Cl-based system. Furthermore, ILs constituted by the anions $[C_1CO_2]^-$ ($pK_{a1} = 4.54$) and $[C_2CO_2]^-$ ($pK_{a1} = 4.75$) are those that are only able to form ABS up to a pH value of 5, due to their higher pK_a values. On the other hand, ILs with $[Gly]^-$ ($pK_{a1} = 14.78$ and $pK_{a2} = 3.53$) and $[Lac]^-$ ($pK_{a1} = 14.59$ and $pK_{a2} = 3.78$) can go further and down to a pH value of 4 since their second pK_a values are smaller and, therefore, there is a larger amount of ionic species at lower pH values. In fact, and for all ILs studied, the ability for ABS formation as a function of pH is related to the pK_a of the acid corresponding to IL anion, *i.e.*, when completely protonated acids are present, there is no more formation of liquid-liquid systems (or their salting-out effect over the polymer).

After the determination of the ternary phase diagrams and evaluation of the pH effect, the reversible IL-based ABS behaviour was ascertained by the alternate addition of aqueous solutions of the acid which corresponds to the precursor of the IL anion studied and [Ch][OH]. Experimental details are given in the **Materials and experimental procedure Chapter (section 2.2.1)**. The pH-driven switchable behaviour of the studied systems is illustrated in **Figure 4.1.2**, using as example the [Ch][C_1CO_2]-based ABS. A mixture point in the biphasic region at $pH \approx 9$ was prepared (13 wt% [Ch][C_1CO_2] + 34 wt% PPG 400), resulting in a top PPG-rich phase and in a bottom IL-rich phase. An acetic acid aqueous solution (50 wt%) was further added down to $pH \approx 4$, resulting in a homogenous solution. Then, an aqueous solution of cholinium hydroxide (46 wt%) was added, ensuing the creation of a biphasic system again – *cf.* **Figure 4.1.2**. As previously highlighted, these compounds were chosen to be able to change the pH of the aqueous medium while maintaining the initial ABS species. Two dyes (sudan III and pigment blue 27) were added to the system shown in **Figure 4.1.2** to better allow the identification of the two phases. When the ABS is formed, sudan III preferentially migrates for the PPG-rich phase while pigment blue 27 partitions preferentially for the IL-rich phase, which is a direct result of their affinity for each phase as confirmed by their octanol-water partition coefficients (K_{ow}) ($\log(K_{ow})$ of sudan III = 7.47; $\log(K_{ow})$ of pigment blue 27: -0.26³⁷). The cyclic reversibility of these systems was proved, at least for three times, with small changes in the overall mixture compositions ($\pm 1-3.5$ wt%). In summary, it is possible to design reversible IL-based ABS playing around with the IL anion speciation, achieved at temperatures close to room temperature and using low-cost acids and bases. The large impact of the pH on these systems behaviour can be further tailored to design

effective separation platforms, as demonstrated below with an example on the separation of DNA from HSA.

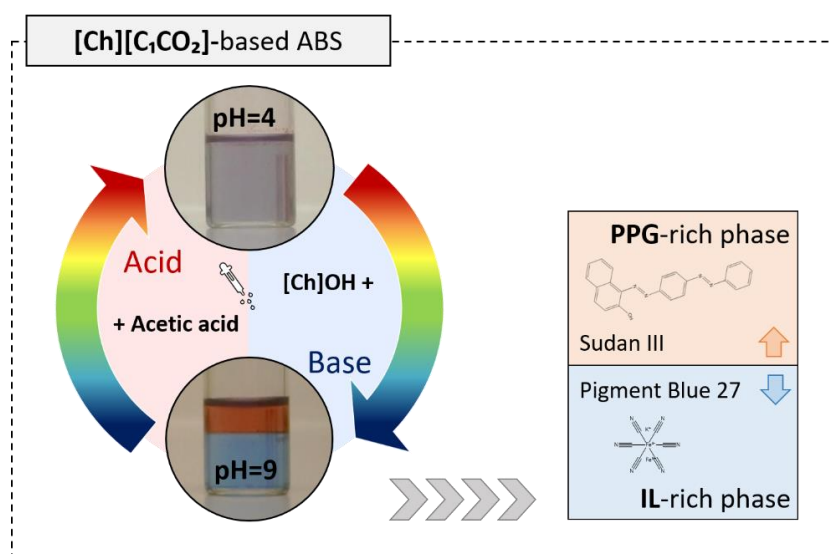


Figure 4.1.2. Illustration of the pH-driven behaviour of $[\text{Ch}][\text{C}_1\text{CO}_2]$ -based ABS; two dyes were added to better illustrate the phase separation.

After ascertaining the pH-triggered reversibility of IL-PPG-based ABS by the proper speciation of the IL anion, these systems were evaluated in what concerns their ability for the selective separation of mixtures of DNA and HSA. Both species are present in human serum and their separation is useful to improve the analysis of DNA.^{1,38} The extraction efficiency of the different IL-based ABS at different pH values (pH 1-9) for pure DNA and pure HSA was initially appraised. The pH was adjusted using the corresponding acid of each IL anion. Further experimental details are given in the **Materials and experimental procedure** Chapter (section 2.2.1). **Figure 4.1.3** depicts the percentage extraction efficiencies ($EE\%$) and recovery yields ($Y\%$) of the studied ABS for both DNA and HSA. The extraction efficiencies are defined as the percentage ratio between the total weight of DNA or HSA in the IL-rich phase to that in both phases, whereas the percentage yield is defined as the total percentage ratio between the total weight of DNA or HSA quantified in both liquid phases to that initially added. Detailed results are given in the **Appendix B.1 (Tables B.1.8 and B.1.9)**.

Remarkable extraction efficiencies of DNA to the IL-rich phase were obtained with all investigated systems, ranging between 90 and 100%, achieved in a single-step. Furthermore, no significant losses of DNA are observed, as appraised by the respective yields (100%). These results confirm a preferential migration of DNA to the IL-rich phase even when the IL acts as the salting-out species in the studied systems. This preferential affinity may be a direct result of preferential hydrogen-bonding and electrostatic interactions between ILs and DNA, as already

demonstrated by MacFarlane and co-workers.²⁷ The unique exception to this trend was observed for the ABS formed at pH 1 with [Ch]Cl, in which DNA is denatured.

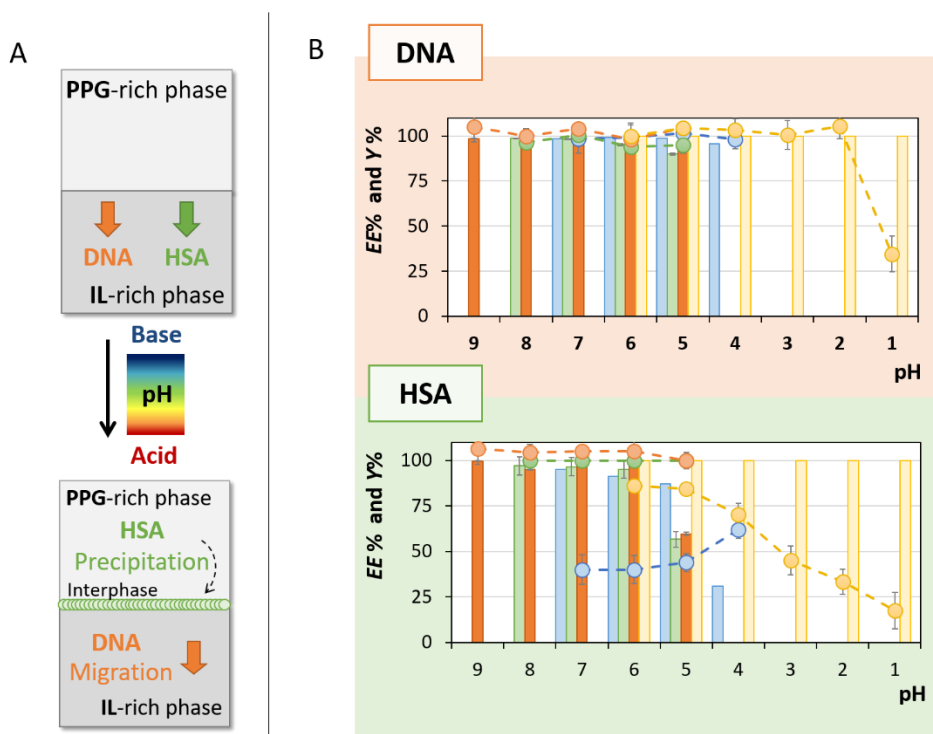


Figure 4.1.3. (A) Scheme of the separation of the DNA from HSA. **(B)** DNA extraction efficiency to the IL-rich phase ($EE\%$, bars) and HSA yield ($Y\%$, symbols) in ABS formed by: (orange bars) [Ch][C₁CO₂], (green bars) [Ch][C₂CO₂], (blue bars) [Ch][Gly] and (yellow bars) [Ch]Cl.

Anderson and co-workers³⁹ applied water-miscible ILs to DNA aqueous solutions, and then added LiNTf₂ to promote the *in situ* formation of a water immiscible IL, allowing the phase separation and the enrichment of DNA at the IL-rich phase (with an extraction efficiency of *ca.* 49%; calculated by us according to the definition given above). Solutions of DNA at low concentrations ($< 0.01 \text{ mg}\cdot\text{mL}^{-1}$) were preferentially used by the authors to be able to achieve the highest extraction efficiencies. The authors demonstrated that when using DNA solutions at higher concentrations ($> 0.1 \text{ mg}\cdot\text{mL}^{-1}$) the IL-rich phase reaches the saturation and, consequently, the extraction efficiency for DNA decreases down to 35% (calculated by us according to the definition given above).³⁹ In our work, we avoid the use of fluorinated species and the creation of water-immiscible ILs, we promote the phase separation by the addition of a biocompatible polymer, and higher DNA concentrations ($\approx 0.5 \text{ mg}\cdot\text{mL}^{-1}$) are used without saturation of the IL-rich phase. Furthermore, extraction efficiencies of 100%, *i.e.* the complete extraction of DNA, to the IL-rich phase, is achieved in a single-step.

Given the high performance of the systems to enrich DNA at the IL-rich phase, these systems were then optimized aiming at selectively separating DNA from HSA. They were then evaluated

in terms of extraction performance for HSA. The results obtained in terms of extraction efficiency and yield for HSA are given in **Figure 4.1.3**. With the exception of the system formed by [Ch]Cl, HSA preferentially partitions to the IL-rich phase at higher pH values, and gradually shifts to the polymer-rich phase with the pH decrease. The studied protein has a pI of 4.9,⁴⁰ meaning that when positively charged (acidic media) it prefers the polymer-rich phase whereas when negatively charged it prefers the IL-rich medium. Therefore, it seems that there are preferential interactions between the IL cation and the negatively charged protein at higher pH values responsible for its partition switch between the ABS coexisting phases. Interestingly, significant precipitation of HSA in the [Ch][Gly]- and [Ch]Cl-based ABS was also observed, particularly at acidic media, as identified by the low recovery yields shown in **Figure 4.1.3**. Both ILs are amongst the most hydrophilic ILs investigated, meaning that the respective PPG-rich phase has a lower water amount, being not suitable for the enrichment of the protein at this phase. In particular the system formed by [Ch]Cl, despite allowing a complete extraction of HSA to the IL-rich phase, leads to significant precipitation of the protein, creating a new protein-rich interphase and fitting within the IL three-phase partitioning approach.^{41, 42}

Based on all gathered results, the selective separation of DNA and HSA depends on two criteria: IL hydrophilicity and medium pH. If these conditions are properly tailored, DNA can be enriched at the IL-rich phase and the protein can be separated by inducing its precipitation. The best identified ABS is the one composed of [Ch][Gly]. It was additionally confirmed that DNA remains stable in presence of aqueous [Ch][Gly] solutions at pH values between 4 and 7 (**Appendix B.1, Figure B.1.3A**).

ABS formed by [Ch][Gly] at different pH values (7-4) were finally investigated to separate DNA from HSA mixtures (employing also different weight ratio of DNA to HSA, namely 1:1 to 1:5) – additional details are given in the **Materials and experimental procedure** Chapter, **section 2.2.1**. With the exception of the ABS at pH 7, all remaining systems allow to effectively separate DNA from HSA (detailed results given in **Appendix B.1; Figure B.1.2** and **Tables B.1.10** and **B.1.11**). After the extraction step, DNA was isolated from the IL-bottom phase using ice cold ethanol, re-dissolved in a phosphate buffer aqueous solution (0.01M, pH 7.2). The UV-Vis spectrum of DNA is characterized by a single characteristic absorbance band at 260 nm, while the purity of DNA may be appraised by the absorbance ratio at 260 nm and 280 nm. For pure DNA in water this value corresponds to 1.8.⁴³ It should be remarked that this assessment on purity is also based on the additional absorbance of the protein at 280 nm. As shown in **Figure 4.1.4A**, an increase in the DNA:HSA ratio in water leads to a decrease on the DNA purity. This is an expected trend given that cold ethanol also induces the precipitation of proteins. According to the data given in **Figure 4.1.4A**, the best system to purify DNA is the one formed by [Ch][Gly],

at pH 5. Furthermore, for the DNA:HSA weight ratio of 1:1, 1:2 and 1:3, it is possible to obtain DNA with a purity > 98%. To the best of our knowledge, there is only one work reporting on the use of IL-based ABS to purify DNA,³¹ however, DNA was recovered with lower purity (absorbance ratio at 260 nm and 280 nm = 1.7³¹). In addition to the higher DNA purity achieved by us, the [Ch][Gly]-PPG-based ABS investigated avoids the use of less benign imidazolium-based ILs paired with fluorinated anions and the use of high concentrations of inorganic salts.

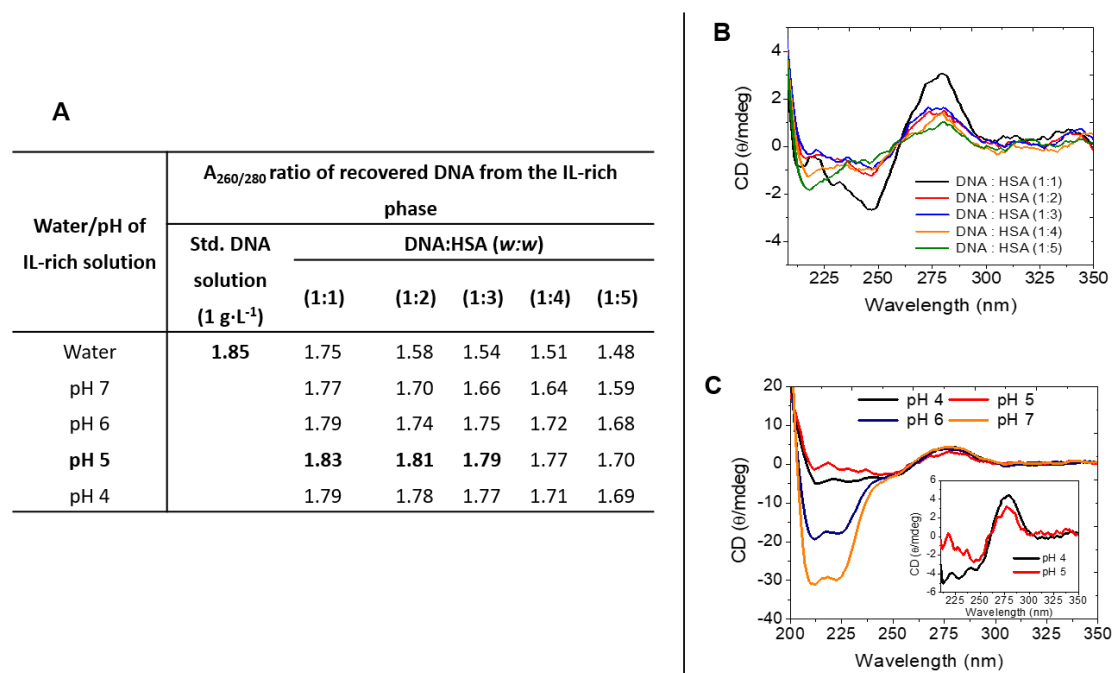


Figure 4.1.4. (A) A_{260} to A_{280} ratio for DNA samples after recovery from the IL-rich phase. (B) Circular dichroism (CD) spectra of samples of DNA:HSA at different weight ratio after recovery from the IL-rich phase at pH 5. (C) CD spectra of the DNA:HSA sample at a 1:1 weight ratio after recovery from the IL-rich phase at different pH values.

The structural and conformational stability of the recovered DNA was appraised by Circular dichroism (CD) - **Figures 4.1.4B** and **4.1.4C**. Further data are given in the **Materials and experimental procedure** Chapter (**section 2.2.1**). Also in terms of DNA stability, the best identified ABS is the one formed by [Ch][Gly] at pH 5, particularly at a DNA:HSA weight ratio of 1:1. The CD spectrum of stable β -form of DNA is characterized by a positive band at 277 nm, corresponding to π - π base interactions, and a less intense negative band at 246 nm, corresponding to the DNA helicity (see **Appendix B.1, Figure B.1.3A**, with the CD spectrum of DNA in PBS aqueous solutions). At these conditions, DNA with the highest purity (**Figure 4.1.4C** showing that HSA is not present) and stability (**Figure 4.1.3B** showing that the DNA β -form was not changed) was obtained. The long term stability of DNA (up to six months) at room temperature (*ca.* 25 °C) in the IL-rich phase was finally appraised (detailed data shown in

Appendix B.1, Figure B.1.3B). According to the respective CD spectra, there is no DNA conformational changes, confirming the structural and chemical stability of DNA for at least six months in the ABS IL-rich phase. It should be noted however that DNA stored in PBS aqueous solutions (0.01M, pH 7.2) was found to be degraded at the end of the six months of storage. These results support the potential of appropriate ILs aqueous solutions to act as preservation media of DNA, in agreement with previous results published by Sharma *et al.*³⁰. In summary, designed IL-based ABS can be used to separate DNA from complex matrices, and the respective IL-rich phase further used to preserve the nucleic acid up to use.

Conclusions

Novel pH-driven reversible ABS composed of water, polymers and ILs able to undergo speciation through their anion are here disclosed. The determined phase diagrams confirm that changes between homogeneous and biphasic regimes may occur in a wide range of pH values and compositions, which can be further tailored to a target separation process. The cyclic reversibility was demonstrated for at least three times, with no significant changes on the overall mixture composition. Taking advantage of the biocompatible nature of the phase-forming components and large pH impact on these systems behavior, they were finally investigated as separation platforms for relevant biomolecules, namely for the separation of DNA from HSA. Using the most promising ABS, DNA preferentially migrates to the IL-rich phase, maintains its structural integrity under storage at room temperature in the IL-rich phase for at least six months, and can be recovered with a purity > 98%. In summary, designed IL-based ABS at appropriate pH values can be used as simultaneous separation and preservation systems of relevant biopolymers.

References

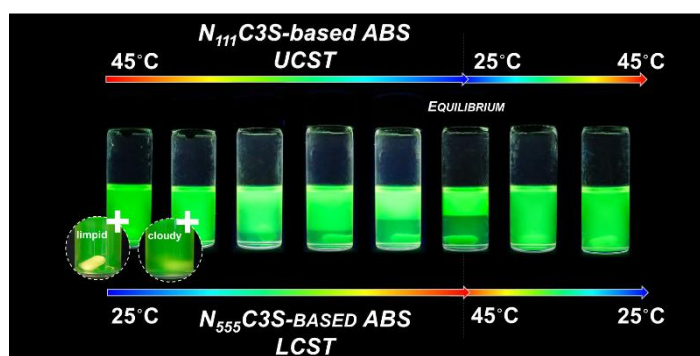
1. S. C. Tan and B. C. Yiap, *J. Biomed. Biotechnol.*, 2009, **2009**, 0-10.
2. M. Martínez-Aragón, S. Burghoff, E. L. V. Goetheer and A. B. de Haan, *Sep. Purif. Technol.*, 2009, **65**, 65-72.
3. P.-A. Albertsson, *Nature*, 1958, **182**, 709-711.
4. J. F. B. Pereira, L. P. N. Rebelo, R. D. Rogers, J. A. P. Coutinho and M. G. Freire, *Phys. Chem. Chem. Phys.*, 2013, **15**, 19580-19583.
5. K. E. Gutowski, G. A. Broker, H. D. Willauer, J. G. Huddleston, R. P. Swatloski, J. D. Holbrey and R. D. Rogers, *J. Am. Chem. Soc.*, 2003, **125**, 6632-6633.
6. R. D. Rogers and K. R. Seddon, *Science*, 2003, **302**, 792-793.
7. M. G. Freire, A. F. Cláudio, J. M. Araujo, J. A. P. Coutinho, I. M. Marrucho, J. N. Canongia Lopes and L. P. Rebelo, *Chem. Soc. Rev.*, 2012, **41**, 4966-4995.
8. J. R. Harjani, R. D. Singer, M. T. Garcia and P. J. Scammells, *Green Chem.*, 2009, **11**, 83-90.
9. J. K. Blusztajn, *Science*, 1998, **281**, 794-795.
10. M. T. Zafarani-Moattar, S. Hamzehzadeh and S. Nasiri, *Biotechnol. Prog.*, 2012, **28**, 146-156.
11. Z. Li, X. Liu, Y. Pei, J. Wang and M. He, *Green Chem.*, 2012, **14**, 2941-2950.

12. C. P. Song, R. N. Ramanan, R. Vijayaraghavan, D. R. MacFarlane, E.-S. Chan, J. A. P. Coutinho, L. Fernandez and C.-W. Ooi, *J. Chem. Thermodyn.*, 2017, **115**, 191-201.
13. H. Passos, A. Luís, J. A. P. Coutinho and M. G. Freire, *Sci. Rep.*, 2016, **6**, 1-7.
14. P. G. Jessop, S. M. Mercer and D. J. Heldebrant, *Energy Environ. Sci.*, 2012, **5**, 7240-7253.
15. P. Nockemann, B. Thijs, S. Pittois, J. Thoen, C. Glorieux, K. Van Hecke, L. Van Meervelt, B. Kirchner and K. Binnemans, *J. Phys. Chem. B*, 2006, **110**, 20978-20992.
16. S. Saita, Y. Kohno and H. Ohno, *Chem. Commun.*, 2013, **49**, 93-95.
17. D. E. Bergbreiter, P. L. Osburn, A. Wilson and E. M. Sink, *J. Am. Chem. Soc.*, 2000, **122**, 9058-9064.
18. T. V. Hoogerstraete, B. Onghena and K. Binnemans, *Int. J. Mol. Sci.*, 2013, **14**, 21353-21377.
19. D. Xiong, G. Cui, J. Wang, H. Wang, Z. Li, K. Yao and S. Zhang, *Angew. Chem. Int. Ed.*, 2015, **54**, 7265-7269.
20. M. Iqbal, Y. Tao, S. Xie, Y. Zhu, D. Chen, X. Wang, L. Huang, D. Peng, A. Sattar, M. A. B. Shabbir, H. I. Hussain, S. Ahmed and Z. Yuan, *Biol. Proced. Online*, 2016, **18**, 18.
21. P. W. K. Rothmund, *Nature*, 2006, **440**, 297-302.
22. D. Yang, M. J. Campolongo, T. N. Nhi Tran, R. C. H. Ruiz, J. S. Kahn and D. Luo, *Wiley Interdiscip. Rev. Nanomed. Nanobiotechnol.*, 2010, **2**, 648-669.
23. A. Chandran, D. Ghoshdastidar and S. Senapati, *J. Am. Chem. Soc.*, 2012, **134**, 20330-20339.
24. S. A. Markarian, A. M. Asatryan, K. R. Grigoryan and H. R. Sargsyan, *Biopolymers*, 2006, **82**, 1-5.
25. H. Zhao, *J. Chem. Technol. Biotechnol.*, 2015, **90**, 19-25.
26. H. Tateishi-Karimata and N. Sugimoto, *Nucleic Acids Res.*, 2014, **42**, 8831-8844.
27. R. Vijayaraghavan, A. Izgorodin, V. Ganesh, M. Surianarayanan and D. R. MacFarlane, *Angew. Chem. Int. Ed.*, 2010, **49**, 1631-1633.
28. K. Fujita and H. Ohno, *Chem. Commun.*, 2012, **48**, 5751-5753.
29. C. Mukesh, D. Mondal, M. Sharma and K. Prasad, *Chem. Commun.*, 2013, **49**, 6849-6851.
30. M. Sharma, D. Mondal, N. Singh, N. Trivedi, J. Bhatt and K. Prasad, *RSC Adv.*, 2015, **5**, 40546-40551.
31. D. J. Huang and D. C. Huang, *Future Material Research and Industry Application*, 2012, **455-456**, 477-482.
32. M. G. Freire, C. M. S. S. Neves, I. M. Marrucho, J. A. P. Coutinho and A. M. Fernandes, *J. Phys. Chem. A*, 2010, **114**, 3744-3749.
33. F. Hofmeister, *Arch. Exp. Pathol. Pharmacol.*, 1888, **24**, 247-260.
34. K. A. Kurnia, M. G. Freire and J. A. P. Coutinho, *J. Phys. Chem. B*, 2014, **118**, 297-308.
35. M. T. Zafarani-Moattar and S. Hamzehzadeh, *Fluid Ph. Equilibria*, 2011, **304**, 110-120.
36. S. Li, C. He, H. Liu, K. Li and F. Liu, *J. Chromatogr. B*, 2005, **826**, 58-62.
37. Chemspider, The free chemical database, <http://www.chemspider.com>, (accessed September 2017).
38. O. Nacham, K. D. Clark and J. L. Anderson, *Anal. Chem.*, 2016, **88**, 7813-7820.
39. T. Li, M. D. Joshi, D. R. Ronning and J. L. Anderson, *J. Chromatogr. A*, 2013, **1272**, 8-14.
40. C. P. Song, R. N. Ramanan, R. Vijayaraghavan, D. R. MacFarlane, E.-S. Chan and C.-W. Ooi, *ACS Sustain. Chem. Eng.*, 2015, **3**, 3291-3298.
41. E. Alvarez-Guerra and A. Irabien, *Separation of Proteins by Ionic Liquid-Based Three-Phase Partitioning*, Elsevier, Amsterdam, 2014, chapter 6, 207-234.
42. A. G. Enrique and I. Angel, *J. Chem. Technol. Biotechnol.*, 2015, **90**, 939-946.
43. W. W. Wilfinger, K. Mackey and P. Chomczynski, *BioTechniques*, 1997, **22**, 474-476.

4.2. Temperature-responsive aqueous biphasic systems composed of ammonium-based zwitterions and salts

Based on the published communication:⁴

A. M. Ferreira, H. Passos, A. Okafuji, M. G. Freire, J. A. P. Coutinho and H. Ohno, "Designing the thermal behaviour of aqueous biphasic systems composed of ammonium-based zwitterions", *Green Chem.*, 2017, **19**, 4012-4016.



Design of the thermal behaviour - from an upper critical solution temperature (UCST) to a lower critical solution temperature (LCST) - of aqueous biphasic systems composed of water-soluble ammonium-based zwitterions.

Abstract

The ability of water-soluble ammonium-based zwitterions (ZIs) to form aqueous biphasic systems (ABS) in presence of salts aqueous solutions is here disclosed. These systems are thermoreversible at temperatures close to room temperature and further allow the design of their thermal behaviour, from an upper critical solution temperature (UCST) to a lower critical solution temperature (LCST), by increasing the ZIs alkyl chains length. The investigated thermoreversible ABS are more versatile than typical liquid-liquid systems, and can be applied in a wide range of temperatures and compositions envisaging a target separation process. An example is given regarding their ability to selectively separate mixtures of aromatic and aliphatic amino acids in a single-step.

⁴**Contributions:** M.G.F., J.A.P.C. and H.O. conceived and directed this work. A.M.F., H.P. and A.O. acquired the experimental data. A.M.F., H.P., M.G.F. and J.A.P.C. interpreted the experimental data. The manuscript was mainly written by A.M.F., H.P., J.A.P.C and M.G.F. with contributions from the remaining authors.

Introduction

The use of ionic liquids (ILs) in liquid-liquid extractions has been a hot topic of research in the past decades.¹⁻⁶ Their unique properties, namely negligible vapour pressures, high thermal and chemical stabilities, and high solvation ability for a large range of compounds, make of ILs remarkable alternatives over volatile organic solvents. Furthermore, the possibility of changing the ILs properties by the structural design of both the cation and anion is considered one of their most interesting characteristics, allowing to tailor these fluids for specific applications.

Recently, it was proposed that the ILs properties could be further fine-tuned by using ILs mixtures.⁷ However, whenever IL-containing systems lead to the formation of more than one phase, ILs mixtures may lead to a different partitioning of their ions between the coexisting phases, leading therefore to changes in the composition of the phases.⁸ To overcome some of these unwanted trends, some authors⁸⁻¹³ proposed the use of zwitterions (ZIs), compounds where the cation and the anion are covalently tethered, instead of ILs. These ion pairs remain covalently linked even after adding strong acids, such as lithium salts¹⁴ and Brønsted acids.¹⁵

Since 2012, when Ohno and co-workers^{9, 10} proposed the use of ZIs as additives in IL-water systems to improve the water content in hydrophobic IL-rich phases, and consequently to increase the IL-phase ability to dissolve and extract proteins, several authors^{8, 11-13} addressed the study of ZIs applications in liquid-liquid extractions. In these works,⁸⁻¹³ ZIs with a high hydrophobic character were investigated, whereas more hydrophilic ZIs have been described as unable to induce phase separation with water, even by temperature changes. These compounds, that did not seem very attractive for use in liquid-liquid extractions from aqueous media, are here evaluated regarding their ability to form aqueous biphasic systems (ABS) with conventional salts. ABS were first reported in the 50's as more benign liquid-liquid separation processes for biomolecules due to their water-rich environment.¹⁶ These systems consist in two immiscible aqueous-rich phases, that are created by the mixture of two polymers, a polymer and a salt or two salts in aqueous media.^{17, 18}

In the past few years, the research on dynamic and reversible biphasic systems involving ILs or ZIs has attracted much attention towards the development of novel and more efficient separation processes, either by changes in pH,¹⁹ temperature^{8, 13, 20-22} or CO₂/N₂ addition.²³ Systems displaying an UCST- or LCST-type phase behaviour can be used to move between monophasic and biphasic regimes by inducing temperature-dependent phase transitions, shown to be highly advantageous for the separation of proteins,²⁰ metals²¹ and catalysts.²² However, most of the phase transitions in these systems occur at temperatures far from room temperature, or are confined to narrow mixture compositions. Therefore, the design of novel

systems with UCST- or LCST-type phase behaviour occurring at temperatures close to room temperature has been object of a great deal of work; yet, only a limited number of systems has been identified.^{13, 20, 24}

Herein we study the ability of water-soluble ammonium-based ZIs to form ABS by mixing them with salts (K_2HPO_4 , $K_3C_6H_5O_7 \cdot H_2O$, K_3PO_4 , K_2CO_3 , KH_2PO_4 , $Na_3C_6H_5O_7$ and $NaH_2PO_4 \cdot 2H_2O$) aqueous solutions. The definition of the salts is provided in the in the **List of acronyms**. Since the cation and anion of ZIs are covalently tethered, there is no ion exchange between the coexisting phases. The effect of temperature on the respective phase diagrams was also evaluated to appraise their thermal behaviour. Five ammonium-based ZIs with different alkyl side chains length (**Figure 4.2.1**) were synthesized and used in the creation of ABS. The definition of the ZIs acronyms is provided in the in the **List of acronyms**. The detailed synthetic procedure for their preparation is given in the **Materials and experimental procedure** Chapter (**section 2.2.2**). The chemical structure and purity of the ZIs were confirmed by 1H NMR and elemental analysis, and their thermal properties were evaluated by DSC and TGA (*cf.* the **Appendix B.2**, with detailed information in the subsection “NMR spectrum data of the synthesized ZIs”).

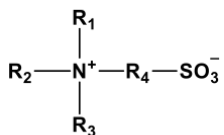
	Acronym	R_1, R_2, R_3	R_4
	$N_{111}C3S$	CH_3	$(CH_2)_3$
	$N_{111}C4S$	CH_2CH_3	$(CH_2)_4$
	$N_{222}C3S$	$(CH_2)_2CH_3$	$(CH_2)_3$
	$N_{333}C3S$	$(CH_2)_3CH_3$	$(CH_2)_3$
	$N_{555}C3S$	$(CH_2)_4CH_3$	$(CH_2)_3$

Figure 4.2.1. Chemical structures and acronyms of the ZIs used.

Results and discussion

The phase diagrams of ternary mixtures constituted by each ZI (**Figure 4.2.1**), each salt (K_3PO_4 , $K_3C_6H_5O_7$, K_2CO_3 , K_2HPO_4 and KH_2PO_4), and water, were initially determined at 25 °C to address the ability of water-soluble ammonium-based ZIs to create ABS. **Figure 4.2.2A** displays an example of the ternary liquid-liquid phase diagrams obtained. Further details on the experimental procedure are given in the **Materials and experimental procedure** Chapter (**section 2.2.2**), whereas detailed experimental weight fraction data and the representation of the remaining phase diagrams are given in the **Appendix B.2** (**Table B.2.2 to B.2.8**, **Figures B.2.1 and B.2.2**). All solubility curves are represented in molality units in order to better interpret the salting-in/-out effects obtained, while avoiding the effect of the different species molecular weights.

Figure 4.2.2A depicts the solubility curves for systems composed of $N_{555}C3S$, potassium-based salts and water, allowing the evaluation of the salt anion effect on the formation of ZI-based ABS. The solubility curves represent the limit between the monophasic and biphasic regimes, in which mixture compositions above the solubility curve result in biphasic liquid-liquid systems, and those below fall in the monophasic region. The larger the monophasic region of each phase diagram the higher is the amount of ZI and/or salt required to induce the ABS or two-phase formation. From the gathered results, and at the molality of ZI at which it equals the molality of salt in each binodal curve (*i.e.*, $[ZI] = [salt]$), the ability of the potassium-based salt anions to induce the formation of ABS follows the order: $PO_4^{3-} > C_6H_5O_7^{3-} > CO_3^{2-} > HPO_4^{2-} \gg H_2PO_4^-$. This salt anions trend is in good agreement with the Hofmeister series,²⁵ and with previously reported ranks for IL-based ABS.²⁶ This trend indicates that potassium-based salts act as salting-out species. In the studied systems composed of salts with high charge density ions and ZIs, the former are more able to create hydration complexes and to induce the salting-out of the more hydrophobic ZIs.

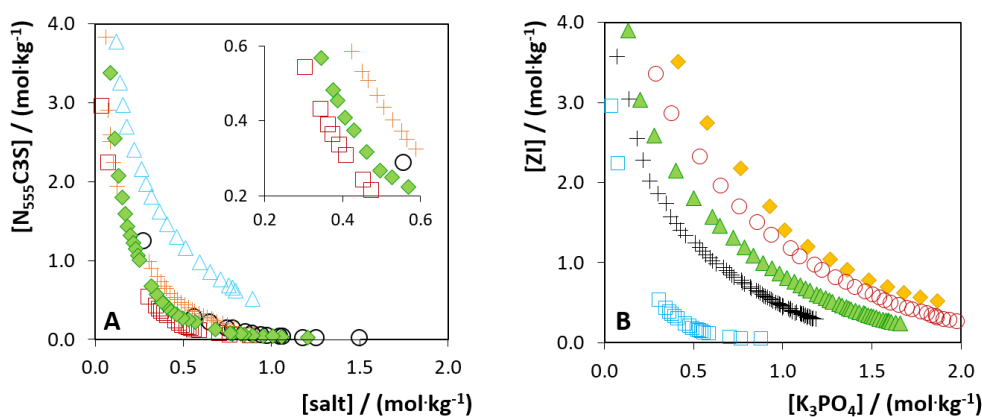


Figure 4.2.2. (A) Salt anion effect in the phase diagrams of ternary systems composed of water, $N_{555}C3S$ and potassium-based salts at 25 °C: K_3PO_4 (□), $K_3C_6H_5O_7$ (◆), K_2CO_3 (○), K_2HPO_4 (+) and KH_2PO_4 (△). **(B)** ZIs alkyl chains length effect in the phase diagrams of ternary systems composed of water, K_3PO_4 and ZIs at 25 °C: $N_{555}C3S$ (□), $N_{333}C3S$ (+), $N_{222}C3S$ (▲), $N_{111}C4S$ (○) and $N_{111}C3S$ (◆).

The phase diagrams obtained with the salts $Na_3C_6H_5O_7$ and $K_3C_6H_5O_7$, and KH_2PO_4 and NaH_2PO_4 , with a given ZI, allow us to address the salt cations ability to promote the formation of ZI-based ABS (**Appendix B.2, Figure B.2.2**). The results obtained demonstrate that the salt cation has no significant effect on the binodal curves of $N_{555}C3S$ -based ABS. However, when a more hydrophilic ZI is used, such as $N_{333}C3S$, the salting-out ability of the citrate-based salts cations follows the order: $Na^+ > K^+$, in good agreement with trends observed for IL-based ABS.²⁶

This trend was also verified with phosphate-based salts, in which only NaH_2PO_4 was able to induce phase separation with $\text{N}_{333}\text{C3S}$ – cf. the **Appendix B.2, Figure B.2.2**.

Figure 4.2.2B depicts the influence of the ZIs alkyl chain length on the formation of ABS with a given salt (K_3PO_4). The solubility curves show a strong dependency on the ZI alkyl side chains length – effect even more pronounced than that verified with the salt ions. At the solubility curve, namely when $[\text{ZI}] = [\text{salt}]$ ($\text{mol}\cdot\text{kg}^{-1}$), the tendency of ZIs to form ABS by the addition of K_3PO_4 follows the order: $\text{N}_{555}\text{C3S} > \text{N}_{333}\text{C3S} > \text{N}_{222}\text{C3S} > \text{N}_{111}\text{C4S} > \text{N}_{111}\text{C3S}$. The longer the cation/anion alkyl chains of the ZI, representing an increase in the ZI hydrophobicity and capability for being salted-out, the better it is their ability to undergo liquid-liquid demixing in presence of salts aqueous solutions. This trend also supports the loss in the ability to form ABS with salts of weaker salting-out strength displayed by ZIs with smaller alkyl side chains – cf. the **Appendix B.2, Figure B.2.2**.

After appraising the possibility of forming ZI-salt-based ABS, the temperature effect on this type of systems was studied. Additional phase diagrams were determined at 35 and 45 °C, and compared with the solubility curves obtained at 25 °C discussed above. The detailed experimental procedure is given in the **Materials and experimental procedure** Chapter (**section 2.2.2**), and the remaining results, *i.e.*, the weight fraction data, and the representation of the phase diagrams for the others ZIs, are given in the **Appendix B.2 (Table B.2.9 to B.2.11 and Figure B.2.3)**.

Figure 4.2.3 depicts the temperature dependency of the $\text{N}_{555}\text{C3S}$ -, $\text{N}_{333}\text{C3S}$ - and $\text{N}_{111}\text{C3S}$ - K_3PO_4 -based ABS phase diagrams. Remarkably, within the studied series of ZIs, a change in the temperature dependency was observed. For $\text{N}_{555}\text{C3S}$ -based ABS, an increase in temperature enlarges the two-phase region (**Figure 4.2.3A**), whereas the opposite effect is observed with $\text{N}_{111}\text{C3S}$ (**Figure 4.2.3C**). In this line, a negligible effect of temperature occurs in the $\text{N}_{333}\text{C3S}$ -based ABS (**Figure 4.2.3B**). It was previously shown that $\text{N}_{555}\text{C3S}$ presents a LCST-type phase transition behaviour with water⁸ and, consequently, the phase's separation is favoured at higher temperatures – a phenomenon that seems to prevail in the respective ABS. This behaviour is similar to that reported for polymer-salt ABS,^{27, 28} in which the temperature dependency is dominated by hydrogen-bonding interactions between the polymer and water. On the opposite, when more hydrophilic ZIs are used, such as $\text{N}_{222}\text{C3S}$, $\text{N}_{111}\text{C3S}$ and $\text{N}_{111}\text{C4S}$, an increase in temperature decreases the two-phase region of the respective ABS (**Figure 4.2.3C** and additional data in the **Appendix B.2, Figure B.2.3**), demonstrating the presence of an UCST-type phase behaviour in systems dominated by non-directional interactions. For ZIs of intermediate alkyl chains length, such as $\text{N}_{333}\text{C3S}$, the temperature seems to have a negligible impact upon the binodal curves, with their overlapping at different temperatures – **Figure 4.2.3B**. In summary, as

the ZIs hydrophobicity decreases, by the decrease of their alkyl side chains length, a shift in the dominant interactions between the ZIs and water occurs, from directional hydrogen bonding to non-directional interactions, allowing therefore the design of the thermal behaviour of ZI-based ABS.

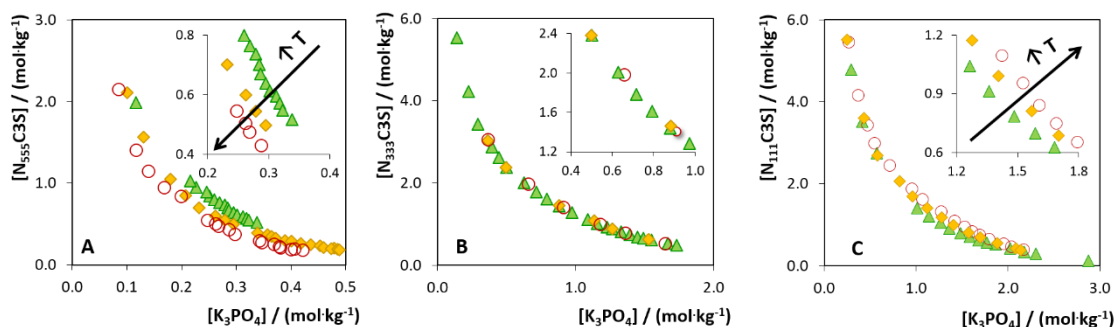


Figure 4.2.3. Temperature (T) effect in the phase diagrams of ternary systems composed of ZI + K_3PO_4 + water at 25 °C (▲), 35 °C (◆), and 45 °C (○): (A) $N_{555}C3S$, (B) $N_{333}C3S$, and (C) $N_{111}C3S$.

Upon the establishment of the temperature dependency of the studied ABS, their temperature-reversible behaviour was further appraised. A mixture point between the solubility curves at 25 and 45 °C was prepared for systems composed of $N_{555}C3S$ (30 wt% ZI + 4 wt% K_3PO_4) or $N_{111}C3S$ (19.5 wt% ZI + 19.5 wt% K_3PO_4). For the $N_{555}C3S$ + K_3PO_4 + water ABS, a mixture point between these two solubility curves results in a homogeneous solution at 25 °C – cf. **Figure 4.2.3**. However, when the temperature increases up to 45 °C, the phase separation occurs, resulting in a top ZI-rich phase and in a bottom salt-rich phase. If the temperature is decreased again to 25 °C, the initial monophasic system is recovered. Since $N_{111}C3S$ -based ABS presents the opposite temperature dependency behaviour, the formation of two phases occurs at lower temperatures (25 °C) that disappear on heating up to 45 °C. The thermoreversible behaviour of the studied systems is illustrated in **Figure 4.2.4**, for both $N_{555}C3S$ - and $N_{111}C3S$ -based ABS. A luminescent molecule – fluorescein – was added to each system to highlight the phase separation phenomenon by a change in temperature. Fluorescein partitions almost completely to the ZI-rich phases when the phases separation occurs.

The potential application of the studied thermoreversible systems was finally investigated to separate mixtures of amino acids that could exist in protein hydrolysates or in fermentation broths. As an example of this type of mixtures, aromatic and aliphatic amino acids, namely L-tryptophan (Try) and glycine (Gly), were studied. The previously described ABS mixture compositions were used. Details on the quantification of both amino acids are given in the **Materials and experimental procedure** Chapter (section 2.2.2). The obtained results are depicted in **Figure 4.2.5**. Data are shown in percentage extraction efficiencies ($EE_{AA}\%$) of each

amino acid for each phase. $EE_{AA}\%$ correspond to the percentage ratio between the amount of each amino acid in a given phase and that in the total mixture.

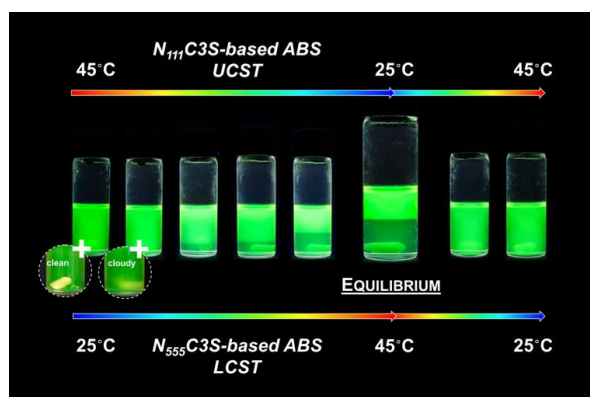


Figure 4.2.4. Illustration of the thermoreversible behaviour of ZI-based ABS.

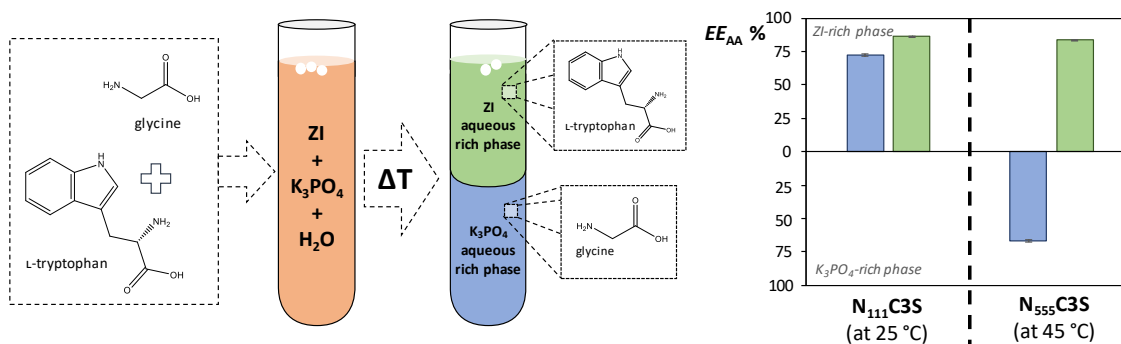


Figure 4.2.5. Partition of L-tryptophan (Try) and glycine (Gly) in $N_{111}C3S$ - and $N_{555}C3S$ -based ABS formed at 25 °C and 45 °C, respectively: $EE_{Try}\%$ (green bars), $EE_{Gly}\%$ (blue bars).

In general, there is a high impact of the ZI alkyl chain length on the separation performance of the studied ABS (Figure 4.2.5). In $N_{111}C3S$ -based ABS both amino acids preferentially partition to the ZI-rich phase, with extraction efficiencies ranging between 72 and 86%. However, in the $N_{555}C3S$ -based ABS, glycine partitions to the opposite phase ($EE_{AA}\% = 67\%$), the salt-rich phase instead of the ZI-rich phase, while the phase for which L-tryptophan partitions and its extraction extent ($EE\% = 84\%$) is almost not affected. The trends obtained are in good agreement with the hydrophilic/hydrophobic character of each amino acid ($\log(K_{ow})_{Try} = -1.09$ and $\log(K_{ow})_{Gly} = -3.41$, with K_{ow} defined as the octanol-water partition coefficient).²⁹ With the ZI alkyl chain length increase there is an increase in the hydrophobicity of the corresponding phase; therefore, an inversion on the partition trend of the most hydrophilic amino acid occurs, preferentially migrating to the more hydrophilic salt-rich phase. The selectivity of the $N_{111}C3S$ - and $N_{555}C3S$ -

based ABS for the separation of L-tryptophan from glycine are 2.4 and 6.8, respectively, meaning that an increase in the ZI alkyl chain length improves (3-fold increase) the selectivity of ABS (**Appendix B.2, Figure B.2.4**). In summary, the separation of aromatic (L-tryptophan) and aliphatic (glycine) amino acids can be achieved in a single-step using adequate ZI-based ABS, further supporting the tailoring ability of the investigated liquid-liquid systems.

Conclusions

It was here demonstrated that water-soluble ZIs can form ABS with aqueous solutions of salts, and that their thermoreversible behaviour can be designed by playing around with the ZI alkyl chains length, while allowing their tuning according to specific requirements of a given separation process, as demonstrated with their use in the separation of mixtures of amino acids. These reversible ZI-based ABS occur at temperatures close to room temperature, avoiding additional energetic consumptions or thermal degradation of some target products. Furthermore, the temperature range of operation can be selected based on the ternary mixture compositions to fit the requirements of a specific process and is not restricted to fixed temperatures imposed by the thermodynamic nature of binary liquid-liquid systems.

References

1. A. E. Visser, R. P. Swatloski, S. T. Griffin, D. H. Hartman and R. D. Rogers, *Sep. Sci. Technol.*, 2001, **36**, 785-804.
2. K. Nakashima, F. Kubota, T. Maruyama and M. Goto, *Anal. Sci.*, 2003, **19**, 1097-1098.
3. G. T. Wei, Z. Yang, C. Y. Lee, H. Y. Yang and C. R. Wang, *J. Am. Chem. Soc.*, 2004, **126**, 5036-5037.
4. J. Wang, Y. Pei, Y. Zhao and Z. Hu, *Green Chem.*, 2005, **7**, 196-202.
5. Y. Pei, K. Wu, J. Wang and J. Fan, *Sep. Sci. Technol.*, 2008, **43**, 2090-2102.
6. Y. Shimoyama, K. Ikeda, F. Su and Y. Iwai, *J. Chem. Eng. Data*, 2010, **55**, 3151-3154.
7. H. Niedermeyer, J. P. Hallett, I. J. Villar-Garcia, P. A. Hunt and T. Welton, *Chem. Soc. Rev.*, 2012, **41**, 7780-7802.
8. S. Saita, Y. Mieno, Y. Kohno and H. Ohno, *Chem. Comm.*, 2014, **50**, 15450-15452.
9. Y. Ito, Y. Kohno, N. Nakamura and H. Ohno, *Chem. Comm.*, 2012, **48**, 11220-11222.
10. Y. Ito, Y. Kohno, N. Nakamura and H. Ohno, *Int. J. Mol. Sci.*, 2013, **14**, 18350-18361.
11. D. Dupont, S. Raiguel and K. Binnemans, *Chem. Comm.*, 2015, **51**, 9006-9009.
12. D. Dupont, E. Renders and K. Binnemans, *Chem. Comm.*, 2016, **52**, 4640-4643.
13. Y. Mieno, Y. Kohno, S. Saita and H. Ohno, *Chem. Eur. J.*, 2016, **22**, 12262-12265.
14. M. Yoshizawa, M. Hirao, K. Ito-Akita and H. Ohno, *J. Mater. Chem.*, 2001, **11**, 1057-1062.
15. M. Yoshizawa and H. Ohno, *Chem. Comm.*, 2004, **0**, 1828-1829.
16. P. A. Albertsson, *Nature*, 1958, **182**, 709-711.
17. P. A. Albertsson, *Partitioning of Cell Particles and Macromolecules*, Wiley, New York, 3rd edn., 1986.
18. B. Y. Zaslavsky, *Aqueous Two-Phase Partitioning*, Marcel Dekker, Inc., New York, 1994.
19. A. M. Ferreira, A. F. M. Cláudio, M. Valega, F. M. J. Domingues, A. J. D. Silvestre, R. D. Rogers, J. A. P. Coutinho and M. G. Freire, *Green Chem.*, 2017, **19**, 2768-2773.
20. H. Passos, A. Luís, J. A. P. Coutinho and M. G. Freire, *Sci. Rep.*, 2016, **6**, 1-7.
21. P. Nockemann, B. Thijs, S. Pittois, J. Thoen, C. Glorieux, K. Van Hecke, L. Van Meervelt, B. Kirchner and K. Binnemans, *J. Phys. Chem. B*, 2006, **110**, 20978-20992.
22. D. E. Bergbreiter, P. L. Osburn, A. Wilson and E. M. Sink, *J. Am. Chem. Soc.*, 2000, **122**, 9058-9064.
23. P. G. Jessop, S. M. Mercer and D. J. Heldebrant, *Energy Environ. Sci.*, 2012, **5**, 7240-7253.

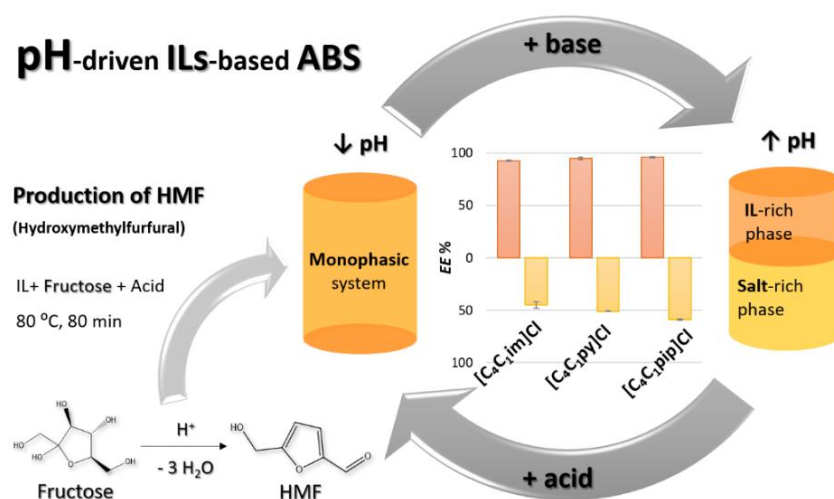
24. Y. Kohno and H. Ohno, *Chem. Comm.*, 2012, **48**, 7119-7130.
25. F. Hofmeister, *Arch. Exp. Pathol. Pharmacol.*, 1888, **24**, 247-260.
26. S. Shahriari, C. M. S. S. Neves, M. G. Freire and J. A. P. Coutinho, *J. Phys. Chem. B*, 2012, **116**, 7252-7258.
27. D. Fontana and G. Ricci, *J. Chromatogr. B Biomed. Sci. Appl.*, 2000, **743**, 231-234.
28. H. D. Willauer, J. G. Huddleston, M. Li and R. D. Rogers, *J. Chromatogr. B Biomed. Sci. Appl.*, 2000, **743**, 127-135.
29. Chempider, The free chemical database, <http://www.chemspider.com> (accessed July 2017).

5. INTEGRATED IL-BASED PROCESSES

5.1. Integrated production-separation platforms applying reversible pH-driven aqueous biphasic systems

Based on the published communication:⁵

A. M. Ferreira, A. F. Cláudio, M. Válega, F. M. J. Domingues, A. J. D. Silvestre, R. D. Rogers, J. A. P. Coutinho and M. G. Freire, "Switchable (pH-Driven) Aqueous Biphasic Systems formed by Ionic Liquids as Integrated Production-Separation Platforms", *Green Chem.*, 2017, **19**, 2768 - 2773.



pH-driven reversible aqueous biphasic systems are remarkable production-separation platforms and can be easily prepared by playing around with the speciation of at least one of the phase-forming components.

Abstract

The ability to induce reversible transitions between homogeneous solutions and biphasic systems is of paramount relevance in separation processes. In this context, pH-triggered aqueous biphasic systems (ABS) composed of ionic liquids (ILs) and salts are here disclosed as switchable mono/biphasic systems, and their potential application further demonstrated through an integrated approach comprising both the production and separation of hydroxymethylfurfural (HMF) from fructose.

⁵Contributions: M.G.F., J.A.P.C. and A.J.D.S. conceived and directed this work. A.M.F. acquired the experimental data. M.V. and F.M.J.D. helped in the HMF and fructose quantification by HPLC. A.M.F., A.F.C., R.D.R., M.G.F. and J.A.P.C. interpreted the experimental data. The manuscript was mainly written by A.M.F. and M.G.F. with contributions from the remaining authors.

Introduction

Liquid-liquid extraction processes are of technological simplicity and of low cost, and are frequently a preferred strategy in separation processes engineering.¹ Nevertheless, the use of molecular and volatile organic solvents in separation routes presents major drawbacks due to their high volatility and recurrent toxicity.² In this context, and in addition to their tailoring ability, ionic liquids (ILs) represent a viable alternative as a result of their non-volatile nature at ambient conditions.^{3, 4} The research in liquid-liquid extractions from aqueous media using ILs has been focused on two main approaches: (i) the direct use of non-water miscible hydrophobic ILs; and (ii) the use of aqueous biphasic systems (ABS) composed of ILs and organic/inorganic salts. Within the two types of systems, ABS constitute a “greener” and more benign option since they are mainly composed of water (up to 70 wt% in the overall system).⁵⁻⁸ Moreover, a more efficient « tuning of the phases polarities can be achieved with IL-based ABS, resulting in systems that usually allow the complete extraction and purification of a wide variety of compounds.⁵⁻⁸

More recently, there has been a large interest on the use/applications of dynamic and reversible mono/biphasic systems formed by ILs.⁹⁻¹¹ It was demonstrated that phase transitions in IL-containing mixtures can be induced by a temperature-driven phenomenon or by CO₂/N₂ flushing.¹²⁻¹⁶ Both upper critical solution temperature (UCST)¹⁷⁻¹⁹ and lower critical solution temperature (LCST)²⁰⁻²² phase behaviours have been reported for IL-solvent mixtures, whereas these temperature-dependent phase transitions have shown to be advantageous in the selective separation of proteins²³ and metals.²⁴ Reversible liquid-liquid systems have been also gathered with molecular solvents that react with CO₂ forming salts and/or ILs, and applied in the separation of aliphatic and aromatic amines¹²⁻¹⁴, and in the synthesis/separation of gold (Au) porous films.¹⁵ However, common UCST and LCST behaviours in systems involving ILs typically occur at temperatures well above room temperature and a high energy input is required to trigger their phase switch, while the CO₂/N₂-dependent reversibility pattern requires the use of specific equipment. Furthermore, these systems are usually composed of an IL-rich phase (typically with hydrophobic characteristics) and a more hydrophilic molecular-solvent-rich phase.^{18, 20-24} These systems are thus restricted in polarity differences amongst the coexisting phases, hindering improved extraction and selectivity performances to be obtained when dealing with the separation/fractionation of complex matrices. In this line, IL-based ABS can be seen as promising options, although the investigation on their use as reversible systems lagged behind. To the best of our knowledge, only temperature-dependent reversible behaviours of IL-based ABS have been reported.²⁵ Contrarily to most IL-based ABS, which display a weak dependence on temperature, it was recently found²⁵ that ABS formed by protic ILs and polymers

are highly temperature dependent, allowing therefore to trigger reversible phase separations by small changes in temperature.

Given the potential of applications of switchable (aqueous-rich) biphasic systems discussed above, in this work we demonstrate the reversibility of IL-based ABS attained by a pH-driven phenomenon and their use as integrated platforms, comprising both the production and separation of 5-hydroxymethylfurfural (HMF) from fructose.

Results and discussion

Aiming at evaluating the possibility of moving from monophasic to biphasic regimes (and *vice-versa*) by a proper tailoring of the pH of the aqueous media, ABS formed by a wide range of chloride-based ILs and potassium citrate/citric acid were investigated. The chemical structures of the investigated ILs are given in **Figure 5.1.1**. The definition of the ILs acronyms is provided in the **List of acronyms**. ILs with no speciation capability were chosen, and as such, the pH-triggered reversible phenomenon is a result of the salt (potassium citrate) speciation as a function of the pH. Citric acid presents 4 acidic dissociation constants (pK_a) values, namely 3.05, 4.67, 5.39 and 13.92.²⁶ The speciation curves of citric acid are depicted in the **Appendix C.1 (Figure C.1.1)**. At pH values lower than 3.05, the non-charged citric acid is the dominant species present, whereas at pH values above 3.07, 4.67 and 5.39, there is the prevalence of the monovalent, divalent and trivalent charged dihydrogencitrate, hydrogencitrate and citrate anions, respectively. All these citrate-based species can be ranked within the Hofmeister series,⁶ in which higher charge density and higher charge valence anions are better hydrated and stronger salting-out species, being thus more favourable to the creation of IL-based ABS. In fact, previous works have been published on the pH effect towards the formation of IL-based ABS,²⁷⁻²⁹ although no investigations on their reversible behaviour have been carried out hitherto. To be able to change the pH in the investigated ABS and to trigger the phase transition while avoiding the introduction of new species into the overall system, citric acid ($C_6H_8O_7$) and potassium hydroxide (KOH) were here used. The pair potassium citrate/citric acid also was selected due to their biodegradable and non-toxic characteristics.³⁰

Figure 5.1.2 sketches the principle of the reversible process under investigation, where the transitions between the monophasic and the biphasic regimes could be attained by the alternate addition of an acidic or an alkaline species to the overall aqueous system. For mixture compositions above each solubility curve there is the formation of a two-phase system at given conditions, while mixture compositions below the same curve result in the formation of a homogeneous solution (no phase-separation).

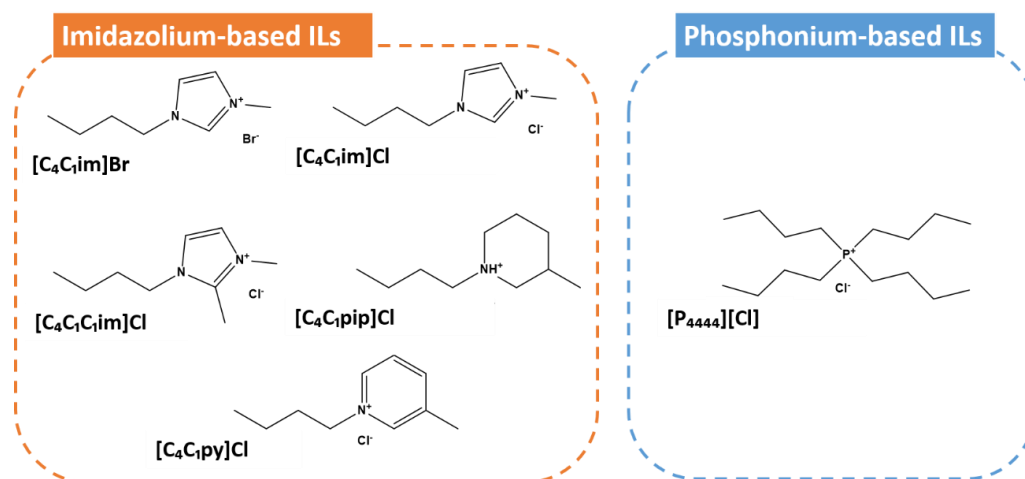


Figure 5.1.1. Chemical structures of the ILs investigated.

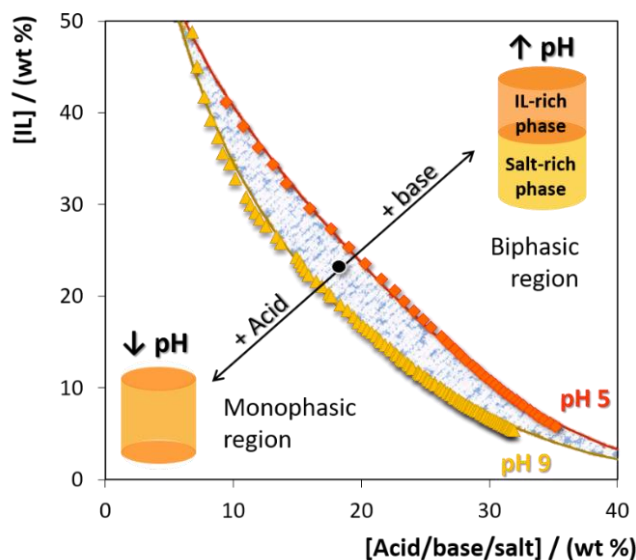


Figure 5.1.2. Ternary phase diagrams of an IL-based ABS at 25 °C, at pH \approx 9 (\blacktriangle) and pH \approx 5 (\blacklozenge). In all the investigated ABS, the top phase corresponds to the IL-rich phase while the bottom phase is mainly composed of salt and water.

We firstly determined the liquid-liquid ternary phase diagrams at different pH values of ABS composed of ILs + $K_3C_6H_5O_7/C_6H_8O_7$ + water. These were determined at pH values ranging between 5 and 9 for the following hydrophilic ILs: $[C_4C_1im]Cl$, $[C_4C_1C_1im]Cl$, $[C_4C_1pip]Cl$, $[C_4C_1py]Cl$, $[C_4C_1im]Br$ and $[P_{4444}]Cl$. Further details on the experimental procedure adopted are provided in the **Materials and experimental procedure** Chapter (section 2.3.1).

The ternary phase diagrams at 25 °C for the ABS composed of $[P_{4444}]Cl$ at different pH values are illustrated in Figure 5.1.3. The depicted ABS phase diagrams at the most acidic pH values

also denote the limit in compositions and pH values for which ABS no longer form. The experimental weight fraction data, as well as the representation of the phase diagrams for the remaining ILs, are given in the **Appendix C.1 (Table C.1.1 to C.1.11 and Figure C.1.2)**. All the phase diagrams were further characterized by the determination of tie-lines to infer on the phases compositions for given mixture compositions (*cf.* the **Appendix C.1, Tables C.1.12 and C.1.13**). In general, and for all ILs, there is a decrease on the ability for ABS formation with the pH decrease - the higher the pH of the aqueous medium the larger is the biphasic region, and the lower the IL/salt amounts required to induce phase separation. Given that ILs with no speciation capability have been chosen, the observed dependency of the ABS formation on the pH is related to the speciation performance of potassium citrate. As discussed before, at pH values lower than 3.05 and 4.07, the non-charged citric acid and monovalent dihydrogen citrate anion are, respectively, the prevalent species, and none of these species is able to form ABS with the ILs investigated. At pH values above 4.67 and 5.39 there is the main presence of the divalent and trivalent charged hydrogencitrate and citrate anions, respectively. IL-based ABS are only formed at pH values higher than 5, meaning that only the divalent and trivalent citrate-based anions induce phase separation. This behaviour is in agreement with the Hofmeister series⁶ since higher charge density and higher charge valence anions are stronger salting-out species able to induce the salting-out of the IL, further resulting in the creation of IL-based ABS.

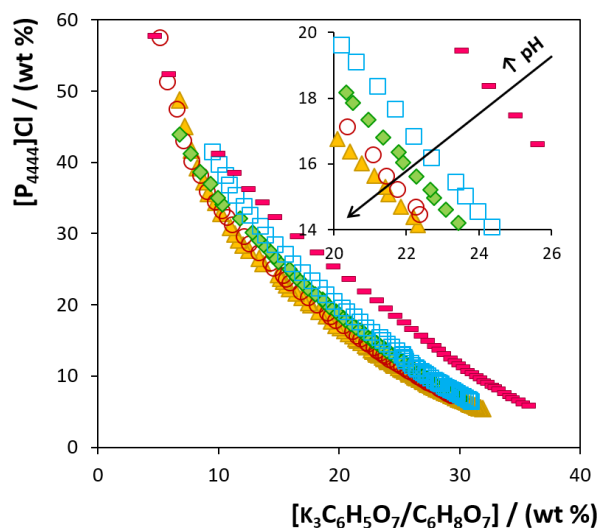


Figure 5.1.3. Phase diagrams of ABS composed of $[P_{4444}]Cl$ + water + $K_3C_6H_5O_7/C_6H_8O_7$ at pH ≈ 9 (\blacktriangle), pH ≈ 8 (\circ), pH ≈ 7 (\blacklozenge), pH ≈ 6 (\square) and pH ≈ 5 (\blacksquare).

At a fixed pH, the IL ability to form ABS follows the order: $[P_{4444}]Cl > [C_4C_{1m}]Br > [C_4C_{1py}]Cl \approx [C_4C_{1pip}]Cl > [C_4C_{1C_{1im}}]Cl \approx [C_4C_{1im}]Cl$ (*cf.* the **Appendix C.1, Figure C.1.3**). More hydrophobic ILs, resulting either from cations with longer and more aliphatic moieties or from anions of lower

hydrogen-bond basicity^{31, 32}, are more capable of forming ABS, *i.e.* are able to form two-phase systems at lower pH values or require lower amounts of the phase-forming components for phase separation. Examples of this are seen with [P₄₄₄₄]Cl and [C₄C₁im]Br, the only two ILs that form ABS at pH 5. On the other hand, ILs such as [C₄C₁im]Cl and [C₄C₁C₁im]Cl, which are amongst the most hydrophilic ILs investigated, do not form ABS even at a pH of 6, being 7 the minimum pH value required for ABS formation with these ILs. This pattern also mirrors the salting-out effect of the citrate-based salt over the IL.⁵⁻⁸ A summary of the overall results according to the ability of each IL to form ABS at all studied pH values is given in the **Appendix C.1 (Table C.1.14)**.

After establishing the ternary phase diagrams, which describe the mixture compositions and pH values for which the liquid-liquid demixing occurs, the reversible IL-based ABS behaviour was appraised by the alternate addition of citric acid and potassium hydroxide. For this purpose, an initial ternary mixture at the biphasic region (IL at 25 wt% + K₃C₆H₅O₇ at 35 wt% + water at 40 wt%) was prepared and allowed for phase separation at 25 °C. At this initial mixture composition the pH values of the aqueous media of all IL-containing systems are *ca.* 9. An aqueous solution of citric acid at 50 wt% was added dropwise, under constant agitation, until the mixture became homogeneous (monophasic). Then, an aqueous solution of potassium hydroxide at 50 wt% was added, under agitation, to recover the initial pH value of 9 and the biphasic system. During these manipulations the pH of the aqueous solutions was experimentally controlled. **Figure 5.1.2** depicts the procedure carried out to attain the reversible process under investigation. It should be remarked that the differences in the phases' compositions are negligible after each addition step since a small amount of each aqueous solution (± 0.6 wt%) is enough to trigger the phase transition. The pH-driven reversibility was experimentally confirmed with all the ILs investigated, at least 3 times, with no significant changes in the phases' composition.

In summary, it is possible to prepare reversible IL-based ABS playing around with the speciation behaviour of the organic salt. This phase reversibility takes place at room temperature (25 °C) and is achieved with cheap compounds already present in the original mixture and with no need of sophisticated equipment. Hence, IL-based ABS can be envisaged as potential alternatives to the more complex reversible systems that require additional energy inputs or the addition of gases and more specific equipment. Their reversibility is however a major advantage in liquid-liquid extractions to attain selective separations, and as demonstrated hereinafter.

We investigated the possibility of using the proposed systems for the production of hydroxymethylfurfural (HMF) through fructose dehydration at acidic pH, and then to proceed with an integrated separation step of HMF from the unreacted precursor by an increase in the pH and consequent formation of two-phase systems. The dehydration of carbohydrates (*e.g.*

cellulose, glucose, fructose, sucrose, inulin, and cellobiose) to produce HMF has attracted large attention in the past few years.^{33, 34} In fact, HMF is nowadays considered a key biomass-derived building block relevant in bio-based industries.^{33, 35} The current applications of HMF are widespread and comprise the production of solvents³⁶, biofuels (dimethylfuran),³⁷ polymeric materials (mainly based on its 2,5-furandicarboxylic acid derivative),³⁸ fine chemicals³⁹, among others. Recently, a short-time synthesis of the active pharmaceutical ingredient ranitidine (Zantac) also was reported making use of HMF.⁴⁰ Typically, HMF is produced from fructose via a dehydration reaction, generally catalysed by acids (pH values ranging between 1.5 and 3).⁴¹ However, high temperatures (> 200 °C), reduced pressure and long reaction times are usually required.⁴¹ More recently, IL-acid mixtures or acidic ILs have been used for sugars dehydration and production of HMF in high yields, obtained at lower temperatures (< 120 °C) and within short reaction times.⁴² Although good results using ILs for the fructose dehydration have been described, the development of a cost-effective, integrated and more sustainable production-separation process is still in crucial demand. In this line, we propose herein the discussed switchable ABS as an integrated and more benign platform for the production and separation of HMF.

The production of HMF was carried out through fructose dehydration in acidic medium (pH *ca.* 1.5), at 80 °C for 80 min, in the IL-based ABS monophasic regions. After reaction, an aqueous solution of KOH was added to stop the reaction and to move the system into the biphasic region by a pH increase – **Figure 5.1.2**. The creation of two-phase systems is intended for the selective separation (migration for opposite phases) of HMF and unreacted fructose. Further experimental details are given in the **Materials and experimental procedure** Chapter (**section 2.3.1**).

Figure 5.1.4 depicts the results on the production of HMF in citric acid aqueous solutions at the monophasic region (corresponding to a mixture composition of 40 wt% of IL + 30 wt% of citric acid). The respective reactions were also carried out in the absence of ILs, as well as in the absence of citric acid, for comparison purposes. As shown, the use of an acidic medium is required for the production of HMF through the dehydration of fructose – when no acid was used a maximum yield of 0.00281 g·L⁻¹ of HMF was obtained. On the other hand, without IL, a maximum yield of HMF of 2.28 g·L⁻¹ was found. However, when ILs are used in acidic medium, HMF yields ranging between 4.61 and 6.37 g·L⁻¹ have been observed, supporting the need of the presence of both the IL and the acidic medium to maximise the HMF production yield. These results are consistent with previous studies describing the requirement of the addition of ILs and acid catalysts to obtain high HMF yields.^{42, 43}

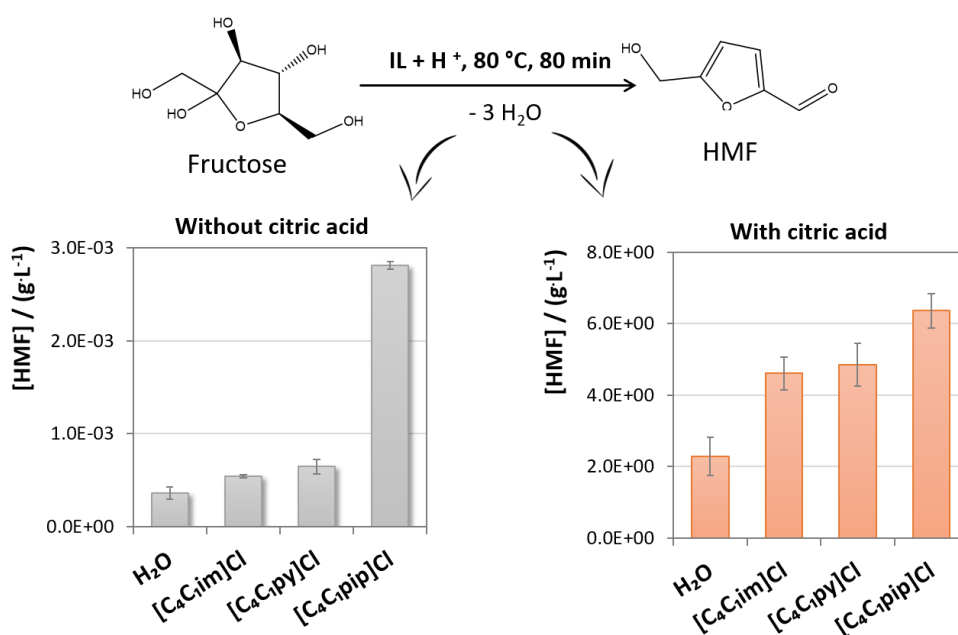


Figure 5.1.4. Production of HMF through fructose dehydration in presence (or not) of citric acid and ILs, at 80 °C for 80 min.

After the HMF production, the reaction was stopped and the two-phase systems simultaneously formed by the addition of aqueous KOH (up to pH 7). **Figure 5.1.5** depicts the results regarding the selective separation of HMF from fructose using IL-based ABS. The results are given in extraction efficiencies of both HMF and fructose ($EE_{\text{HMF}}\%$ and $EE_{\text{Fructose}}\%$) for opposite phases. The extraction efficiencies are defined as the percentage ratio between the total weight of HMF or fructose in one of the phases to that in the total mixture (detailed results are given in the **Appendix C.1, Tables C.1.15** and **C.1.16**). The results in partition coefficients values, defined as the concentration of HMF between the IL-rich phase and the salt-rich phase, as well as selectivity of the systems to HMF, also are provided in the **Appendix C.1 (Figure C.1.4)**.

In all investigated systems, HMF preferentially migrates to the IL-rich phase while fructose is enriched in the opposite layer, allowing thus the separation of the two compounds. Remarkable extraction efficiencies of HMF to the IL-rich phase ranging between 92 and 96%, and of fructose to the salt-rich phase ranging between 53 and 64%, were obtained in a single-step. This migration for opposite phases and selective separation results from the higher affinity of HMF to more hydrophobic (IL-rich) phases in contrast to the higher affinity of fructose to more hydrophilic (salt-rich) phases, as reflected by their octanol-water partition coefficients (K_{ow}) ($\log(K_{\text{ow}})$ of HMF = -0.10; $\log(K_{\text{ow}})$ of fructose = -2.76).²⁶ Although the almost complete extraction of HMF to the IL-rich phase was achieved in a single-step in all studied systems, the extraction of fructose to the opposite phase seems to be more dependent on the nature of the IL employed; the selective separation of HMF and fructose increases in the following order:

$[C_4C_{1im}]Cl < [C_4mpy]Cl < [C_4mpip]Cl$. This trend follows the IL hydrophobic nature as described by their ternary phase diagrams at a fixed pH, shown in the **Appendix C.1 (Figure C.1.3)**.

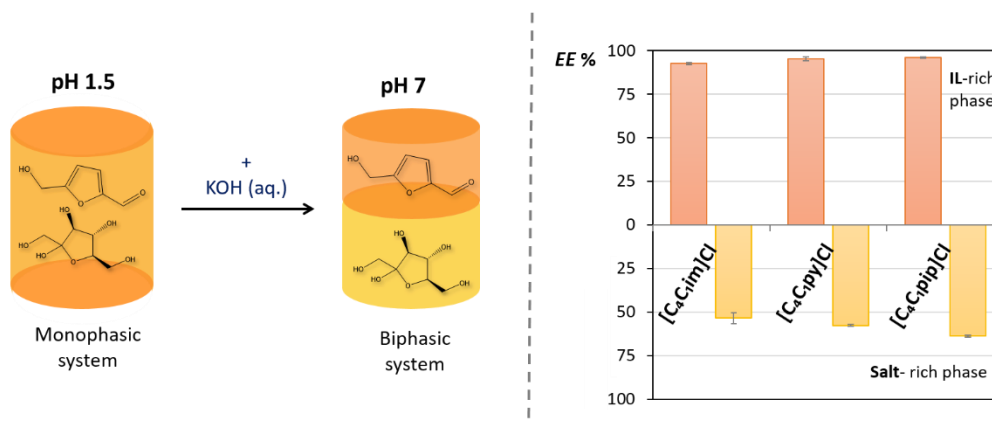


Figure 5.1.5. Selective separation of HMF (red bars) from fructose (yellow bars) that did not react through the addition of KOH and formation of ABS.

In what concerns the extraction performance and selectivity of the systems to HMF (ranging between 14 and 48; detailed data shown in the **Appendix C.1, Figure C.1.4 and Table C.1.17**), our results are quite promising when compared to those reported in the literature.^{44, 45} Partition coefficients of HMF ranging between 0.5 and 2.0 have been reported, with biphasic systems composed of water and butanol, methyl-iso-butylketone (MIBK), toluene, dichloromethane or other mixtures of organic volatile solvents.⁴⁴ More recently, Blumenthal *et al.*⁴⁵ suggested biphasic systems formed by water and *o*-propylphenol or *o*-isopropylphenol for the separation of HMF from the aqueous reaction medium, in which an increase up to five times in the partition coefficients was reported when compared to the previously applied solvents.⁴⁴ The partition coefficients obtained in the current work range between 9 and 17 (*cf.* the **Appendix C.1, Figure C.1.4 and Table C.1.17**). Our results on the separation of HMF are thus better than the most promising ones reported hitherto in the literature. Moreover, with IL-based ABS, the use of volatile and often toxic organic solvents is avoided; instead, aqueous-rich media are used. Additionally, an integrated methodology is here proposed for the separation of HMF by the creation of two-phase systems only through a pH increase, representing thus a step forward on the development of more sustainable production-separation processes.

Conclusions

The results here reported demonstrate that pH-driven reversible ABS composed of ILs can be easily prepared by playing around with the speciation of at least one of the phase-forming components. Furthermore, these systems show potential to become remarkable integrated

platforms, in which reaction and separation steps can be carried out sequentially by taking advantage of their switchable behaviour, as demonstrated here with the HMF production and separation from fructose as the reaction precursor. In addition to the example shown herein, reversible IL-based ABS can be certainly tailored to fit the requirements of other separation processes. Additional reactions or separation processes that occur at other pH values can be carried out with the proposed systems. The studied systems are only constrained by the minimum pH value at which they are able to form two phases to proceed with the separation step.

References

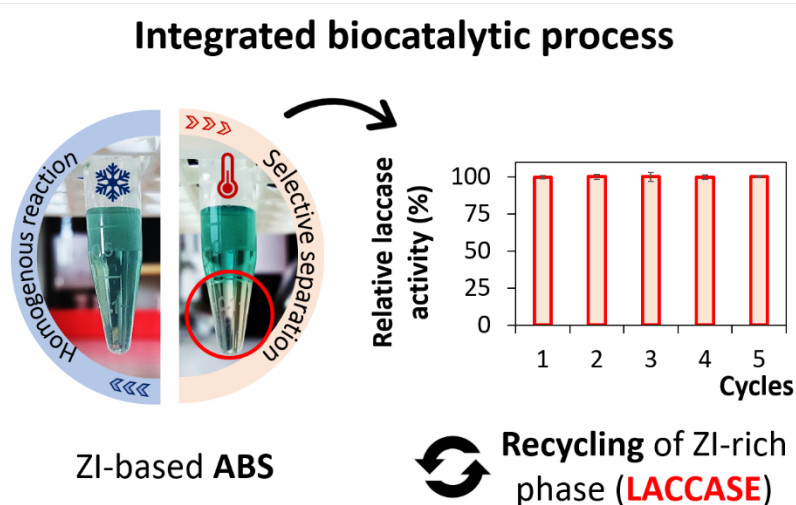
1. F. W. Fifield and D. Kealey, *Principles and Practice of Analytical Chemistry*, 5th edn., 2000.
2. J. Rydberg, M. Cox, C. Musikas and G. R. Choppin, *Principles and practices of solvent extraction. Second Edition, Revised and Expanded*, 2nd edn., 2004.
3. R. D. Rogers and K. R. Seddon, *Science (New York, N.Y.)*, 2003, **302**, 792-793.
4. M. J. Earle, J. M. S. S. Esperanca, M. A. Gilea, J. N. Canongia Lopes, L. P. N. Rebelo, J. W. Magee, K. R. Seddon and J. A. Widegren, *Nature*, 2006, **439**, 831-834.
5. K. E. Gutowski, G. A. Broker, H. D. Willauer, J. G. Huddleston, R. P. Swatloski, J. D. Holbrey and R. D. Rogers, *J. Am. Chem. Soc.*, 2003, **125**, 6632-6633.
6. M. G. Freire, A. F. M. Cláudio, J. M. M. Araújo, J. A. P. Coutinho, I. M. Marrucho, J. N. C. Lopes and L. P. N. Rebelo, *Chem. Soc. Rev.*, 2012, **41**, 4966-4995.
7. M. G. Freire, C. L. S. Louros, L. P. N. Rebelo and J. A. P. Coutinho, *Green Chem.*, 2011, **13**, 1536-1545.
8. M. G. Freire, C. M. S. S. Neves, I. M. Marrucho, J. N. Canongia Lopes, L. P. N. Rebelo and J. A. P. Coutinho, *Green Chem.*, 2010, **12**, 1715-1718.
9. Y. Kohno and H. Ohno, *Chem. Commun.*, 2012, **48**, 7119-7130.
10. P. G. Jessop, S. M. Mercer and D. J. Heldebrant, *Energy Environ. Sci.*, 2012, **5**, 7240-7253.
11. J. Luo, T. Xin and Y. Wang, *New J. Chem.*, 2013, **37**, 269-273.
12. S. Saita, Y. Kohno, N. Nakamura and H. Ohno, *Chem. Commun.*, 2013, **49**, 8988-8990.
13. Y. Kohno, H. Arai and H. Ohno, *Chem. Commun.*, 2011, **47**, 4772-4774.
14. D. Xiong, H. Wang, Z. Li and J. Wang, *ChemSusChem*, 2012, **5**, 2255-2261.
15. D. Z. Xiong, G. K. Cui, J. J. Wang, H. Y. Wang, Z. Y. Li, K. S. Yao and S. J. Zhang, *Angew. Chem. Int. Ed.*, 2015, **54**, 7265-7269.
16. G. Yu, Y. Lu, X. Liu, W.-J. Wang, Q. Yang, H. Xing, Q. Ren, B.-G. Li and S. Zhu, *Ind. Eng. Chem. Res.*, 2014, **53**, 16025-16032.
17. M. G. Freire, C. M. S. S. Neves, K. Shimizu, C. E. S. Bernardes, I. M. Marrucho, J. A. P. Coutinho, J. N. C. Lopes and L. P. N. Rebelo, *J. Phys. Chem. B*, 2010, **114**, 15925-15934.
18. P. Nockemann, B. Thijs, S. Pittois, J. Thoen, C. Glorieux, K. Van Hecke, L. Van Meervelt, B. Kirchner and K. Binnemans, *J. Phys. Chem. B*, 2006, **110**, 20978-20992.
19. Y. Lu, G. Yu, W.-J. Wang, Q. Ren, B.-G. Li and S. Zhu, *Macromolecules*, 2015, **48**, 915-924.
20. S. Saita, Y. Kohno and H. Ohno, *Chem. Commun.*, 2013, **49**, 93-95.
21. J. Lachwa, J. Szydłowski, A. Makowska, K. R. Seddon, J. M. S. S. Esperanca, H. J. R. Guedes and L. P. N. Rebelo, *Green Chem.*, 2006, **8**, 262-267.
22. K. Fukumoto and H. Ohno, *Angew. Chem. Int. Ed.*, 2007, **46**, 1852-1855.
23. Y. Kohno, S. Saita, K. Murata, N. Nakamura and H. Ohno, *Polym. Chem.*, 2011, **2**, 862-867.
24. Z.-L. Xie and A. Taubert, *ChemPhysChem*, 2011, **12**, 364-368.
25. H. Passos, A. Luis, J. A. P. Coutinho and M. G. Freire, *Sci. Rep.*, 2016, **6**, 1-7.
26. Chemspider, The free chemical database, <http://www.chemspider.com>, (accessed October 2016).
27. M. T. Zafarani-Moattar and S. Hamzehzadeh, *Fluid Phase Equilib.*, 2011, **304**, 110-120.
28. S. Li, C. He, H. Liu, K. Li and F. Liu, *J. Chromatogr. B*, 2005, **826**, 58-62.

29. K. A. Kurnia, M. G. Freire and J. A. P. Coutinho, *J. Phys. Chem. B*, 2014, **118**, 297-308.
30. J. S. L. Hong-Shum, in *Food Additives Data Book*, ed. B. S. Ltd, Blackwell Science Ltd, Wiley-Blackwell, 2003, DOI: 10.1002/9780470995327.fmatter, pp. i-xix.
31. A. F. M. Cláudio, A. M. Ferreira, S. Shahriari, M. G. Freire and J. A. P. Coutinho, *J. Phys. Chem. B*, 2011, **115**, 11145-11153.
32. A. F. M. Cláudio, L. Swift, J. P. Hallett, T. Welton, J. A. P. Coutinho and M. G. Freire, *Phys. Chem. Chem. Phys.*, 2014, **16**, 6593-6601.
33. A. A. Rosatella, S. P. Simeonov, R. F. M. Frade and C. A. M. Afonso, *Green Chem.*, 2011, **13**, 754-793.
34. J. Song, B. Zhang, J. Shi, H. Fan, J. Ma, Y. Yang and B. Han, *RSC Adv.*, 2013, **3**, 20085-20090.
35. R.-J. van Putten, J. C. van der Waal, E. de Jong, C. B. Rasrendra, H. J. Heeres and J. G. de Vries, *Chem. Rev.*, 2013, **113**, 1499-1597.
36. S. K. M. Konduri, S. K. Thoota, C. Javvadi, P. R. Muddasani, K. S. B. R. Adibhatla and V. C. Nannapaneni, *WO/2015/155784*, 2015.
37. Y. Roman-Leshkov, C. J. Barrett, Z. Y. Liu and J. A. Dumesic, *Nature*, 2007, **447**, 982-985.
38. A. F. Sousa, C. Vilela, A. C. Fonseca, M. Matos, C. S. R. Freire, G.-J. M. Gruter, J. F. J. Coelho and A. J. D. Silvestre, *Polym. Chem.*, 2015, **6**, 5961-5983.
39. P. Gupta, S. K. Singh, A. Pathak and B. Kundu, *Tetrahedron*, 2002, **58**, 10469-10474.
40. M. Mascal and S. Dutta, *Green Chem.*, 2011, **13**, 3101-3102.
41. F. Salak Asghari and H. Yoshida, *Ind. Eng. Chem. Res.*, 2006, **45**, 2163-2173.
42. S. P. Teong, G. Yi and Y. Zhang, *Green Chem.*, 2014, **16**, 2015-2026.
43. C. Sievers, I. Musin, T. Marzioletti, M. B. Olarte, P. K. Agrawal and C. W. Jones, *ChemSusChem*, 2009, **2**, 665-671.
44. C. Fan, H. Guan, H. Zhang, J. Wang, S. Wang and X. Wang, *Biomass Bioenergy*, 2011, **35**, 2659-2665.
45. L. C. Blumenthal, C. M. Jens, J. Ulbrich, F. Schwering, V. Langrehr, T. Turek, U. Kunz, K. Leonhard and R. Palkovits, *ACS Sustain. Chem. Eng.*, 2016, **4**, 228-235.

5.2. Integrated production-separation platforms applying thermoreversible aqueous biphasic systems

Comunicacion submitted⁶

A. M. Ferreira, H. Passos, A. Okafuji, A. P. M. Tavares, H. Ohno, M. G. Freire and J. A. P. Coutinho, "An integrated process for enzymatic catalysis allowing product recovery and enzyme reuse by applying thermoreversible aqueous biphasic systems", *Green Chem.*, 2018,**20**, 1218-1223.



Integrated biocatalysis-separation process where the reaction step occurs in homogeneous medium, followed by the enzyme and products separation in a liquid-liquid system promoted by temperature changes.

Abstract

Thermoreversible aqueous biphasic systems (ABS) composed of ammonium-based zwitterions (ZIs) and polymers are here disclosed to act as integrated bioreaction-separation processes. The biocatalytic reaction involving laccase occurs in homogeneous media, after which small changes in temperature induce the formation of two phases and the complete separation of the enzyme from the products in a single-step. These systems also allow the recover and reuse of the enzyme, along with the ZI-rich phase, contributing towards the development of sustainable biocatalytic processes.

⁶**Contributions:** M.G.F., J.A.P.C., A.P.M.T. and H.O. conceived and directed this work. A.M.F., H.P. and A.O. acquired the experimental data. A.M.F., H.P., M.G.F., A.P.M.T. and J.A.P.C. interpreted the experimental data. The manuscript was mainly written by A.M.F., H.P. and M.G.F. with significant contributions from the remaining authors.

Introduction

In the past years, there has been an increased interest on the development of sustainable and efficient production processes, in which biocatalysis plays a pivotal role.¹ Enzymes display a high activity, specificity and selectivity, minimizing the consumption of raw materials and the production of by-products when compared to their synthetic counterparts, thus contributing towards the development of sustainable catalytic processes.^{1,2} Enzymes and biocatalysis have been used in several sectors, such as in soil bioremediation, nanobiotechnology, and biosensors, and by the textile, pulp and paper, cosmetic, food and pharmaceutical industries.³ Significant developments have been reported in the pharmaceutical industry with a decrease of the respective E-factor.⁴ Despite their advantages, the major challenges associated to enzyme-catalysed bioprocesses rely on the maintenance of the enzymes structural stability and activity, and on their reusability.⁵ Efforts have been made to overcome these issues, whereas one of the main strategies is the enzyme immobilization where the biocatalyst is adsorbed on, bound to, or encapsulated in a solid matrix.^{6,7} Albeit this approach allows the reuse of the biocatalyst, immobilization may present some disadvantages, such as conformational changes of the enzymes, loss of activity, and their heterogeneity on the support.^{6,8} Therefore, new approaches to recover biocatalysts from the reaction medium have been proposed, including for instance the use of membranes, centrifugation, liquid-liquid extraction,⁹ and immobilization of chemically modified enzymes.^{7,10}

Liquid-liquid systems appear as an interesting alternative in biocatalysis since they could allow the integration of the reaction and separation steps. Although liquid-liquid systems have been widely employed in the chemical industry for separation purposes due to their simplicity, low cost, and easy scale-up¹¹, the commonly employed volatile organic solvents can be harmful to biologically active biomolecules. However, a milder environment to biomolecules can be afforded by water-rich systems, such as aqueous biphasic systems (ABS).¹² ABS are composed of two immiscible aqueous-rich phases and can be formed by the mixture of two water soluble phase-forming components, such as two polymers, a polymer and a salt, or two salts, dissolved in aqueous media.¹³ Polymer-based ABS have shown to be biocompatible to deal with the separation of proteins, enzymes, viruses, cells, cell organelles, and other biological materials.¹⁴ Nevertheless, these systems are limited by a narrow polarity range preventing high extraction efficiencies and selectivities. This drawback may be overcome by ABS composed of ionic liquids (ILs).^{12,15} Compared to the more conventional polymer-based systems, IL-based ABS display a lower viscosity, a faster phases separation, and higher extraction performance and selectivity.¹²

Previous studies on IL-based ABS have focused on the determination of the respective phase diagrams and on evaluation of their extraction efficiency for a wide range of compounds.¹² Furthermore, recently, there has been a significant interest on the development of dynamic and reversible IL-based systems induced by changes of pH,¹⁶ temperature¹⁷ or by the addition of gases^{17, 18}, that could ultimately lead to the development of integrated reaction-separation processes. However, only few works investigated the reversible behaviour of IL-based ABS in separation processes. For instance, they have been investigated for the extraction of proteins (by temperature change),¹⁹ and in the production and separation of 5-hydroxymethylfurfural (HMF) from fructose (by pH change).²⁰

In addition to the widely studied IL-based systems, novel ABS composed of water soluble ammonium-based zwitterions (ZIs) and inorganic salts were recently proposed,²¹ and their application in the selective separation of amino acids demonstrated. ZIs were suggested as substitutes of ILs, where the cation and the anion are covalently tethered, thus avoiding possible ions exchange between the ABS coexisting phases.²² However, the salts employed may lead to biocompatibility concerns when dealing with solutes sensitive to ionic strength, like proteins and enzymes.²³ To minimize these issues, salts are here proposed to be replaced by polymers, such as polyethylene glycol (PEG), generally recognized as safe (GRAS) and used as additive in food products and drugs.^{10, 24, 25} Furthermore, ZI-based reversible ABS have not previously been considered as potential integrated reaction-separation platforms.

Based on the need of finding integrated reaction-separation processes for biocatalysis, in this work we investigated and designed novel ZI-polymer-based ABS with a thermal switchable behaviour, at temperatures amenable to deal with proteins. These systems were tested as integrated reaction-separation platforms, where a homogeneous catalytic reaction followed by the enzyme separation from the product, by a change in temperature, is performed in one-step. To this end, laccase (EC 1.10.3.2) was used as the biocatalyst and 2,2'-azinobis(3-ethylbenzthiazoline-6-sulfonate) (ABTS) as the substrate. Laccase was chosen since it has been attracting a large attention in the past years due to its ability to degrade a wide variety of substrates, being currently considered a promising biocatalyst in bio-based industries.^{6, 26}

Results and discussion

Three water-soluble ammonium-based ZIs ($N_{555}C3S$, $N_{333}C3S$ and $N_{111}C3S$), with different alkyl chain lengths, were synthesized and used in the preparation of ABS. Their molecular structures are depicted in **Figure 5.2.1**, while their definition is given in the **List of acronyms**.

Their synthesis was previously described¹³, while details on their purity are given in the **Appendix C.2** (subsection “NMR spectrum data of the synthesized ZIs”).

The ability of each ZI to form an ABS when mixed with PEGs of different molecular weight (1540, 2000, 4000 and 6000 g·mol⁻¹) was firstly evaluated, and the respective ternary phase diagrams were determined at 25 °C. Further details on the experimental procedure are given in the **Materials and experimental procedure** Chapter (section 2.3.2), and the detailed experimental weight fraction data are given in the **Appendix C.2 (Tables C.2.1 to C.2.5)**.

Both N₅₅₅C3S and N₁₁₁C3S ZIs are able to form ABS at 25 °C with all polymers studied; however, N₃₃₃C3S, the ZI of intermediate alkyl chain length, does not undergo phase separation with any of the investigated polymers. A summary of the ZIs ability to form ZI-PEG-based ABS is provided in the **Appendix C.2 (Table C.2.6)**. To the best of our knowledge, this irregular trend on the ABS formation with the increase of the alkyl side chain length of one of the phase-forming components was never observed, and is certainly a result of a change in the balance of competing interactions between the compounds present in the investigated ternary systems due to the increase of the ZI alkyl chains.^{27, 28}

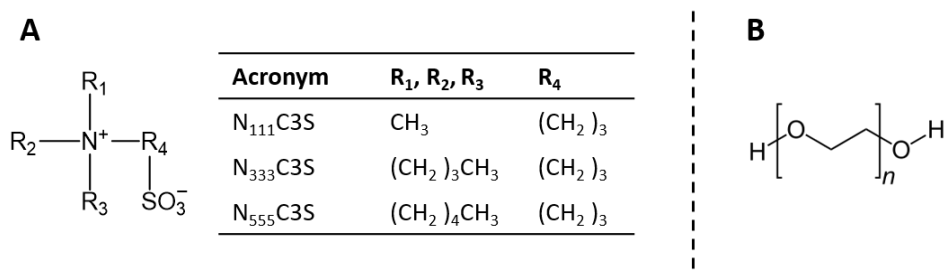


Figure 5.2.1. (A) Chemical structures and acronyms of the ZIs used. **(B)** Chemical structure of PEG with the molecular formula H-(O-CH₂-CH₂)_n-OH.

By plotting all the phase diagrams at 25 °C (*cf.* **Appendix C.2, Figure C.2.1**), it is possible to appraise the influence of the length of the aliphatic moiety of the ZI, as well as of the molecular weight of PEG on the solubility curves. The solubility curves indicate the minimum composition required to form an ABS, where mixtures with compositions above the curve are biphasic while those below are monophasic. The larger the biphasic region, the higher the ability of the ZI to induce liquid-liquid phase separation in polymer aqueous solutions. ZIs with shorter alkyl side chains are more prone to form ABS with polymers, while the ability of PEG to induce phase separation increases with its molecular weight, in agreement with trends previously observed for ABS composed of polymer/salt²⁹ or polymer/IL.³⁰ This is a consequence of the increasing hydrophobicity of PEG with higher molecular weight.³⁰

After the previous assessment on the ZI-PEG potential to form ABS at a common temperature (25 °C), these were then appraised at 35 and 45 °C, taking into account the operational temperature range of most enzymes and to avoid their activity loss. The optimum operation temperature of laccase is around 40 °C,³¹ although this temperature can vary with the pH and the laccase source, between 30 and 50 °C.³² **Figure 5.2.2** depicts the phase diagrams obtained for ZI-PEG 6000-based ABS at several temperatures. The detailed experimental procedure used and the experimental data obtained for PEG 6000 and remaining polymers at different temperatures are provided in the **Appendix C.2 (Figure C.2.2)**. It should be noted that N₅₅₅C3S does not form ABS with PEG 6000 at 45 °C. As previously observed for ZI-salt-based ABS,²¹ ZI-polymer-based ABS also present two distinct behaviours with temperature, which depend on the ZIs alkyl chains length: (i) an increase of the immiscibility region with an increase in temperature for N₁₁₁C3S-based ABS; and (ii) a decrease of the biphasic region with a decrease in temperature for the N₅₅₅C3S-based systems. ABS composed of ZIs with smaller alkyl chains (N₁₁₁C3S) display a lower critical solution temperature (LCST)-type behaviour when mixed with polymers, following the same behaviour as polymer-salt ABS.³³ Their formation seems thus to be dominated by a salting-out phenomenon, where the ZI acts as the salting-out species.³⁰ On the other hand, the ABS formed by the most hydrophobic ZI investigated - N₅₅₅C3S - present an upper critical solution temperature (UCST)-type behaviour, similar to those of polymer-polymer ABS.³⁴ At higher temperatures, the interactions between the polymer and ZI are more favourable, enhancing thus their mutual solubility and reducing their ability to form ABS.³⁵

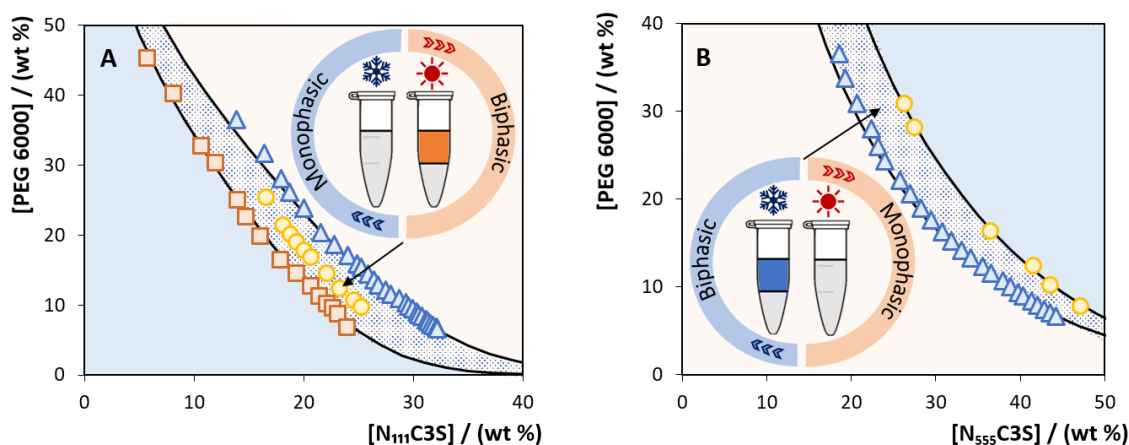


Figure 5.2.2. Temperature effect in the phase diagrams of ternary systems composed of ZI + PEG 6000 + H₂O at 25 °C (▲), 35 °C (●) and 45 °C (■). **(A)** N₁₁₁C3S- and **(B)** N₅₅₅C3S-based ABS. There is no formation of ABS comprising PEG 6000 and N₅₅₅C3S at 45°C.

The temperature-reversible behaviour of the studied systems is also depicted in **Figure 5.2.2**. To confirm this behaviour, a ternary mixture at the monophasic region was prepared at 25 °C for the system composed of N₁₁₁C3S, and at 45 °C for the system composed of N₅₅₅C3S. Then, the temperatures were changed to 45 °C and 25 °C for the systems composed of N₁₁₁C3S and N₅₅₅C3S, respectively, to induce the formation of a biphasic system. Details on these mixtures compositions are described below, corresponding to the same mixtures at which biocatalysis was carried out. When the phase's separation occurs, a top polymer-rich phase and a bottom ZI-rich phase are formed. This proves the thermoreversible behaviour of the studied systems, which were then applied to develop integrated reaction-separation biocatalytic processes.

The homogeneous biocatalytic oxidation of ABTS by laccase was carried out in the monophasic region, followed by the separation of laccase from the oxidation product by promoting the phases' separation by temperature changes (increase or decrease according to the ZI employed in the ABS formation). The oxidation of ABTS occurred through the addition of laccase and ABTS to a monophasic mixture composed of ZI, PEG 6000 and water. The mixture was carefully mixed during 1 min, at 40 °C for the ZI N₁₁₁C3S (20 wt% ZI + 20 wt% PEG 6000), and at 25 °C for the ZI N₅₅₅C3S (39 wt% ZI + 13 wt% PEG 6000) – experimental details are given in the **Materials and experimental procedure** Chapter (**section 2.3.2**). The negligible effect of laccase, ABTS and PBS in the phase diagrams behaviour and ABS phase compositions was confirmed by the determination of an additional phase diagram in presence of all these components at the concentrations used in the separation assays (*cf.* **Appendix C.2, Figures C.2.3**).

For the two studied thermoreversible ABS, it was observed that laccase successfully catalysed the oxidation of ABTS (colourless) to a highly stable green-coloured ABTS⁺ radical³⁶ (**Figure 5.2.3A**). ABTS is a standard substrate used to appraise the laccase activity, for which the yield of reaction is considered as 100%. After that, a temperature change (from 25 to 40 °C or *vice-versa*) was applied, inducing the separation of the system into two phases, while allowing the selective separation of the oxidized substrate and laccase, as shown in **Figure 5.2.3**. Further experimental details are given in the **Materials and experimental procedure** Chapter (**section 2.3.2**).

Figure 5.2.3B (*cf.* **Appendix C.2, Table C.2.9**) shows the extraction efficiencies (*EE%*) of the studied systems for both laccase and oxidized ABTS, which correspond to the percentage recovery of each compound to a given phase. Remarkably, laccase and the reaction product partition to opposite phases, with extraction efficiencies higher than 81% achieved in a single-step. For the two studied ABS, laccase preferentially partitions to the ZI-rich phase and the reaction product to the PEG-rich phase, allowing thus the selective separation of the enzyme and product. The trend obtained for the oxidized ABTS is in good agreement with its hydrophobic character ($\log(K_{ow}) = 1.93$,³⁷ where K_{ow} is defined as the octanol-water partition

coefficient), meaning that ABTS tends to enrich in more hydrophobic phases, corresponding to the polymer-rich phase. On the other hand, proteins and enzymes tend to preferentially migrate to more hydrophilic (water-rich) phases, and particularly laccase as demonstrated in the literature,^{38, 39} therefore preferentially migrating to the ZI-rich phase. Previous works on the separation of proteins using ABS formed by ILs and polymers support this behaviour.^{40, 41}

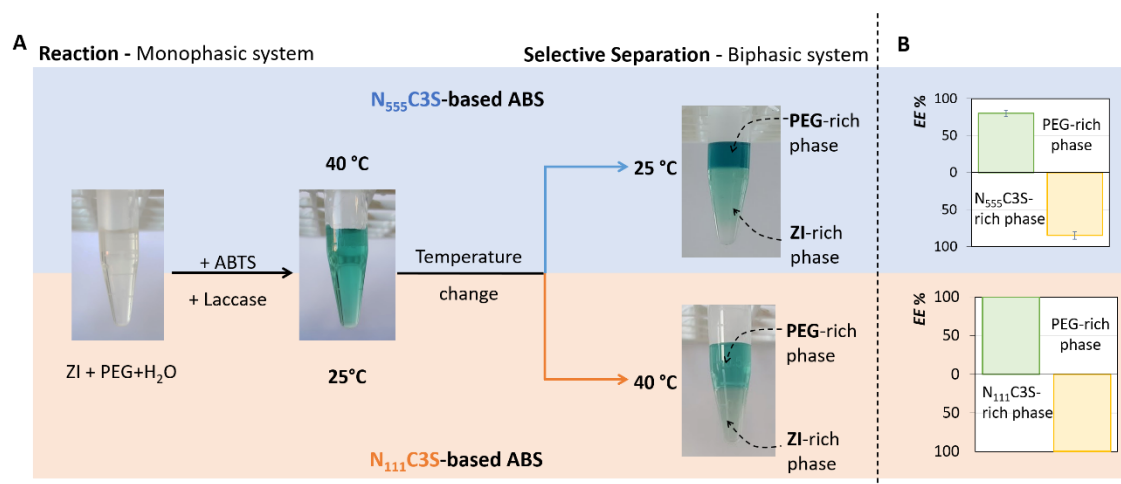


Figure 5.2.3. (A) Oxidation of ABTS using laccase and their selective separation from the reaction product by changes in temperature. **(B)** Extraction efficiencies of laccase ($EE\%$, yellow bars) and extraction efficiencies of the green-coloured $ABTS^+$ radical ($EE\%$, green bars) in ABS formed by PEG 6000 and $N_{555}C3S$ or $N_{111}C3S$.

A remarkable extraction efficiency of 100% was obtained with the $N_{111}C3S$ -based ABS, *i.e.* laccase and the oxidized ABTS are completely separated for opposite phases with no losses or cross-contamination. It should be remarked that complete separations could also be achieved with other ZI-based ABS by a proper tailoring of the phases' hydrophobicity, either by changing the PEG molecular weight, ZI employed, or mixture composition.

In addition to the complete separation of the enzyme and the reaction product, it was further confirmed that laccase maintains its biocatalytic activity after the separation step (experimental details are given in the **Materials and experimental procedure** Chapter (section 2.3.2)). This maintenance in activity is of crucial relevance when envisaging the development of processes in which the enzyme can be recovered and reused. To prove this concept, the phase enriched in laccase (ZI-rich) was recovered and reused for the creation of a novel ternary system, as a new biocatalytic reaction medium. A summary of the enzyme recovery/reuse process is depicted in **Figure 5.2.4A**; experimental details are given in the **Materials and experimental procedure** Chapter (section 3.2.2). Remarkably, it is possible to recover laccase and reuse it without losses in the catalytic activity, for at least 5 consecutive cycles (**Figure 5.2.4B**). This approach not only

allows the recovery and reuse of the enzyme, but also allows the recovery and reuse of the ZI-rich phase required to form ABS, contributing towards the development of sustainable biocatalytic processes. If a sustainable method is being proposed, the PEG-rich phase should also be recovered and reused. An ultrafiltration step was finally applied to the PEG-rich phase, allowing the recovery of the oxidized ABTS and ZI from the polymer-rich solution (experimental details are given in **Materials and experimental procedure** Chapter, **section 2.3.2**), showing that it is also possible to recover the polymer with negligible losses (*cf.* **Appendix C.2, Figures C.2.4 and C.2.5**).

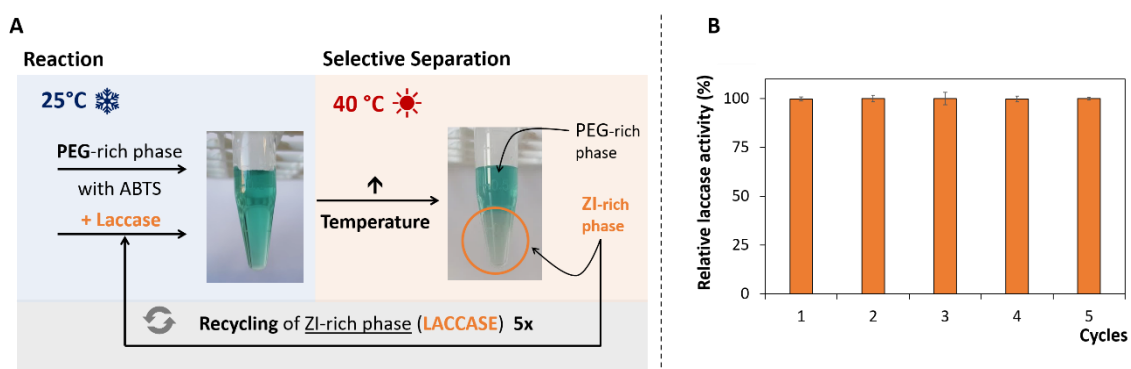


Figure 5.2.4. (A) Flowchart of the integrated reaction-separation process developed, including the enzyme and ZI-rich phase recyclability. **(B)** Relative laccase activity in the ZI-rich phase in 5 cycles of oxidative reaction, comprising both the recovery and reuse of the enzyme and ZI-rich phase.

Two works using two-phase systems with laccase as a biocatalyst were previously reported.^{42,43} In the first work, it was shown the occurrence of enzymatic reactions (using laccase from *Polyporus versicolor*) in a two-phase system, yet composed of one organic solvent, such as hexane, toluene, tetrahydrofuran, acetone, among others, comprising the substrate and products, and an aqueous phase which contains the enzyme.⁴² However, the enzymatic reaction occurs in heterogeneous media, *i.e.* at the interface, being thus essentially different from the approach here proposed. In addition to the use of hazardous organic solvents, the authors³⁶ were not able to characterize the compounds obtained in aqueous solution due to difficulties in obtaining them in sufficient amounts. Nicotra *et al.*⁴³ isolated and characterized four C-C and -O dimers from the steroid hormone 17 β -estradiol, formed by a catalytic reaction using laccase from *Trametes pubescens* in a biphasic system, formed by ethyl acetate and an aqueous buffered salt solution. Also in this approach, biocatalysis occurred at the interface. These heterogeneous reaction media usually require vigorous shaking and stirring to ensure the transfer of substrates and products between the phases, which can cause enzyme inactivation.⁴⁴ This may be responsible for the low yield obtained, *ca.* 27%.⁴³ Andersson and Hahn-Hägerdal⁹ reviewed

others works on bioconversion in conventional (polymer-salt and polymer-polymer) ABS, using different enzymes or living cells, but in all these cases ABS were used as heterogeneous media, *i.e.* with systems involving two-phases with the reaction occurring at the interface. Moreover, in these works, it was not possible to adequately separate the enzyme and the product for opposite phases. To overcome this problem, the use of ultrafiltration units has been proposed.⁹ The thermoreversible systems here suggested thus overcome these limitations, allowing a homogeneous biocatalytic reaction, with all the advantages in terms of kinetics and yield, followed by a complete separation of the products and enzyme by a small temperature change.

Conclusions

In this work it was demonstrated that temperature-driven reversible ABS composed of ZIs and polymers are efficient and sustainable integrated reaction-separation platforms in biocatalytic processes. Reaction and separation steps can be carried out sequentially by taking advantage of their temperature switchable behaviour. The reaction step occurs at a homogeneous medium, followed by the enzyme and products separation in liquid-liquid systems promoted by small changes in temperature. This approach avoids the need of vigorous stirring to improve mass transfer, as typically carried out in heterogeneous reactions, thus contributing to the maintenance of the enzyme activity. Furthermore, the thermoreversible nature of ZI-PEG-ABS occurs at temperatures amenable for keeping the enzymes stability and activity (25-45 °C). These systems further allow the complete separation of the enzyme and the products in one-step, which are enriched in opposite phases, followed by the recovery and reuse of both the ZI-rich phase and enzyme. In addition to the example here discussed, reversible ZI-based ABS can be tailored to fit the requirements of other biocatalytic processes comprising value-added products.

References

1. S. Datta, L. R. Christena and Y. R. S. Rajaram, *3 Biotech.*, 2013, **3**, 1-9.
2. S. C. Silvério, O. Rodríguez, A. P. M. Tavares, J. A. Teixeira and E. A. Macedo, *J. Mol. Catal. B: Enzym.*, 2013, **87**, 37-43.
3. A. Kunamneni, S. Camarero, C. García-Burgos, F. J. Plou, A. Ballesteros and M. Alcalde, *Microb. Cell Fact.*, 2008, **7**, 32-47.
4. R. A. Sheldon, *Green Chem.*, 2017, **19**, 18-43.
5. M. Misson, H. Zhang and B. Jin, *J. Royal Soc. Interface*, 2015, **12**, 1-20.
6. M. Fernández-Fernández, M. Á. Sanromán and D. Moldes, *Biotechnol. Adv.*, 2013, **31**, 1808-1825.
7. Y. Zhang, J. Ge and Z. Liu, *ACS Catal.*, 2015, **5**, 4503-4513.
8. A. K. Vahidi, Y. Yang, T. P. N. Ngo and Z. Li, *ACS Catal.*, 2015, **5**, 3157-3161.
9. E. Andersson and B. Hahn-Hägerdal, *Enzyme Microb. Technol.*, 1990, **12**, 242-254.
10. A. Akelah, *Functionalized Polymeric Materials in Agriculture and the Food Industry*, Springer US, Boston, MA, 2013, 195-248.
11. M. Martínez-Aragón, S. Burghoff, E. L. V. Goetheer and A. B. de Haan, *Sep. Purif. Technol.*, 2009, **65**, 65-72.

12. M. G. Freire, A. F. Cláudio, J. M. Araujo, J. A. P. Coutinho, I. M. Marrucho, J. N. Canongia Lopes and L. P. Rebelo, *Chem. Soc. Rev.*, 2012, **41**, 4966-4695.
13. M. Martínez-Aragón, S. Burghoff, E. L. V. Goetheer and A. B. de Haan, *Sep. Purif. Technol.*, 2009, **65**, 65-72.
14. P.-A. Albertsson, *Nature*, 1958, **182**, 709-711.
15. K. E. Gutowski, G. A. Broker, H. D. Willauer, J. G. Huddleston, R. P. Swatloski, J. D. Holbrey and R. D. Rogers, *J. Am. Chem. Soc.*, 2003, **125**, 6632-6633.
16. F. A. S. Cunha, A. S. G. Pereira, J. P. A. Fernandes, W. S. Lyra, M. C. U. Araújo and L. F. Almeida, *Food Anal. Methods*, 2017, **10**, 921-930.
17. Y. Kohno and H. Ohno, *Chem. Commun.*, 2012, **48**, 7119-7130.
18. P. G. Jessop, S. M. Mercer and D. J. Heldebrant, *Energy Environ. Sci.*, 2012, **5**, 7240-7253.
19. H. Passos, A. Luís, J. A. P. Coutinho and M. G. Freire, *Sci. Rep.*, 2016, **6**, 1-7.
20. A. M. Ferreira, A. F. M. Cláudio, M. Valega, F. M. J. Domingues, A. J. D. Silvestre, R. D. Rogers, J. A. P. Coutinho and M. G. Freire, *Green Chem.*, 2017, **19**, 2768-2773.
21. A. M. Ferreira, H. Passos, A. Okafuji, M. G. Freire, J. A. P. Coutinho and H. Ohno, *Green Chem.*, 2017, **19**, 4012-4016.
22. S. Saita, Y. Mieno, Y. Kohno and H. Ohno, *Chem. Commun.*, 2014, **50**, 15450-15452.
23. M. Iqbal, Y. Tao, S. Xie, Y. Zhu, D. Chen, X. Wang, L. Huang, D. Peng, A. Sattar, M. A. B. Shabbir, H. I. Hussain, S. Ahmed and Z. Yuan, *Biol. Proced. Online*, 2016, **18**, 1-18.
24. A. Pitto-Barry and N. P. E. Barry, *Polymer Chemistry*, 2014, **5**, 3291-3297.
25. R. B. Greenwald, *J. Control. Release*, 2001, **74**, 159-171.
26. T. Itoh, *Chem. Rev.*, 2017, **117**, 10567-10607.
27. J. F. Pereira, K. A. Kurnia, O. A. Cojocar, G. Gurau, L. P. Rebelo, R. D. Rogers, M. G. Freire and J. A. P. Coutinho, *Phys. Chem. Chem. Phys.*, 2014, **16**, 5723-5731.
28. J. F. Pereira, L. P. Rebelo, R. D. Rogers, J. A. P. Coutinho and M. G. Freire, *Phys. Chem. Chem. Phys.*, 2013, **15**, 19580-19583.
29. Y.-M. Lu, Y.-Z. Yang, X.-D. Zhao and C.-B. Xia, *Food Bioprod. Process.*, 2010, **88**, 40-46.
30. M. G. Freire, J. F. Pereira, M. Francisco, H. Rodriguez, L. P. Rebelo, R. D. Rogers and J. A. P. Coutinho, *Chem. Eur. J.*, 2012, **18**, 1831-1839.
31. S. Z. Mazlan and S. A. Hanifah, *Int. J. Polym. Sci.*, 2017, **2017**, 1-8.
32. L. I. Ramírez-Cavazos, C. Junghanns, N. Ornelas-Soto, D. L. Cárdenas-Chávez, C. Hernández-Luna, P. Demarche, E. Enaud, R. García-Morales, S. N. Agathos and R. Parra, *J. Mol. Catal. B: Enzym.*, 2014, **108**, 32-42.
33. H. D. Willauer, J. G. Huddleston, M. Li and R. D. Rogers, *J. Chromatogr. B Biomed.*, 2000, **743**, 127-135.
34. H. Walter and E. J. Krob, *J. Chromatogr. A*, 1988, **441**, 261-273.
35. A. F. M. Cláudio, J. F. B. Pereira, P. D. McCrary, M. G. Freire, J. A. P. Coutinho and R. D. Rogers, *Phys. Chem. Chem. Phys.*, 2016, **18**, 30009-30019.
36. G. Gramss, *Fermentation*, 2017, **3**, 27.
37. Chemspider, The free chemical database, <http://www.chemspider.com>, (accessed October 2017).
38. E. Nazaruk, A. Michota, J. Bukowska, S. Shleev, L. Gorton and R. Bilewicz, *J. Biol. Inorg. Chem.*, 2007, **12**, 335-344.
39. S. Sittthisak, K. Howieson, C. Amezola and R. K. Jayaswal, *Appl. Environ. Microbiol.*, 2005, **71**, 5650-5653.
40. M. V. Quental, M. Caban, M. M. Pereira, P. Stepnowski, J. A. P. Coutinho and M. G. Freire, *Biotechnol. J.*, 2015, **10**, 1457-1466.
41. D. Mondal, M. Sharma, M. V. Quental, A. P. M. Tavares, K. Prasad and M. G. Freire, *Green Chem.*, 2016, **18**, 6071-6081.
42. G. Lugaro, G. Carrea, P. Cremonesi, M. M. Casellato and E. Antonini, *Arch. Biochem. Biophys.*, 1973, **159**, 1-6.
43. S. Nicotra, A. Intra, G. Ottolina, S. Riva and B. Danieli, *Tetrahedron: Asymmetry*, 2004, **15**, 2927-2931.
44. D. Monti, G. Ottolina, G. Carrea and S. Riva, *Chem. Rev.*, 2011, **111**, 4111-4140.

6. CONCLUSIONS & FUTURE WORK

This thesis is based on the use of aqueous solutions of ILs as alternative solvents for the extraction and separation of high-value biomolecules and on the design of more cost-effective, sustainable and integrated extraction/recovery strategies.

In **Chapter 3.1** it was shown that aqueous solutions of ILs and salts containing the tosylate anion (taking advantage of the hydrotrophy concept) can enhance the solubility and extraction yield of caffeine from biomass. Studies using mixtures of ILs and salts showed that the ions in aqueous solution, and not the initial ion pair, are the key factor behind the improvement in caffeine solubility and extraction yield. Moreover, the total caffeine content in SCG (0.74 wt%) can be extracted with aqueous solutions of ILs or salts at 0.75 M, at a solvent-liquid ratio of 1:10 and at 25 °C. The obtained results demonstrate that aqueous solutions of adequate ILs or salts are promising alternative solvents for the extraction of caffeine or other value-added compounds from biomass, avoiding the use of volatile organic solvents, sophisticated equipment and/or high energetic inputs. To design sustainable processes other types of ILs, ideally natural-derived and biocompatible, should be chosen instead. In this line, and trying to overwhelm the need of the target compounds recovery and additional steps in the overall extraction/recovery process, an additional work on the use of aqueous solutions of AGB-ILs for the extraction of HMR from Norway spruce knots was developed (**Chapter 3.2**). The extraction yields obtained showed to be better than those achieved with traditional extraction methods and solvents; outstanding HMR extraction yields up to 9.46 wt% were obtained at 25 °C with an aqueous solution of 1.5 M of $[(C_2)_3NC_2]Br$, a solid-liquid ratio of 0.01, for 280 minutes of extraction. Furthermore, it was found that the antioxidant potential of IL aqueous solutions enriched in HMR are more promising than the recovered HMR-rich solid extracts, and that these solutions can be safely used in nutraceutical and cosmetic applications. These results support a new idea on the possibility of using directly the IL-HMR-extracts aqueous solutions without requiring an additional isolation/recovery step.

Within the separations field, novel reversible pH- and temperature-driven ABS were identified and characterized. In **Chapter 4** new reversible IL-based ABS are disclosed, with some examples of their applications in the separation of several biocompounds. In **Chapter 4.1**, pH-driven IL-based ABS by playing with the ILs speciation behaviour were designed, *i.e.*, changes between homogeneous (at acidic pH values) and biphasic (at alkaline pH values) regimes were found to occur in a wide range of pH values and compositions. The significant impact of pH was then used to explore these systems applicability in the separation of DNA from one of the major proteins present in human plasma, HSA. With the optimized systems it was simultaneously induced the precipitation of the protein (HSA) and the complete extraction of DNA to the IL-rich phase, which maintains its integrity at least up to 6 months of storage at the IL-rich phase. In the

following chapter, **Chapter 4.2**, temperature-switchable ABS composed of water-soluble ammonium-based ZIs and salts aqueous solutions were described. A shift from an UCST to a LCST behaviour was observed by increasing the ZIs alkyl side chains length (from N₁₁₁C4S to N₅₅₅C3S), evidencing a change on the type of dominant interactions in ZI-salt ABS with the ZI increasing alkyl chains. These thermoreversible systems showed be efficient for the separation of aromatic (L-tryptophan) and aliphatic (glycine) amino acids.

Reversible IL-based ABS were finally designed to act as integrated production-separation platforms (**Chapter 5**). In **Chapter 5.1** it was shown the influence of pH to promote reversible ABS, and these systems feasibility to be used in the production and separation of HMF from fructose. HMF was produced from fructose at acidic pH, and then separated from the unreacted precursor by an increase in the pH and consequent formation of two-phase systems. In all investigated systems, HMF preferentially migrates to the IL-rich phase ($EE\% \approx 92-96\%$), while fructose is enriched in the opposite layer ($EE\% \approx 45-59\%$), allowing the separation of the two compounds. **Chapter 5.2** is an additional example of production-separation platforms by the application of switchable ABS. The developed biocompatible thermoreversible ABS, formed by ZIs and PEG of different molecular weights, were applied in biocatalytic processes. The biocatalytic reaction involving laccase occurred in homogeneous media, and by temperature changes, the formation of two phases was induced allowing the complete separation of the enzyme from the product (oxidized ABTS) in a single-step. Furthermore, it was demonstrated that it is possible to maintain the enzymatic activity of laccase at least in 5 recyclability cycles, representing a step forward on the development of more sustainable production-separation processes. In summary, these two works on reversible systems have potential to be used as integrated platforms, in which reaction and separation steps can be carried out sequentially and allowing the IL and remaining solvents recyclability, taking by this way advantage of their switchable behaviour by the application of an external stimulus.

As future work and taking advantage of the results achieved and discussed above, it would be interesting to:

- Conjugate two of the processes presented, *i.e.* solid-liquid extractions of value-added compounds from biomass using ILs aqueous solutions followed by their purification using IL-based ABS, including their use in centrifugal partition chromatography to appraise their feasibility at a large scale;
- Use of aqueous solutions of ILs with ions displaying biological activities to extract value-added compounds from biomass with similar features, aiming at using directly IL-biomass-extracts with improved biological activities directed to nutraceutical and cosmetic applications;
- Development of pH-dependent IL-based ABS through CO₂/N₂ addition to design pH-driven switchable systems, yet without changes in their phases' compositions;
- Explore other applications of switchable IL-based ABS by taking advantage of the applied stimulus in order to develop other integrated production-separation processes;
- Development of multi-responsive IL-based ABS by combining different stimulus in the same system, such as simultaneous pH- and temperature-driven phenomena.
- Development of IL-based aqueous multiphasic systems to act as one-step separation platforms of complex mixtures.

LIST OF PUBLICATIONS

List of publications in the current thesis

1. **Ana M. Ferreira,*** Helena Passos,* Akiyoshi Okafuji, Ana P. M. Tavares, Hiroyuki Ohno, Mara G. Freire and João A. P. Coutinho, "An integrated process for enzymatic catalysis allowing product recovery and enzyme reuse by applying thermoreversible aqueous biphasic systems", *Green Chemistry*, 2018. 20 (6): p. 1218-1223, (*equally contributing authors). Research Highlight in Nature Catalysis (Nature Catalysis, 2018. 1 (4): p. 235).
2. **Ana M. Ferreira,*** Helena Passos,* Akiyoshi Okafuji, Mara G. Freire, João A. P. Coutinho and Hiroyuki Ohno, "Designing the thermal behaviour of aqueous biphasic systems composed of ammonium-based zwitterions", *Green Chemistry*, 2017. 19 (12): p. 4012-4016 (*equally contributing authors). 2017 Green Chemistry Hot Articles and International Symposium on Green Chemistry 2017 Special Issue.
3. **Ana M. Ferreira,** Ana Filipa M. Cláudio, Mónica Válega, Fernando M. J. Domingues, Armando J. D. Silvestre, Robin D. Rogers, João A. P. Coutinho and Mara G. Freire, "Switchable (pH-Driven) Aqueous Biphasic Systems Formed by Ionic Liquids as Integrated Production-Separation Platforms", *Green Chemistry*, 2017. 19 (12): p. 2768-2773, Green Chemistry 2017 Emerging Investigators Special Issue.
4. **Ana M. Ferreira,** Eduarda S. Morais, Ana Cláudia Leite, Aminou Mohamadou, Bjarne Holmbom, Thomas Holmbom, Bruno M. Neves, João A. P. Coutinho, Mara G. Freire and Armando J. D. Silvestre, "Enhanced Extraction and Biological Activity of 7-Hydroxymatairesinol Obtained from Norway Spruce Knots Using Aqueous Solutions of Ionic Liquids", *Green Chemistry*, 2017. 19 (11): p. 2626-2635.

Other publications

1. Ana Cláudia Leite,* **Ana M. Ferreira,*** Eduarda S. Morais, Imran Khan, Mara G. Freire, and João A. P. Coutinho", Cloud point extraction of chlorophylls from spinach leaves using aqueous solutions of non-ionic surfactants", *ACS Sustainable Chemistry & Engineering*, 2018. 6 (1), pp 590–599 (*equally contributing authors).
2. **Ana M. Ferreira,*** Vânia F. M. Faustino,* Dibyendu Mondal, João A. P. Coutinho and Mara G. Freire, "Improving the Extraction and Purification of Immunoglobulin G by the Use of Ionic Liquids as Adjuvants in Aqueous Biphasic Systems", *Journal of Biotechnology*, 2016. 236: p. 166-175 (*equally contributing authors).
3. Helena Passos, Daniel J. P. Tavares, **Ana M. Ferreira,** Mara G. Freire, João A. P. Coutinho, "Are Aqueous Biphasic Systems Composed of Deep Eutectic Solvents Ternary or Quaternary Systems?", *ACS Sustainable Chemistry & Engineering*, 2016. 4 (5): p. 2881-2886.
4. **Ana M. Ferreira,*** Pedro D. O. Esteves,* Isabel Boal-Palheiros, Ana B. Pereira, Luis Paulo N. Rebelo, Mara G. Freire, "Enhanced tunability afforded by aqueous biphasic systems formed by fluorinated ionic liquids and carbohydrates", *Green Chemistry*, 2016. 18 (4): p. 1070-1079 (*equally contributing authors).
5. **Ana M. Ferreira,** João A. P. Coutinho, Ana M. Fernandes and Mara G. Freire, "Complete removal of textile dyes from aqueous media using ionic-liquid-based aqueous two-phase systems", *Separation and Purification Technology*, 2014. 128 (0): p. 58-56.
6. Ana Filipa M. Cláudio, **Ana M. Ferreira,** Mara G. Freire and João A. P. Coutinho, "Enhanced extraction of caffeine from guarana seeds using aqueous solutions of ionic liquids", *Green Chemistry*, 2013. 15 (7): p. 2002-2010.

7. Ana Filipa M. Cláudio, **Ana M. Ferreira**, Carmen S. R. Freire, Armando J. D. Silvestre, Mara G. Freire, and João A. P. Coutinho, "Optimization of the Gallic Acid Extraction using Ionic-Liquid-Based Aqueous Two-Phase Systems", *Separation and Purification Technology*, 2012, 97 (0): p. 142-149.
8. Ana Filipa M. Cláudio, **Ana M. Ferreira**, Shahla Shahriari, Mara G. Freire and João A. P. Coutinho, "Critical Assessment on the Formation of Ionic-Liquid-Based Aqueous Two-Phase Systems in Acidic Media", *Journal of Physical Chemistry B*, 2011, 115 (38): p. 11145–11153.

APPENDIX A

A.1. Extraction of caffeine from spent coffee grounds using aqueous solutions of ionic liquids and salts

Caffeine solubility

Table A.1.1. Influence of the hydrotropes (ILs, salts and the mixture ILs + salts) concentration in the solubility of caffeine in aqueous solutions at 25 °C.

Aqueous solution	Caffeine solubility / (g·L ⁻¹)							
	0.25 M		0.50 M		0.75 M		1.00 M	
NaCl	19.2	± 0.9	17.3	± 1.2	15.0	± 1.2	13.0	± 1.2
[C ₄ C ₁ im]Cl	27.7	± 2.2	29.5	± 1.9	31.7	± 0.9	32.8	± 1.0
NaCl + [C ₄ C ₁ im][Tos] (1:1 in a mole basis)	33.4	± 1.0	37.0	± 0.5	38.3	± 0.9	40.3	± 1.1
Na[Tos] + [C ₄ C ₁ im]Cl (1:1 in a mole basis)	32.9	± 1.0	36.8	± 1.1	38.5	± 1.0	40.1	± 0.5
[C ₄ C ₁ im][Tos]	44.6	± 0.9	51.7	± 2.3	53.5	± 2.6	57.1	± 0.9
Na[Tos]	44.3	± 1.2	50.7	± 1.3	53.7	± 0.8	58.5	± 1.8

Caffeine extraction

Table A.1.2. Caffeine extraction yields with different aqueous solutions of ILs, salts, and their mixtures at different concentrations (T = 25 °C, t = 30 min) for a S/L ratio = 0.10.

Extraction solution	Caffeine extraction yields / (wt. %)							
	1.00 M		0.75 M		0.50 M		0.25 M	
NaCl	0.56	± 0.01	0.56	± 0.01	0.56	± 0.01	0.57	± 0.02
[C ₄ C ₁ im]Cl	0.64	± 0.02	0.62	± 0.03	0.60	± 0.02	0.58	± 0.03
NaCl + [C ₄ C ₁ im][Tos] (1:1 in a mole basis)	0.69	± 0.02	0.67	± 0.02	0.66	± 0.01	0.64	± 0.03
Na[Tos] + [C ₄ C ₁ im]Cl (1:1 in a mole basis)	0.70	± 0.01	0.69	± 0.03	0.68	± 0.02	0.66	± 0.02
[C ₄ C ₁ im][Tos]	0.74	± 0.03	0.72	± 0.03	0.69	± 0.03	0.65	± 0.02
Na[Tos]	0.74	± 0.03	0.71	± 0.01	0.70	± 0.02	0.64	± 0.03

A.2. Extraction of 7-hydroxymatairesinol from Norway Spruce knots using aqueous solutions of ionic liquids

Surface Response Methodology – Experimental procedure

Table A.2.1. 2^3 factorial planning.

Experiment	χ_1	χ_2	χ_3
1	-1	-1	-1
2	1	-1	-1
3	-1	1	-1
4	1	1	-1
5	-1	-1	1
6	1	-1	1
7	-1	1	1
8	1	1	1
9	-1.68	0	0
10	1.68	0	0
11	0	-1.68	0
12	0	1.68	0
13	0	0	-1.68
14	0	0	1.68
15	0	0	0
16	0	0	0
17	0	0	0
18	0	0	0
19	0	0	0
20	0	0	0

Table A.2.2. Coded levels of independent variables used in the first and second factorial planning.

Studied parameters	Symbol	Level				
		Axial -1.68	Factorial -1	Central 0	Factorial 1	Axial 1.68
Concentration (M)	C	0.2	0.6	1.1	1.7	2.0
Extraction time (min)	t	29	90	180	270	331
Solid-liquid ratio	Ratio S/L	0.01	0.05	0.10	0.15	0.19

HMR extraction**Table A.2.3.** HMR extraction yield from Norway spruce knots with different aqueous solutions of ILs (at 1.5 M) and volatile solvents (T = 25 °C, t = 180 min) for a S/L ratio = 0.10 and for a S/L ratio = 0.02. Ratio of HMR2/ HMR1 for a S/L ratio = 0.10 or for a S/L ratio = 0.02.

Solvents	HMR Total Yield (wt%)		Ratio HMR 2/1	
	S/L ratio= 0.02	S/L ratio= 0.10	S/L ratio= 0.02	S/L ratio= 0.10
Acetone		5.00 ± 0.20		0.94 ±
Water		4.38 ± 0.25		1.12 ± 0.15
[C ₄ C ₁ im][Tos]	6.86 ± 0.19	6.52 ± 0.24	1.65 ± 0.13	1.43 ± 0.28
[C ₄ C ₁ im][C ₁ CO ₂]	6.22 ± 0.17	5.83 ± 0.09	1.65 ± 0.10	1.60 ± 0.11
[C ₄ C ₁ im]Cl	6.46 ± 0.02	5.52 ± 0.00	1.74 ± 0.02	1.55 ± 0.09
[C ₄ C ₁ im]Br	7.37 ± 0.31	5.91 ± 0.09	1.41 ± 0.27	1.24 ± 0.06
[C ₁ PyrNC ₂]Br	5.49 ± 0.05	5.22 ± 0.14	1.57 ± 0.11	1.56 ± 0.04
[(C ₂) ₃ NC ₂]Br	5.64 ± 0.07	5.30 ± 0.08	1.76 ± 0.02	1.68 ± 0.11
[(C ₃) ₃ NC ₂]Br	5.82 ± 0.08	5.55 ± 0.20	1.84 ± 0.15	1.73 ± 0.04
[(C ₄) ₃ NC ₂]Br	5.66 ± 0.27	5.11 ± 0.13	1.52 ± 0.18	1.53 ± 0.04

Surface Response Methodology**Table A.2.4.** Experimental data and response surface predicted values of the factorial planning.

Experiment t	t (min)	C (M)	Ratio S/L	Experimental yield of HMR Total (wt%)	Predicted yield of HMR Total (wt%)	Relative deviation (%)
1	331	1.1	0.10	8.04	7.56	-6.26
2	270	0.6	0.05	6.43	6.55	1.91
3	270	1.7	0.05	8.09	8.37	3.33
4	270	0.6	0.15	5.41	5.72	5.42
5	270	1.7	0.15	7.38	7.74	4.66
6	180	0.2	0.10	3.96	3.84	-3.18
7	180	2.0	0.10	7.47	7.10	-5.14
8	180	1.1	0.01	8.53	8.44	-1.00

9	180	1.1	0.19	7.80	7.40	-5.44
10	180	1.1	0.10	7.40	7.36	-0.56
11	180	1.1	0.10	6.95	7.36	5.54
12	180	1.1	0.10	7.40	7.36	-0.56
13	180	1.1	0.10	7.47	7.36	-1.56
14	180	1.1	0.10	7.50	7.36	-1.92
15	180	1.1	0.10	7.34	7.36	0.24
16	90	0.6	0.05	5.78	5.76	-0.29
17	90	1.7	0.05	7.60	7.63	0.44
18	90	0.6	0.15	5.08	5.15	1.26
19	90	1.7	0.15	7.00	7.22	3.03
20	30	1.1	0.10	6.48	6.47	-0.21

Table A.2.5. Regression coefficients of the predicted second-order polynomial model for the HMR extraction yield obtained from the RSM, $R^2 = 0.954$ and $r_{adj} = 0.913$. The statistical results obtained are in terms of the coded values of the factors.

	Regression coefficients	Standard deviation	t-student (10)	P-value
Interception	7.359	0.136	53.970	<0.05
Time	0.326	0.091	3.607	<0.05
Concentration	0.971	0.091	10.727	<0.05
Solid-liquid ratio	-0.311	0.091	-3.439	<0.05
Time ²	-0.122	0.088	-1.381	0.197
Concentration ²	-0.668	0.088	-7.576	<0.05
Solid-liquid ratio ²	0.199	0.088	2.258	<0.05
Time × Concentration	-0.014	0.118	-0.119	0.907
Time × Solid-liquid ratio	-0.054	0.118	-0.458	0.657
Solid-liquid ratio × Concentration	0.050	0.118	0.421	0.682

Table A.2.6. ANOVA data for the extraction of HMR obtained from the RSM design.

	Sum of squares	Degrees of freedom	Mean square	F-value	P-value
Regression	23.20926	9	2.578807	23.07013	0.000015
Residuals	1.11781	10	0.111781		
Total	24.32708				

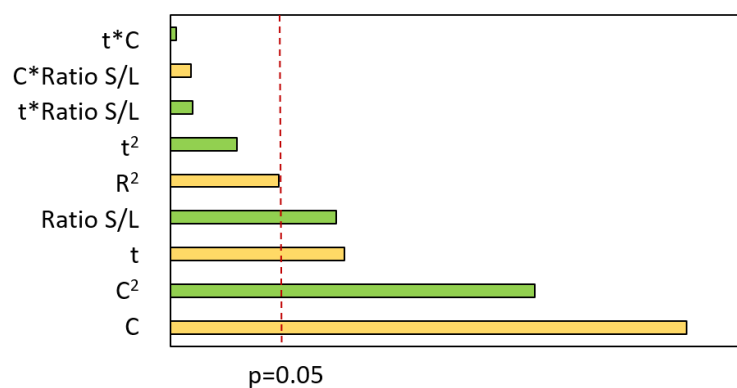


Figure A.2.1. Pareto chart for the standardized main effects (positive (yellow) and negative (green)) in the factorial planning for the HMR extraction. The vertical line indicates the statistical significance of the effects.

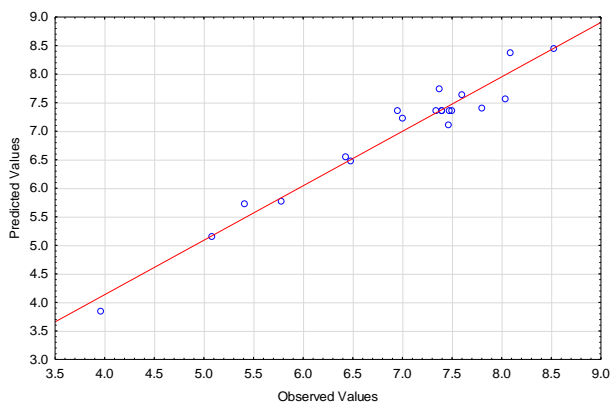


Figure A.2.2. Observed values vs Predicted values.

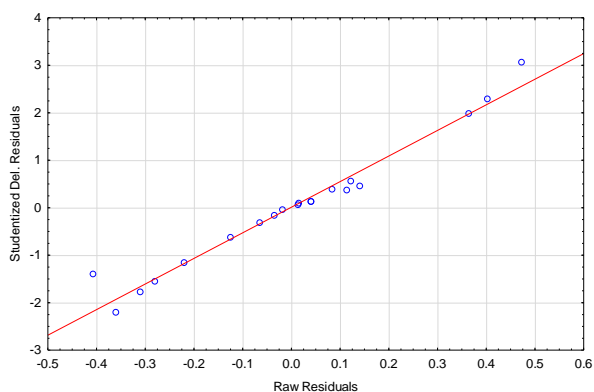


Figure A.2.3. Distribution of residuals.

Table A.2.7. Predicted yield of HMR total (wt%) using an IL concentration at 1.5 M and a solid-liquid ratio of 0.01 at different extractions times.

t (min)	predicted yield of HMR total (wt%)
220	8.94
240	9.00
260	9.04
280	9.10
300	9.11
320	9.13
340	9.13

Recyclability of the biomass

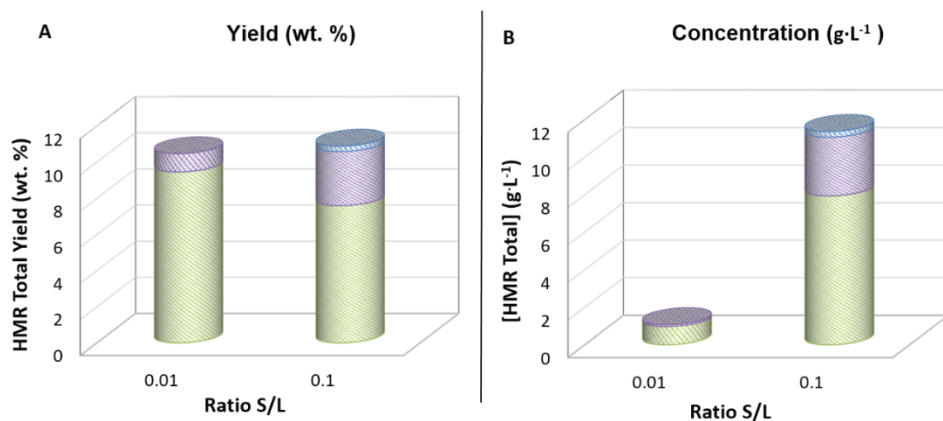
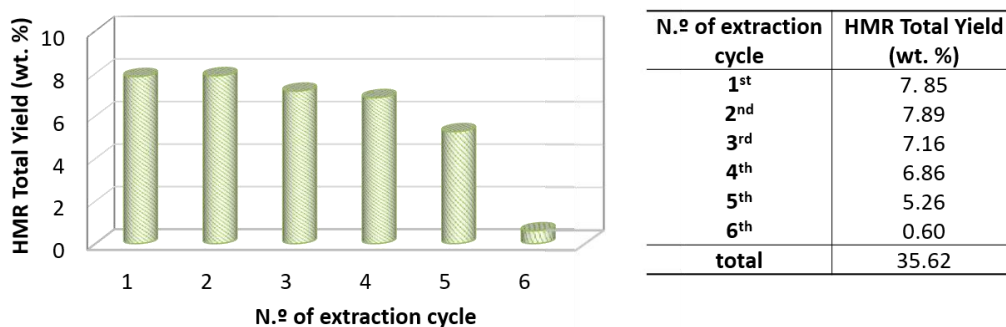
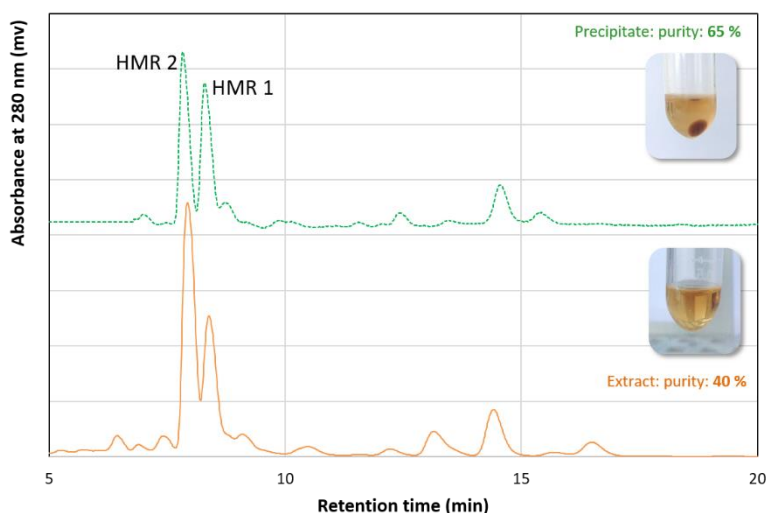


Figure A.2.4. Results on the use of new aqueous solutions of $[(C_2)_3NC_2]Br$ at 1.5 M for 3 successive extractions of the same biomass sample, at the optimized operational conditions (solid-liquid ratio of 0.1 or 0.01 during 280 min and at 25 °C). **(A)** HMR total extraction yield and **(B)** concentration obtained during the biomass recyclability studies. (green bars) 1st cycle, (purple bars) 2nd cycle and (blue bars) 3rd cycle.

Table A.2.8. HMR total extraction yield and concentration obtained during the biomass recyclability studies.

	HMR Total Yield (wt%)		[HMR Total] (g·L ⁻¹)	
	S/L ratio = 0.01	S/L ratio = 0.10	S/L ratio = 0.01	S/L ratio = 0.10
1 st Cycle	9.46	7.59	0.97	7.93
2 nd Cycle	1.01	3.00	0.10	3.13
3 rd Cycle	0.00	0.30	0.00	0.30
4 th Cycle	0.00	0.00	0.00	0.00

**Figure A.2.5.** HMR extraction yield according to the reusability of the aqueous solution of $[(C_2)_3NC_2]Br$ at 1.5 M. This solution was used for 6 successive extractions at the optimized operational conditions (solid-liquid ratio of 0.1 for 280 min and at 25 °C) using new biomass samples in each cycle.**Figure A.2.6.** HPLC-DAD chromatograms of the HMR extract in aqueous solutions of IL (—) and precipitated HMR (---).

Antioxidant activity assays

Table A.2.9. Antioxidant activity of the different HMR extracts.

Type of extract	Time (h)	$\mu\text{g AAE}\cdot\text{mg}^{-1}$ of extract
Soxhlet Extract	0.5	21.61 ± 3.57
	1.5	20.32 ± 3.04
	2	19.47 ± 3.02
IL+Extract	0.5	21.82 ± 6.97
	1.5	19.51 ± 6.54
	2	18.97 ± 6.89
Precipitated Extract	0.5	2.56 ± 0.61
	1.5	2.20 ± 0.4
	2	2.25 ± 0.51

Analysis of the scale-up potential of the proposed process

To appraise the extraction process scale-up viability, the following equation was used:

$$R = [C_{prod} \times \epsilon_{prod} - \epsilon_{biom}] - [V_{IL} \times \epsilon_{IL} \times r_{IL\ lost} \times \delta + \beta] \quad (\text{Eq. A.2.1})^1$$

This equation was proposed by Passos *et al.*² as a simplified model that relates the return (R) associated to the extraction of a particular value-added compound when ILs are used as extraction solvents. In **Eq. (A.2.1)** the return *per* kg of treated biomass is equal to the gain, defined by the extracted concentration of the target compound in the biomass (C_{prod}), times its price *per* kg (ϵ_{prod}), minus the cost associated to the biomass (ϵ_{biom}), and the extraction process that we assume to be proportional to the cost of the IL lost in each kg of biomass treated. The cost of the IL lost in the process is given by the volume of the IL needed to treat one kg of biomass (V_{IL}), times its price per kg (ϵ_{IL}), times the ratio of IL lost during the recycling approach ($r_{IL\ lost}$), that in our case is of 100% because we do not pretend to recycle the IL. The factor δ represents the proportional costs of the process, and the non-proportional constant β represents other constant costs. Through the application of **Eq (A.2.1)** it is possible to understand which variables display the most relevant impact on the return of a given process.¹

In the developed process, taking in account a solid–liquid ratio of 1:10 and an IL concentration of 1.5 M, and that the solution will be reused five times until saturation, 0.8 kg of $\text{IL}\cdot\text{kg}_{\text{biomass}}^{-1}$ are needed, with an IL price of 110 € kg^{-1} (small scale) and without the recovery of

the IL (r_{IL} lost = 100%). In **Figure A.2.7A** it is possible to see a linear relationship between the return and the production cost if a negligible cost of the biomass is assumed ($\$_{biom} = 0$). Thus, as it is possible to obtain a high concentration of the target compound (37 wt% of HMR), the cost of the ILs is the main factor responsible for the final product cost, mainly because we do not aim the IL recycling. Therefore, for this process to become economically viable it is necessary to employ ILs with a cost lower than 11 € kg^{-1} (**Figure A.2.7B**), which is perfectly achievable if the process is scaled-up and industrial reagents are acquired,^{2,3} instead of using those available at a lab-scale.

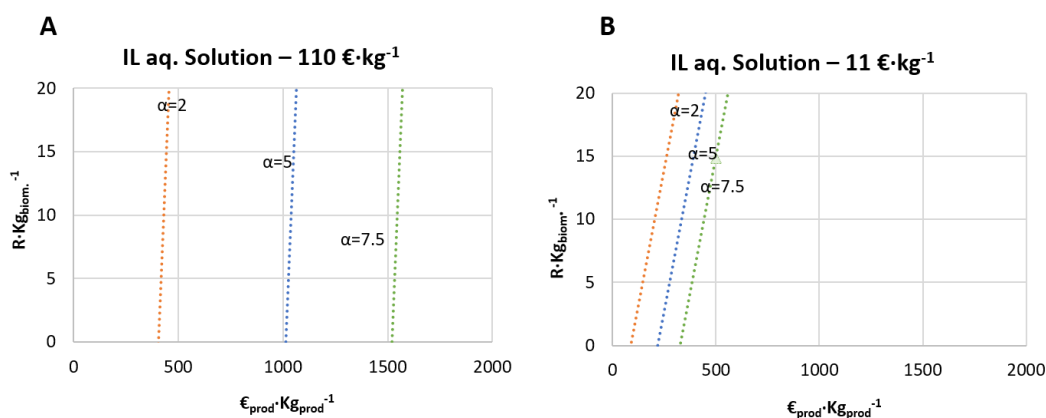


Figure A.2.7. Return obtained for each kg of treated biomass as a function of the IL cost, **(A)** IL price of $110 \text{ €} \cdot \text{kg}^{-1}$ **(B)** IL price of $11 \text{ €} \cdot \text{kg}^{-1}$.

References

1. H. Passos, M. G. Freire and J. A. P. Coutinho, *Green Chem.*, 2014, **16**, 4786-4815.
2. Merckmillipore, <http://www.merckmillipore.com/DE/en/product/>, (accessed March 2017).
3. Alibaba, <https://www.alibaba.com>, (accessed March 2017).

APPENDIX B

B.1. pH-responsive aqueous biphasic systems formed by ionic liquids and polymers

Determination of the ABS phase diagrams and tie-lines (TLs)

Table B.1.1. Experimental weight fraction data for the systems composed of PPG 400 (1) + [Ch]Cl (2) + H₂O (3) at 25 °C and atmospheric pressure.

pH ≈ 6		pH ≈ 5		pH ≈ 4		pH ≈ 3	
100 w ₁	100 w ₂	100 w ₁	100 w ₂	100 w ₁	100 w ₂	100 w ₁	100 w ₂
59.7532	4.1395	52.8723	5.5387	52.7824	5.9084	58.3564	5.3205
49.4185	5.3248	46.4150	6.4181	42.9307	7.1386	49.2396	6.3663
35.8966	6.9097	40.7974	7.1892	39.2582	7.7223	40.4128	7.3836
32.4552	7.4524	36.8239	7.6400	36.4770	7.9673	31.6416	9.6679
29.6019	8.2317	33.6122	8.3820	34.5635	8.3681	28.8933	10.3231
26.7506	9.4906	27.6148	10.3735	31.2450	9.3932	27.0617	11.0236
24.4788	10.5980	25.7613	10.9259	28.4750	10.1740	25.6632	11.8768
18.4968	13.3364	23.7786	11.8542	26.2602	11.1482	21.7211	13.9509
17.5558	14.0857	22.2997	12.6928	24.6853	12.1823	20.4996	14.8983
16.6818	14.8366	20.9626	13.5935	23.0535	13.0662	19.2025	15.8738
15.5831	15.9160	19.8542	14.4509	21.8673	13.7015	18.0334	16.3081
14.8640	16.7543	18.5097	15.7845	20.4640	14.8041	17.1847	17.2285
14.3194	17.0226	17.1164	16.7403	19.3719	15.2737	16.0937	18.0482
13.6968	17.6815	15.8749	17.9693	18.2690	16.1415	15.5562	18.3674
13.2829	18.1224	15.1095	18.6685	15.6427	17.4720	15.0386	18.9172
12.8191	18.3980	14.1274	19.8070	14.3531	19.0349	14.5618	19.4484
12.4294	18.8661	13.1325	20.6890	13.3947	19.9554	14.0055	20.0191
0.0000	0.0000	12.2130	21.6637	12.6118	20.9712	13.5096	20.3838
11.6097	19.9104	11.5915	22.4241	11.9627	21.6976	13.1025	20.7967
11.1937	20.2424	10.7515	23.4144	11.4323	22.2675	12.5953	21.3281
10.7458	20.7799	10.0731	24.4786	10.8227	23.0596	12.0384	21.8452
10.4340	21.0027			10.2984	23.7361	11.6476	22.2494
10.0677	21.4114					11.1255	22.9989
9.6171	22.0911					10.6908	23.6781
9.3013	22.5695					10.2762	24.0234
8.9851	22.9893					9.9460	24.4708
8.6572	23.3424					9.5722	25.0197
8.3524	23.6269						
8.0836	24.0514						
7.7731	24.3902						

Table B.1.2. Experimental weight fraction data for the systems composed of PPG 400 (1) + IL (2) + H₂O (3) at 25 °C and atmospheric pressure.

[Ch]Cl				[Ch][C ₁ CO ₂]	
pH ≈ 2		pH ≈ 1		pH ≈ 9	
100 w ₁	100 w ₂	100 w ₁	100 w ₂	100 w ₁	100 w ₂
46.7755	6.9008	57.0021	5.8068	62.2434	2.5662
40.8679	7.2435	48.8889	6.4576	53.3027	3.6444
34.6006	8.5195	43.0007	7.1546	45.0223	4.2765
32.1922	9.0772	39.2462	8.0611	40.2374	4.8220
30.1997	9.7495	24.0966	13.6377	35.7533	5.5826
28.5268	10.7455	22.9697	13.9400	32.3194	5.9866
26.2866	11.6911	21.5344	14.6861	30.3054	6.3806
24.4148	12.5483	20.0900	15.3788	28.0351	6.8690
22.6845	13.6216	19.2542	15.9541	23.8764	7.8872
21.0476	14.9172	18.2562	16.6517	22.4079	8.4851
19.0809	16.3731	17.3228	16.9136	20.7062	9.2137
17.5593	17.5620	16.2446	17.9112	19.2778	9.9999
16.2876	18.5948	15.2223	18.6531	16.0776	11.1828
15.5805	19.4104	14.2998	19.7305	15.4904	11.4911
14.8130	20.2956	13.5687	20.5798	14.9912	11.8453
14.0085	21.2632	12.8833	20.8624	14.4345	12.3824
13.4975	21.8212	12.5215	21.2633	13.8961	12.6638
12.9722	22.3954	12.0080	21.8916	13.3943	12.9397
				12.9830	13.4865
				12.4644	13.9071
				12.0131	14.2372
				11.6145	14.5842
				11.1326	14.8984
				10.8677	15.1538
				10.5030	15.5629
				10.1721	15.9009
				9.8193	16.2896
				9.4237	16.6121
				8.9030	17.6248
				8.6957	18.0559

Table B.1.3. Experimental weight fraction data for the systems composed of PPG 400 (1) + [Ch][C₁CO₂] (2) + H₂O (3) at 25 °C and atmospheric pressure.

pH ≈ 8		pH ≈ 7		pH ≈ 6		pH ≈ 5	
100 w ₁	100 w ₂	100 w ₁	100 w ₂	100 w ₁	100 w ₂	100 w ₁	100 w ₂
54.6031	5.0394	56.4943	6.8460	48.0396	9.5022	54.1295	9.8833
48.8655	6.0096	51.4596	7.7135	46.2564	9.9356	51.0816	11.6533
29.9665	11.8524	47.5712	8.3634	44.6495	10.7930	49.3503	13.3356
27.9906	12.7336	44.6179	9.2990	43.3274	11.0511	46.2413	14.5185
26.6476	13.4651	34.2213	10.9544	40.6562	11.9750	42.4865	18.0246
24.7729	13.9703	32.3083	11.2973	39.1273	12.7216	39.4951	20.9362
23.3359	14.6873	30.9894	11.7560	37.7614	13.7091		
22.0874	15.1576	29.4847	12.0318	36.7350	14.0281		
20.6967	15.8834	28.5021	12.4839	35.3484	14.8988		
19.4767	16.8004	27.5649	12.9219	34.5000	15.2042		
18.2613	17.3891	26.6191	13.4923	33.2758	16.0089		
17.3460	17.8304	25.0059	14.1441	31.7019	16.4039		
16.3928	18.4987			30.5723	17.4661		
15.5605	19.0674			28.6270	18.7499		
14.8769	19.3999			26.9100	19.9894		
				25.2884	21.4396		
				23.5715	23.2259		
				22.2588	24.7318		
				20.9626	25.8128		
				19.6128	27.7123		
				18.3490	29.6039		
				17.0761	31.8186		
				15.6422	34.9359		

Table B.1.4. Experimental weight fraction data for the systems composed of PPG 400 (1) + [Ch][C₂CO₂] (2) + H₂O (3) at 25 °C and atmospheric pressure.

pH ≈ 8		pH ≈ 7		pH ≈ 6		pH ≈ 5	
100 w ₁	100 w ₂	100 w ₁	100 w ₂	100 w ₁	100 w ₂	100 w ₁	100 w ₂
44.5952	5.7175	56.4943	6.8460	55.5307	8.2453	61.4200	8.8946
41.3783	6.1279	51.4596	7.7135	51.6542	9.3539	56.8397	11.2466
34.4822	6.8389	47.5712	8.3634	49.8029	10.3037	52.4439	12.9165
32.4571	7.1200	44.6179	9.2990	46.8573	11.2386	50.1136	13.6458
31.1750	7.4391	34.2213	10.9544	44.4757	11.7993	47.5044	15.5158
27.6950	8.6203	32.3083	11.2973	42.6258	12.5584	45.3968	17.0625
26.3713	8.9673	30.9894	11.7560	40.6863	13.2181		
24.7850	9.7275	29.4847	12.0318	35.6820	14.9487		
23.1773	10.0498	28.5021	12.4839	34.2739	15.3597		
21.9820	10.7785	27.5649	12.9219	32.6688	16.1998		
20.5827	11.3181	26.6191	13.4923	31.3793	16.3884		

19.3680	11.6819	25.0059	14.1441	30.4884	16.8421
18.4598	12.2914	23.9300	14.7874	29.8749	17.5404
17.2735	12.6296	22.7203	15.4359	29.0650	17.8387
16.5801	13.1291	21.4602	16.4649	27.9969	18.9169
15.7179	13.7294	20.0449	17.4179	27.0550	19.7528
14.8602	14.4935	18.7946	18.1425	26.0586	20.4862
13.9646	15.0787	17.4092	19.0483		
13.3363	15.3438	16.6174	19.6840		
12.6596	15.9378	15.7684	20.4511		
12.1134	16.4191	14.8904	21.1748		
11.4332	17.1174	14.1233	21.8795		
11.0200	17.5610	13.3370	22.9640		
10.4604	18.1920	12.5012	23.9935		
9.9837	18.6085	11.6981	25.2076		
9.5463	19.0402	10.7417	27.0962		
9.1016	19.5564				

Table B.1.5. Experimental weight fraction data for the systems composed of PPG 400 (1) + [Ch][Lac] (2) + H₂O (3) at 25 °C and atmospheric pressure.

pH ≈ 7		pH ≈ 6		pH ≈ 5		pH ≈ 4	
100 w ₁	100 w ₂	100 w ₁	100 w ₂	100 w ₁	100 w ₂	100 w ₁	100 w ₂
56.9575	3.5283	58.7605	4.7414	46.7239	9.1828	54.8035	11.3515
35.5059	6.2014	56.0807	5.4008	44.6863	9.9975	50.4094	14.4250
33.0561	6.6436	53.6867	5.8983	43.2509	10.3578	46.9767	16.8815
30.0739	7.6275	50.0782	6.3409	41.5848	10.9828	44.1931	18.7172
26.6982	8.4305	48.2521	6.8630	35.2355	13.0357	41.5404	20.4667
23.8971	9.0050	45.0155	7.5570	33.2873	13.9893	38.7645	22.5816
22.0381	9.5716	42.3031	8.0129	31.2925	14.8492	35.8946	25.0858
20.4718	10.5160	39.8886	8.3647	29.7590	15.5212	33.5717	27.1607
19.1057	11.3305	38.5278	8.7424	27.9996	16.3845	31.7752	28.8225
17.6568	12.1084	37.3275	9.1039	25.9459	17.6506		
16.4701	12.6995	36.1461	9.4873	24.4075	18.4441		
15.6712	13.0326	34.2409	9.8379	21.0115	21.2016		
14.9078	13.5705	32.7047	10.2688	19.8296	21.9969		
14.1921	14.1030	31.0008	10.7548	18.5687	22.7285		
13.5151	14.5670	28.7951	11.5977	17.4251	23.7080		
13.0089	15.0409	26.8138	12.5599	16.2915	24.7439		
12.3006	15.5938	25.0422	13.3312	15.6619	25.4254		
11.7019	15.9777	23.3603	14.0865	14.7127	26.3039		
11.1916	16.5126	22.2641	14.9301	13.5136	27.6597		
10.7446	16.9131	20.9622	15.7390	12.6090	28.8469		
10.3590	17.2277	19.7527	16.4743	11.6030	30.3170		
9.9392	17.6969	18.5438	17.4251	10.9748	32.0263		
9.5100	18.0761	17.2843	18.1701	10.1309	33.1935		

16.2173	18.8301	9.2899	34.5470
15.4649	19.4988		
14.5479	20.1697		
13.6239	20.9971		
12.8825	21.5915		
12.1359	22.6195		
11.1002	23.4026		
10.3702	24.4070		
9.6582	25.0032		
8.7701	26.0296		

Table B.1.6. Experimental weight fraction data for the systems composed of PPG 400 (1) + [Ch][Gly] (2) + H₂O (3) at 25 °C and atmospheric pressure.

pH ≈ 7		pH ≈ 6		pH ≈ 4	
100 w_1	100 w_2	100 w_1	100 w_2	100 w_1	100 w_2
62.9671	3.1708	59.7877	4.9948	57.8111	6.7937
51.3010	4.0717	51.4078	5.9067	51.0564	8.0817
43.8295	5.1693	46.3200	6.6792	47.5512	9.0382
36.9375	5.7690	42.8885	7.3476	44.5361	10.0949
28.0324	7.2200	39.8920	7.9482	41.6892	10.8792
25.7823	7.6551	37.0065	8.4363	39.8818	11.7668
24.0925	8.1523	34.5014	8.8010	37.6512	12.2464
22.4759	9.0019	32.6456	9.3662	34.0591	13.6205
20.8381	9.6107	30.6550	9.6897	31.3547	14.6370
19.3942	10.3030	28.7295	10.7020	28.8978	15.6352
18.1418	11.0393	26.4707	11.4722	27.6539	15.9857
16.9162	11.7583	24.7902	12.0716	25.8482	16.8336
15.9441	12.3304	23.6134	13.3213	23.9382	18.1751
15.0238	12.7526	22.2632	13.7163	22.4799	19.2959
14.2388	13.4776	20.5797	15.4497	20.7106	20.5423
13.5185	13.7305	19.3834	15.9492	19.2389	21.3595
12.8304	14.3680	18.1396	17.0536	17.9515	22.7080
12.1284	14.8950	16.7612	17.7890	16.6972	23.6229
11.4602	15.6133	16.0667	18.3390	15.4629	24.7914
10.8353	16.0448	15.0440	19.5769	14.4042	26.0293
10.2723	16.6132	13.9212	20.1407	13.3780	27.3638
9.6447	17.1678	12.4944	22.3703	12.4233	28.5322
		11.5647	23.1238	11.2612	30.4304
		10.8146	23.7316	10.3707	31.4536
		9.9253	24.4484		

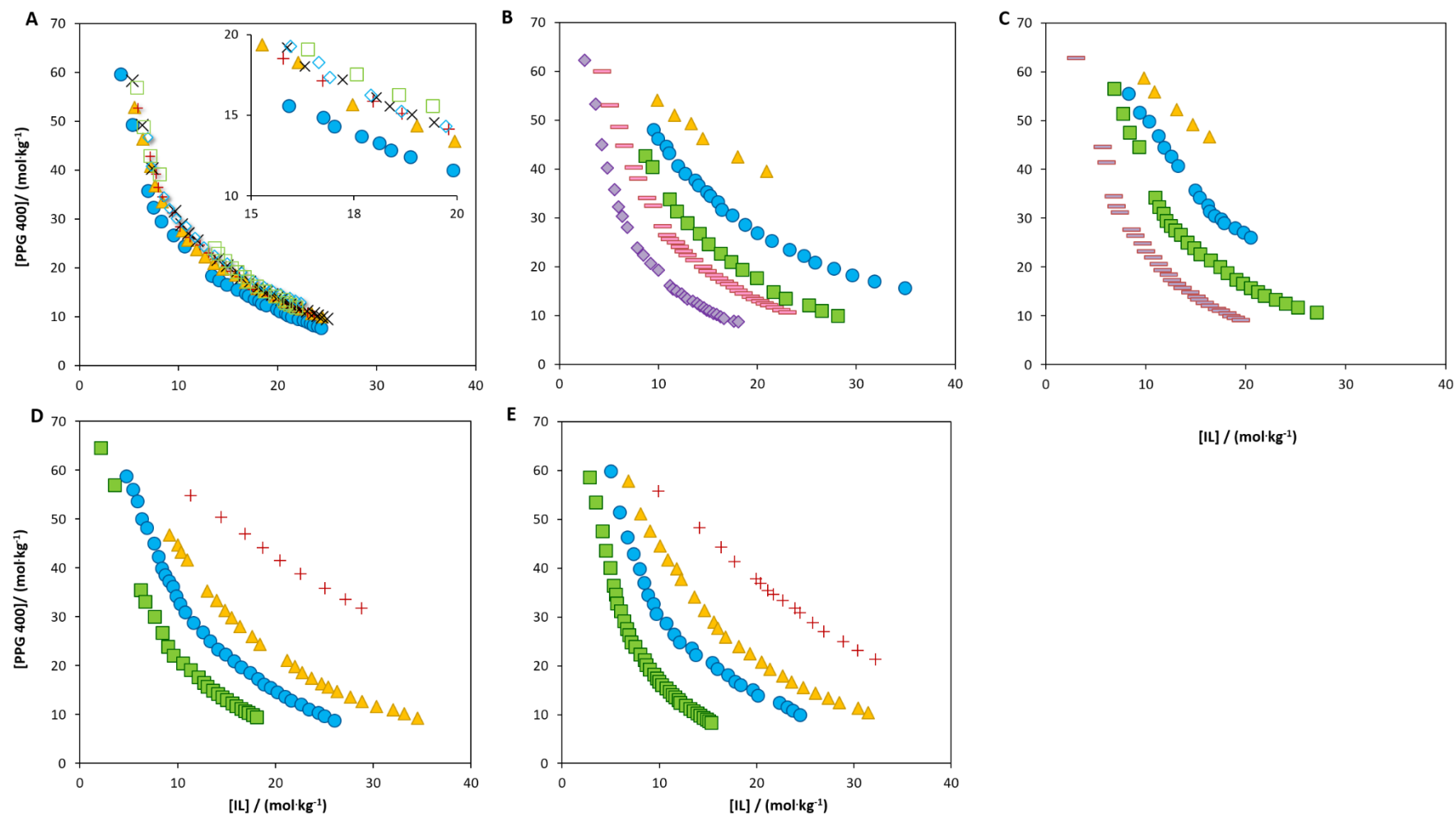


Figure B.1.1. Evaluation of the pH effect in the ternary phase diagrams, at 25 °C and atmospheric pressure, composed of PPG 400 + water + IL at pH \approx 9 (\blacklozenge), pH \approx 8 ($-$), pH \approx 7 (\blacksquare), pH \approx 6 (\bullet), pH \approx 5 (\blacktriangle), pH \approx 4 ($+$), pH \approx 3 (\times), pH \approx 2 (\blacklozenge) and pH \approx 1 (\square). ILs: (A) [Ch]Cl, (B) [Ch][C₁CO₂], (C) [Ch][C₂CO₂], (D) [Ch][Lac] and (E) [Ch][Gly].

Table B.1.7. Identification of the systems able (✓) or not able (✗) to form two-phase systems as a function of the pH, at 25 °C and atmospheric pressure.

pH	9	8	7	6	5	4	3	2	1
[Ch]Cl					✓	✓	✓	✓	✓
[Ch][C ₁ CO ₂]	✓	✓	✓	✓	✓	✗	✗	✗	✗
[Ch][Gly]			✓	✓		✓	✗	✗	✗
[Ch][Lac]			✓	✓	✓	✓	✗	✗	✗
[Ch][C ₂ CO ₂]		✓	✓	✓	✓	✗	✗	✗	✗

Separation of HSA and DNA**Table B.1.8.** Extraction efficiency to the IL-rich phase and yield of DNA and HSA.

IL	pH	DNA				HSA			
		EE%		Y%		EE%		Y%	
[Ch][Gly]	7	98.56	± 0.08	98.29	± 1.00	95.00	± 0.50	40.00	± 8.00
	6	99.28	± 0.11	99.16	± 1.73	91.18	± 1.34	40.00	± 7.87
	5	98.91	± 0.17	101.46	± 1.78	87.03	± 2.00	43.96	± 5.00
	4	95.65	± 0.84	98.00	± 4.89	30.94	± 4.00	62.00	± 5.00
[Ch][C ₂ CO ₂]	8	98.78	± 0.17	96.43	± 6.49	97.00	± 5.00	100.00	± 2.00
	7	98.13	± 0.21	100.41	± 5.14	96.42	± 5.00	100.00	± 2.00
	6	95.20	± 0.62	94.03	± 0.43	95.03	± 4.98	100.00	± 3.84
	5	90.00	± 0.48	95.00	± 6.21	56.59	± 4.46	100.00	± 4.49
[Ch][C ₁ CO ₂]	9	98.56	± 0.12	105.00	± 8.00	99.61	± 0.06	106.32	± 8.41
	8	98.00	± 1.09	100.00	± 6.04	95.00	± 0.10	104.48	± 4.17
	7	98.78	± 0.06	104.00	± 3.63	97.93	± 0.05	105.00	± 2.37
	6	98.67	± 0.01	98.00	± 2.00	96.79	± 0.54	105.00	± 8.00
	5	93.32	± 0.09	104.21	± 7.02	59.66	± 1.00	100.00	± 2.00
[Ch]Cl	6	100.00	± 0.09	100.00	± 1.50	100.00	± 1.00	86.00	± 2.00
	5	99.81	± 0.02	104.33	± 0.30	100.00	± 0.99	84.31	± 1.97
	4	99.80	± 0.02	103.42	± 1.39	100.00	± 0.87	70.20	± 6.23
	3	99.83	± 0.02	100.46	± 0.52	100.00	± 1.01	45.00	± 8.00
	2	99.81	± 0.01	105.52	± 0.74	100.00	± 1.32	33.28	± 7.00
	1	99.95	± 0.05	34.46	± 5.00	100.00	± 0.88	17.35	± 7.00

Table B.1.9. Identification of the ABS with precipitation (✓) or not (✗) of HSA and DNA at different pH values.

pH	DNA				HSA			
	[Ch][Gly]	[Ch][C ₂ CO ₂]	[Ch][C ₁ CO ₂]	[Ch][Cl]	[Ch][Gly]	[Ch][C ₂ CO ₂]	[Ch][C ₁ CO ₂]	[Ch][Cl]
1	---	---	---	✓	---	---	---	✓
2	---	---	---	✗	---	---	---	✓
3	---	---	---	✗	---	---	---	✓
4	✗	---	---	✗	✓	---	---	✓
5	✗	✗	✗	✗	✓	✗	✗	✓
6	✗	✗	✗	✗	✓	✗	✗	---
7	✗	✗	✗	---	✓	✗	✗	---
8	---	✗	✗	---	---	✗	✗	---
9	---	---	✗	---	---	---	✗	---

Purification of DNA using [Ch][Gly]-based ABS

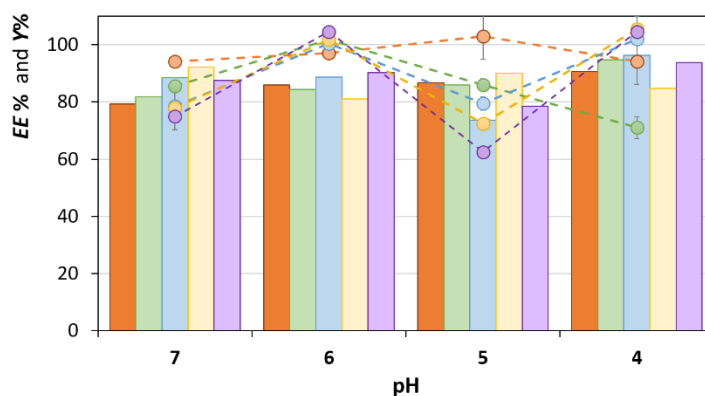
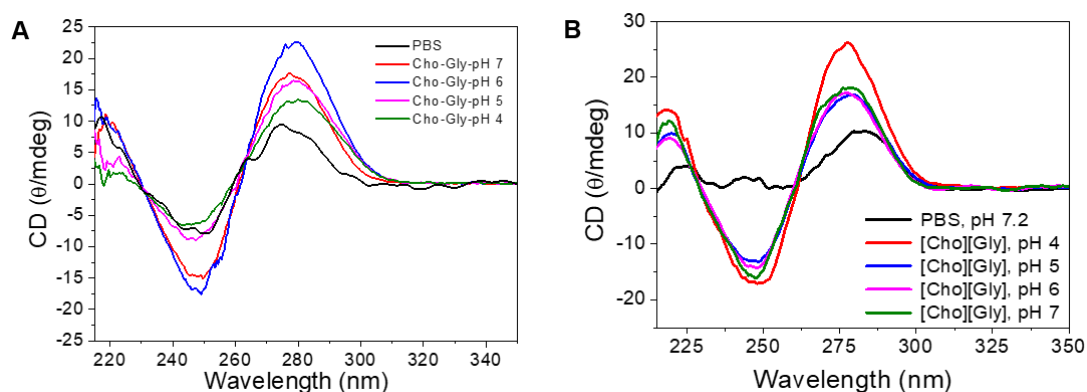

Figure B.1.2. DNA extraction efficiency to the IL-rich phase ($EE\%$, bars) and HSA yield ($Y\%$, symbols) in ABS composed of [Ch][Gly] at different pH values. DNA:HSA mole ratios: (orange) 1:1, (green) 1:2, (blue) 1:3, (yellow) 1:4 and (purple) 1:5.

Table B.1.10. Extraction efficiency of DNA to the IL-rich phase and respective yield in the ABS formed by [Ch][Gly] at different pH values.

pH	Y%					EE%				
	ADN:HSA ratio (w/w)					ADN:HSA ratio (w/w)				
	(1:1)	(1:2)	(1:3)	(1:4)	(1:5)	(1:1)	(1:2)	(1:3)	(1:4)	(1:5)
4	94.10	71.00	101.90	105.50	104.60	90.60	94.70	96.30	92.20	93.80
5	103.00	86.00	79.50	72.50	62.50	86.70	85.90	73.70	81.00	78.50
6	97.00	101.70	100.50	101.80	104.60	85.90	84.40	88.60	90.10	90.30
7	94.10	85.50	78.60	78.00	74.90	79.20	81.90	88.50	84.70	87.60

Table B.1.11. Identification of the systems with precipitation (✓) or not (✗) of HSA in ABS formed by [Ch][Gly] at different pH values.

pH	DNA: HSA weight ratio				
	(1:1)	(1:2)	(1:3)	(1:4)	(1:5)
7	✗	✗	✗	✗	✗
6	✗	✓	✓	✓	✓
5	✓	✓	✓	✓	✓
4	✓	✓	✓	✓	✓

**Figure B.1.3.** Circular dichroism (CD) spectra of standard DNA and DNA recovered from the bottom phase of [Ch][Gly]-based ABS at different pH values: **(A)** after extraction and immediate recovery; **(B)** after storage for six months at room temperature (*ca.* 25 °C) and recovery. All CD spectra were recorded in PBS (0.01 M, pH 7.2).

B.2. Temperature-responsive aqueous biphasic systems composed of ammonium-based zwitterions and salts

NMR spectrum data of the synthesized ZIs:

N₅₅₅C3S: δ_{H} (400 MHz; D₂O; δ /ppm relative to TMS): 0.77 (9H, t, $J=7.00$), 1.22 (12H), 1.52 (6H), 2.01 (2H), 2.83 (2H, t, $J=7.00$), 3.10 (6H), 3.25 (2H). Elemental analysis (%) for C₁₈H₃₉NO₃S: Found: C, 61.37; H, 11.67; N, 3.76; C/N, 16.32. Calculated: C, 61.85; H, 11.25; N, 4.01; C/N, 15.42.

N₃₃₃C3S: δ_{H} (400 MHz; D₂O; δ /ppm relative to TMS): 0.83 (9H, t, $J=7.30$), 1.55 (6H), 1.98 (2H), 2.83 (2H t, $J=7.00$), 3.06 (6H), 3.26 (2H). Elemental analysis (%) for C₁₂H₂₇NO₃S: Found: C, 53.22; H, 10.50; N, 44.89; C/N, 10.89. Calculated: C, 54.31; H, 10.25; N, 45.28; C/N, 10.29.

N₂₂₂C3S: δ_{H} (400 MHz; D₂O; δ /ppm relative to TMS): 1.16 (9H, t, $J=7.30$), 2.01 (2H), 2.86 (2H t, $J=7.10$), 3.22 (8H). Elemental analysis (%) for C₉H₂₁NO₃S: Found: C, 47.77; H, 9.55; N, 5.92; C/N, 8.07. Calculated: C, 48.4; H, 9.48; N, 6.27; C/N, 7.72.

N₁₁₁C3S: δ_{H} (400 MHz; D₂O; δ /ppm relative to TMS): 2.12 (2H), 2.86 (2H, t, $J=7.30$), 3.03 (9H), 3.37 (2H). Elemental analysis (%) for C₆H₁₅NO₃S: Found: C, 39.60; H, 8.51; N, 7.38; C/N, 5.36. Calculated: C, 39.76; H, 8.34; N, 7.73; C/N, 5.14.

N₁₁₁C4S: δ_{H} (400 MHz; D₂O; δ /ppm relative to TMS): 1.68 (2H), 1.82 (2H), 2.85 (2H, t, $J=7.30$), 3.00 (9H), 3.25 (2H). Elemental analysis (%) for C₇H₁₇NO₃S: Found: C, 41.19; H, 8.93; N, 6.48; C/N, 6.35. Calculated: C, 39.42; H, 8.98; N, 6.57; C/N, 6.00.

Table B.2.1. Thermal properties of the synthesised ZIs: T_m – melting temperature. T_d – decomposition temperature.

ZI	T _m (°C)	T _d (°C)
N ₅₅₅ C3S	170	268
N ₃₃₃ C3S	228	282
N ₂₂₂ C3S	186	300
N ₁₁₁ C3S	195	368
N ₁₁₁ C4S	185	353

Determination of the ABS phase diagrams

Table B.2.2. Experimental weight fraction data for the systems composed of N₅₅₅C3S (1) + salt (2) + H₂O (3) at 25 °C and atmospheric pressure.

K ₃ PO ₄		KH ₂ PO ₄		K ₂ HPO ₄		K ₂ CO ₃	
100 w ₁	100 w ₂	100 w ₁	100 w ₂	100 w ₁	100 w ₂	100 w ₁	100 w ₂
53.89	0.78	67.81	1.04	68.61	0.84	33.17	3.57
50.06	1.44	62.93	1.34	60.23	1.07	10.29	7.12
46.98	1.54	59.87	1.63	53.44	1.24	8.12	8.19
43.93	2.42	56.28	1.89	50.56	1.46	5.77	9.29
27.24	4.60	53.97	2.12	49.73	1.46	5.57	9.69
24.89	5.07	51.63	2.35	47.02	1.78	3.89	10.51
23.96	5.22	48.72	2.91	43.46	2.11	2.52	11.47
23.17	5.40	46.08	3.44	28.01	5.02	2.03	11.81
22.54	5.59	43.79	3.79	26.22	5.27	1.66	12.78
21.68	5.69	41.73	4.14	23.99	5.78	1.22	14.71
20.90	5.73	39.02	4.71	22.36	6.11		
20.13	5.89	36.56	5.24	21.12	6.40		
19.45	6.02	33.90	5.89	20.44	6.58		
19.00	6.21	31.37	6.54	18.77	6.88		
18.40	6.33	27.78	7.46	17.34	7.28		
17.77	6.41	25.33	8.17	16.68	7.49		
17.65	6.03	23.05	8.82	15.60	7.84		
16.94	6.69	21.31	9.35	14.69	8.10		
14.60	6.78	20.54	9.56	13.70	8.45		
13.33	7.12	19.71	9.78	12.82	8.76		
12.56	7.36	16.88	10.81	12.16	8.96		
11.75	7.66			11.35	9.30		
10.87	7.96			10.51	9.68		
8.74	8.75			9.83	9.98		
7.86	9.14			9.17	10.30		
6.92	9.47			8.79	10.44		
6.25	9.87			8.13	10.72		
5.74	10.10			7.40	11.20		
5.51	10.32			6.83	11.57		
4.95	10.57			6.14	12.07		
4.38	11.07						
3.00	12.95						
2.28	13.93						
2.06	15.70						

Table B.2.3. Experimental weight fraction data for the systems composed of N₅₅₅C3S (1) + salt (2) + H₂O (3) at 25 °C and atmospheric pressure.

K₃C₆H₅O₇		Na₃C₆H₅O₇		NaH₂PO₄			
100 w₁	100 w₂	100 w₁	100 w₂	100 w₁	100 w₂	100 w₁	100 w₂
70.74	1.56	41.18	3.64	63.44	1.15	17.45	9.08
57.13	2.56	36.36	4.09	60.18	1.58	17.00	9.20
50.14	3.33	33.49	4.58	55.37	1.95	16.44	9.39
45.04	3.91	31.09	5.02	51.56	2.26	15.98	9.55
41.57	4.43	28.19	5.87	49.12	2.61	15.50	9.72
38.63	4.91	26.46	6.24	46.57	2.85	14.99	9.93
36.13	5.29	25.06	6.44	44.78	3.10	14.58	10.07
34.23	5.75	23.11	7.03	43.00	3.34	14.20	10.20
32.66	6.18	19.61	7.82	41.18	3.62	13.84	10.33
31.15	6.57	18.42	8.17	39.66	3.80	13.49	10.46
29.64	6.86	17.26	8.57	37.78	4.23	13.18	10.57
28.49	7.16	16.27	8.90	36.54	4.43	12.87	10.69
21.03	8.83	15.44	9.16	34.94	4.77	12.59	10.81
18.33	9.58	14.48	9.53	34.14	4.93	12.24	10.96
15.96	10.32	13.80	9.75	32.61	5.27	11.83	11.17
15.21	10.62	12.99	10.08	31.78	5.43	11.44	11.36
13.88	11.06	12.08	10.51	30.47	5.75	11.04	11.57
12.86	11.62	11.33	10.77	29.62	5.90	10.68	11.76
11.12	12.40	10.75	11.05	28.43	6.19	10.18	12.03
9.55	13.19	10.09	11.34	27.32	6.45	9.76	12.28
8.97	13.91	9.43	11.74	26.23	6.70		
8.11	14.83	8.33	12.40	24.97	7.02		
4.65	17.27	7.38	12.99	24.17	7.21		
3.21	18.99	6.05	14.18	23.17	7.52		
2.66	20.15	2.93	15.91	22.47	7.69		
2.54	19.26	2.44	19.32	21.81	7.84		
2.32	20.56			20.98	8.11		
1.97	21.47			20.38	8.25		
1.57	23.56			19.62	8.48		
1.50	22.61			19.09	8.61		
1.38	24.45			18.47	8.79		
0.77	26.97			17.87	8.99		

Table B.2.4. Experimental weight fraction data for the systems composed of N₃₃₃C3S (1) + salt (2) + H₂O (3) at 25 °C and atmospheric pressure.

K ₃ PO ₄		K ₂ HPO ₄		K ₂ CO ₃		K ₃ C ₆ H ₅ O ₇	
100 w ₁	100 w ₂	100 w ₁	100 w ₂	100 w ₁	100 w ₂	100 w ₁	100 w ₂
57.59	0.96	55.23	1.07	44.91	4.17	64.88	3.11
48.70	1.48	47.42	1.85	38.43	6.55	59.52	4.15
44.69	2.79	40.25	3.50	33.73	8.24	52.93	6.45
40.40	3.75	36.85	4.20	30.12	9.72	47.74	8.18
37.77	4.38	36.13	4.44	26.89	11.08	43.36	10.76
34.92	5.11	35.20	4.74	20.66	13.26	41.09	12.02
33.14	5.99	34.69	4.93	19.04	14.29	38.79	13.34
31.60	6.81	33.78	5.24	15.68	15.77	34.79	16.13
29.53	7.33	33.14	5.48	14.79	16.27	32.14	17.98
28.34	7.88	32.47	5.76	14.06	16.55	29.95	19.52
27.24	8.29	31.70	6.10	13.33	16.94	27.62	21.24
26.29	8.80	30.73	6.49	12.68	17.13	25.42	22.97
24.88	9.78	29.68	6.92	12.09	17.43	22.80	24.99
24.02	10.15	28.92	7.32	11.54	17.69	21.29	26.14
23.27	10.49	27.71	7.89	11.15	18.16	19.78	27.33
22.54	10.73	26.67	8.41	10.62	18.35	18.94	27.99
21.94	11.17	25.99	8.85	10.16	18.57	17.68	28.99
21.43	11.38	24.94	9.46	9.77	18.76	16.49	29.94
20.82	11.71	23.50	10.18	9.52	19.01	15.55	30.74
19.91	12.42	22.71	10.84	9.18	19.20	14.87	31.37
19.38	12.70	21.53	11.37	8.84	19.18	13.92	32.23
18.86	12.94	20.41	12.21	8.62	19.40	12.20	33.85
18.44	13.14	18.85	13.19	8.41	19.61	11.35	34.70
17.93	13.39	17.10	14.43	8.21	19.86		
17.18	14.03	15.34	15.79	7.93	19.89		
16.76	14.07	14.42	16.71	7.76	20.15		
16.32	14.27	11.93	18.38	7.42	20.63		
15.69	14.77	9.02	20.49	7.05	20.76		
15.32	14.88	7.24	22.43	6.78	21.04		
14.77	15.31			6.59	21.06		
14.48	15.49			6.33	21.42		
14.18	15.65			6.16	21.44		
13.88	15.82			6.02	21.41		
13.56	15.96			5.91	21.62		
13.32	16.07			5.80	21.76		
13.05	16.28			5.66	21.77		
12.76	16.44			5.56	21.91		
12.22	16.68			5.46	22.05		
11.86	16.96			5.34	22.02		
11.20	17.31			5.25	22.13		

11.00	17.45		5.18	22.26
10.48	17.48		5.01	22.53
10.13	18.12		4.87	22.73
9.90	18.06		4.69	22.83
9.44	18.27		4.55	23.01
9.07	18.51		4.42	23.12
8.79	19.00		4.30	23.28
8.49	18.97		4.15	23.62
8.20	19.20		4.02	23.64
8.00	19.57		3.87	23.84
7.73	19.73			
7.51	19.91			
7.27	20.10			

Table B.2.5. Experimental weight fraction data for the systems composed of N₃₃₃C3S (1) + salt (2) + H₂O (3) at 25 °C and atmospheric pressure.

Na₃C₆H₅O₇		NaH₂PO₄	
100 w₁	100 w₂	100 w₁	100 w₂
59.89	1.00	59.10	1.13
56.37	1.88	54.34	2.08
51.89	2.53	46.13	6.41
48.06	3.08	42.94	8.16
44.33	4.40	40.08	9.63
42.40	4.91	37.85	10.82
39.61	5.90	34.97	12.57
36.93	6.95		
33.16	8.64		
29.55	10.43		
24.36	13.31		
20.63	15.56		
16.31	18.18		

Table B.2.6. Experimental weight fraction data for the systems composed of N₂₂₂C3S (1) + salt (2) + H₂O (3) at 25 °C and atmospheric pressure.

K₃PO₄		K₂HPO₄		K₂CO₃	
100 w₁	100 w₂	100 w₁	100 w₂	100 w₁	100 w₂
59.14	0.84	54.56	4.12	54.97	2.68
46.60	2.76	40.00	5.64	43.70	4.00
40.41	4.10	34.66	7.34	29.84	6.89
36.71	5.62	31.74	9.01	27.81	7.72
32.52	7.86	28.58	10.04	15.94	11.82
28.76	9.62	23.46	13.05	15.34	12.00
26.00	11.40	22.35	14.16	14.77	12.22
24.60	12.08	21.04	14.82	14.20	12.40
22.73	13.27	20.11	15.45	13.45	12.93
21.11	14.30	18.53	17.07	12.61	13.24
19.56	15.09	17.74	17.59	11.89	13.56
18.26	15.87	17.00	17.89	11.23	13.75
17.23	16.62	15.99	18.90	10.76	14.15
16.23	17.24	15.37	19.27	10.33	14.11
15.35	17.84	14.79	19.59	9.95	14.46
14.53	18.46	14.30	19.90	9.46	14.61
13.83	18.92	13.58	20.84	8.90	14.98
13.23	19.30	13.12	21.08	8.39	15.33
12.64	19.65	12.68	21.33	7.61	16.10
11.96	20.16	12.10	21.89	4.66	18.94
11.51	20.44	11.72	22.15	54.97	2.68
11.04	20.82	11.23	22.72	43.70	4.00
10.65	21.09	10.90	22.88	29.84	6.89
10.26	21.32	10.62	23.09	27.81	7.72
9.78	21.81	10.20	23.60	15.94	11.82
9.43	22.04	9.81	24.00		
9.07	22.38	9.53	24.16		
8.80	22.51	9.24	24.38		
8.56	22.67	8.98	24.66		
8.22	23.00	8.68	25.05		
7.92	23.27	8.40	25.40		
7.64	23.57	8.06	25.43		
7.43	23.66	7.77	25.74		
7.17	23.87	7.49	26.14		
6.93	24.10	7.29	26.36		
6.75	24.24	7.10	26.57		
6.52	24.44	6.78	26.91		
6.32	24.65	6.61	27.12		
6.13	24.88	6.36	27.33		
5.95	25.09	6.21	27.50		
5.79	25.27				
5.68	25.60				
5.52	25.42				

Table B.2.7. Experimental weight fraction data for the systems composed of $N_{111}C4S$ (1) + salt (2) + H_2O (3) at 25 °C and atmospheric pressure.

K_3PO_4		K_2HPO_4		K_2CO_3	
100 w_1	100 w_2	100 w_1	100 w_2	100 w_1	100 w_2
58.16	2.52	53.33	5.86	32.38	8.43
45.92	4.27	42.07	9.15	25.61	10.97
39.55	5.74	33.00	12.67	18.65	13.68
35.87	7.40	29.83	13.82	13.01	16.09
31.20	10.18	27.71	15.45	7.71	18.69
27.66	12.12	25.85	16.62	5.94	20.36
24.93	13.85	24.33	17.84	3.78	23.16
22.68	15.37	22.93	18.51		
20.82	16.57	21.74	19.31		
18.70	18.13	20.79	20.08		
17.41	18.86	19.14	21.81		
16.02	19.98	18.28	22.21		
15.07	20.57	17.46	22.84		
13.83	21.56	16.08	24.07		
12.91	22.29	15.54	24.61		
12.02	22.93	15.00	25.23		
11.11	23.67	14.04	26.12		
10.51	24.18	13.63	26.39		
9.93	24.65	12.90	27.00		
9.43	25.01	12.58	27.30		
9.00	25.37	12.23	27.57		
8.45	25.93	11.88	27.75		
7.93	26.46	11.38	28.41		
7.52	26.80	10.77	29.16		
7.09	27.35	9.85	29.84		
6.71	27.72	9.62	29.92		
6.37	28.03	9.44	30.16		
6.13	28.28	9.06	30.66		
5.82	28.35	8.87	30.73		
5.50	28.77	8.58	31.16		
5.25	29.11	8.27	31.42		
4.92	29.57	8.00	31.80		
		7.75	32.14		
		7.46	32.21		
		7.34	32.32		
		7.12	32.75		
		6.95	33.13		
		6.78	33.31		
		6.52	33.65		
		6.28	33.97		
		6.03	34.29		
		5.83	34.50		
		5.69	34.64		
		5.56	34.79		

	5.44	34.98	
	5.34	35.06	
	5.12	35.44	
	4.94	35.66	

Table B.2.8. Experimental weight fraction data for the systems composed of N₁₁₁C3S (1) + salt (2) + H₂O (3) at 25 °C and at atmospheric pressure.

K ₃ PO ₄		K ₂ HPO ₄		K ₂ CO ₃	
100 w ₁	100 w ₂	100 w ₁	100 w ₂	100 w ₁	100 w ₂
46.56	5.85	39.90	9.29	24.36	14.12
38.97	8.05	36.08	11.23	12.54	19.46
33.31	10.88	32.89	13.11	3.29	28.28
28.38	13.94	28.97	16.52		
23.63	16.46	26.99	17.65		
20.35	17.67	24.28	20.04		
17.93	19.50	22.82	20.84		
15.94	21.16	20.78	22.69		
14.23	22.39	19.18	24.09		
12.49	23.95	17.76	25.38		
11.28	25.19	16.58	26.31		
10.21	26.30	15.59	27.25		
9.37	27.31	14.70	28.10		
8.65	28.37	13.83	28.71		
7.08	30.06	12.85	29.85		
5.78	31.59	12.18	30.47		
5.14	32.86	11.60	30.96		
2.22	37.89	10.88	31.86		
		10.44	32.26		
		9.84	33.00		
		9.50	33.35		
		9.13	33.63		
		8.70	34.30		
		8.29	34.87		
		7.87	35.19		
		7.57	35.56		
		7.25	35.94		
		6.95	36.28		
		6.69	36.63		
		6.38	37.12		
		6.22	37.18		
		5.97	37.63		
		5.76	37.94		
		5.63	38.05		
		5.45	38.27		
		5.30	38.54		

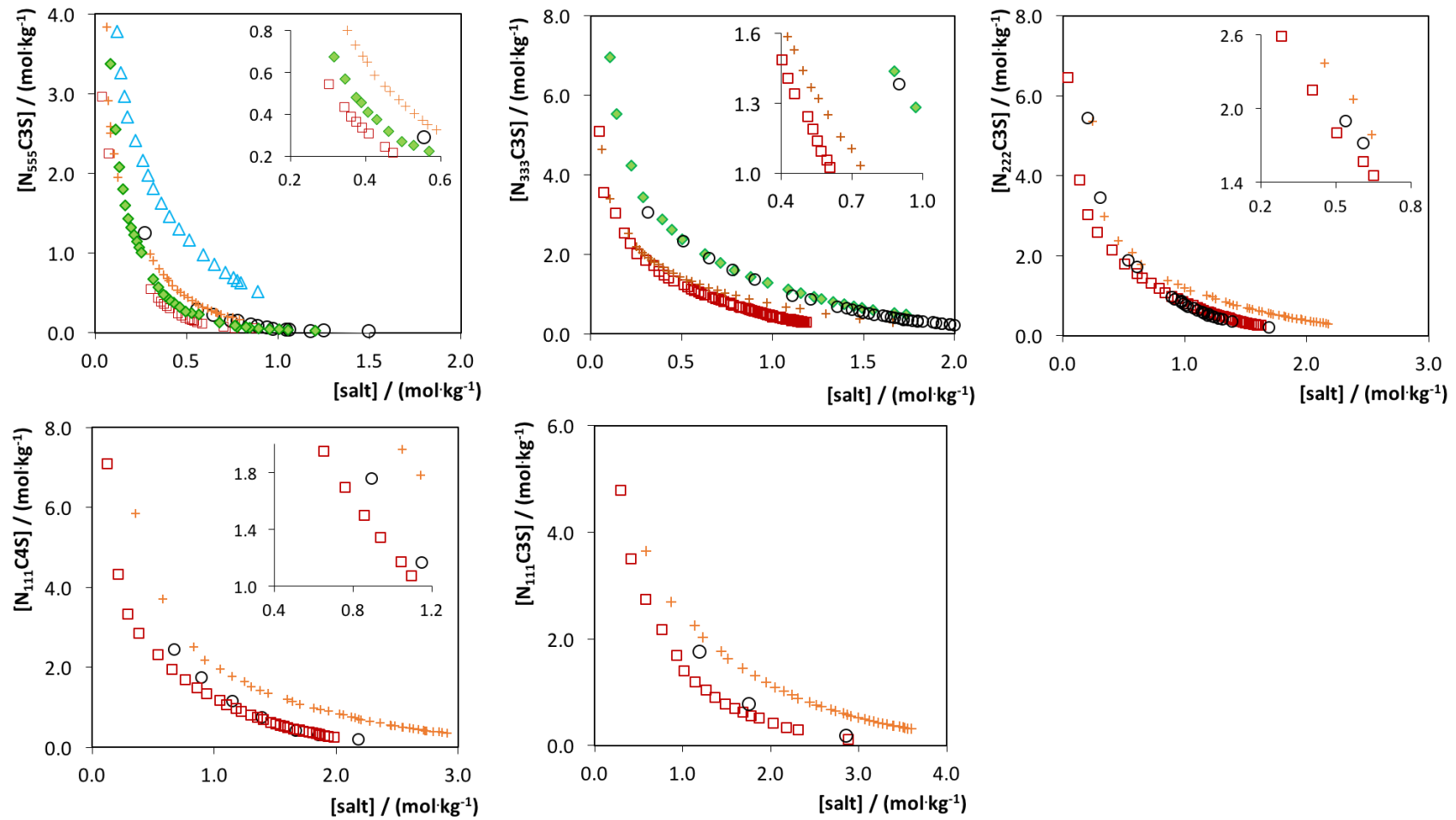


Figure B.2.1. Salt anion effect in the phase diagrams of ternary systems, at 25 °C and atmospheric pressure, composed of water, ZIs, and the following potassium-based salts: K₃PO₄ (□), K₃C₆H₅O₇ (◆), K₂CO₃ (○), K₂HPO₄ (+) and KH₂PO₄ (△).

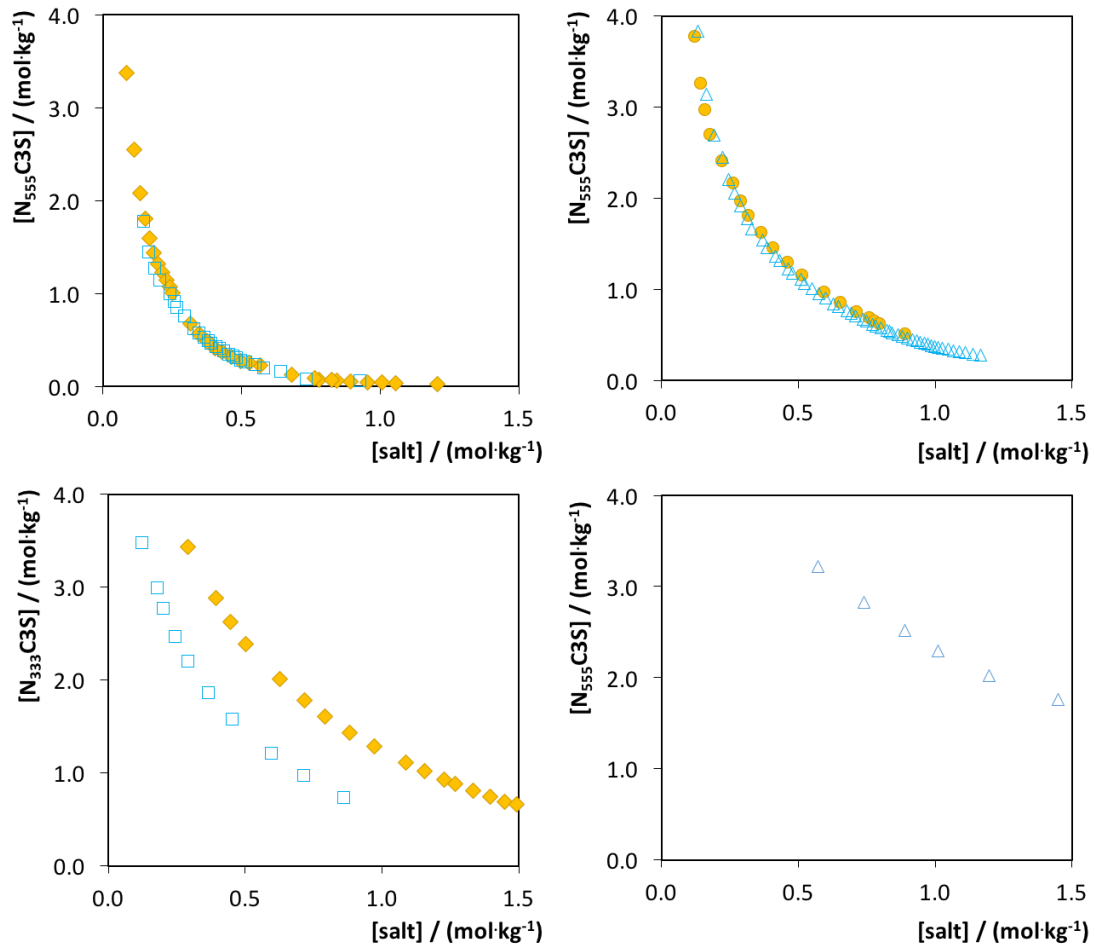


Figure B.2.2. Cation salt effect in the phase diagrams of ternary systems, at 25 °C and atmospheric pressure, composed of water, ZIs, and the following salts: $\text{Na}_3\text{C}_6\text{H}_5\text{O}_7$ (\square), $\text{K}_3\text{C}_6\text{H}_5\text{O}_7$ (\blacklozenge), NaH_2PO_4 (\triangle) and KH_2PO_4 (\bullet).

Table B.2.9. Experimental weight fraction data for the systems composed of ZI (1) + K₃PO₄ (2) + H₂O (3) at 35 °C and 45 °C and atmospheric pressure.

N ₅₅₅ C3S				N ₃₃₃ C3S			
35 °C		45 °C		35 °C		45 °C	
100 w ₁	100 w ₂	100 w ₁	100 w ₂	100 w ₁	100 w ₂	100 w ₁	100 w ₂
45.40	2.09	45.96	1.77	49.55	2.01	57.81	0.98
38.13	2.70	35.71	2.41	39.28	3.72	50.93	1.87
29.22	3.68	31.21	2.86	36.10	5.09	40.96	3.42
25.11	4.22	27.20	3.44	32.62	6.15	38.42	4.04
21.65	4.69	24.88	4.05	32.06	6.30	36.05	4.55
19.13	5.27	17.74	4.98	30.02	7.15	33.06	5.78
17.70	5.59	16.60	5.26	29.07	7.90	30.47	6.93
16.42	5.90	15.81	5.38	28.77	7.73	28.34	7.68
13.40	6.71	14.52	5.74	27.21	8.48	25.42	9.29
12.73	7.04	12.83	5.93	25.94	9.42	24.11	9.67
12.12	7.18	10.57	6.77	25.64	9.19	22.12	10.68
11.43	7.33	9.72	6.85	24.44	9.81	19.88	12.16
10.45	7.64	9.08	7.27	23.15	10.74	18.14	13.17
10.18	7.85	8.28	7.43	22.20	11.16	16.90	13.73
9.38	8.16	7.69	7.48	20.41	12.04	15.49	14.64
8.85	8.47	7.32	7.93	18.92	12.85	14.41	15.24
8.32	8.77	6.99	7.82	17.73	13.40	13.44	15.81
7.77	8.90	6.68	8.20	17.09	13.80	12.51	16.41
7.44	9.23	6.35	8.45	16.55	14.07	11.71	16.92
7.16	9.13	5.89	8.75	15.93	14.42	11.01	17.41
6.98	9.33	5.55	9.08	15.46	14.68	10.25	17.93
6.71	9.40	5.27	9.11	14.80	15.24	9.73	18.19
6.53	9.47	5.11	9.30	14.36	15.42	9.06	18.67
6.38	9.56	4.85	9.32	13.94	15.57	8.64	18.83
6.18	9.88	4.68	9.55	13.60	15.79	8.48	18.85
5.89	10.11			13.14	15.89	7.97	19.34
5.65	10.05			12.47	16.29	7.55	19.62
5.47	10.22			12.22	16.34	6.95	20.20
5.26	10.45			11.90	16.61	6.59	20.46
				11.48	16.75	6.46	20.50
				11.08	17.31	5.53	21.50
				10.80	17.22		
				10.65	17.35		
				10.24	17.66		
				10.09	17.73		
				9.91	17.86		
				9.59	18.07		
				9.26	18.30		

		8.97	18.46
		8.69	18.55
		8.33	18.81
		8.14	19.02
		8.06	19.05
		7.84	19.17
		7.50	19.46
		7.43	19.46
		7.34	19.49
		7.21	19.62
		7.07	19.73
		7.00	19.79

Table B.2.10. Experimental weight fraction data for the systems composed of ZI (1) + K₃PO₄ (2) + H₂O (3) at 35 °C and 45 °C and atmospheric pressure.

N ₂₂₂ C3S				N ₁₁₁ C4S			
35 °C		45 °C		35 °C		45 °C	
100 w ₁	100 w ₂	100 w ₁	100 w ₂	100 w ₁	100 w ₂	100 w ₁	100 w ₂
56.67	2.51	44.99	4.14	54.55	2.59	47.95	4.17
38.52	5.61	40.40	5.46	45.20	5.18	40.44	5.64
35.58	6.85	37.02	6.46	40.37	7.13	35.35	8.54
33.03	7.95	34.64	7.49	33.63	9.66	31.26	10.57
29.85	9.86	32.72	8.40	29.62	12.02	29.41	11.28
28.10	10.56	30.81	9.29	25.44	14.91	25.39	14.02
25.77	12.10	29.45	9.87	23.09	16.31	22.14	16.14
23.84	13.46	28.00	10.45	21.03	17.43	19.34	18.39
22.75	13.79	25.32	12.56	18.82	18.86	17.52	19.78
20.67	15.33	23.83	12.82	17.01	20.12	16.05	20.87
19.71	15.66	22.92	13.23	15.49	21.21	14.66	21.85
18.05	16.95	21.61	14.28	14.25	22.03	12.91	23.35
16.95	17.46	20.89	14.62	13.64	22.22	12.54	23.38
16.23	17.69	19.60	15.60	11.83	24.07	11.47	24.41
15.14	18.61	18.66	16.22	11.30	24.31	10.79	24.88
14.05	19.28	18.08	16.30	10.54	24.90	9.70	26.09
12.95	19.64	17.20	17.02	9.74	25.58	9.21	26.39
12.29	20.51	16.79	17.18	9.31	25.83	7.92	27.96
12.01	20.57	16.16	17.49	8.68	26.36	7.67	28.00
11.67	20.65	15.34	18.23	8.18	26.80	7.07	28.62
11.03	21.11	14.66	18.35	7.51	27.56	6.45	29.37
10.60	21.55	13.92	19.02			6.11	29.65
10.26	21.80	13.31	19.29			5.75	30.03
10.05	21.79	13.01	19.40				

9.45	22.59	12.29	20.26		
9.26	22.56	11.81	20.38		
8.83	23.06	11.14	20.87		
8.68	23.06	10.38	21.51		
8.52	23.06	10.10	21.45		
8.29	23.13	9.53	22.03		
7.81	23.88	9.02	22.37		
7.54	23.88	8.56	22.84		
		7.96	23.15		

Table B.2.11. Experimental weight fraction data for the systems composed of $N_{111}C_3S$ (1) + K_3PO_4 (2) + H_2O (3) at 35 °C and 45 °C and atmospheric pressure.

35 °C		45 °C	
100 w_1	100 w_2	100 w_1	100 w_2
50.05	4.95	49.83	5.37
39.60	8.45	43.03	7.25
32.80	10.90	38.41	9.11
27.25	14.79	35.25	10.40
23.43	16.98	30.76	13.10
20.30	19.16	25.44	16.84
17.60	21.33	22.76	18.50
15.28	22.98	19.28	21.23
12.87	24.99	16.62	23.18
11.10	26.54	14.79	24.46
9.09	28.57	13.27	25.44
7.10	30.71	12.00	26.41
6.52	31.21	10.62	27.56
		8.79	29.33
		7.87	30.17
		6.60	31.56

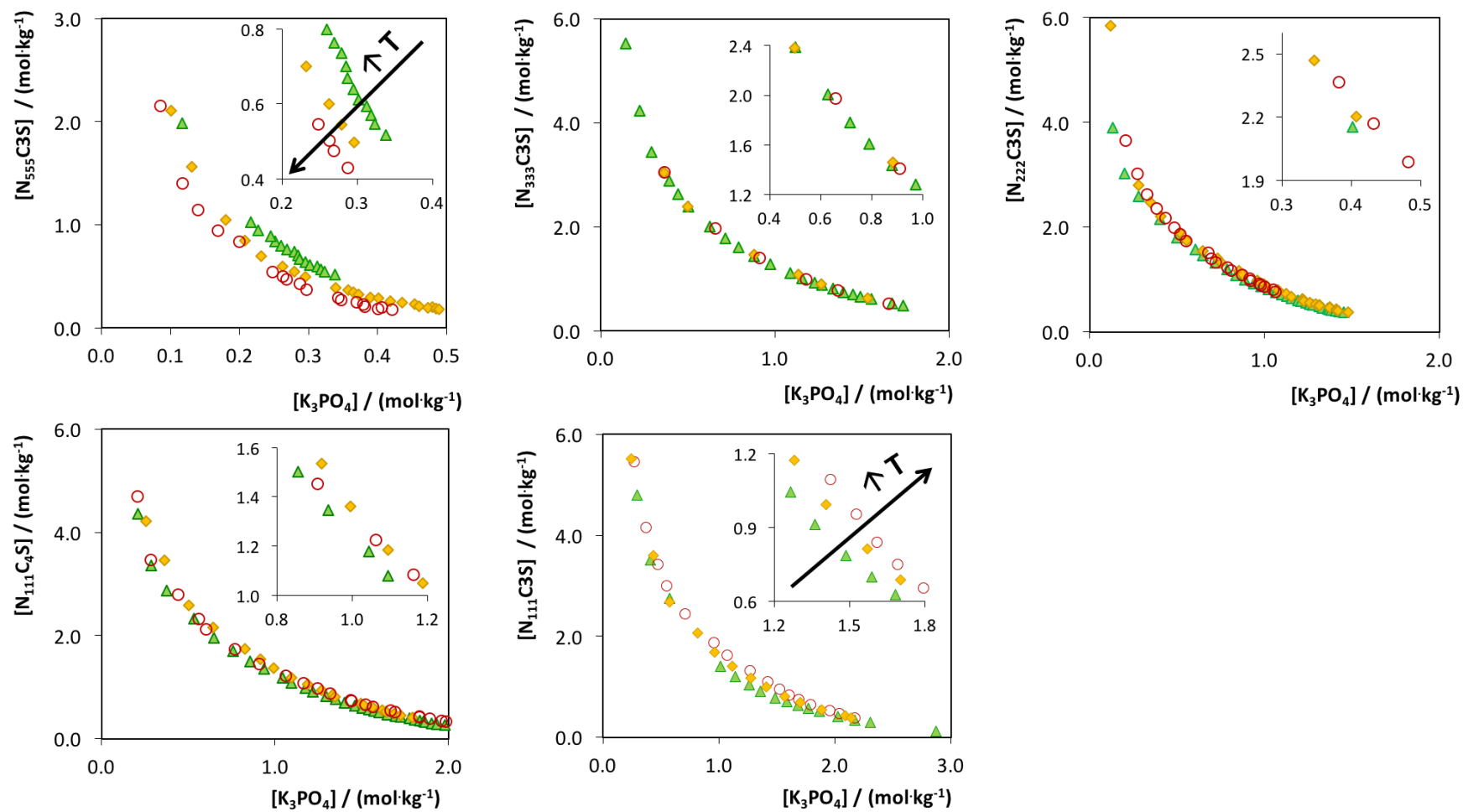


Figure B.2.3. Temperature effect in the phase diagrams of the ternary systems, at 25 °C and atmospheric pressure, composed of ZI + K_3PO_4 + water at 25 °C (\blacktriangle), 35 °C (\blacklozenge), and 45 °C (\circ).

Partition of amino acids

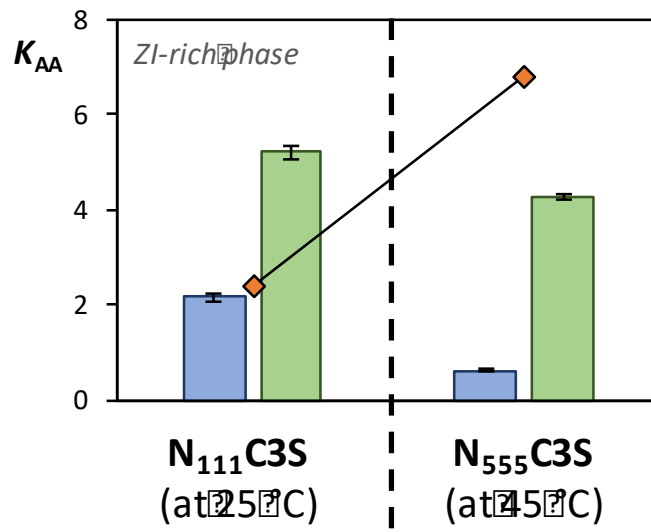


Figure B.2.4. Partition coefficient (K_{AA}) of L-tryptophan (green bars) and glycine (blue bars) in N₁₁₁C3S- and N₅₅₅C3S-based ABS at 25 °C and 45 °C, respectively, and selectivity (\diamond).

APPENDIX C

C.1. Integrated production-separation platforms applying reversible pH-driven aqueous biphasic systems

Determination of the ABS phase diagrams and tie-lines (TLs)

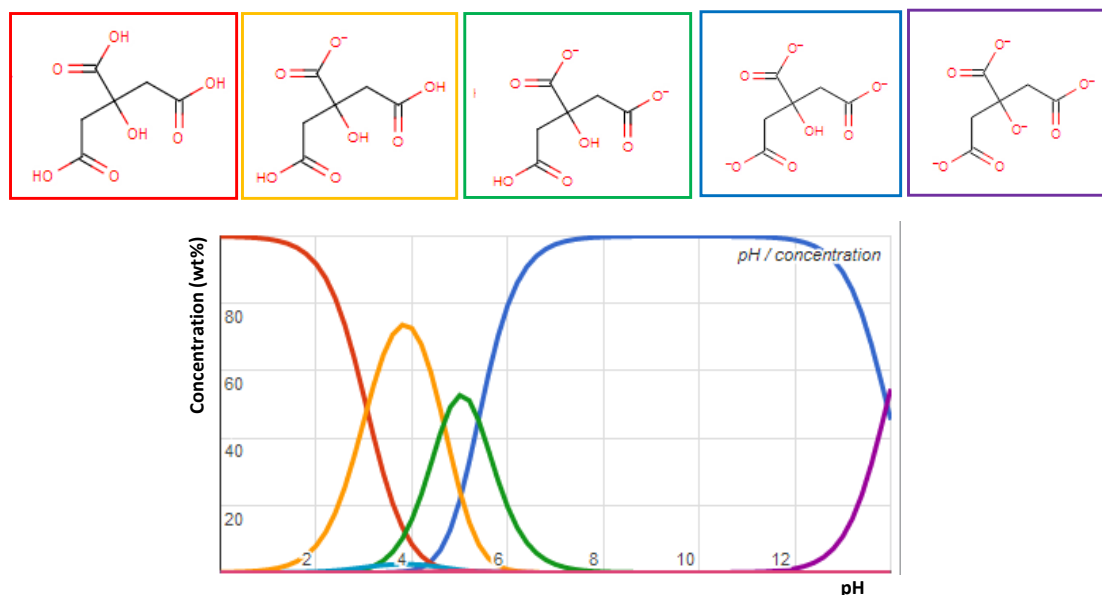


Figure C.1.1. Speciation curves of citric acid as a function of pH.¹

Table C.1.1. Experimental weight fraction data for the systems composed of [C₄C₁im]Cl (1) + salt (2) + H₂O (3) at 25 °C and at atmospheric pressure.

pH≈9		pH≈8		pH≈7	
100 w1	100 w2	100 w1	100 w2	100 w1	100 w2
16.0591	39.9485	16.3947	39.7533	14.7563	42.5266
17.9726	37.6514	18.1351	37.5613	16.5634	40.2903
19.6938	35.5432	20.6379	34.6574	18.1753	38.2234
21.1447	33.6433	22.9777	32.3000	20.4143	35.8728
22.9233	31.5002	24.8409	30.2236	22.3989	33.6556
25.3400	28.4100	26.5139	28.3980	23.6100	32.1799
28.3300	25.8100	28.5845	26.3586	25.3891	30.4357
30.9800	23.1000	29.8132	24.9234	26.9197	28.8631
32.3000	21.8400	31.7043	23.2323	28.1425	27.4771
33.7700	20.5200	33.1419	21.8759	29.3640	26.1079
34.9000	19.3900	33.9817	20.9766	30.5421	24.8985
35.9100	18.5100	35.0461	19.9804	31.6398	23.8687
37.4900	17.0100	36.1685	19.0202	32.9935	22.6317

39.0000	15.8200	36.8758	18.3354	33.8930	21.7312
42.9530	13.7150	37.8069	17.5496	34.7234	20.9158
49.4490	9.4070	38.6094	16.8158	35.8402	19.9569
54.4870	6.5200	39.3870	16.1450	36.5202	19.2637
58.9900	4.3630	40.6013	15.3096	37.6967	18.3265
62.7670	2.9200	41.4766	14.6329	38.7095	17.4915
68.6300	1.5800	42.2971	14.0321	39.5328	16.7724
		43.2780	13.3493	40.2287	16.1767
		44.3115	12.6948	41.1063	15.5093
		44.9843	12.1720	41.7192	14.9869
		45.7937	11.6260	42.4183	14.4346
		46.4473	11.1761	43.2104	13.8353
		46.9252	10.8470	43.8263	13.3640
		47.6044	10.4271	44.6029	12.8143
		48.2284	10.0283	45.1577	12.4218
		48.7219	9.7110	45.7855	11.9815
		49.3645	9.3324	46.3013	11.6199
		49.9221	9.0053	46.6216	11.3363
		50.4147	8.7071	47.0996	11.0136
		51.0178	8.3643	47.6565	10.6718
		55.9191	6.2504	48.0247	10.4504
		62.8618	2.9875	48.5419	10.1118
		71.7474	1.5942	49.1112	9.7797
				49.6217	9.4639
				50.0253	9.2153
				50.3852	8.9873

Table C.1.2. Experimental weight fraction data for the systems composed of [C₄C₁im]Cl (1) + salt (2) + H₂O (3) at 25 °C and at atmospheric pressure.

pH≈9		pH≈8		pH≈7	
100 w ₁	100 w ₂	100 w ₁	100 w ₂	100 w ₁	100 w ₂
17.5639	39.8362	20.7075	36.3945	22.4236	35.3274
20.0557	37.4146	22.5899	34.4799	23.3368	33.4880
21.6310	35.2678	23.9211	32.5651	26.1175	30.6571
23.6885	33.0411	25.0982	30.8423	27.8648	28.8437
25.6583	31.0179	27.2221	28.6135	28.7956	27.7530
26.5884	29.8473	28.9819	27.0687	29.9169	26.9052
27.6666	28.4244	30.3432	25.5562	30.7609	25.6530
29.1333	26.8809	32.8459	23.5999	32.6215	23.9410
30.6602	25.3975	33.3921	22.6689	34.7080	22.2041
31.9121	24.1263	33.9155	21.9135	35.4705	21.1840

32.9990	22.9993	35.1220	20.7665	36.1866	20.3259
33.8364	22.0619	36.6756	19.5156	37.4028	19.2026
35.7135	20.6511	37.1041	18.8897	38.4585	18.3004
36.7707	19.6852	38.2027	17.9040	39.3304	17.5438
37.4674	18.9073	39.3748	17.0284	39.8576	16.9852
38.2935	18.1959	40.0938	16.4192	40.3881	16.5001
39.1099	17.4737	40.3612	16.1345	41.2282	15.8913
39.6331	16.9411	41.1552	15.4867	41.7614	15.4316
40.3374	16.3041	42.1021	14.8585	42.5672	14.7401
40.9630	15.7582	42.7267	14.3328	43.0529	14.3983
41.8435	15.1113	43.3789	13.8474	43.5522	13.9208
42.6419	14.5066	44.3593	13.2308	44.0532	13.5694
43.1248	14.0310	44.7070	12.8436	44.7276	13.0196
43.9949	13.4263	45.1969	12.4955	45.1257	12.7364
44.7581	12.8835	45.7177	12.0789	45.7717	12.2850
45.8031	12.2799	46.0371	11.8184	46.4527	11.7919
46.4520	11.8184	46.5260	11.4930	47.1620	11.3652
47.0710	11.3796	47.1892	11.0339	48.2544	10.6519
47.5449	11.0071	47.8669	10.5941	48.7955	10.2831
48.1635	10.6226	48.3715	10.2174	49.1995	9.9937
48.6019	10.3021	49.0378	9.7943	49.8791	9.5702
49.0689	9.9799	49.7889	9.3565	50.7905	9.0487
49.5037	9.6697	50.2905	9.0643	51.9121	8.4121
50.0581	9.3561	50.7832	8.7779	52.5663	7.9932
50.5745	9.0419	51.1282	8.5133	53.2454	7.6860
42.4123	14.5350	51.6471	8.2342	53.7612	7.4004
49.8258	9.1656	52.0449	7.9955	54.4843	7.0120
53.1731	7.3481	52.4355	7.7726		
56.8969	5.3008	59.8442	4.8006		
59.9870	3.7771	80.7466	1.5373		

Table C.1.3. Experimental weight fraction data for the systems composed of [C₄C₁pip]Cl (1) + salt (2) + H₂O (3) at 25 °C and at atmospheric pressure.

pH≈9		pH≈8		pH≈7		pH≈6	
100 w ₁	100 w ₂	100 w ₁	100 w ₂	100 w ₁	100 w ₂	100 w ₁	100 w ₂
11.8779	42.0814	18.5918	34.7445	19.1288	34.2900	27.7645	27.8446
13.2137	40.2890	20.8318	32.2317	21.7665	31.4809	29.1664	25.8716
13.8002	39.4154	22.1675	30.4867	23.7906	29.1489	30.3075	24.5749
15.1159	37.6963	24.0414	28.4860	25.3628	27.2222	32.1771	22.5954
16.1873	36.2783	25.6902	26.6967	27.2252	25.2342	33.3385	21.3135

17.2135	34.8857	27.5645	24.7879	29.2963	23.1948	34.8580	19.8117
18.8257	33.2705	28.9116	23.3592	30.9309	21.5805	38.9572	16.7164
19.6583	32.2197	30.4896	21.8523	32.7478	19.8526	40.0301	15.6677
20.9142	30.8794	31.2913	20.9193	33.9099	18.7602	41.2147	14.5968
21.5887	29.9564	32.4779	19.8362	35.3521	17.4506	42.6312	13.4330
22.7780	28.7832	33.6068	18.7931	36.9450	16.1302	43.9236	12.4418
23.7344	27.7078	34.9018	17.6500	37.9718	15.2572	45.4226	11.3171
24.6492	26.7513	36.1462	16.5798	39.0318	14.3832	47.8643	9.6811
25.5752	25.7733	38.5627	14.5789	40.3601	13.3873	64.4868	1.6150
26.5109	24.8309	39.4598	13.8450	41.5498	12.4932		
27.4363	23.9149	40.5345	13.0524	42.3966	11.8384		
28.9490	22.3683	41.7785	12.1531	43.5867	11.0112		
29.6948	21.6456	44.0910	10.6062	45.2099	9.9857		
30.3373	20.9788	44.7628	10.0927	46.5449	9.1533		
30.9753	20.3619	45.9167	9.3553	47.7960	8.3586		
31.4895	19.8072	46.8941	8.7397	50.9636	6.6636		
32.2745	19.1440	48.9936	7.6139	56.2140	3.5958		
33.5724	17.9547	49.5723	7.0979	63.3822	2.2685		
34.2235	17.3762	53.5122	5.0866				
34.4711	17.1436	68.5290	1.7860				
34.9649	16.6948						
35.4650	16.3068						
35.9407	15.9036						
36.3142	15.5403						
37.4033	14.7061						
37.7808	14.3866						
38.2987	13.9777						
38.5338	13.7857						
38.9518	13.4665						
39.4754	13.1443						
39.8736	12.8322						
40.4423	12.4411						
44.2930	10.1380						
51.2880	6.5760						

Table C.1.4. Experimental weight fraction data for the systems composed of [C₄C₁py]Cl (1) + salt (2) + H₂O (3) at 25 °C and at atmospheric pressure.

pH≈9		pH≈8		pH≈7		pH≈6	
100 w ₁	100 w ₂	100 w ₁	100 w ₂	100 w ₁	100 w ₂	100 w ₁	100 w ₂
10.3520	43.9106	16.1550	35.7374	21.5230	31.5972	20.1890	37.1099
10.9390	42.6182	17.3005	34.1121	24.1622	28.7340	21.8798	33.9768
12.1725	40.3244	19.1243	32.1241	26.6534	26.1362	21.9294	33.8754
12.7275	39.2124	20.1184	30.6920	28.9522	23.8002	23.3702	32.1461
13.2595	38.3247	21.5311	29.0830	30.9445	21.8262	24.2277	31.3730
13.7627	37.2681	23.4651	27.3004	31.9832	20.8481	26.4111	28.9153
15.1317	35.7952	24.1238	26.2884	37.4705	16.3452	28.2444	26.8664
16.2410	34.3927	25.2560	25.1026	40.8486	13.8405	29.8631	25.0636
16.6722	33.5235	26.3273	23.9771	45.7694	10.5323	31.2613	23.5228
17.7926	32.4672	27.3393	22.9533	48.1000	9.1209	32.9111	21.9934
18.2788	31.8734	28.2592	22.0161	50.9472	7.4900	34.2906	20.6312
18.5719	31.1133	29.4633	20.9673	53.3648	6.2672	35.6823	19.2698
19.5507	30.0672	30.2357	20.2155			36.7937	18.1956
20.8888	28.6347	30.9456	19.4711			37.9766	17.1577
21.7727	27.7161	31.9261	18.6081			39.2486	16.0311
22.0155	27.1612	32.7787	17.8515			40.2094	15.2015
22.8139	26.3470	33.5242	17.1840			41.2908	14.3338
23.5572	25.5278	34.3287	16.5383			42.2571	13.5635
24.2755	24.8298	35.0301	15.9536			42.9198	13.0848
24.9947	24.1091	35.8603	15.3058			43.9808	12.3111
25.6083	23.4746	36.7579	14.8650			45.1592	11.4777
26.1681	22.8390	37.1963	14.5139			46.2131	10.7239
26.7165	22.2807	37.8043	14.0119			47.5453	9.8649
27.1404	21.7079	42.6186	12.0786			48.9056	9.0284
27.6823	21.1891	45.2390	10.4194			74.1362	1.2936
28.1828	20.6464	47.2672	9.2849				
28.4209	20.3486	49.6622	7.8631				
29.2571	19.7281	51.2425	7.1452				
29.6596	19.2829	53.0469	6.3009				
29.9995	18.8759	54.7933	5.5007				
30.7441	18.3101	56.6343	4.6833				
31.0773	17.9129	58.4954	3.8977				
31.4224	17.5977	75.3583	0.9350				
32.2555	16.8272						
32.8425	16.3991						
33.6176	15.7280						
34.6460	14.8366						
35.9625	13.8039						
36.6668	13.2573						

Table C.1.5. Experimental weight fraction data for the systems composed of [P₄₄₄₄]Cl (1) + salt (2) + H₂O (3) at 25 °C and at atmospheric pressure.

pH≈9					
100 w ₁	100 w ₂	100 w ₁	100 w ₂	100 w ₁	100 w ₂
5.3948	31.9074	11.0171	25.1436	29.1193	11.6832
5.4979	31.7579	11.2365	24.9242	29.9589	11.3385
5.5927	31.6088	11.5073	24.5869	30.8292	10.9785
5.6934	31.4443	11.6487	24.4848	32.7905	10.1775
5.7746	31.3460	11.8039	24.4161	34.4216	9.7388
5.8626	31.2440	12.0945	24.0175	35.5912	9.1585
5.9770	31.0747	12.2515	23.9305	37.2858	8.7838
6.0899	30.8912	12.4937	23.6946	39.2541	8.2486
6.2028	30.7388	12.6651	23.5927	41.7165	7.7237
6.3186	30.5726	12.9623	23.2558	45.0090	7.1845
6.4329	30.4180	13.0995	23.1312	48.7886	6.7607
6.5407	30.2694	13.2689	23.0590		
6.6636	30.0961	13.5524	22.7698		
6.7980	29.9059	13.7589	22.6892		
6.9469	29.6917	14.1365	22.3069		
7.0262	29.6338	14.3801	22.1978		
7.1624	29.4611	14.7046	21.8403		
7.2862	29.3033	15.0868	21.4970		
7.4572	29.0782	15.3047	21.4193		
7.5971	28.8946	15.6354	21.1153		
7.7403	28.7135	16.0217	20.7685		
7.8911	28.5028	16.3874	20.4539		
7.9884	28.4275	16.7671	20.0977		
8.1354	28.2129	17.1680	19.7297		
8.2793	28.0402	17.7517	19.3876		
8.4275	27.8636	18.4587	18.9242		
8.5682	27.7119	19.0499	18.3418		
8.7140	27.5760	19.9655	17.6546		
8.8988	27.3352	20.3343	17.4617		
9.0417	27.2270	21.0431	16.9084		
9.2235	26.9862	21.6530	16.4435		
9.3407	26.9228	22.3247	15.8673		
9.5300	26.6785	22.8310	15.6092		
9.7514	26.4223	23.3095	15.3755		
9.9206	26.2841	23.7648	15.1701		
10.0740	26.1489	24.2746	14.9452		
10.3403	25.7647	25.7977	13.7085		
10.4598	25.7122	26.4988	13.3945		
10.6775	25.4512	27.6162	12.5410		
10.8818	25.2190	28.4037	12.0422		

Table C.1.6. Experimental weight fraction data for the systems composed of [P₄₄₄₄]Cl (1) + salt (2) + H₂O (3) at 25 °C and at atmospheric pressure.

pH≈8					
100 w ₁	100 w ₂	100 w ₁	100 w ₂	100 w ₁	100 w ₂
57.5547	5.1133	21.9022	16.7962	11.3907	25.1182
51.3753	5.7210	21.0825	17.4168	11.1177	25.4472
47.5050	6.4933	20.0351	18.1653	10.8229	25.6632
43.0923	7.0668	18.9056	18.9747	10.5643	25.9218
40.1382	7.7242	18.4039	19.2313	10.2648	26.2606
38.2240	8.4985	17.8655	19.6852	10.0261	26.4734
35.8977	9.0434	17.1444	20.3577	9.8045	26.7087
34.5148	9.7294	16.2847	21.0846	9.5972	26.8828
33.2760	10.2711	15.2364	21.7508	9.1832	27.2877
32.3099	10.6881	14.7070	22.2491	9.0141	27.4496
31.2601	11.0874	14.4866	22.3586	8.8087	27.6920
29.6716	12.1152	13.9772	22.8716	8.4320	28.1528
28.6393	12.4888	13.6519	23.0838	8.3148	28.2237
27.3283	13.2994	13.2699	23.4331	8.2061	28.2859
25.9506	14.2791	13.0134	23.6562	7.9859	28.5354
25.1962	14.5425	12.7424	23.8372	7.7987	28.7652
24.1979	15.3099	12.3581	24.1644	7.6536	28.9181
23.6382	15.6013	12.0469	24.5081	7.4963	29.1136
23.1173	15.8606	11.7097	24.8224	7.3494	29.2819

Table C.1.7. Experimental weight fraction data for the systems composed of [P₄₄₄₄]Cl (1) + salt (2) + H₂O (3) at 25 °C and at atmospheric pressure.

pH≈7					
100 w ₁	100 w ₂	100 w ₁	100 w ₂	100 w ₁	100 w ₂
6.7891	30.1625	12.1061	25.1963	38.5866	8.4976
6.8782	30.0836	12.2740	25.1079	41.1608	7.7125
6.9942	29.9324	12.5806	24.7897	43.8623	6.7416
7.0871	29.8433	12.9027	24.5157		
7.1796	29.7243	13.2231	24.2613		
7.2703	29.5901	13.5461	23.9753		
7.3761	29.4990	13.8776	23.7010		
7.4807	29.3996	14.2109	23.4382		
7.6123	29.2241	14.6087	23.0861		
7.7444	29.0704	14.9831	22.7630		
7.8074	29.0439	15.2195	22.6639		
7.8610	28.9736	15.6287	22.2673		
7.9287	28.9499	16.0507	21.9113		
8.0980	28.7172	16.3493	21.7874		
8.2263	28.6113	16.8117	21.3660		

8.3018	28.6086	17.3418	20.9465
8.4850	28.3765	17.8555	20.5213
8.6043	28.2238	18.1681	20.3472
8.7466	28.0892	18.7362	19.9064
8.8816	27.9928	19.1292	19.7115
9.0161	27.8187	19.7536	19.1752
9.1718	27.6760	20.3100	18.8208
9.3336	27.5277	20.7504	18.6420
9.4743	27.3823	21.5071	18.0248
9.5719	27.3279	22.3061	17.4067
9.7326	27.2039	22.9839	17.0111
9.9034	27.0569	23.7585	16.5123
10.0889	26.8950	24.3950	16.2060
10.2366	26.7504	24.9565	15.8711
10.4231	26.5817	26.0625	14.9920
10.6205	26.4069	26.7792	14.6135
10.8005	26.2040	27.5793	14.2128
10.9003	26.1948	28.3617	13.7621
11.1271	25.9765	29.1461	13.2893
11.3244	25.8604	30.0949	12.8133
11.4516	25.7708	32.1408	11.8075
11.6962	25.5666	34.1085	10.3152
11.8454	25.4751	35.0160	9.9361
12.1061	25.1963	36.9793	9.3338

Table C.1.8. Experimental weight fraction data for the systems composed of [P₄₄₄₄]Cl (1) + salt (2) + H₂O (3) at 25 °C and at atmospheric pressure.

pH≈6					
100 w ₁	100 w ₂	100 w ₁	100 w ₂	100 w ₁	100 w ₂
41.5610	9.4338	17.6874	21.6882	10.0606	27.3306
39.8025	10.0148	16.8498	22.1895	9.8021	27.5614
38.1769	10.5583	16.2087	22.6783	9.5076	27.8837
36.8672	10.8672	15.4576	23.3484	9.3654	28.0262
35.4010	11.3902	15.0291	23.6087	9.1816	28.1641
33.8517	12.0940	14.5723	23.9605	9.0279	28.3228
32.6151	12.6011	14.0916	24.3544	8.9228	28.3978
31.0253	13.4039	13.5857	24.7420	8.6930	28.6809
29.8230	13.8782	13.0761	25.2134	8.4773	28.8730
28.5100	14.6504	12.9396	25.2058	8.3147	29.0162
27.1956	15.4978	12.6996	25.3586	8.1654	29.1964
25.8070	16.1369	12.4731	25.4425	7.9760	29.3996
24.6101	16.8965	12.2056	25.4959	7.7789	29.5979
23.4508	17.7110	11.8010	25.8939	7.6032	29.7881

22.3471	18.3558	11.5617	26.0623	7.3574	30.0296
21.4818	18.8986	11.2675	26.3211	7.1839	30.2386
20.5104	19.5391	11.0216	26.4946	6.9413	30.4722
19.6346	20.2063	10.7197	26.7594	6.7763	30.6786
19.1031	20.6049	10.4980	26.9721	6.6610	30.7860
18.3677	21.1999	10.2920	27.1530	6.5208	30.9234

Table C.1.9. Experimental weight fraction data for the systems composed of [P₄₄₄₄]Cl (1) + salt (2) + H₂O (3) at 25 °C and at atmospheric pressure.

pH≈5					
100 w ₁	100 w ₂	100 w ₁	100 w ₂	100 w ₁	100 w ₂
57.7084	4.1732	18.3660	24.0994	9.9574	30.8217
52.3413	5.3498	17.4716	24.8313	9.6061	31.1558
41.1731	9.4540	16.5868	25.4299	9.2556	31.4689
38.4940	10.7645	15.6178	26.2426	8.9596	31.7383
36.2354	11.9482	14.8823	26.7742	8.6081	32.1045
34.3652	13.0916	14.1684	27.3257	8.3384	32.3654
32.2713	14.1512	13.6598	27.7164	8.0661	32.6489
29.5863	15.9934	13.0798	28.1534	7.5930	33.1546
27.3230	17.6217	12.4625	28.7098	7.1679	33.5836
25.3565	18.9943	12.0134	29.0412	6.8786	33.8693
23.5731	20.2839	11.5925	29.3615	6.5060	34.3004
21.8258	21.5693	11.1492	29.7298	6.1373	34.7029
20.5767	22.5930	10.7012	30.1348	5.7658	35.1614
19.4395	23.3356	10.3057	30.4901		

Table C.1.10. Experimental weight fraction data for the systems composed of [C₄C₁im]Br (1) + salt (2) + H₂O (3) at 25 °C and at atmospheric pressure.

pH≈9		pH≈8				pH≈7	
100 w ₁	100 w ₂	100 w ₁	100 w ₂	100 w ₁	100 w ₂	100 w ₁	100 w ₂
14.0588	31.4976	74.6692	1.7071	14.7402	31.1274	14.0554	34.0102
15.6686	29.9014	62.2292	3.5899			15.8671	32.1716
17.3798	28.2620	55.7952	4.5687			18.9328	29.3782
19.2837	26.5865	53.7379	5.4895			20.5407	28.0655
20.8123	25.3568	52.4385	6.0282			22.2259	26.6261
22.7626	23.7899	51.1184	6.5971			24.2693	24.9879
25.2484	21.8864	49.2717	7.6222			26.4308	23.3838
28.1199	19.8442	47.9687	8.3090			28.6680	21.6541
31.3557	17.4650	46.8307	8.7596			31.3276	19.7129
34.4359	15.4745	45.6325	9.3666			34.2345	17.5869

37.2668	13.7305	43.9663	10.2978	37.0418	15.7384
43.0663	9.7932	42.5776	11.0643	40.0378	13.7155
46.5773	7.9639	41.4969	11.7464	43.6035	11.3177
48.9797	7.2517	40.4967	12.3258	46.6277	9.6972
53.6390	5.3732	39.2647	13.0520	48.9873	8.5396
57.2031	4.3649	38.3023	13.6647	52.7198	6.5982
60.7843	3.2181	36.8416	14.6905	54.5368	5.9419
66.6892	1.9342	35.3456	15.7034	57.8177	4.2714
14.0588	31.4976	34.2934	16.4524	61.0892	2.7458
15.6686	29.9014	33.0183	17.3642	63.6529	1.8296
17.3798	28.2620	31.1062	18.8453	78.0200	0.4262
19.2837	26.5865	30.2517	19.3823	14.0554	34.0102
20.8123	25.3568	28.7960	20.4784	15.8671	32.1716
22.7626	23.7899	27.8623	21.1637	18.9328	29.3782
25.2484	21.8864	27.0973	21.7318	20.5407	28.0655
28.1199	19.8442	26.6466	22.0029	22.2259	26.6261
31.3557	17.4650	25.9514	22.5344	24.2693	24.9879
34.4359	15.4745	25.2505	23.0745	26.4308	23.3838
37.2668	13.7305	24.1415	23.9091	28.6680	21.6541
43.0663	9.7932	23.5451	24.3393	31.3276	19.7129
46.5773	7.9639	20.8741	25.2211	34.2345	17.5869
48.9797	7.2517	20.2310	25.7807	37.0418	15.7384
53.6390	5.3732	19.5592	26.3928	40.0378	13.7155
57.2031	4.3649	18.9190	26.9909	43.6035	11.3177
60.7843	3.2181	18.3783	27.4884	46.6277	9.6972
66.6892	1.9342	17.6814	28.1693	48.9873	8.5396
		17.0936	28.7205	52.7198	6.5982
		16.3846	29.4266	54.5368	5.9419
		15.5370	30.3036	57.8177	4.2714

Table C.1.11. Experimental weight fraction data for the systems composed of [C₄C₁im]Br (1) + salt (2) + H₂O (3) at 25 °C and at atmospheric pressure.

pH≈7		pH≈6				pH≈5	
100 w ₁	100 w ₂	100 w ₁	100 w ₂	100 w ₁	100 w ₂	100 w ₁	100 w ₂
61.0892	2.7458	13.1289	40.9277	42.5059	13.0330	48.8255	11.8806
63.6529	1.8296	14.6369	37.8062	42.8610	12.7617	52.7982	9.5053
78.0200	0.4262	15.4353	36.7627	43.2331	12.5204	53.0294	9.3376
		16.6319	35.4319	43.5518	12.2803	53.3424	9.1489
		18.0233	34.0131	43.9026	12.0745	53.7521	8.8781
		18.6667	33.2197	44.2004	11.8618	54.2591	8.5404
		19.9499	32.0458	44.6306	11.5841	54.4792	8.3756
		21.4402	30.7913	45.0522	11.3258	54.8214	8.1616
		22.6211	29.6228	45.3365	11.1196	55.1614	7.9445
		23.4683	28.6192	45.8005	10.8714	55.7765	7.5528

24.7265	27.5343	46.1277	10.6633	56.0490	7.3768
26.1772	26.3980	46.4046	10.4826	56.3058	7.2228
26.9795	25.6396	46.6931	10.2876	56.5910	7.0483
27.5439	25.0612	46.9333	10.1271		
28.6331	24.2187	47.2513	9.9269		
29.3257	23.5222	47.4015	9.7540		
30.4280	22.7180	47.7184	9.5641		
30.9947	22.1325	48.0615	9.3802		
31.6755	21.5690	48.3586	9.2140		
32.4393	20.8683	48.6681	9.0465		
32.8501	20.4090	48.9684	8.8754		
33.3331	19.9721	49.2857	8.7043		
34.0746	19.4849	49.6341	8.5348		
34.4802	19.0562	50.0614	8.2920		
35.3174	18.4711	50.8046	7.8751		
35.6522	18.0907	51.1411	7.7314		
36.3547	17.6037	51.3609	7.6091		
36.7720	17.2347	51.6497	7.4731		
37.5590	16.7515	52.0009	7.3234		
37.8739	16.4092	52.2130	7.2098		
38.4874	16.0096	52.5221	7.0811		
38.7591	15.6990	52.9099	6.8869		
39.2165	15.3895	53.5474	6.5863		
39.5462	15.1067	54.4502	6.1986		
40.0778	14.7448	54.9257	6.0009		
40.5598	14.4099	54.9483	5.8978		
40.9810	14.0989	56.2662	5.4754		
41.3850	13.8069	58.0126	4.7360		
41.8287	13.5066	69.9374	1.6121		

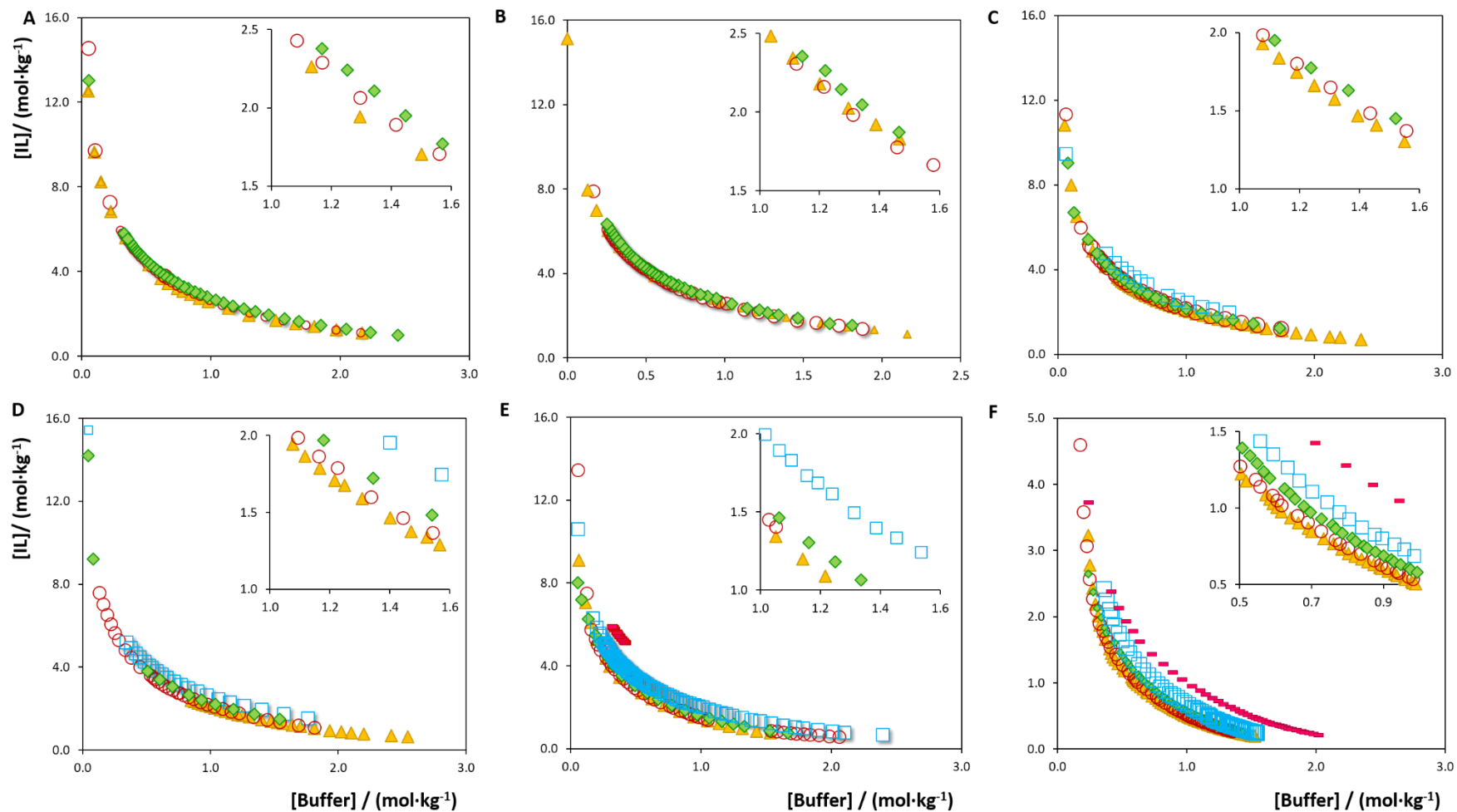


Figure C.1.2. Evaluation of the pH effect in the ternary phase diagrams, at 25 °C and atmospheric pressure, composed of IL + water + $\text{K}_3\text{C}_6\text{H}_5\text{O}_7$ / $\text{C}_6\text{H}_8\text{O}_7$ at pH \approx 9 (\blacktriangle), pH \approx 8 (\circ), pH \approx 7 (\blacklozenge), pH \approx 6 (\square) and pH \approx 5 (\blacksquare). The ILs are: **(A)** $[\text{C}_4\text{C}_{1\text{im}}]\text{Cl}$, **(B)** $[\text{C}_4\text{C}_{1\text{C}_{1\text{im}}}\text{im}]\text{Cl}$, **(C)** $[\text{C}_4\text{C}_{1\text{pip}}]\text{Cl}$, **(D)** $[\text{C}_4\text{C}_{1\text{py}}]\text{Cl}$, **(E)** $[\text{C}_4\text{C}_{1\text{im}}]\text{Br}$ and **(F)** $[\text{P}_{4444}]\text{Cl}$.

Table C.1.12. Values for the constants A , B and C , obtained by the regression of the experimental binodal data as described originally by Merchuk *et al.*² (and respective standard deviations, σ , and correlation coefficients, R^2), at 25 °C and atmospheric pressure.

IL	pH	$A \pm \sigma$		$B \pm \sigma$		$10^6 (C \pm \sigma)$		R^2
[C ₄ C ₁ C ₁ im]Cl	9	86.8	± 0.7	-0.181	± 0.002	7.37	± 0.25	0.9990
	8	103.8	± 1.6	-0.235	± 0.005	3.13	± 0.68	0.9939
	7	86.7	± 0.7	-0.178	± 0.003	7.34	± 0.34	0.9987
[C ₄ C ₁ im]Cl	9	88.7	± 0.9	-0.197	± 0.004	7.72	± 0.47	0.9986
	8	88.7	± 0.8	-0.178	± 0.003	9.29	± 0.37	0.9982
	7	91.8	± 0.3	-0.201	± 0.001	6.73	± 0.06	1.0000
[C ₄ C ₁ pip]Cl	9	88.3	± 0.4	-0.217	± 0.001	8.07	± 0.14	0.9996
	8	90.3	± 0.9	-0.219	± 0.003	6.62	± 0.51	0.9986
	7	83.9	± 0.9	-0.195	± 0.004	8.56	± 0.57	0.9983
	6	79.8	± 0.8	-0.165	± 0.004	9.88	± 0.76	0.9985
[C ₄ C ₁ py]Cl	9	90.5	± 1.4	-0.243	± 0.004	7.18	± 0.19	0.9996
	8	95.6	± 1.0	-0.239	± 0.004	8.36	± 0.63	0.9978
	7	87.6	± 0.9	-0.199	± 0.004	9.71	± 0.58	0.9995
	6	94.4	± 0.4	-0.215	± 0.001	5.01	± 0.17	0.9997
[C ₄ C ₁ im]Br	9	93.1	± 0.6	-0.237	± 0.003	18.30	± 0.57	0.9997
	8	90.8	± 1.4	-0.218	± 0.005	20.69	± 0.87	0.9981
	7	85.6	± 0.8	-0.192	± 0.004	18.51	± 0.79	0.9975
	6	90.7	± 0.2	-0.204	± 0.001	10.57	± 0.11	0.9998
	5	76.3	± 0.6	-0.107	± 0.003	46.96	± 1.91	0.9999
[P ₄₄₄₄]Cl	9	150.0	± 4.6	-0.458	± 0.010	20.69	± 1.23	0.9964
	8	154.5	± 5.3	-0.464	± 0.012	17.76	± 1.97	0.9953
	7	97.2	± 1.0	-0.308	± 0.003	34.64	± 0.41	0.9996
	6	124.0	± 3.6	-0.354	± 0.009	31.75	± 0.91	0.9995
	5	99.8	± 1.4	-0.275	± 0.005	26.10	± 0.60	0.9990

Table C.1.13. Weight fraction percentage (wt%) composition of the initial mixture and of the coexisting phases of IL-based ABS, and respective values of tie-line length (TLL) and pH values of each phase, at 25 °C and atmospheric pressure

IL	Weight fraction composition / wt%								TLL
	[IL] _{IL}	[salt] _{IL}	pH _{IL}	[IL] _M	[salt] _M	[IL] _{salt}	[salt] _{salt}	pH _{salt}	
[C ₄ C ₁ im]Cl	53.04	7.13	9.32	25.25	35.03	5.77	54.58	9.30	66.98
[C ₄ C ₁ C ₁ im]Cl	47.88	10.76	8.93	25.02	34.90	9.78	51.00	8.67	55.42
[C ₄ C ₁ pip]Cl	55.91	4.46	9.26	25.13	34.75	4.40	55.15	9.34	72.27
	66.45	1.00	6.40	40.07	20.80	13.35	42.05	6.36	57.79
	62.07	2.00	6.19	33.18	24.83	18.12	36.73	6.29	56.02
[C ₄ C ₁ py]Cl	55.74	5.13	8.44	24.62	35.47	4.39	55.19	8.16	71.71
	54.52	6.56	6.24	32.86	24.75	23.28	32.80	6.20	40.80
	61.48	4.05	6.24	37.06	23.58	20.56	36.12	6.16	55.53
[C ₄ C ₁ im]Br	76.93	0.65	8.93	35.08	32.04	0.42	58.03	8.92	95.64
	51.51	7.57	6.00	33.54	21.54	20.82	31.42	5.93	38.87
	62.69	3.28	6.07	34.33	25.39	8.38	45.64	6.01	68.88
[P ₄₄₄₄]Cl	39.60	8.92	9.00	30.10	15.04	8.88	28.25	8.89	36.32
	72.93	3.06	9.34	24.97	35.03	0.58	51.29	9.14	86.95
	56.00	4.60	5.99	27.84	23.12	1.54	40.46	5.84	65.20
	63.15	3.28	5.62	33.29	21.97	1.13	42.11	5.90	73.17

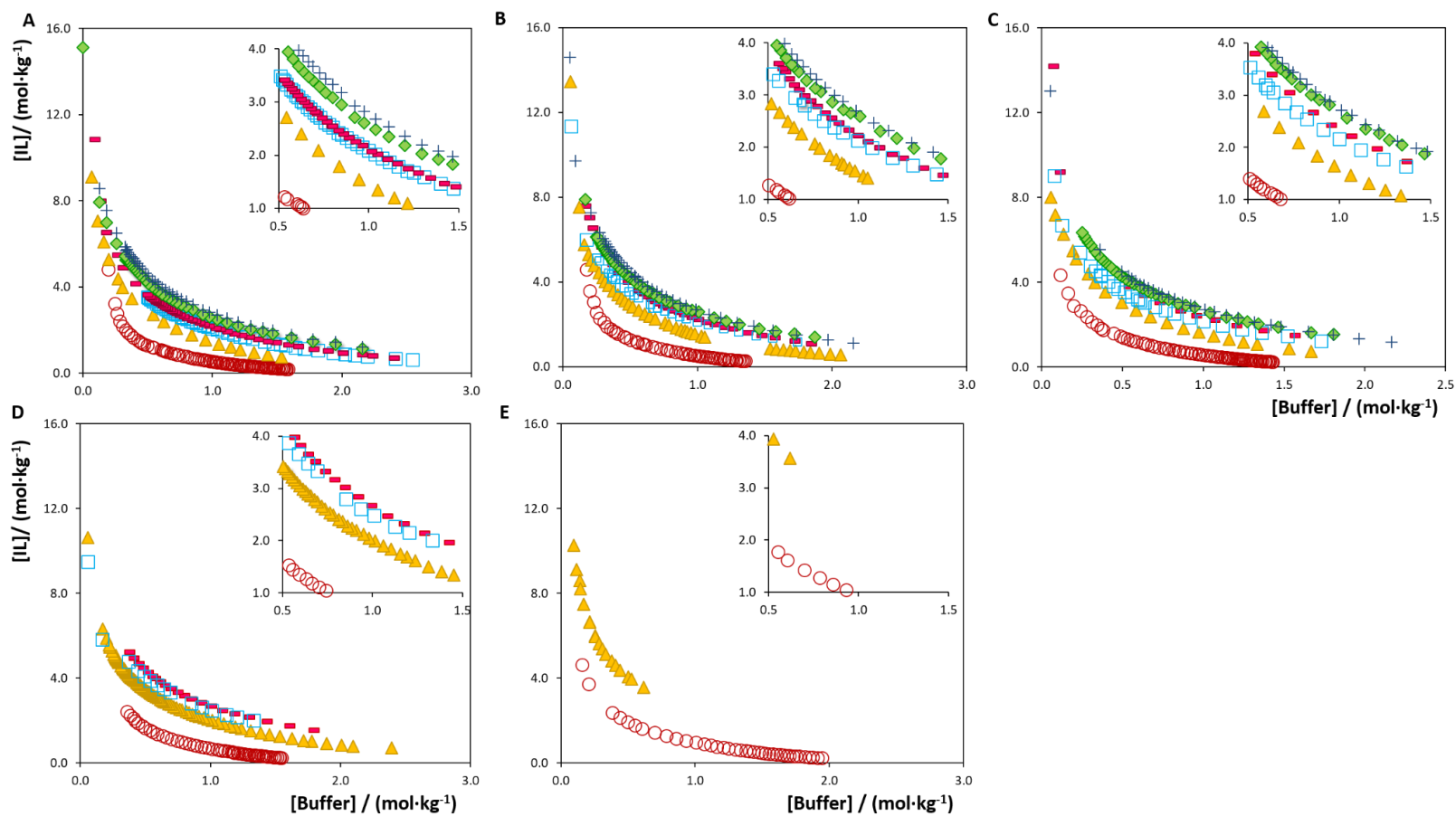


Figure C.1.3. Phases diagrams for the different IL-based ABS at 25 °C, atmospheric pressure and at fixed pH: pH \approx 9 (A); pH \approx 8 (B); pH \approx 7 (C); pH \approx 6 (D); and pH \approx 5 (E). ILs investigated: [P₄₄₄₄]Cl (○), [C₄C₁im]Br (▲), [C₄C₁pip]Cl (□), [C₄C₁py]Cl (■), [C₄C₁C₁im]Cl (◆) and [C₄C₁im]Cl (+).

Table C.1.14. Identification of the systems able (✓) or not able (✗) to form two-phase systems as a function of the pH, at 25 °C and atmospheric pressure.

pH	9	8	7	6	5
[C ₄ C ₁ im]Cl	✓	✓	✓	✗	✗
[C ₄ C ₁ C ₁ im]Cl	✓	✓	✓	✗	✗
[C ₄ C ₁ pip]Cl	✓	✓	✓	✓	✗
[C ₄ C ₁ py]Cl	✓	✓	✓	✓	✗
[C ₄ C ₁ im]Br	✓	✓	✓	✓	✓
[P ₄₄₄₄]Cl	✓	✓	✓	✓	✓

Production and separation of HMF

Table C.1.15. Production yields of HMF through fructose dehydration in presence (or not) of citric acid and ILs.

	[HMF] / g·L ⁻¹	
	Without citric acid	With citric acid
H ₂ O	(53.84 ± 1.65) × 10 ⁻⁵	2.28 ± 0.53
[C ₄ C ₁ im]Cl	(64.61 ± 7.88) × 10 ⁻⁵	4.61 ± 0.46
[C ₄ C ₁ py]Cl	(36.09 ± 6.37) × 10 ⁻⁵	4.85 ± 0.60
[C ₄ C ₁ pip]Cl	(281.36 ± 4.02) × 10 ⁻⁵	6.37 ± 0.48

Table C.1.16. Extraction efficiencies (*EE*%) of the systems studied for HMF and fructose.

	<i>EE</i> _{HMF} (IL-rich phase) %		<i>EE</i> _{Fructose} (salt-rich phase) %	
[C ₄ C ₁ im]Cl	92.50	± 0.50	53.41	± 3.13
[C ₄ C ₁ py]Cl	95.09	± 1.09	57.66	± 0.44
[C ₄ C ₁ pip]Cl	95.89	± 0.45	63.72	± 0.56

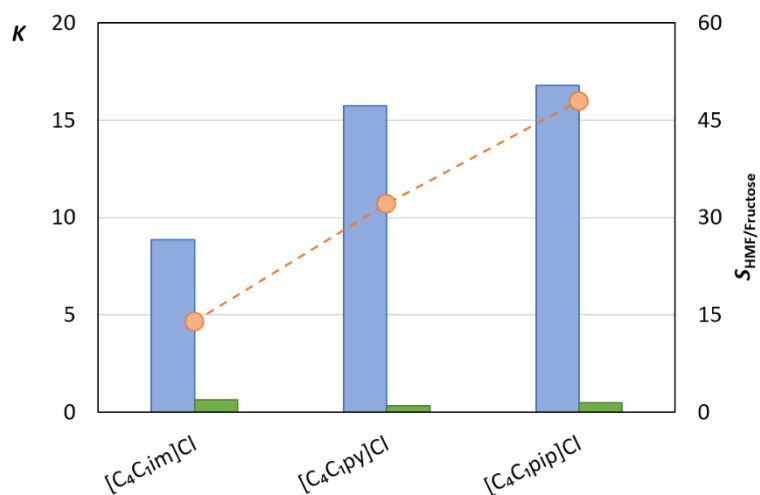


Figure C.1.4. Partition coefficient (K) of HMF (blue bars) and fructose (green bars) in IL-based systems studied at 25 °C, and selectivity (S , ●).

Table C.1.17. Partition coefficients (K) of HMF and selectivity (S) values of the systems studied

	K_{HMF}		K_{fructose}		$S_{\text{HMF/Fructose}}$	
[C ₄ C ₁ im]Cl	8.87	± 0.50	0.64	± 0.04	13.94	± 0.07
[C ₄ C ₁ py]Cl	15.73	± 0.67	0.49	± 0.01	32.14	± 0.02
[C ₄ C ₁ pip]Cl	16.79	± 1.78	0.35	± 0.04	47.89	± 0.03

References

1. Chemspider, The free chemical database, <http://www.chemspider.com>, (accessed October 2016).
2. J. C. Merchuk, B. A. Andrews and J. A. Asenjo, *J. Chromatogr. B Biomed. Sci. Appl.*, 1998, **711**, 285-293.

C.2. Integrated production-separation platforms applying thermoreversible aqueous biphasic systems

NMR spectrum data of the synthesized ZIs:

N₅₅₅C3S: δ_H (400 MHz; D₂O; δ /ppm relative to TMS): 0.77 (9H, t, $J = 7.00$), 1.22 (12H), 1.52 (6H), 2.01 (2H), 2.83 (2H, t, $J = 7.00$), 3.10 (6H), 3.25 (2H). Elemental analysis (%) for C₁₈H₃₉NO₃S: Found: C, 61.37; H, 11.67; N, 3.76; C/N, 16.32. Calculated: C, 61.85; H, 11.25; N, 4.01; C/N, 15.42.

N₃₃₃C3S: δ_H (400 MHz; D₂O; δ /ppm relative to TMS): 0.83 (9H, t, $J = 7.30$), 1.55 (6H), 1.98 (2H), 2.83 (2H, t, $J = 7.00$), 3.06 (6H), 3.26 (2H). Elemental analysis (%) for C₁₂H₂₇NO₃S: Found: C, 53.22; H, 10.50; N, 44.89; C/N, 10.89. Calculated: C, 54.31; H, 10.25; N, 45.28; C/N, 10.29.

N₁₁₁C3S: δ_H (400 MHz; D₂O; δ /ppm relative to TMS): 2.12 (2H), 2.86 (2H, t, $J = 7.30$), 3.03 (9H), 3.37 (2H). Elemental analysis (%) for C₆H₁₅NO₃S: Found: C, 39.60; H, 8.51; N, 7.38; C/N, 5.36. Calculated: C, 39.76; H, 8.34; N, 7.73; C/N, 5.14.

Determination of the ABS phase diagrams and tie-line

Table C.2.1. Experimental weight fraction data for the systems composed of PEG (1) + N₁₁₁C3S (2) + H₂O (3) at 25 °C and atmospheric pressure.

PEG 1540		PEG 2000		PEG 4000		PEG 6000	
100 w_1	100 w_2	100 w_1	100 w_2	100 w_1	100 w_2	100 w_1	100 w_2
61.7421	6.0918	34.0487	18.7480	4.5019	39.9471	36.5480	13.8659
55.4399	8.5957	31.8726	20.3877	38.5272	14.1616	31.6993	16.3996
48.1452	12.2903	30.3512	21.6191	33.8958	17.2392	28.1107	17.9649
42.1343	15.3750	28.3233	22.1655	30.0458	19.7265	26.1921	18.7581
34.7956	20.4897	25.5365	24.1730	28.0121	20.6579	23.8267	20.0611
28.1009	25.5694	23.2277	25.7972	25.4302	22.5751	20.3927	21.5968
23.3294	29.1927	21.4455	26.7825	23.1789	24.0596	18.6645	22.8338
19.9088	31.9590	19.3712	28.6400	20.7934	25.9579	17.0672	24.0653
16.9317	33.9948	18.0385	29.5860			15.8596	24.9044
3.6458	51.5846	16.7994	30.6240			15.3595	25.2720
13.7774	37.1920	16.1899	30.8026			14.4565	25.8687
20.6973	31.1082	15.1847	31.4162			13.6024	26.3826
25.9894	26.6601	14.4760	32.2904			12.9157	26.7802
32.2135	21.7758	13.4289	33.2900			12.1127	27.4744
38.6463	17.1432	13.0566	33.4685			11.5231	27.9370
45.5854	12.8555	12.7045	33.6969			10.9030	28.6900
		11.8409	34.5139			10.2791	29.3006
		11.5821	34.7636			9.8782	29.5406
		11.2841	34.9267			9.4401	29.9541
		11.0058	34.9162			8.9751	30.3724

10.7818	35.0899	8.6531	30.5118
10.5888	35.2309	8.3425	30.7703
10.2064	35.7282	7.9672	31.1481
9.8278	36.1299	7.6797	31.3330
9.4236	36.3663	7.3563	31.5805
9.1261	36.6079	7.0926	31.7867
8.7886	36.8812	6.8398	32.0830
8.5036	37.1197	6.6460	32.1985
8.2073	37.3645	6.5345	32.1756
7.7852	38.0516	5.1742	33.3822
7.4631	38.4183	5.0224	33.4928
7.2257	38.5334	4.8670	33.6513
6.9512	38.9100	4.7271	33.8350
6.7573	39.0754	4.5967	34.0021
6.6478	39.0029	4.4796	34.0722
		4.3459	34.2717

Table C.2.2. Experimental weight fraction data for the systems composed of PEG (1) + N₅₅₅C3S (2) + H₂O (3) at 25 °C and atmospheric pressure.

PEG 2000		PEG 4000		PEG 6000	
100 w ₁	100 w ₂	100 w ₁	100 w ₂	100 w ₁	100 w ₂
22.2531	38.6759	31.8241	25.8809	36.5072	18.5734
17.8769	42.2702	29.4176	26.9142	33.7211	19.3230
13.2438	46.1743	27.4069	27.9340	30.8400	20.6449
		24.9894	29.1468	28.0395	22.3740
		22.5272	31.2166	26.0183	23.1997
		20.8345	32.6053	24.3382	23.9173
		18.2265	35.5452	22.0932	25.7930
				20.5848	26.9534
				18.9978	28.2837
				17.6259	29.4506
				16.3132	30.7081
				15.2276	31.8042
				14.1827	33.0016
				13.3341	34.1333
				12.3330	35.5667
				11.5755	36.5125
				10.7007	37.9364
				10.0149	38.8572
				9.3636	39.7651
				8.9328	40.3753
				8.3697	41.2818
				7.8662	42.0420
				7.4306	42.8574

		7.0137	43.5142
		6.6308	44.1926
		6.2891	44.8622

Table C.2.3. Experimental weight fraction data for the systems composed of PEG (1) + N₁₁₁C3S (2) + H₂O (3) at 35 °C and 45 °C and atmospheric pressure.

PEG 1540				PEG 2000			
35 °C		45 °C		35 °C		45 °C	
100 w ₁	100 w ₂	100 w ₁	100 w ₂	100 w ₁	100 w ₂	100 w ₁	100 w ₂
2.5799	52.4192	12.3438	30.7170	37.8487	14.1892	2.7565	35.8610
4.6128	42.3991	20.0573	25.4501	29.3328	19.5811	6.2559	31.7276
6.1163	39.3528	24.8130	21.0591	22.8144	24.0034	41.1505	10.2282
9.1282	35.5950	28.1497	18.7405	20.3801	25.3364	37.0615	12.4077
14.0020	31.4270	29.1972	17.3232	18.1173	27.6502	34.0536	13.8191
20.6191	26.1840	33.3398	15.2324	14.7896	29.5112	31.2460	15.2157
21.4814	25.1298	36.0052	13.7126	12.8064	31.7178	29.1164	16.1726
29.4090	20.0588	38.0713	12.6729	11.3756	32.8514	26.9461	17.1540
34.6321	16.5671	38.9525	11.4103	10.0079	33.8398	25.2384	17.9872
40.6361	13.0729	39.8117	10.1940	9.2179	34.6020	18.9339	21.7057
		45.3637	8.1480	7.2448	36.4122	17.5744	22.7771
				6.3520	37.7940	16.6291	23.4499
				5.8848	38.2306	15.0332	24.8597
				5.6474	38.2865	14.2061	25.8340
				5.4368	38.5683	13.7490	25.9092
				4.9457	39.7139		
				4.7770	39.7568		

Table C.2.4. Experimental weight fraction data for the systems composed of PEG (1) + N₁₁₁C3S (2) + H₂O (3) at 35 °C and 45 °C and atmospheric pressure.

PEG 4000				PEG 6000			
35 °C		45 °C		35 °C		45 °C	
100 w ₁	100 w ₂	100 w ₁	100 w ₂	100 w ₁	100 w ₂	100 w ₁	100 w ₂
40.5840	11.8056	2.5259	34.7317	40.5129	11.4816	45.2757	5.7506
36.8467	13.8912	3.6572	31.4290	25.4078	16.5983	40.2826	8.0785
33.2146	15.9229	4.7655	29.7844	21.4521	18.0844	32.8029	10.6718
30.2343	17.6603	8.1131	26.8450	20.1425	18.8188	30.4045	11.9240
25.7113	20.0444	41.6749	9.5992	19.0414	19.3449	25.0506	13.9550
24.0681	21.2838	36.2602	11.0490	17.8234	19.9910	22.6949	14.7161
20.5196	23.8284	33.2506	12.7646	16.8645	20.6571	19.8310	15.9964
18.7608	24.7111	30.9704	14.1185	14.5630	22.1402	16.4714	17.8744
16.7048	25.7350	28.7147	15.0193	12.3231	23.2632	14.6027	19.3607
14.9147	27.0727	25.2678	16.8539	10.6804	24.5741	12.7138	20.6243
13.2412	28.2875	22.5188	18.7483	9.7350	25.2282	11.2953	21.4441

12.1310	29.1904			10.1615	22.1220
10.7508	29.8224			9.6225	22.6210
9.9066	31.2383			8.7220	23.1279
8.5305	32.7156			6.8447	23.9302
7.6329	33.4654				

Table C.2.5. Experimental weight fraction data for the systems composed of PEG 6000 (1) + N₅₅₅C3S (2) + H₂O (3) at 35 °C and atmospheric pressure.

35 °C	
100 w_1	100 w_2
30.8761	26.2935
28.1694	27.4792
16.4114	36.4320
12.4479	41.5483
10.2233	43.5569
7.8140	47.1157

Table C.2.6. Identification of the ZI-PEG systems able (✓) or not able (✗) to form ABS at 25 °C and atmospheric pressure.

Polymer	N ₅₅₅ C3S	N ₃₃₃ C3S	N ₁₁₁ C3S
PEG 1540	✗	✗	✓
PEG 2000	✓	✗	✓
PEG 4000	✓	✗	✓
PEG 6000	✓	✗	✓

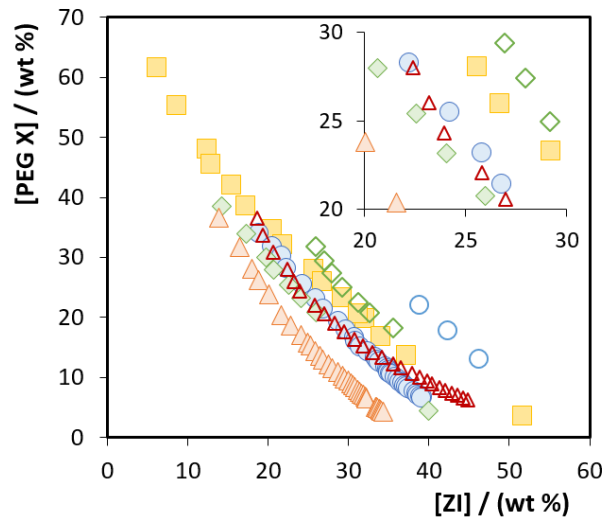


Figure C.2.1. Ternary phase diagrams of ZI-PEG-based ABS at 25 °C and atmospheric pressure. N₁₁₁C3S (full symbols); N₅₅₅C3S (open symbols): PEG 1540 (■), PEG 2000 (●), PEG 4000 (◆) and PEG 6000 (▲).

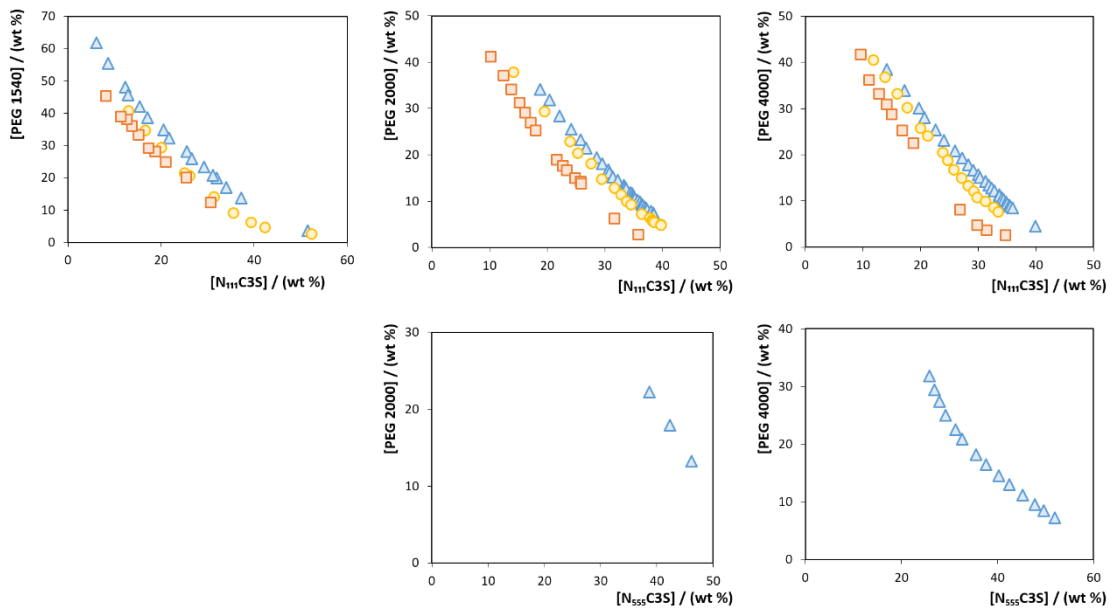


Figure C.2.2. Temperature effect in the phase diagrams of ternary systems composed of ZI + water + PEG at 25 °C (▲), 35 °C (●) and 45 °C (■), and atmospheric pressure.

Table C.2.7. Values for the constants A , B and C , obtained by the regression of the experimental binodal data as described originally by Merchuk *et al.*¹ Respective standard deviations, σ , and correlation coefficients, R^2 , are also given. ^aNot determined due to insufficient experimental data to describe the binodal curve; ^bestimated, atmospheric pressure.

ZI	PEG	T (°C)	$A \pm \sigma$		$B \pm \sigma$		$10^6(C \pm \sigma)$	
N ₅₅₅ C3S	2000	25 ^a						
	4000	25 ^a						
	6000	25	333.8	± 10.4	-0.524	± 0.004	0.48	± 0.08
		35	413.4	± 13.5	-0.488	± 0.009	0.57	± 0.13
	1540	25	110.5	± 4.9	-0.234	± 0.014	1.23	± 0.13
		35	108.6	± 32.4	-0.259	± 0.078	1.95	± 0.48
45		85.1	± 16.7	-0.220	± 0.060	2.32	± 0.81	
N ₁₁₁ C3S	2000	25	78.0	± 1.3	-0.154	± 0.002	2.44	± 0.05
		35	84.0	± 11.0	-0.192	± 0.033	2.61	± 0.18
		45	106.0	± 19.6	-0.281	± 0.054	3.75	± 0.62
	4000	25	81.3	± 16.3	-0.178	± 0.053	2.72	± 0.43
		35	92.8	± 12.0	-0.225	± 0.036	3.27	± 0.30
		45	94.2	± 27.2	-0.255	± 0.088	5.67	± 1.22
	6000	25	103.8	± 1.2	-0.269	± 0.009	3.76	± 0.14
		35	253.3	± 2.0	-0.524	± 0.011	3.85	± 0.72
		45	96.5	± 2.0	-0.302	± 0.011	7.90	± 0.72
40 ^b		168.2	± 0.6	-0.434	± 0.001	5.49	± 0.04	

Table C.2.8. Weight fraction percentage (wt%) composition of the initial mixture and of the coexisting phases of the ZI-based ABS used in the enzyme recovery, pH value, atmospheric pressure.

ZI	PEG	T (°C)	Weight fraction composition / wt%						
			[PEG] _{PEG}	[ZI] _{PEG}	[PEG] _M	[ZI] _M	[PEG] _{ZI}	[ZI] _{ZI}	pH
N ₁₁₁ C3S	6000	40	30.4	20.0	20.0	35.03	2.9	30.9	4.6

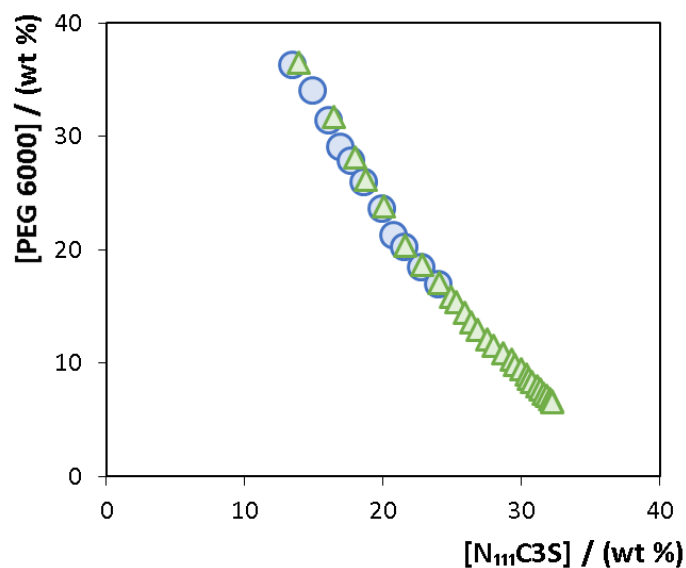


Figure C.2.3. Ternary phase diagram of the $N_{111}C3S$ -PEG 6000-based ABS at 25 °C and atmospheric pressure. (\blacktriangle) ABS composed of $N_{111}C3S$, PEG 6000 and water; (\bullet) ABS composed of $N_{111}C3S$, PEG 6000 and water, in presence of laccase, ABTS and PBS, at concentrations of $2.50 \text{ g}\cdot\text{L}^{-1}$, $4.00 \times 10^{-2} \text{ g}\cdot\text{L}^{-1}$ and $4.83 \times 10^{-4} \text{ g}\cdot\text{L}^{-1}$, respectively.

Oxidation reaction and separation of Laccase

Table C.2.9. Extraction efficiencies ($EE\%$) of the studied systems for oxidized ABTS and laccase for opposite phases in ZI-PEG-ABS.

	EE_{ABTS} (PEG-rich phase) %			$EE_{laccase}$ (ZI-rich phase) %		
$N_{111}C3S$	100	---	---	100	---	---
$N_{555}C3S$	80.9	\pm	4.0	85.0	\pm	3.6

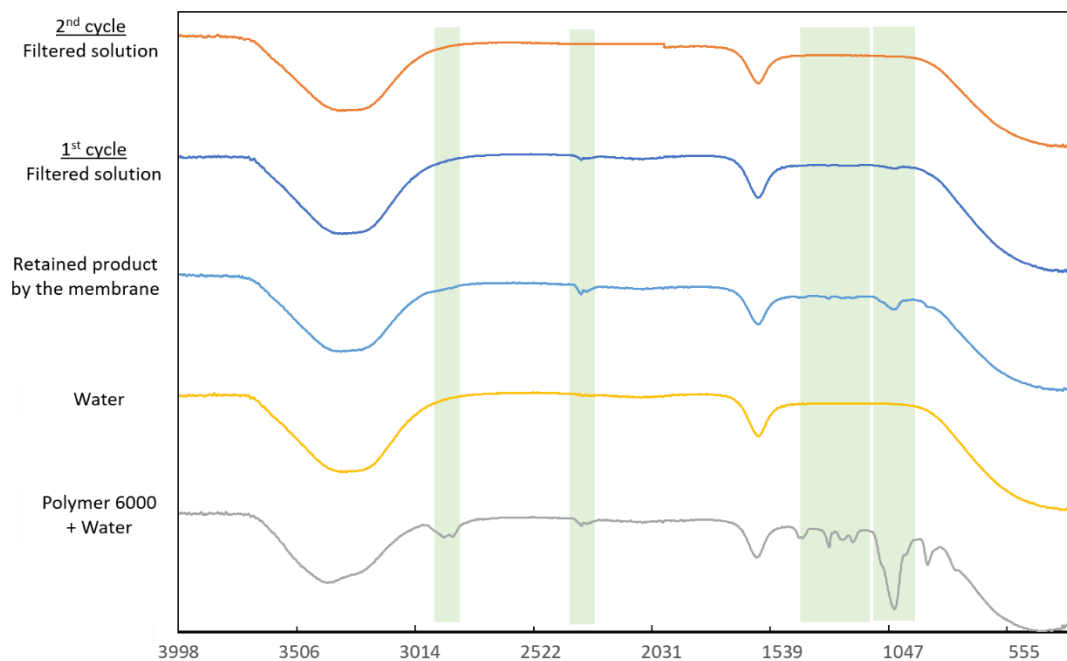


Figure C.2.4. FT-IR (Fourier-transform infrared) spectroscopy spectra corresponding to the PEG-recovery assays.

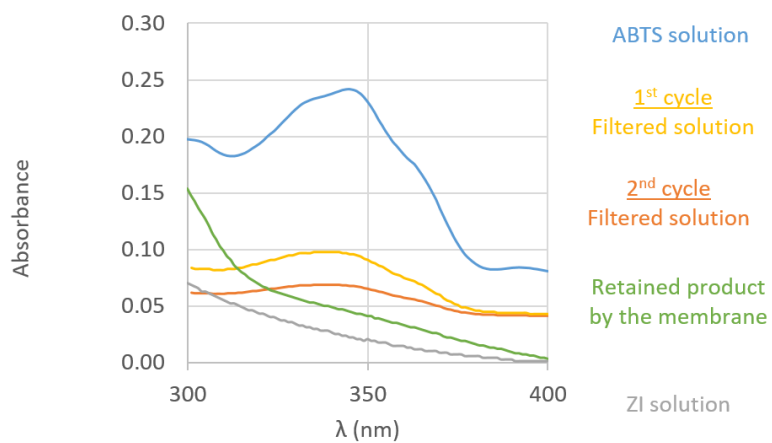


Figure C.2.5. UV-Vis spectroscopy spectra corresponding to the PEG-recovery assays.

References

1. J. C. Merchuk, B. A. Andrews and J. A. Asenjo, *J. Chromatogr. B Biomed. Sci. Appl.*, 1998, **711**, 285-293.